



MONASH University

**Synthesis, Characterisation and Bioactivity Evaluation of
Group 10 Metal *N*-Heterocyclic Carbene (NHC) Complexes**

Choo Kar Bee

A thesis submitted for the degree of Doctor of Philosophy at

Monash University

Faculty of Science

2019

COPYRIGHT NOTICE

© Choo Kar Bee (2019).

I certify that I have made all reasonable efforts to secure copyright permissions for third-party content included in this thesis and have not knowingly added copyright content to my work without the owner's permission.

ABSTRACT

N-heterocyclic carbenes (NHCs) are heterocyclic species containing a carbene carbon and at least one nitrogen atom within the ring structures. Metal *N*-heterocyclic carbene (NHC) complexes have emerged as a new platform to look for novel therapeutic alternatives to treat cancers and infectious diseases over the past two decades. Their therapeutic potential is further accentuated by a number of patents held by several universities and “Big Pharma” in recent years.

In this thesis, a series of racemic pyridine-functionalised nickel, palladium and platinum NHC complexes were synthesized and characterized. The *in vitro* antimicrobial activities of these metal NHC complexes were tested against a panel of microorganisms. Besides, the metal NHC complexes were tested against three selected human cancer cell lines for their *in vitro* cytotoxicity effect as potential anticancer candidates.

Chapter 1 provides a brief background on NHCs and development of metal NHC complexes as novel therapeutic alternatives. Emphasis is placed on group 10 metal NHC complexes (nickel, palladium and platinum) and their antimicrobial and anticancer activities were discussed.

Chapter 2 highlights the synthesis and characterization of a series of racemic pyridine-functionalised nickel, palladium and platinum metal NHC complexes. The basic backbone of the NHC ligands were prepared in two stepwise reactions: reduction of the commercially available 2-benzoylpyridine, followed by halogenation to yield 2-(chloro(phenyl)methyl)pyridine. Subsequent reactions with different imidazoles gave the desired imidazolium salts (or NHC precursors) with different R groups at the *N* wingtip (R = Me, Ph, *t*Bu). Transmetalation of the imidazolium salts (NHC precursors) into palladium and platinum NHC complexes were achieved by using Ag₂O mediated method with Pd(CH₃CN)₂Cl₂ and Pt(cod)Cl₂ as the transmetalating agents respectively. On the other hand, nickel NHC complexes were obtained via one pot synthesis method with nickel chloride as the transmetalating agents and reflux with presence of a base. The racemic metal NHC complexes have a chiral centre within the NHC chelate ring. Characterization of these synthesized precursors, imidazolium salts and metal NHC complexes were performed using ¹H and ¹³C nuclear magnetic resonance (NMR) spectroscopy as well as mass spectrometry. The racemic palladium NHC complexes were separated into enantiomers via optical resolution approach which involved three steps: formation of diastereomers pair upon coordination with sodium salt of chiral amino acid, separation of the diastereomic pair by fractional crystallization, followed by treatment with 1 M HCl to get the optical active metal NHC complexes as a result of cleavage of chiral amino acid auxiliary. Following recrystallisation, the molecular structure of a platinum NHC complex had been successfully elucidated via single crystal X ray diffraction (XRD) analysis. The six-membered ring

of the platinum NHC complexes adopted a boat conformation with the phenyl ring arranged at the axial position. Meanwhile, two unexpected nickel complexes, i.e. simple nickel coordination complex and nickelate complex, were obtained upon recrystallisation from Ni NHC complexes and studied using XRD.

The antimicrobial activities of the previously described metal NHC complexes were studied in Chapter 3. They were tested against a panel of clinically relevant microorganisms including Gram positive and Gram bacteria, as well as yeasts using broth microdilution assays. It was observed that the platinum and palladium NHC complexes displayed enhanced antimicrobial activities upon coordination to metals, as compared to the corresponding imidazolium salts i.e. NHC precursors, with minimum inhibitory concentration (MIC) values in micromolar (μM) range. A couple of platinum NHC complexes synthesized exhibited antimicrobial activities with MIC as low as $2 \mu\text{M}$, which are comparable to silver NHC complexes with renowned antimicrobial profiles. Besides, the optically resolved *R* enantiomers of palladium NHC complexes have shown evident antimicrobial activities compared to *S* enantiomers, resembling chiral drugs with only one bioactive enantiomer out of two.

In Chapter 4, the anticancer potential of the synthesized metal NHC complexes were investigated. The cytotoxicity of these complexes was evaluated against three selected human carcinoma cell lines, including breast (MCF7), oral (H103) and colon (HCT116) cancer cells via MTT cell viability assay. Their half maximal inhibitory concentration (IC_{50}) were determined along with cisplatin. Similarly, upon coordination to the metals, the cytotoxicity effects of the palladium and platinum NHC complexes increased significantly as compared to the imidazolium salts. Among all, one of the platinum NHC complexes synthesized displayed significant cytotoxicities towards the cancer cells with IC_{50} values that are two to three times lower than that of the anticancer benchmark cisplatin. Evidence of variable cytotoxicities were also observed for the *R* and *S* enantiomer of palladium NHC complexes, in which latter was less cytotoxic towards the cancer cells tested.

In essence, a series of racemic pyridine-functionalised nickel, palladium and platinum NHC complexes had been synthesized and characterised with various spectroscopic techniques. Evidences for the influence of metals, wingtip substituents on the NHC ring and optical isomerism on the biological activities of these metal NHC complexes have been found. Although the mechanism of action for the reported biological activities is not known at present, it is apparent from this work that these Group 10 metal NHC complexes, especially the platinum NHC complexes, could be some potential drug candidates in the future.

DECLARATION

This thesis contains no material which has been accepted for the award of any other degree or diploma at any university or equivalent institution and that, to the best of my knowledge and belief, this thesis contains no material previously published or written by another person, except where due reference is made in the text of the thesis.

Signature

: 

Print Name : Choo Kar Bee

Date : 21 February 2019

PUBLICATIONS DURING ENROLMENT

Publication #1

CHOO, K. B., MAH, W. L., LEE, S. M., LEE, W. L. & CHEOW, Y. L. 2018. Palladium complexes of bidentate pyridine N-heterocyclic carbenes: Optical resolution, antimicrobial and cytotoxicity studies. *Applied Organometallic Chemistry*, 32, e4377.

Abstract:

A series of bidentate pyridine-functionalized palladium N-heterocyclic carbene (Pd NHC) complexes with various wingtip substituents (R = methyl, phenyl and *tert*-butyl) has been synthesized and evaluated for their potential biomedical applications as antimicrobials and antiproliferative drug candidates. The obtained Pd NHC complexes have been applied in a standard broth microdilution assay for determination of their antimicrobial activities against thirteen strains of pathogenic microorganisms. In addition to that, cytotoxic activities of the Pd complexes were also evaluated against three human cancer cell lines, including breast (MCF7), colon (HCT116) and oral (H103) cancer cells using a standard MTT assay. Upon coordination to palladium, the Pd NHC complexes have shown significant antimicrobial activities with MIC at micromolar range, and they were cytotoxic to the tested carcinomas with IC₅₀ ranging from 13 μ M to 38 μ M. Evidences for influence of both wingtip substituents and optical isomerism on the biological activities of the complexes have been found.

Poster Presentation #1

Optical Resolution and Bioactivities of Palladium *N*-Heterocyclic Carbene (NHC) Complexes

6th Asian Conference on Coordination Chemistry, 23-28 July 2017 (Melbourne, Australia)

Poster Presentation #1

Palladium Complex of Racemic Bidentate Pyridine *N*-Heterocyclic Carbene (NHC): Antimicrobial and Cell Cytotoxicity Studies

18th Asian Edition Tetrahedron Symposium, 24-26 July 2017 (Melbourne, Australia)

Manuscript #1

Platinum *N*-heterocyclic carbenes complexes: Synthesis, characterization, and bioactivity studies

Manuscript #2

Antimicrobial and antibiofilm potential of dichloro(1,5-cyclooctadiene)platinum(II), Pt(cod)Cl₂

ACKNOWLEDGEMENTS

First and foremost, I would like to express my profound gratitude and deep regards towards my supervisor, Dr. Cheow Yuen Lin, for his unconditional patience, encouragement and guidance during my candidature period. In addition, I would like to thank Dr. Lee Sui Mae and Dr. Lee Wai Leng for their guidance in microbiology and cell biology aspects of this study.

I am grateful for the financial supports from the Ministry of Higher Education (MOHE), Malaysia via Fundamental Research Grant Scheme (FRGS) (FRGS/1/2014/ST01/MUSM/03/1) and the School of Science, Monash University Malaysia. Many thanks for Monash University Malaysia for providing me a Merit Scholarship. Without these, my PhD journey would not be possible.

Besides that, I would like to acknowledge the laboratory administrative office and technical officers from School of Science, Monash University including Mr. Ragavan, Ms. Darshini, Ms. Nurul, Mr. Jegan, Mr. Syafiq, Mr. Syamil and Ms. Amreeta Sarjit for providing me helps whenever I seek upon it. Also, special thanks to Dr. Tan Wooi Boon and Ms. Nurulnadia from School Research Office who always provide assistances on the milestone progress and candidature related issues.

Also, I would like to express my gratitude to Ms. Felicia Lim, Ms. Tan Ping Wey and Dr. Anton from the NMR Platform of Monash University Malaysia for technical supports in the numerous NMR of this study. Not to forget Ms. Nurziana from the LC-MS/MS Platform of Monash University Malaysia who provide technical assistance on the MS results included in this study. Last but not least, I would like to thank Dr. Tan Kong Wai from University of Malaya (UM) and Mr. Mohammad Fadzlee from Universiti Kebangsaan Malaysia (UKM) for their competent technical assistance and analysis on the X ray crystallography data obtained in this study.

Special thanks to my fellow research group mate, Wee Li, for his valuable help and feedback throughout my candidature, which helped me a lot in finalizing this study within the limited timeframe. Besides that, I would like to express my thankfulness towards Dr. Mae's research group and Dr. Lee's research group who provide valuable advices and supports on the antimicrobial and anticancer studies of this work. Many thanks to fellow lab mates for their helps and supports throughout these years including Amy, Andrew, Calvin, Carrie, Chew Ee, Chong Wey, Christina, Hikari, Hong Sheng, Irene, Janet, Jing Yun, Kak Ming, Kit Yee, Mei Mun, Patric, Pei Sheng, Peng Nian, Shawn, Siew Yin, Si Hui, Siyin, Shu Kee, Steven, Xin Hui, Yi Yi, Yiing Yng and others.

Last but not least, I would like to express utmost gratitude to my family and friends for their unconditional love and support which accompanying me along the journey towards completion of this PhD. Most importantly, I would like to thank myself for completing this journey while wading through the darkest period of my life involving grief, mental and physical traumas. You've done it!

TABLE OF CONTENT

COPYRIGHT NOTICE	I
ABSTRACT	II
DECLARATION	IV
PUBLICATIONS DURING ENROLMENT	V
ACKNOWLEDGEMENTS	VI
TABLE OF CONTENT	VII
LIST OF ABBREVIATIONS	XII
LIST OF TABLES	XV
LIST OF FIGURES	XVII
LIST OF SCHEMES	XXII
CHAPTER 1 INTRODUCTION AND LITERATURE REVIEW	1
1.1. Transition metals as metallodrugs	1
1.2. Emergence of Bioorganometallic Drugs	1
1.3. <i>N</i>-heterocyclic carbenes (NHC)	3
1.3.1. Synthesis of <i>N</i> -heterocyclic carbenes (NHC)	4
1.3.2. Complexation of <i>N</i> -heterocyclic carbenes (NHC) to metals	8
1.3.3. Characteristic features of biologically studied metal NHC complexes	9
1.4. Group 10 metal NHC complexes with therapeutic potentials	10
1.5. Group 10 metal NHC complexes with anticancer activities	11
1.5.1. Platinum <i>N</i> -Heterocyclic carbene (Pt NHC) complexes	12

1.5.2. Palladium <i>N</i> -Heterocyclic carbene (Pd NHC) complexes	19
1.5.3. Nickel <i>N</i> -Heterocyclic carbene (Ni NHC) complexes	26
1.6. Group 10 metal NHC complexes with antimicrobial activities	27
1.6.1. Palladium <i>N</i> -Heterocyclic carbene (Pd NHC) complexes	29
1.7. Summary and Research Gaps	30
1.8. Research Objectives	32

CHAPTER 2 SYNTHESIS, CHARACTERISATION AND OPTICAL RESOLUTION OF PALLADIUM, PLATINUM AND NICKEL <i>N</i>-HETEROCYCLIC CARBENE (NHC) COMPLEXES	33
2.1. Introduction	33
2.2. Results and Discussion	35
2.2.1. Synthesis and characterisation of imidazolium salts (NHC precursors) 64	35
2.2.1.1. Synthesis and characterisation of 1-methyl-3-[phenyl(pyridin-2-yl)methyl]-1H-imidazolium chloride, 64a	36
2.2.1.2. Synthesis and characterisation of 1-phenyl-3-[phenyl(pyridin-2-yl)methyl]-1H-imidazolium chloride, 64b	37
2.2.1.3. Synthesis and characterisation of 1-tert-butyl-3-[phenyl(pyridin-2-yl)methyl]-1H-imidazolium chloride, 64c	37
2.2.2. Synthesis and Characterisation of Racemic Metal NHC Complexes	38
2.2.2.1. Synthesis and characterization of racemic palladium NHC complexes	38
2.2.2.1.1. Characterisation of racemic complex Pd-65a	39
2.2.2.1.2. Characterisation of racemic complex Pd-65b	39
2.2.2.1.3. Characterisation of racemic complex Pd-65c	40
2.2.2.2. Optical resolution of racemic palladium NHC complexes	41
2.2.2.2.1. Optical resolution of racemic Pd-65a complex	41
2.2.2.2.2. Optical resolution of racemic Pd-65b complex	43
2.2.2.2.3. Optical resolution of racemic Pd-65c complex	45
2.2.2.3. Synthesis and characterisation of racemic platinum NHC complexes	46
2.2.2.3.1. Characterisation of racemic complex Pt-65a	46
2.2.2.3.2. Characterisation of racemic complex Pt-65b	49

2.2.2.3.3. Characterisation of racemic complex Pt-65c	50
2.2.2.4. Synthesis and characterisation of racemic nickel NHC complexes	52
2.2.2.4.1. Characterisation of racemic complex Ni-65a	54
2.2.2.4.2. Characterisation of racemic complex Ni-65b	57
2.2.2.4.3. Characterisation of racemic complex Ni-65c	58
2.3. Conclusion	61
2.4. Experimental	62
2.4.1. General procedures	62
2.4.2. Synthesis and characterisation of imidazolium salts (NHC precursors) 64	63
2.4.2.1. Synthesis of phenyl(pyridine-2-yl)methanol, 62	63
2.4.2.2. Synthesis of 2-(chloro(phenyl)methyl)pyridine, 63	64
2.4.2.3. Synthesis of 1-methyl-3-[phenyl(pyridin-2-yl)methyl]-1H-imidazolium chloride, 64a	65
2.4.2.4. Synthesis of 1-phenyl-3-[phenyl(pyridin-2-yl)methyl]-1H-imidazolium chloride, 64b	66
2.4.2.5. Synthesis of 1-tert-butyl-3-[phenyl(pyridin-2-yl)methyl]-1H-imidazolium chloride, 64c	67
2.4.3. Synthesis of racemic palladium NHC complexes	68
2.4.3.1. Synthesis of racemic complex (\pm)- Pd-65a	68
2.4.3.2. Synthesis of racemic complex (\pm)- Pd-65b	69
2.4.3.3. Synthesis of racemic complex (\pm)- Pd-65c	70
2.4.4. Optical resolution of racemic palladium NHC complexes	70
2.4.4.1. Optical resolution of racemic complex Pd-65a	70
2.4.4.2. Optical resolution of racemic complex Pd-65b	72
2.4.5. Synthesis of racemic platinum NHC complexes	73
2.4.5.1. Synthesis of racemic complex (\pm)- Pt-65a	73
2.4.5.2. Synthesis of racemic complex (\pm)- Pt-65b	74
2.4.5.3. Synthesis of racemic complex (\pm)- Pt-65c	75
2.4.5.4. Preparation of racemic dibromide complex (\pm)- 70	76
2.4.5.5. Preparation of racemic diiodo complex (\pm)- 71	77
2.4.6. Synthesis of racemic nickel NHC complexes	78
2.4.6.1. Synthesis of racemic complex (\pm)- Ni-65a	78
2.4.6.2. Synthesis of racemic complex (\pm)- Ni-65b	79
2.4.6.3. Synthesis of racemic complex (\pm)- Ni-65c	80

CHAPTER 3 ANTIMICROBIAL STUDIES OF PALLADIUM, PLATINUM AND NICKEL <i>N</i>-HETEROCYCLIC CARBENE (NHC) COMPLEXES	81
3.1. Introduction	81
3.2. Results and Discussion	82
3.3. Conclusion	93
3.4. Experimental	94
3.4.1. Microorganisms	94
3.4.2. Broth microdilution assay (BMD)	95
CHAPTER 4 CYTOTOXICITY STUDIES OF PALLADIUM, PLATINUM AND NICKEL <i>N</i>-HETEROCYCLIC CARBENE (NHC) COMPLEXES	96
4.1. Introduction	96
4.2. Results and Discussion	97
4.2.1. Cytotoxicity study against human carcinoma cell lines	97
4.2.2. Selectivity index study	103
4.3. Conclusion	106
4.4. Experimental	107
4.4.1. Cell lines	107
4.4.2. Maintenance of cell culture	107
4.4.3. MTT cell viability assay	108
CHAPTER 5 SUMMARY AND FUTURE DIRECTIONS	109
5.1. Summary	109
5.2. Future Directions	111

REFERENCES	115
APPENDIX 1: X RAY CRYSTALLOGRAPHIC DATA	143
APPENDIX 2: NMR SPECTRAL DATA	146
APPENDIX 3: LCMS SPECTRAL DATA	163
APPENDIX 4: PLOTS OF MTT CELL VIABILITY ASSAY	170
APPENDIX 5: PUBLISHED PUBLICATION #1	178
APPENDIX 6: POSTER PRESENTATION #1	191
APPENDIX 7: POSTER PRESENTATION #2	192

LIST OF ABBREVIATIONS

Ar	aryl group
ATCC	American Type Culture Collection
BMD	broth microdilution assay
br	broad
<i>ca.</i>	Circa
calcd	calculated
CDCL ₃	chloroform-d ₁
CLSI	Clinical and Laboratory Standards Institute
d	doublet (in NMR assignment)
dd	doublet of doublets (in NMR assignment)
ddd	doublet of doublet of doublets (in NMR assignment)
dq	doublet of quadruplets (in NMR assignment)
dt	doublet of triplets (in NMR assignment)
DCM	dichloromethane
DMSO	dimethyl sulfoxide
EA	ethyl acetate
ESI	electrospray ionization
EtOH	ethanol
FBS	fetal bovine serum
h	hour(s)
H ₂ O	water
HCl	hydrochloric acid
HEX	hexane
HPLC	high performance liquid chromatography

Hz	hertz
LC	liquid chromatography
m	multiplets (in NMR assignment)
M	molar/mole per liter
M.p	melting point
MBC	minimum bactericidal concentration
Me	methyl
MEM	minimum essential medium
MeOH	methanol
MHA	Mueller-Hinton agar
MHB	Mueller-Hinton broth
MHz	megahertz
MIC	minimum inhibitory concentration
min	minute(s)
mg	milligram
mg/mL	milligram per milliliter
mL	milliliter
mL/min	milliliter per minute
mM	millimolar/millimole per liter
mmol	millimole
MRSA	methicillin-resistant <i>Staphylococcus aureus</i>
MSSA	methicillin-sensitive <i>Staphylococcus aureus</i>
MS	mass spectrometry
m/z	mass-to-charge ratio
nm	nanometer
NMR	nuclear magnetic resonance

OD	optical density (or absorbance)
PBS	phosphate buffer saline
Ph	phenyl
ppm	parts per million
<i>R</i>	rectus (Latin: right absolute configuration)
<i>S</i>	sinister (Latin: left absolute configuration)
s	singlet (in NMR assignment)
SD	standard deviation
SEM	standard error of mean
SiMe ₄	tetramethylsilane (TMS)
t	triplet (in NMR assignment)
<i>t</i> Bu	<i>tert</i> -butyl
td	triplet of doublets (in NMR assignment)
TLC	thin layer chromatography
TMS	tetramethylsilane
TOF	time-of-flight
μL	microliter
UV	ultraviolet
VRE	vancomycin-resistant <i>Enterococcus faecalis</i>
v/v	volume per volume
w/v	weight per volume
WHO	World Health Organization
XRD	X-ray diffraction
δ	NMR chemical shift in ppm

LIST OF TABLES

Table 1. List of parameters for the optical resolution of racemic complex Pd-65c	45
Table 2. Selected bond lengths (Å) and angles (°) for racemic complex Pt-65a	48
Table 3. ¹ H and ¹³ C NMR spectral data for racemic complex Pt-65b in DMSO- <i>d</i> ₆ and TMS as internal standard, with relative to racemic complex Pd-65b	49
Table 4. ¹ H and ¹³ C NMR spectral data for racemic complex Pt-65c in DMSO- <i>d</i> ₆ and TMS as internal standard, with relative to racemic complex Pd-65c	51
Table 5. List of synthesis parameters for optimizing the synthesis of Ni NHC complexes....	54
Table 6. Selected bond lengths (Å) and angles (°) for unexpected nickel complex 72	55
Table 7. Selected bond lengths (Å) and angles (°) for unexpected nickel complex 73	60
Table 8. List of compounds tested in antimicrobial assay.....	83
Table 9. Antimicrobial activity of precursors, imidazolium salts and imidazoles reported as MIC and MBC in mM. ^a	84
Table 10. Antimicrobial activity of metal salts, transmetalating agents and antibiotics, reported as MIC and MBC in mM. ^a	85
Table 11. Antimicrobial activity of synthesized palladium complexes, reported as MIC and MBC in mM. ^a	85
Table 12. Antimicrobial activity of synthesized platinum and nickel complexes, reported as MIC and MBC in mM. ^a	87
Table 13. The list of microorganisms used in broth microdilution assay to determine the antimicrobial activity of the synthesized compounds.	94
Table 14. Cytotoxicity of all compounds against selected human carcinoma cell lines, reported as IC ₅₀ (concentration required for 50% inhibition <i>in vitro</i>) in terms of μM.....	98

Table 15. Cytotoxicity of selected compounds against selected human normal cell lines, reported as IC ₅₀ (concentration required for 50% inhibition <i>in vitro</i>) in terms of μM...	103
Table 16. Selectivity index (SI) of selected compounds for oral epithelial cells (OKF6) against oral cancer (H103), colon cancer (HCT116), and breast cancer (MCF7) cells.	105
Table 17. Selectivity index (SI) of selected compounds for skin keratinocytes (HACAT) against oral cancer (H103), colon cancer (HCT116), and breast cancer (MCF7) cells.	105
Table 18. Selectivity index (SI) of selected compounds for lung epithelial cells (BEAS2B) against oral cancer (H103), colon cancer (HCT116), and breast cancer (MCF7) cells.	105
Table 19. The list of cell lines used in MTT assay to determine the cytotoxicity of the synthesized compounds, including human carcinoma cell lines and normal cell lines.	107
Table 20. The list of corresponding cell culture media used to culture and maintain the selected human carcinoma cell lines and normal cell lines.....	107
Table 21. Crystallographic data of racemic complex Pt-65a	143
Table 22. Crystallographic data of unexpected nickel complex 72	144
Table 23. Crystallographic data of unexpected nickelate complex 73	145

LIST OF FIGURES

Figure 1. General representation of a <i>N</i> -heterocyclic carbene (NHC) (4) and stabilisation of the singlet carbene structure by the σ -withdrawing and π -donating effects of the nitrogen heteroatoms in a ground-state electronic structure of imidazole-2-ylidenes (Hopkinson et al., 2014).....	4
Figure 2. Five-membered ring scaffolds of NHCs commonly found in literature: imidazolidinylidene (5), imidazolylidene (6), and benzimidazolylidene (7).	5
Figure 3. Molecular structure of racemic complex Pt-65a with thermal ellipsoids at 50% probability. DMSO solvent molecule and hydrogen atoms are omitted for clarity.	48
Figure 4. Rotated view of complex Pt-65a with thermal ellipsoids at 50% probability.....	48
Figure 5. Molecular structure of unexpected nickel complex 72 with thermal ellipsoids at 50% probability. Hydrogen atoms are omitted for clarity.	56
Figure 6. Molecular structure of unexpected nickel complex 73 with thermal ellipsoids at 50% probability. Hydrogen atoms are omitted for clarity.	61
Figure 7. ¹ H NMR spectrum of phenyl(pyridine-2-yl)methanol, 62	146
Figure 8. ¹³ C NMR spectrum of phenyl(pyridine-2-yl)methanol, 62	146
Figure 9. ¹ H NMR spectrum of 2-(chloro(phenyl)methyl)pyridine, 63	147
Figure 10. ¹³ C NMR spectrum of 2-(chloro(phenyl)methyl)pyridine, 63	147
Figure 11. ¹ H NMR spectrum of imidazolium-based salt, 64a	148
Figure 12. ¹³ C NMR spectrum of imidazolium-based salt, 64a	148
Figure 13. ¹ H NMR spectrum of imidazolium-based salt, 64b	149
Figure 14. ¹³ C NMR spectrum of imidazolium-based salt, 64b	149
Figure 15. ¹ H NMR spectrum of imidazolium-based salt, 64c	150
Figure 16. ¹³ C NMR spectrum of imidazolium-based salt, 64c	150

Figure 17. ^1H NMR spectrum of racemic Pd NHC complex (\pm)- Pd-65a	151
Figure 18. ^{13}C NMR spectrum of racemic Pd NHC complex (\pm)- Pd-65a	151
Figure 19. ^1H NMR spectrum of racemic Pd NHC complex (\pm)- Pd-65b	152
Figure 20. ^{13}C NMR spectrum of racemic Pd NHC complex (\pm)- Pd-65b	152
Figure 21. ^1H NMR spectrum of racemic Pd NHC complex (\pm)- Pd-65c	153
Figure 22. ^{13}C NMR spectrum of racemic Pd NHC complex (\pm)- Pd-65c	153
Figure 23. ^1H NMR spectrum of diastereomer Pd-(Rc,Sc)-68a	154
Figure 24. ^{13}C NMR spectrum of diastereomer Pd-(Rc,Sc)-68a	154
Figure 25. ^1H NMR spectrum of diastereomer Pd-(Sc,Sc)-69b	155
Figure 26. ^{13}C NMR spectrum of diastereomer Pd-(Sc,Sc)-69b	155
Figure 27. ^1H NMR spectrum of racemic Pt NHC complex (\pm)- Pt-65a	156
Figure 28. ^{13}C NMR spectrum of racemic Pt NHC complex (\pm)- Pt-65a	156
Figure 29. ^1H NMR spectrum of racemic Pt NHC complex (\pm)- Pt-65b	157
Figure 30. ^{13}C NMR spectrum of racemic Pt NHC complex (\pm)- Pt-65b	157
Figure 31. ^1H NMR spectrum of racemic Pt NHC complex (\pm)- Pt-65c	158
Figure 32. ^{13}C NMR spectrum of racemic Pt NHC complex (\pm)- Pt-65c	158
Figure 33. ^1H NMR spectrum of racemic dibromide Pt NHC complex (\pm)- 70	159
Figure 34. ^{13}C NMR spectrum of racemic dibromide Pt NHC complex (\pm)- 70	159
Figure 35. ^1H NMR spectrum of racemic diiodo Pt NHC complex (\pm)- 71	160
Figure 36. ^{13}C NMR spectrum of racemic diiodo Pt NHC complex (\pm)- 71	160
Figure 37. ^1H NMR spectrum of racemic Ni NHC complex (\pm)- Ni-65a	161

Figure 38. ¹ H NMR spectrum of racemic Ni NHC complex (±)- Ni-65b	161
Figure 39. ¹ H NMR spectrum of racemic Ni NHC complex (±)- Ni-65c	162
Figure 40. LCMS spectrum of phenyl(pyridine-2-yl)methanol, 62	163
Figure 41. LCMS spectrum of 2-(chloro(phenyl)methyl)pyridine, 63	163
Figure 42. LCMS spectrum of imidazolium-based salt, 64a	163
Figure 43. LCMS spectrum of imidazolium-based salt, 64b	164
Figure 44. LCMS spectrum of imidazolium-based salt, 64c	164
Figure 45. LCMS spectrum of racemic Pd NHC complex (±)- Pd-65a	164
Figure 46. LCMS spectrum of racemic Pd NHC complex (±)- Pd-65b	165
Figure 47. LCMS spectrum of racemic Pd NHC complex (±)- Pd-65c	165
Figure 48. LCMS spectrum of diastereomer Pd-(Rc,Sc)-68a	165
Figure 49. LCMS spectrum of enantiomer Pd NHC complex (R)- Pd-65a	166
Figure 50. LCMS spectrum of diastereomer Pd-(Sc,Sc)-69b	166
Figure 51. LCMS spectrum of enantiomer Pd NHC complex (S)- Pd-65b	166
Figure 52. LCMS spectrum of racemic Pt NHC complex (±)- Pt-65a	167
Figure 53. LCMS spectrum of racemic Pt NHC complex (±)- Pt-65b	167
Figure 54. LCMS spectrum of racemic Pt NHC complex (±)- Pt-65c	167
Figure 55. LCMS spectrum of racemic dibromide Pt NHC complex (±)- 70	168
Figure 56. LCMS spectrum of racemic diiodo Pt NHC complex (±)- 71	168
Figure 57. LCMS spectrum of unexpected Ni complex 72	168
Figure 58. LCMS spectrum of unexpected nickelate complex 73	169

- Figure 59.** Cytotoxicity of cisplatin, metal salts, and transmetalating agents against H103 after 48 hours of treatment. Cell viability was assessed using MTT cell viability assay at 570 nm (reference wavelength at 620 nm). The cell viability is reported in mean with error bars of ± 1 SEM..... 170
- Figure 60.** Cytotoxicity of precursors (**62** and **63**), imidazolium salts **64** and different imidazoles against H103 after 48 hours of treatment. Cell viability was assessed using MTT cell viability assay at 570 nm (reference wavelength at 620 nm). The cell viability is reported in mean with error bars of ± 1 SEM..... 170
- Figure 61.** Cytotoxicity of Pd NHC complexes and diastereomers against H103 after 48 hours of treatment. Cell viability was assessed using MTT cell viability assay at 570 nm (reference wavelength at 620 nm). The cell viability is reported in mean with error bars of ± 1 SEM. 171
- Figure 62.** Cytotoxicity of Pt NHC complexes and Ni complexes against H103 after 48 hours of treatment. Cell viability was assessed using MTT cell viability assay at 570 nm (reference wavelength at 620 nm). The cell viability is reported in mean with error bars of ± 1 SEM. 171
- Figure 63.** Cytotoxicity of cisplatin, metal salts, and transmetalating agents against HCT116 after 48 hours of treatment. Cell viability was assessed using MTT cell viability assay at 570 nm (reference wavelength at 620 nm). The cell viability is reported in mean with error bars of ± 1 SEM..... 172
- Figure 64.** Cytotoxicity of precursors (**62** and **63**), imidazolium salts **64** and different imidazoles against HCT116 after 48 hours of treatment. Cell viability was assessed using MTT cell viability assay at 570 nm (reference wavelength at 620 nm). The cell viability is reported in mean with error bars of ± 1 SEM..... 172
- Figure 65.** Cytotoxicity of Pd NHC complexes and diastereomers against HCT116 after 48 hours of treatment. Cell viability was assessed using MTT cell viability assay at 570 nm (reference wavelength at 620 nm). The cell viability is reported in mean with error bars of ± 1 SEM. 173
- Figure 66.** Cytotoxicity of Pt NHC complexes and Ni complexes against HCT116 after 48 hours of treatment. Cell viability was assessed using MTT cell viability assay at 570 nm

(reference wavelength at 620 nm). The cell viability is reported in mean with error bars of ± 1 SEM.	173
Figure 67. Cytotoxicity of cisplatin, metal salts, and transmetalating agents against MCF7 after 48 hours of treatment. Cell viability was assessed using MTT cell viability assay at 570 nm (reference wavelength at 620 nm). The cell viability is reported in mean with error bars of ± 1 SEM.	174
Figure 68. Cytotoxicity of precursors (62 and 63), imidazolium salts 64 and different imidazoles against MCF7 after 48 hours of treatment. Cell viability was assessed using MTT cell viability assay at 570 nm (reference wavelength at 620 nm). The cell viability is reported in mean with error bars of ± 1 SEM.	174
Figure 69. Cytotoxicity of Pd NHC complexes and diastereomers against MCF7 after 48 hours of treatment. Cell viability was assessed using MTT cell viability assay at 570 nm (reference wavelength at 620 nm). The cell viability is reported in mean with error bars of ± 1 SEM.	175
Figure 70. Cytotoxicity of Pt NHC complexes and Ni complexes against MCF7 after 48 hours of treatment. Cell viability was assessed using MTT cell viability assay at 570 nm (reference wavelength at 620 nm). The cell viability is reported in mean with error bars of ± 1 SEM.	175
Figure 71. Cytotoxicity of selected complexes against OKF6 after 48 hours of treatment. Cell viability was assessed using MTT cell viability assay at 570 nm (reference wavelength at 620 nm). The cell viability is reported in mean with error bars of ± 1 SEM.	176
Figure 72. Cytotoxicity of selected complexes against HACAT after 48 hours of treatment. Cell viability was assessed using MTT cell viability assay at 570 nm (reference wavelength at 620 nm). The cell viability is reported in mean with error bars of ± 1 SEM.	176
Figure 73. Cytotoxicity of selected complexes against BEAS2B after 48 hours of treatment. Cell viability was assessed using MTT cell viability assay at 570 nm (reference wavelength at 620 nm). The cell viability is reported in mean with error bars of ± 1 SEM.	177

LIST OF SCHEMES

Scheme 1. Chemical structures of cisplatin (1), carboplatin (2) and oxaliplatin (3).	2
Scheme 2. General representation of synthesis route for imidazolylidenes 9	5
Scheme 3. General synthesis route of symmetrical (left) and unsymmetrical (right) <i>N,N'</i> -substituted imidazolium salts 8	6
Scheme 4. Multicomponent reaction pathway for synthesis of symmetrical <i>N,N'</i> -substituted imidazolium salts.....	7
Scheme 5. Combination of multicomponent cyclization and <i>N</i> -alkylation for synthesis of unsymmetrical <i>N,N'</i> -substituted imidazolium salts 8	7
Scheme 6. Catalytic <i>N</i> -alkylation or <i>N</i> -arylation of imidazole with alkyl halides or aryl halides, respectively.	8
Scheme 7. General illustration of synthesis route of metal NHC complexes.....	8
Scheme 8. General representation for synthesis of metal NHC complexes using the silver(I) oxide-mediated transmetalation method.	9
Scheme 9. Patented monometallic <i>trans</i> -PtI ₂ (NHC)(amine) complexes 11 and the bimetallic <i>trans</i> -[PtI ₂ (NHC)] ₂ (diamine) complexes 12 developed by Marinetti's group.	12
Scheme 10. Luminescent cyclometalated Pt NHC complexes with anticancer activities developed by Che's group.....	14
Scheme 11. Platinum NHC complexes (17-22) with different <i>N</i> -substituted functionalities at NHC ligands with simplified formula of PtI ₂ (NHC)(pyridine).	15
Scheme 12. Pt NHC complexes and subsequent coordination complex with polyethylenimine (PEI) chain to increase their aqueous solubility.....	16
Scheme 13. Pt NHC complex 27 and addition of histidine to increase the bioavailability.	17
Scheme 14. Selected Pt NHC complexes with different <i>cis</i> and <i>trans</i> configurations exhibiting anticancer activities as reported by Schobert et al.	18

Scheme 15. Pd-mono(NHC) complex 36 and Pd-bis(NHC) complex 37 with potent anticancer activities developed by Ray et al.	20
Scheme 16. A series of Pd NHC complexes with different <i>cis</i> and <i>trans</i> arrangement developed by Haque's group.	21
Scheme 17. Tridendate Pd NHC complexes with potent anticancer activities.	22
Scheme 18. A series of Pt NHC complexes with varying NHC ligands and metal multiplicity developed by Ghdayeb et al.	23
Scheme 19. Cyclometalated Pd NHC complexes with anticancer activities developed by Che's group.	24
Scheme 20. Enantiomeric pairs of Pd NHC complexes with anticancer activities.	26
Scheme 21. Nickel NHC complexes reported by Ray <i>et al.</i> (2009) that showed anticancer potential.	27
Scheme 22. Selected metal NHC complexes with significant minimum inhibitory concentration (MIC) below 10 µg/mL: pyridine-linked pincer silver(I) NHC complex (56), rhodium NHC complex (57), ruthenium NHC complex (58) and cationic bis(NHC)gold(I) complex (59).	29
Scheme 23. Palladium NHC complexes that shown significant antimicrobial activity with minimum inhibitory concentration (MIC) in µg/mL range.	30
Scheme 24. General synthesis route of the racemic metal NHC complexes in this study.	34
Scheme 25. Chemical structure of compound phenyl(pyridine-2-yl)methanol, 62	35
Scheme 26. Chemical structure of compound 2-(chloro(phenyl)methyl)pyridine, 63	36
Scheme 27. Structure of imidazolium salt (R = Me), 64a	36
Scheme 28. Structure of imidazolium salt (R = Ph), 64b	37
Scheme 29. Structure of imidazolium salt (R = <i>t</i> Bu), 64c	38

Scheme 30. Two-steps transmetalation of imidazolium salts (or NHC precursors) (64) into racemic palladium NHC complexes (Pd-65), with the generation of a silver NHC complex 66 <i>in situ</i>	38
Scheme 31. Structure of racemic complex Pd-65a	39
Scheme 32. Structure of racemic complex Pd-65b	40
Scheme 33. Structure of racemic complex Pd-65c	40
Scheme 34. Structure of diastereomeric complex Pd-68a	41
Scheme 35. Optical resolution for separation of racemic Pd-65a into their respective enantiomers (<i>Rc</i> or <i>Sc</i>) using sodium-(<i>Sc</i>)-phenylalanate.	42
Scheme 36. Structure of diastereomeric complex Pd-69b	43
Scheme 37. Optical resolution for separation of racemic Pd-65b into their respective enantiomers (<i>Rc</i> or <i>Sc</i>) using sodium-(<i>Sc</i>)-prolinate.	44
Scheme 38. Two-steps transmetalation of the imidazolium salts (or NHC precursors) (64) into racemic platinum NHC complexes (Pt-65), with the generation of a silver NHC complex 66 <i>in situ</i>	46
Scheme 39. Structure of racemic complex Pt-65a	47
Scheme 40. Structure of racemic complex Pt-65b	50
Scheme 41. Structure of racemic Pt NHC complexes Pt-65c , 70 and 71	51
Scheme 42. One-pot synthesis method for the transmetalation of the imidazolium salts (NHC precursors) (64) into racemic nickel NHC complexes (Ni-65).	52
Scheme 43. Overall schematic representation for synthesis and characterisation of Ni NHC complexes in this study.	53
Scheme 44. Structure of racemic complex Ni-65a	54
Scheme 45. Structure of unexpected crystal, nickel complex 72 , obtained from recrystallization of racemic complex Ni-65a	55

Scheme 46. Structure of racemic complex Ni-65b	58
Scheme 47. Structure of racemic complex Ni-65c	59
Scheme 48. Structure of unexpected crystal, nickel complex 73 , obtained from recrystallization of racemic complex Ni-65c	59
Scheme 49. General pathway for enzymatic optical resolution of chiral alcohol complex...	112

CHAPTER 1 INTRODUCTION AND LITERATURE REVIEW

1.1. Transition metals as metallodrugs

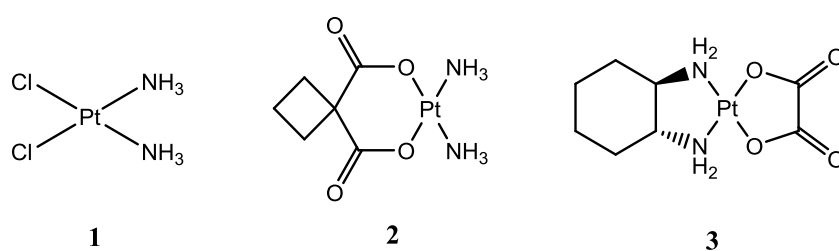
Metals have an esteemed place in medicinal chemistry. The application of metals in therapy and diagnostic of disease in modern medicine is still considered a rather young discipline, though the historically proven utilisation of metals in pharmaceutical potions can be dated back to the ancient civilisations of Mesopotamia, Egypt, India and China.

Transition metals are made up of the *d* block elements, which include group 3 to group 12 elements. The transition metals have an incomplete *d* subshell. They display variable oxidation numbers and electronic configurations, which in turn modulate the variable redox system in the biological system. Some key characteristics of the transition elements are the formation of coloured compounds because of *d–d* electronic transitions and the formation of paramagnetic compounds due to the presence of the unpaired *d* electron. Besides that, transition metals exhibit different oxidation states, which is largely due to the rather low energy gap between different possible oxidation states, and they can interact with various ligands including neutral and negatively charged molecules. These properties of transition metals have laid the foundation for coordination complexes. In general, metal complexes or coordination complex is referring to a structure comprising of a central metal atom bonded to a surrounding array of molecules and anions. Throughout human history, transition metal complexes were known to have a wide range of biological activities including anticancer, antimicrobial, antiparasitic, antiviral, antiinflammation, antidiabetic, antimanic and others (Mjos and Orvig, 2014). In fact, one of the first metallodrugs utilised in therapy were arsenic-based antimicrobial and antiparasitic agents. Another metal that has been extensively used in the treatment of wounds and management of infection is silver. And of course, the star for chemotherapeutic treatment of cancers belongs to platinum, with the accidental discovery of cisplatin's antitumour property back in 1965 (Rosenberg et al., 1965).

1.2. Emergence of Bioorganometallic Drugs

Cisplatin is considered as a classic example of metal-based drugs and the discovery of its antitumour properties have been a major breakthrough in the field of medicine. The clinical success of cisplatin or cis-diamminedichloroplatinum(II) **1**, and its second-generation analogues including carboplatin **2** and oxaliplatin **3**, in the treatment of cancer has had an

enormous impact on the discovery of novel metallopharmaceutical agents (Kelland, 2007, Rixe et al., 1996, Rosenberg et al., 1965, Wang and Lippard, 2005, Wheate et al., 2010) (**Scheme 1**). Nevertheless, platinum-based drugs have several substantial drawbacks (Florea and Busselberg, 2011, Fuertes et al., 2003, Giaccone, 2000, McKeage, 1995). For instance, cisplatin is limited to intravenous administration due to its poor aqueous solubility (1 mg/mL), and the severe side effects including nephrotoxicity, neurotoxicity, ototoxicity, nausea and vomiting have limited the applicable dose for patient. Furthermore, its effectiveness against relatively narrow range of tumour types as well as drug resistance phenomena have lowered the applicability and efficacy of these agents.



Scheme 1. Chemical structures of cisplatin (**1**), carboplatin (**2**) and oxaliplatin (**3**).

In order to circumvent the limitations of current metallodrugs, the scientific community have explored the field of bioorganometallic chemistry to look for novel therapeutic alternatives. It is defined as the study of biomolecules or biological active molecules that contain at least one carbon atom bound to a metal (Hartinger and Dyson, 2009). Organometallic complexes are designed primarily for industrial catalysis (Budagumpi and Endud, 2013, Köhl, 2009, Nolan, 2011). This is largely due to concerns over sensitivity of these complexes towards water and oxygen as well as metal toxicity. Nonetheless, years of research have put forth numerous organometallic complexes which are stable in water and air. Many of these have shown certain degree of toxicity towards certain organisms, a property that is desirable for therapeutic applications. Today, organometallic complexes are a growing interest as pharmaceuticals for the use of diagnostic agents or as chemotherapeutic drugs. This mainly resulted from their wide spectrum of coordination numbers, geometries, reactivities, as well as tunable physicochemical characteristics such as polarity, charge and lipophilicity (Albada and Metzler-Nolte, 2016, Che and Siu, 2010, Gasser and Metzler-Nolte, 2012, Gasser et al., 2011, Ong et al., 2019, Ott and Gust, 2007, Patra and Gasser, 2012, Patra and Gasser, 2017, Ronconi and Sadler, 2007). With its high flexibility, it is suggested that organometallics might offer different mechanisms of drug action compared to conventional organic agents.

Current strategy in the development of organometallic drugs has increasingly focused on the use of transition metal complexes containing organic ligands (Albada and Metzler-Nolte, 2016, Hindi et al., 2009b, Patra and Gasser, 2017, Saleem et al., 2013, Storr et al., 2006, Strohhfeldt and Tacke, 2008). The effectiveness of metallodrugs is highly associated with the choice of ligands. Ligands are most often, but not limited to, organic compounds that bind metal ions, hence modifying the physical and chemical properties of the compounds. Ligands are important for modifying reactivity and lipophilicity, stabilising special oxidation states and contributing to substitution inertness (Storr et al., 2006, Thompson and Orvig, 2006). Most importantly, with its capability to modify the oral/systemic bioavailability of metal ions, ligands can play an integral role in muting the potential toxicity of a metallodrug to have a positive impact for diagnosis and therapy. Organometallic drugs with *N*-heterocyclic carbene (NHC) ligands (4) have, in particular, come into the spotlight over the past decade.

1.3. *N*-heterocyclic carbenes (NHC)

Carbenes are an interesting class of carbon-containing compound. They are defined as neutral compounds containing a divalent carbon atom with two unpaired non-bonding electrons i.e. six-electrons valence shell. However, free carbenes are inherently unstable due to the incomplete electron octet configuration and coordinative unsaturation. Therefore, they are conventionally considered only as highly reactive transient intermediates in organic transformations. Despite the first carbene was reported as early as 1835, the isolation and characterization of a free, uncoordinated carbene remain elusive until the pioneering studies by Bertrand's and Arduengo's group in the late 1980s and early 1990s, where they first successfully isolated and characterized carbenes (Igau et al., 1988, Arduengo et al., 1991, Hopkinson et al., 2014).

With the insightful studies traced back to the early work by Ofele and Wanzlick in 1968 on metal carbene complexes, and to the breakthrough of isolation of the first stable free carbene incorporated into a nitrogen heterocycle by Arduengo's group in 1991, research pertaining *N*-heterocyclic carbenes (NHCs) had experienced an explosion of knowledge with vast libraries of novel NHCs being synthesized and studied (Arduengo et al., 1991, Wanzlick and Schönherr, 1968, Öfele, 1968). *N*-heterocyclic carbenes (NHCs) is an interesting class of ligand similar to phosphine ligand. They are generally derived from persistent carbenes which are stable compounds of divalent carbons. In simpler terms, NHCs are defined as heterocyclic species containing a carbene carbon and at least one nitrogen atom within the ring structures (Bourissou

et al., 2000, de Frémont et al., 2009) (**Figure 1**). The carbene carbon in NHC has zero formal charge as the carbene carbon is incorporated in a nitrogen-containing heterocycle in which its empty p -orbital acts as the acceptor for the π lone pairs of the adjacent nitrogen atoms. In essence, the overall stability of NHC species is contributed by the σ -withdrawing and π -donating effects of the nitrogen heteroatoms, which create a push-and-pull mechanism to stabilise the singlet carbene structures (**Figure 1**) (Hopkinson et al., 2014). Today, as an excellent ligand to the transition metals, NHCs have found multiple applications in various field, particularly highlighted in biology, catalysis and supramolecular chemistry (Budagumpi and Endud, 2013, Budagumpi et al., 2012, Dragutan et al., 2005, Frey et al., 2016, Gautier and Cisnetti, 2012, Hahn et al., 2008, Haque et al., 2015, Hashmi, 2010, He et al., 2012, Henwood et al., 2015, Hindi et al., 2009b, Hu et al., 2009, Kantchev et al., 2007, Kascatan-Nebioglu et al., 2007, Liu and Gust, 2013, Oehninger et al., 2013, Patil et al., 2015, Rit et al., 2011, Samantaray et al., 2011, Zhang and Zi, 2015).

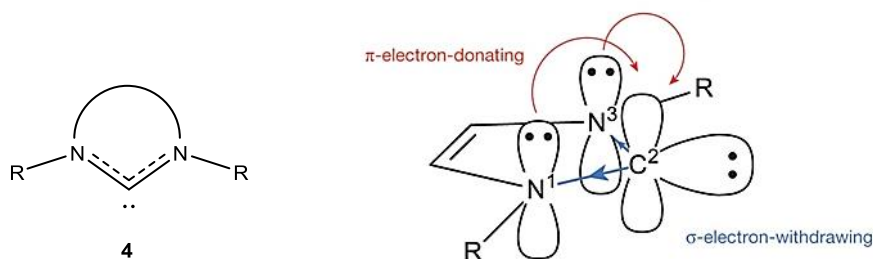


Figure 1. General representation of a *N*-heterocyclic carbene (NHC) (4) and stabilisation of the singlet carbene structure by the σ -withdrawing and π -donating effects of the nitrogen heteroatoms in a ground-state electronic structure of imidazole-2-ylidenes (Hopkinson et al., 2014).

1.3.1. Synthesis of *N*-heterocyclic carbenes (NHC)

A great variety of NHCs bearing different scaffolds have been synthesized since decades ago and reacted with transition elements leading to well-defined complexes. The rise of popularity of NHC ligand could be attributed to the ease of modification of their electronic and steric properties like phosphine ligand, but with much lower sensitivity towards both air and moisture. As such, the synthesis pathway of NHC ligands are generally more hassle free as they can be synthesized under ambient conditions.

Slight changes to the NHC architecture will lead to a dramatic change on the electronic donor properties of the carbene moieties and impose geometric constraints on the *N* substituents,

influencing their steric impact. In other words, these substituents at the *N* wingtip of NHC ring allow modulation of the steric pressure on both the carbene moieties and the coordinated metals. Nonetheless, the five-membered ring moieties, such as imidazolylienes **6** and imidazolidinylienes **5** (**Figure 2**), are extensively utilised to synthesize NHC complexes, while the other frameworks are seldom employed. Generally, differently substituted imidazolylienes **9** can be obtained either by deprotonation of imidazolium salts **8** or by reductive desulfurization of imidazoline-2-thiones **10** as illustrated in **Scheme 2**. In this study, three imidazolium salts with different *N* substituents (NHC precursors), were synthesized based on imidazolylienes.

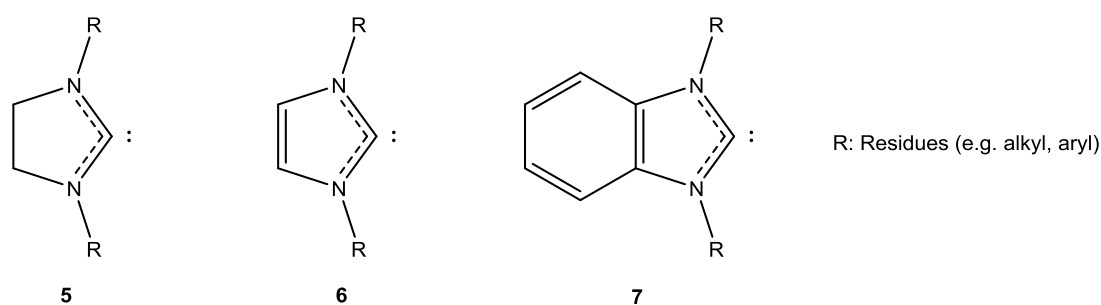
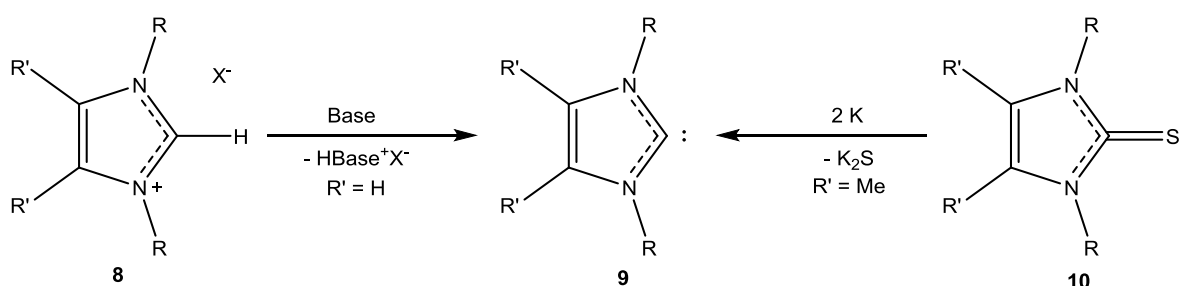


Figure 2. Five-membered ring scaffolds of NHCs commonly found in literature: imidazolidinyliene (5), imidazolyliene (6), and benzimidazolyliene (7).

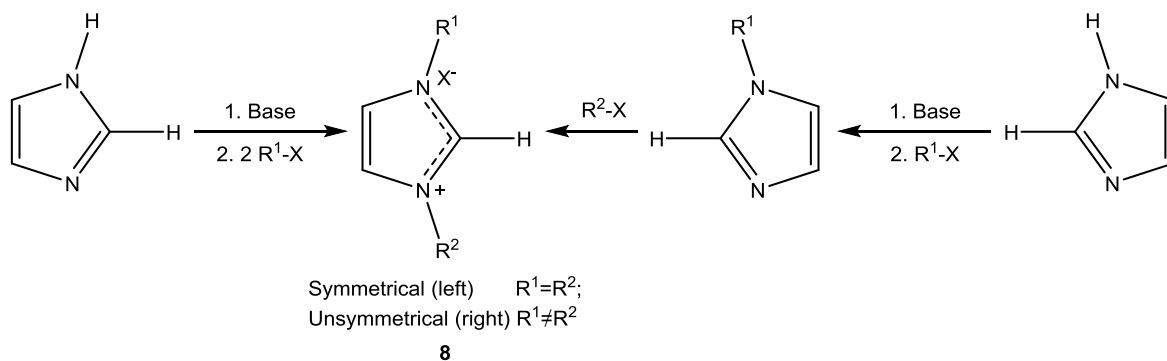


Scheme 2. General representation of synthesis route for imidazolylienes 9.

There are multiple routes of synthesis available for synthesizing imidazolium precursors in literature (de Frémont et al., 2009, Hahn and Jahnke, 2008). In general, the preparation of imidazolium salts **8** can be achieved via two distinct pathways: either by nucleophilic substitution at the nitrogen atoms of the imidazole, or by multicomponent reactions for the synthesis of the *N,N'*-substituted heterocycle.

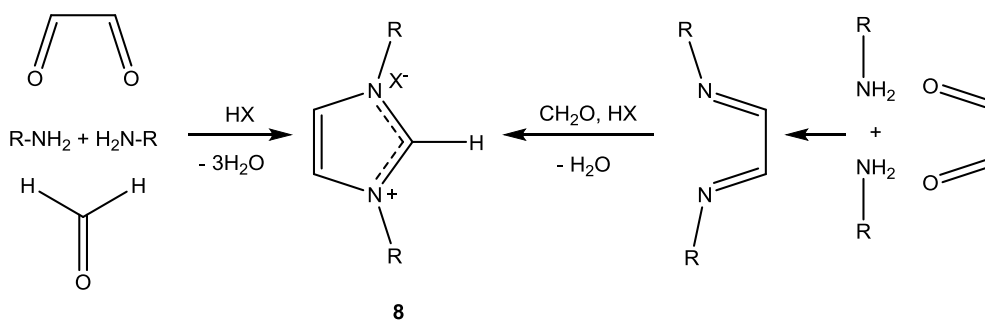
The direct substitution of the nitrogen atoms of imidazole can be applied for introduction of both symmetrical and unsymmetrical *N* substituents by varying the alkyl halides used in the

alkylation step (**Scheme 3**) (Cetinkaya et al., 2003, Chan et al., 1977, Ekkehardt Hahn et al., 2006, Fournari, 1968, Hahn et al., 2004, Herrmann et al., 1997, Herrmann et al., 1996b, Kiyomori et al., 1999, Özdemir et al., 2007). It is started with the deprotonation of the nitrogen atom of the heterocycle. The resulting salts reacts with various alkyl halides under alkylation of the N^l position. Addition of a second equivalent of an alkyl halide drives the continuation of second alkylation to give the N,N' -dialkylimidazolium salt **8**. Generally, this route of synthesis for symmetrical N,N' -substituted imidazolium salts is mainly limited for incorporation of primary alkyl substituents, though introduction of aryl group have been reported. As opposed to the preparation of symmetrical N,N' -substituted imidazolium salts which can be achieved in a one pot synthesis in the presence of a base, the incorporation of different N substituents into the imidazole moieties is required to be done in a stepwise manner to give unsymmetrical N,N' -substituted imidazolium salts.



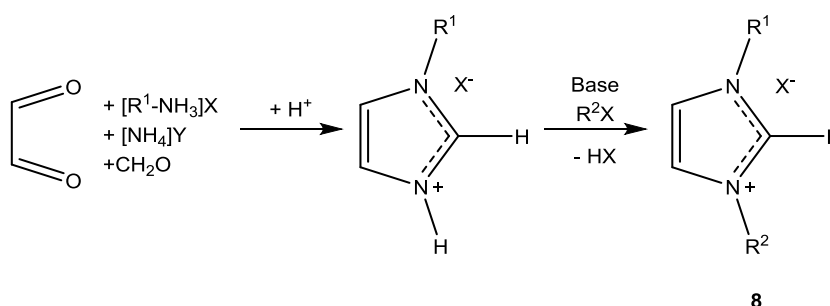
Scheme 3. General synthesis route of symmetrical (left) and unsymmetrical (right) N,N' -substituted imidazolium salts **8.**

On the other hand, the multicomponent reactions for the synthesis of the N,N' -substituted heterocycle is one of the most straightforward way of preparation. It is a simple one-pot synthesis method involving primary amines, glyoxal and formaldehyde in the presence of an acid as shown in **Scheme 4** (Arduengo et al., 1999, Herrmann et al., 1996b, Hintermann, 2007, Jafarpour et al., 2000, Kiyomori et al., 1999, Bildstein et al., 1999, Huang and Nolan, 1999). The reaction proceeds through a coupling reaction between the amine and the glyoxal under acidic condition, which give rise to the corresponding diimine, and subsequent reaction with formaldehyde forms the symmetrically N,N' -substituted imidazolium salts **8**. This synthesis pathway is rather flexible as the initial condensation product (diimine) is isolatable before the cyclization with formaldehyde, thereby enables the preparation of imidazolium salts with unusual or extremely sterically demanding nitrogen substituents.



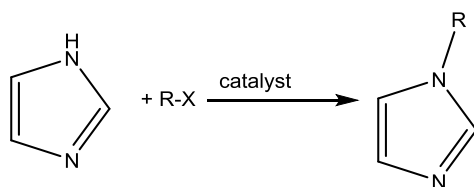
Scheme 4. Multicomponent reaction pathway for synthesis of symmetrical N,N' -substituted imidazolium salts.

For synthesis of unsymmetrical N,N' -substituted imidazolium salts, a multicomponent reaction is combined with an N -alkylation reaction as illustrated in **Scheme 5** (Gridnev and Mihaltseva, 1994, Herrmann et al., 1996a, Herrmann et al., 1996b). An N -alkylimidazolium salt is first obtained upon an initial multicomponent cyclization in acidic condition. The subsequent alkylation at the second nitrogen atom in the heterocyclic ring gives the unsymmetrical N,N' -substituted imidazolium salts.



Scheme 5. Combination of multicomponent cyclization and N -alkylation for synthesis of unsymmetrical N,N' -substituted imidazolium salts 8.

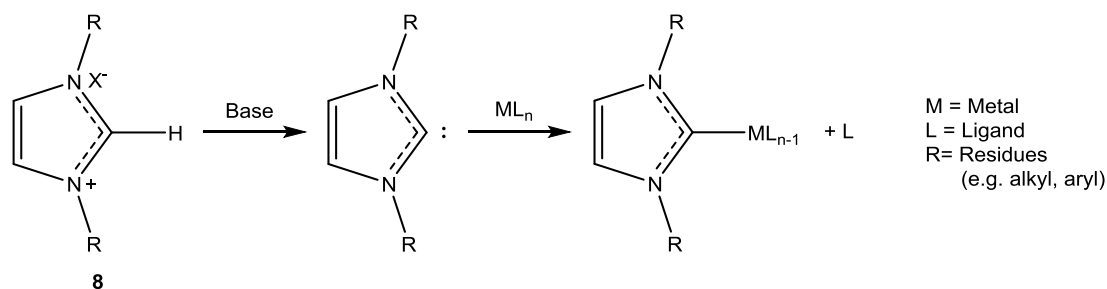
In addition, a catalytic synthesis pathway had been reported for the synthesis of imidazole with different R groups at the N wingtip, which will thereafter be used to synthesize the imidazolium salts. It involves a simple and direct reaction between the readily available imidazole with alkyl halides or aryl halides in the presence of a catalyst, such as copper complexes (Altman and Buchwald, 2006, Suresh and Pitchumani, 2008, Xue et al., 2008). This route of synthesis has provided a great versatility to synthesize various symmetrical and unsymmetrical imidazolylidenes as different functionalities can be straightforwardly introduced into NHCs.



Scheme 6. Catalytic *N*-alkylation or *N*-arylation of imidazole with alkyl halides or aryl halides, respectively.

1.3.2. Complexation of *N*-heterocyclic carbenes (NHC) to metals

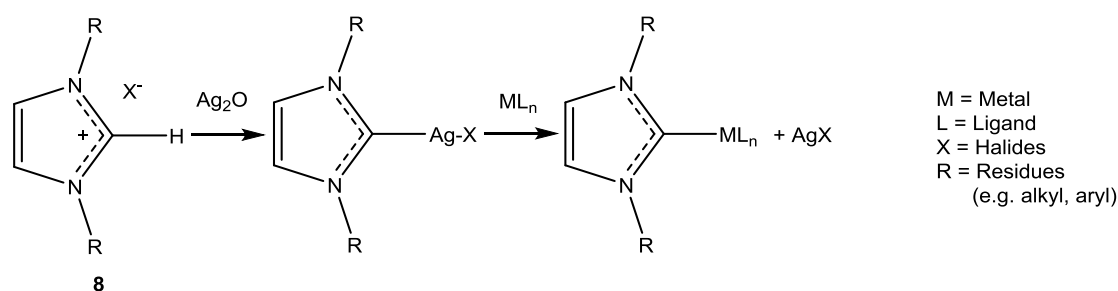
Because of the usefulness of the metal NHC complexes in a wide array of applications, many synthetic pathways have been developed. Most of the metal complexes bearing the NHC ligands are prepared by ligand substitution in the metal centre. Therefore, in such cases, the carbene to be incorporated must be accessible as a stable species, or at least, as a reactive intermediate. This explains the dominance of the stable NHC with five-membered heterocycles in the organometallic NHC coordination chemistry. A general representation for preparation of metal NHC complexes was depicted in **Scheme 7**.



Scheme 7. General illustration of synthesis route of metal NHC complexes.

Common methods for complexation of metals to NHC ligands can be categorized into five different types including (1) reaction of free *N*-heterocyclic carbenes with appropriate metal complexes, (2) reaction of electron-rich olefin dimers with coordinatively unsaturated electrophilic metal complexes, (3) in situ deprotonation of imidazolium salts in the presence of basic metal salts, (4) reaction of imidazolium salts with metal precursors under basic phase catalysis condition, and lastly, (5) a transmetalation method with silver NHC complexes (Herrmann et al., 1996b, Wanzlick and Schönherr, 1968, Lappert, 1988, Wang and Lin, 1998, Lee et al., 1997, Bourissou et al., 2000).

In this study, the metal complexes with NHC ligands was prepared via transmetalation through the corresponding Ag(I) NHC complexes which act as a transfer agent. This method is very well established and very attractive as compared to other procedures, which often required inert or harsher conditions (Rieb et al., 2017). In this method, silver(I) oxide acts as a mild base as well as a metalation agent that deprotonates the imidazolium salts, leading to *in situ* formation of a corresponding Ag(I) NHC complex (**Scheme 8**). The Ag₂O method possesses a number of advantages. These Ag(I) NHC complexes are isolatable sources of NHC ligands. They can be prepared in air at ambient temperature, and no specially purified solvents or any additional base is required. Besides, deprotonation of the imidazolium salts usually occurs at the C² position and other acidic protons in the imidazolium salts are non-reactive in general. Most importantly, this simplicity of the Ag–carbene bond formation attracts interest because of the great affinity of the electron exchange taking place between carbene C and Ag centre. The NHC species are good electronic donors whereby Ag acts as an excellent acceptor of electron density. The overall electronic exchange is the best example of a σ donation from carbene C to the Ag centre and a π back-donation from Ag to carbene C (Aher et al., 2017). In the presence of any organometallic fragment bearing a metal more electronegative than silver, the Ag–carbene bond is broken and the carbene will be transferred to the new metal as the reaction is thermodynamically favoured by the precipitation of solid silver(I) halide. Following this route of synthesis, a number of metal NHC complexes have been synthesized in excellent yields including iridium, ruthenium, rhodium, mercury, copper, silver, gold, nickel, platinum and palladium as previously described in a literature review (Lin and Vasam, 2007).



Scheme 8. General representation for synthesis of metal NHC complexes using the silver(I) oxide-mediated transmetalation method.

1.3.3. Characteristic features of biologically studied metal NHC complexes

Metal NHC complexes are renowned for their widespread application in catalysis since decades ago. The search of novel metallodrugs based on biologically active metal NHC complexes had

gained tremendous interest in recent years because they fit the prerequisites for drug design and fast optimisation (Arduengo et al., 1991). First, NHCs are readily accessible in a few steps as most of the precursors are commercially available (Arduengo et al., 1999, Enders and Gielen, 2001, Herrmann et al., 1996c). Also, their versatility allows them to be manipulated easily for fine-tuning of both the physiochemical properties and reactivity in biological medium of the final metal NHC complexes (Hillier et al., 2003, Huang et al., 1999, Voutchkova et al., 2005). Most importantly, the non-toxic nature of NHC ligands reduces the possibility of these complexes in producing additional toxic metabolites in the biological systems upon dissociation (Che and Sun, 2011, Yan et al., 2010). In general, NHC ligands are more electron donating and sterically demanding compared to phosphine ligands (Crabtree, 2005, Crudden and Allen, 2004, Scott et al., 2005). This results in formation of stronger metal-ligand bonds, thereby a more stable metal NHC complex. This is crucial because high stability of these metal NHC complexes prevent them from dissociating before reaching their target (Albert et al., 2014a, Reedijk, 2008). Besides, NHCs are capable of binding with both hard and soft metals and are readily functionalised, which is a desirable trait for designing targeted pharmaceuticals (Godoy et al., 2011, Lemke et al., 2009, Marion et al., 2007, Zhou et al., 2008). Lastly, the better solubility and/or the ability of their NH moiety to establish hydrogen bonds with a target biomolecule have given metal-NHC complexes a highly favourable characteristic for drug delivery system (Albert et al., 2014b, Ramos-Lima et al., 2010). Altogether, with the versatility provided by numerous possibilities of NHC scaffolds and metals, metal NHC complexes are inevitably becoming a paradigm for the search of new therapeutics.

1.4. Group 10 metal NHC complexes with therapeutic potential

To date, there is a rich diversity of metal NHC complexes with various ligands and oxidation states, spanning most metals from Group 4 to Group 12 (Hahn and Jahnke, 2008). Among all, their biological potential is one of the most active actively research areas in bioorganometallic chemistry. There are over multiple hundreds of transition metal NHC complexes being reported as potential antimicrobials and anti-tumour drugs over the past five years (Liu and Gust, 2016). Their therapeutic potential is further highlighted by a number of patents held by several universities and pharmaceutical companies (Che et al., 2011, Hindi et al., 2009a, Hindi et al., 2008, Mailliet et al., 2009, Youngs et al., 2004, Youngs et al., 2005). In this study, we are

interested in exploring the potential of Group 10 metal NHC complexes as anticancer and antimicrobial agents, including nickel (Ni), palladium (Pd) and platinum (Pt).

Notably, numerous Group 10 metal NHC complexes have been previously reported for their anticancer activities, whereas only a handful of Group 10 metal NHC complexes were reported to exhibit antimicrobial activities. Recent studies have depicted the general mode of action of Group 10 metal NHC complexes as these metal centres appear promising in altering cell migration, DNA replication and condensation or DNA fragmentation (Pages et al., 2015). Interestingly, platinum NHC complexes were recently shown to be interacting with G-quadruplex (G4) structures from telomeric sequence involved in oncogene promoters and thereby causing cell death (Betzer et al., 2016). Apart from the interference with nucleic acids, a recent review by Marloye *et al.* had provided a general insight on the mechanisms of anticancer action of Group 10 metal complexes, which includes reactive oxygen species (ROS) production associated with redox mechanisms, cell cycle arrest, endoplasmic reticulum stress-mediated apoptosis, mitochondria-associated apoptosis and binding to cytochrome, and binding to essential amino acids causing proteins dysfunctions to name a few (Marloye et al., 2016). Therefore, it is interesting to consider the development of Group 10 metal NHC complexes in biomedical applications for treatment of cancers and infectious diseases, due to the increasing mortality cases found in both of the developed and developing countries.

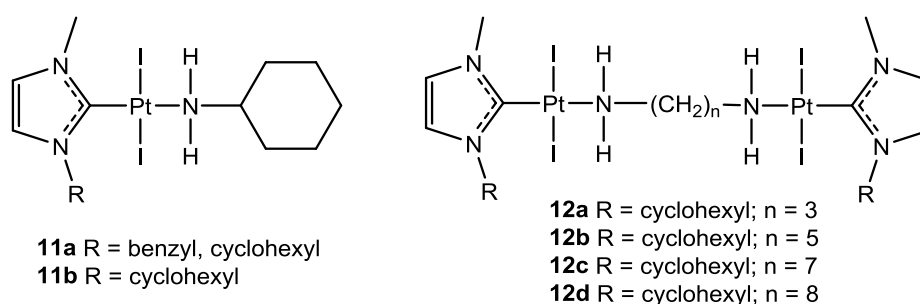
1.5. Group 10 metal NHC complexes with anticancer activities

Cancer is the global second leading cause of death, after cardiovascular diseases. According World Health Organization, cancer is responsible for an estimated 9.6 million deaths globally in 2018, with about 1 in 6 deaths is due to cancer. Undeniably, the unhealthy lifestyle of modern people including unhealthy diet, physical inactivity, tobacco and alcohol uses, is a key factor of the alarming increasing reports of cancer. Cancer is a class of diseases involving groups of cells exhibiting uncontrolled growth that grow beyond their usual boundaries (proliferation), intrusion and destruction of adjacent tissues (invasion), and spreading to other parts of body or organs via lymph or blood (metastasis) (Tandon et al., 2019). When normal cells are damaged beyond repair, they are usually eliminated by apoptosis or programmed cell death, but cancer cells managed to avoid apoptosis and continue to divide uncontrollably (Domagoj, 2008).

1.5.1. Platinum N-Heterocyclic carbene (Pt NHC) complexes

Recently, researchers have shifted the focus towards the synthesis of novel platinum-based drugs by changing the coordinated nitrogen ligand or altering the leaving groups (Edwards et al., 2005, Quirante et al., 2011). Platinum NHC complexes would be the starting point for the search of novel drugs owing to the clinical success of platinum based drugs.

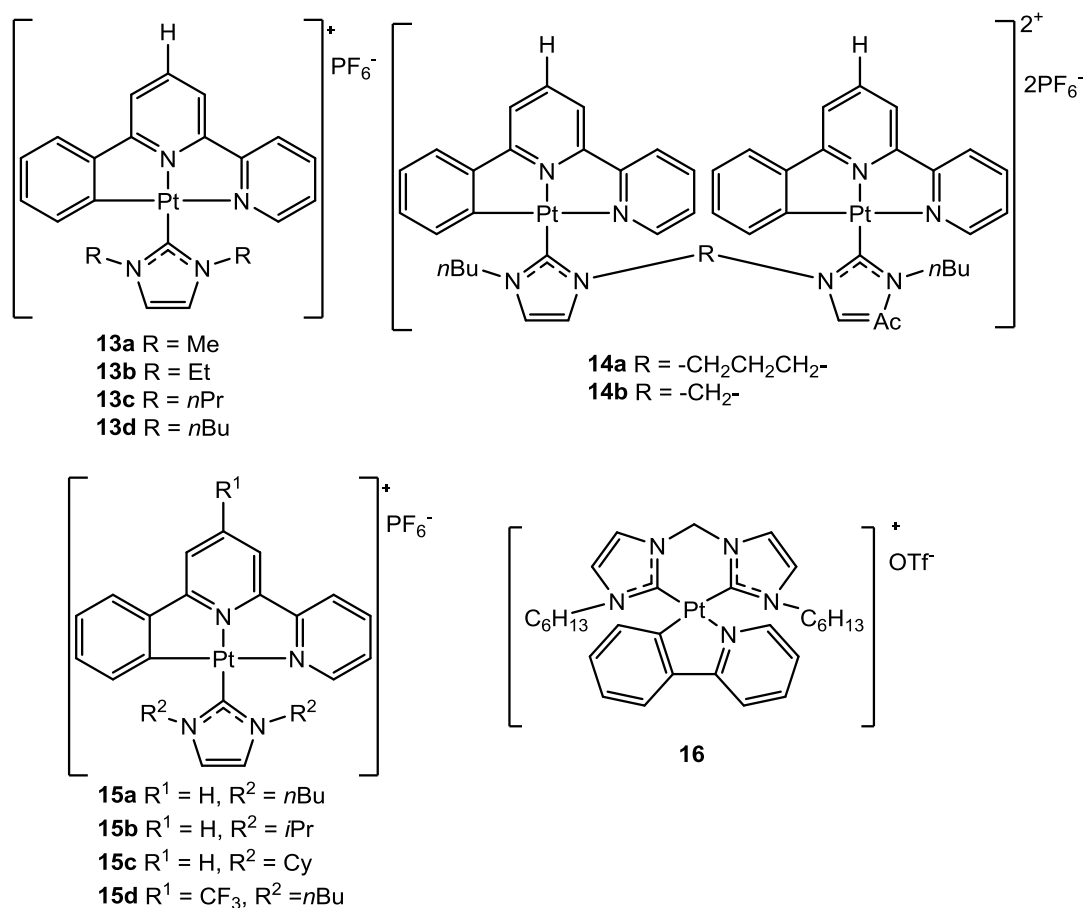
One of the most notable highlight of platinum NHC complexes is the patented monometallic *trans*-PtI₂(NHC)(amine) complexes **11** and the bimetallic *trans*-[PtI₂(NHC)]₂(diamine) complexes **12** developed by Marinetti's group (Scheme 9). They exhibited cytotoxic activities with IC₅₀ at micromolar range against both cisplatin-sensitive (CEM and H460) and cisplatin-resistant (A2780/DDP, CH1/DDP and SKOV3) cell lines (Skander et al., 2010, Mailliet et al., 2009, Chtchigrovsky et al., 2013). Based on the cytotoxicity assay, they even outperformed cisplatin and oxaliplatin, with cytotoxicity that are two- to five-fold higher than the anticancer drugs, under similar experimental condition. Investigation on their cytotoxicity pathway had revealed that these complexes **11** and **12** cause DNA fragmentation and trigger apoptosis by a pathway involving translocation of apoptosis-inducing factor and caspase 12 to the nucleus, instead of inducing cell cycle arrest like cisplatin. In addition, the bimetallic complex **12** may also induce necrosis in the A7280 cells. While the *trans*-configured complexes were previously deemed as inactive in initial anticancer research, they have now been acknowledged for their ability to form different platinum-DNA adducts, less recognized by RNA-repair machinery, and therefore to reduce cross-resistance pertaining to cisplatin (Mauro and Giovanni, 2007, Van Beusichem and Farrell, 1992, Farrell et al., 2004).



Scheme 9. Patented monometallic *trans*-PtI₂(NHC)(amine) complexes **11 and the bimetallic *trans*-[PtI₂(NHC)]₂(diamine) complexes **12** developed by Marinetti's group.**

Che's research group reported numerous luminescent cyclometalated metal NHC complexes and studied their anticancer properties. A key advantage of studying luminescent complexes is

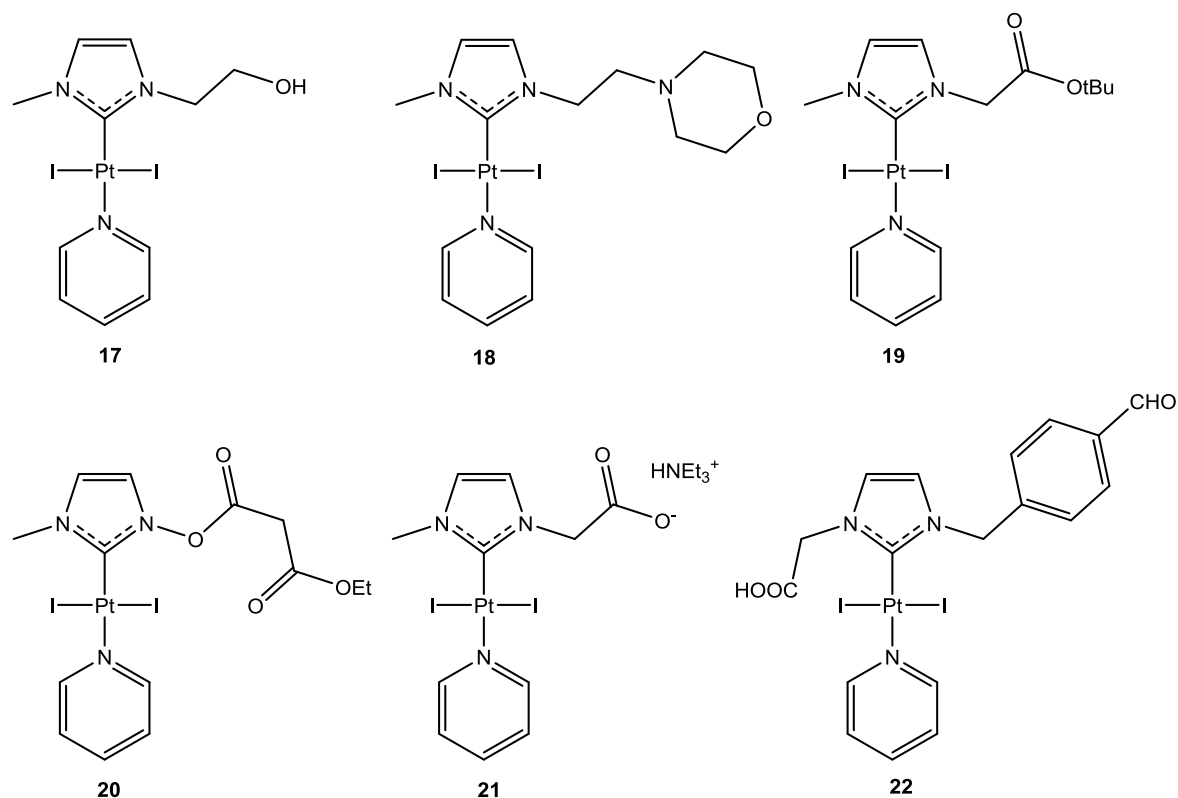
the subcellular delocalisation of the metal NHC complexes can be conveniently visualised via fluorescent microscopy after drug delivery, thereby enabling the elucidation of possible mode of anticancer action of these metal NHC complexes. They have prepared a series of luminescent cyclometalated [Pt(6-phenyl-2,2'-bipyridine)(NHC)] complexes (**13** and **14**) with variable lipophilicity (NHC *N*-substituents) and nuclearity (mono- or bis-), cyclometalated Pt NHC complexes **15** based on C-deprotonated N[^]C[^]N ligands derived from 1,3-di(pyridyl)benzene, as well as Pt NHC complex **16** which made up of 2-phenylpyridine and two NHC ligands with hexyl group, which displayed significant anticancer activities (**Scheme 10**) (Li et al., 2015, Sun et al., 2011, Zou et al., 2013). These Pt NHC complexes were about 5 to 300 folds more potent towards HeLa cells compared with cisplatin. Besides that, **13d** is relatively less toxic towards the normal human lung fibroblast cell line compared to others, thereby suggesting that it has a safety therapeutic window which conferred high specificity towards the cancer cells (Sun et al., 2011). Interestingly, **13d** was found to be displaying a synergistic anticancer effect when co-incubate with cisplatin, as shown by the reduction of IC₅₀ values by half, which means that the HeLa cancer cells can now be inhibited by only half of the concentration required previously. The results put forward that complex **13d** and cisplatin might be working at different target with different anticancer mechanisms. This is important in hope for combination therapy which can be used in the patients to treat cancers more effectively while reducing the risk of side effect caused by cisplatin toxicity. Most importantly, in vivo study with mice have shown that the complex **13d** could inhibit tumour growth significantly with no obvious weight reduction and no induction of acute toxicity. It is one of the very few amount of metal NHC complexes that were evaluated in vivo. The anticancer mechanism study had revealed that, unlike most Pt complexes which localised in the nucleus, they preferentially accumulate in the cytoplasm and mitochondria of the cells, where they act as a survivin (apoptosis inhibitor) suppressant, triggers activation of poly(ADP-ribose) polymerase (PARP), ultimately leading to apoptosis (Li et al., 2015, Sun et al., 2011, Zou et al., 2013). Since DNA is not a primary target for this series of Pt NHC complexes, it was suggested these Pt NHC scaffolds could be a new platinum based anticancer drug offering new therapeutic target different from the conventional antitumor drugs.



Scheme 10. Luminescent cyclometalated Pt NHC complexes with anticancer activities developed by Che's group.

Dahm *et al.* have synthesized and studied a series of platinum NHC complexes (**17-22**) with different *N*-substituted functionalities at NHC ligands with simplified formula of PtI₂(NHC)(pyridine) (**Scheme 11**) (Dahm *et al.*, 2015). Pt NHC complexes **17**, **18**, **19** and **20** featured alcohol, amine, ester and malonate functionalities, respectively, while **21** and **22** are representation of carboxylic functionalities at the nitrogen wingtip of the NHC ligands. Evaluation of their *in vitro* anticancer activities have shown variable anticancer efficacy depending on their *N* substituents at the NHC ligands. The neutral complexes containing esters moieties **19** and **20** were highly cytotoxic to the cells tested with IC₅₀ ranging from 0.01 μM to 1.52 μM. This was followed by complexes **17** and **18** bearing the alcohol and amine functionalities, with IC₅₀ ranging from 1.5 μM to 13.3 μM, which is comparable to that of cisplatin. Lastly, even though complexes **21** and **22** is highly soluble in water, their displayed low to nil cytotoxicity against the panel of cells tested. It is suggested that the low cytotoxicity is caused by the low aptitude of negatively charged organometallics to cross the cell membrane

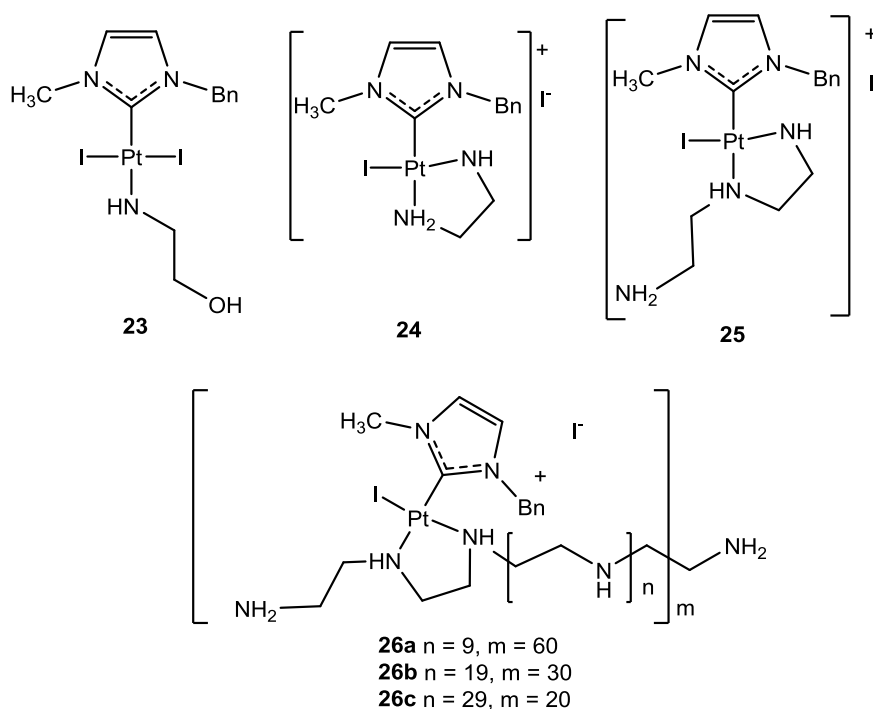
and enter the cells to exert their effects (Dahm et al., 2015, Hartinger et al., 2008, Gasser and Metzler-Nolte, 2012). Nevertheless, this study had provided evidence on the differential anticancer efficacies given rise from the different *N* substituents, which would provide a more versatile and diverse platform for the chemist to explore different functionalized NHC to search for new therapeutic alternatives.



Scheme 11. Platinum NHC complexes (17-22) with different *N*-substituted functionalities at NHC ligands with simplified formula of PtI₂(NHC)(pyridine).

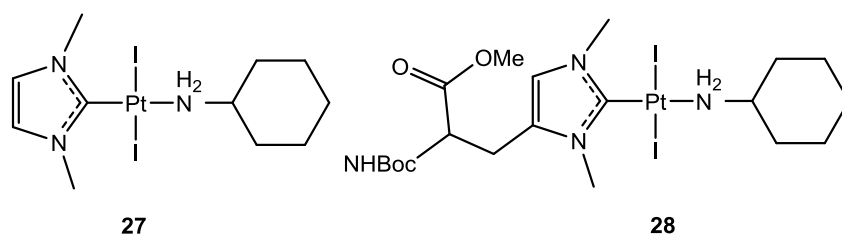
Limited solubility of Pt NHC complexes in aqueous medium has always been a challenge for application of Pt NHC complexes as anticancer agents. In order to circumvent this limitation, Chekkat *et al.* have synthesized a series of Pt NHC complexes and coordinated them along a polyethylenimine (PEI) chain to increase their aqueous solubility (**Scheme 12**) (Chekkat et al., 2016). Three monomeric Pt NHC complexes **23-25** was synthesized from *trans* [(NHC)PtX₂(pyridine)] (NHC = 3-benzyl-1-imidazolilydene) and the nitrogen-containing ligand (aminoethanol, ethylenediamine or diethylene triamine, respectively). Meanwhile, multivalent Pt NHC complex **26a-c** were prepared by using linear PEI as ligand and varying the complex/polymer ratio to obtain Pt NHC-PEI conjugates that contain one Pt complex per 10, 20, or 30 ethylenediamine units (corresponded to 60, 30 and 20 platinum atoms per PEI

chain). The monomeric Pt NHC complex **23** was more potent compared to cisplatin and was comparable to oxaliplatin with IC₅₀ ranging from 28 to 38 μM. Meanwhile the cationic Pt NHC complexes **24** and **25** are determined to be inactive with IC₅₀ more than 100 μM. Nevertheless, after conjugation with PEI (**26a-c**), their cytotoxicities increase tremendously despite their high molecular weight. Interestingly, their cytotoxicity was inversely correlated with the Pt/PEI unit ratio, where the lower Pt/PEI ratio led to higher potency. The linear PEI was thought to be playing an important role in preserving the activity of Pt NHC complexes by shielding the metal from undesirable side reaction with irrelevant molecules, while endowing the inherent properties of PEI (such as interaction of lipid bilayer, buffering capacity over a broad pH range, endosomal release) giving rise to the improved cytotoxicity (Chekkat et al., 2016). Additional studies have indicated that complex **26c** was able to induce higher level of apoptosis in HCT116 cells *in vitro* and in xenograft mouse model, as compared to oxaliplatin at the same concentration, with no side effects observed. In addition, mechanistic studies using Pt NHC complex **26c** have suggested a concurrent cell death mechanism involving mitochondria, such as oxidative stress and apoptosis, along with the classical Pt based mechanisms which involved DNA adduct formation. This may be offering a new line of Pt NHC complexes which offer different mechanism than conventional anticancer drug with better aqueous solubility, which is a highly desirable trait.



Scheme 12. Pt NHC complexes and subsequent coordination complex with polyethylenimine (PEI) chain to increase their aqueous solubility.

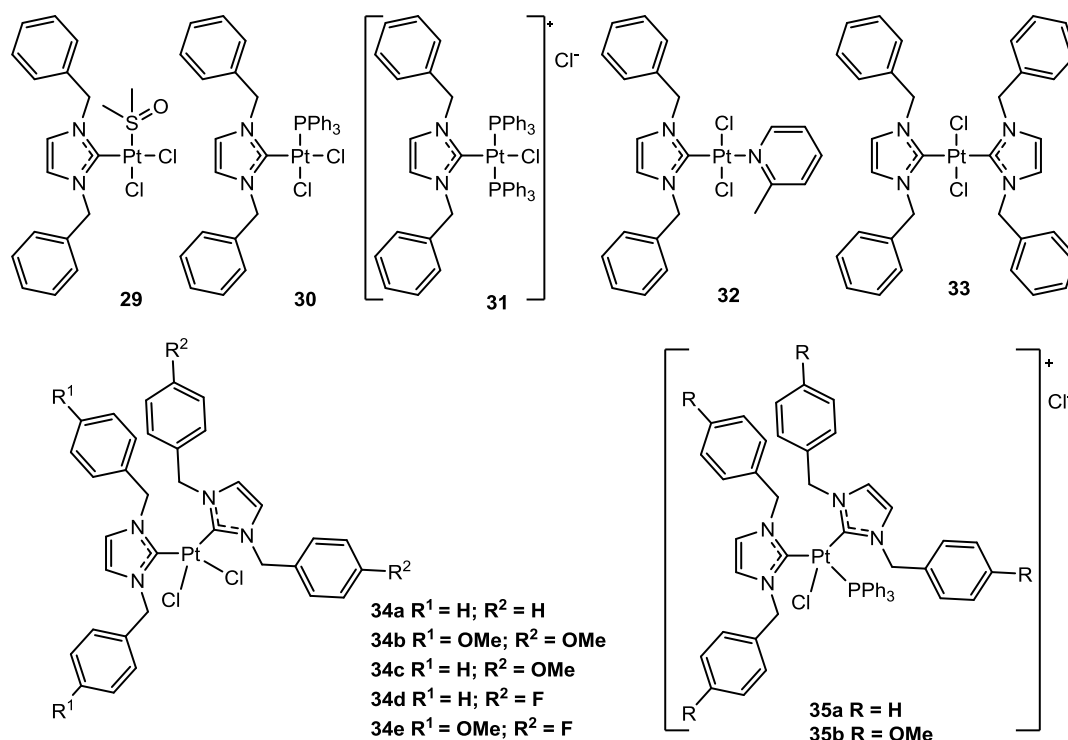
In a recent study conducted by Schmitt *et al.*, they explored an innovative way to increase the bioavailability of Pt NHC complex by adding histidine to Pt NHC complex and studying if the histidine residue is able to acts as an uptake shuttle and efficacy booster (**Scheme 13**) (Schmitt *et al.*, 2016). The 1,3-dimethylimidazol-2-ylidene based Pt NHC complex **27** and its histidine-conjugated Pt NHC complex **28** were tested for their anticancer potential against a panel of carcinoma cell lines. Both Pt NHC complexes **27** and **28** were cytotoxic at single-digit micromolar IC_{50} concentration, with complex **28** twice as potent as complex **27** on average. Notably, the histidine-derived Pt NHC complex **28** was highly effective against HT29 with IC_{50} of 1.5 μ M while **27** was inactive (IC_{50} more than 100 μ M). Apart from HT29 and KB-V1/Vbl, complex **28** was two to twenty-fold more cytotoxic than cisplatin. Mechanistic studies have revealed that complex **28** may augment their cytotoxicity via performance as the transmembrane carriers to increase the cellular accumulation, as well as via initiation of pronounced distortion and unwinding of the supercoiled DNA. Both complexes **27** and **28** caused accumulation of 518A2 melanoma cells in S-phase and G2/M phase of the cell cycle, as well as a slight reduction of cells in G1-phase. They also performed an *in vivo* study observing the effect of both **27** and **28** on the extraembryonic blood vessels in the chorioallantoic membrane (CAM) of fertilized chicken eggs, where disruption of blood vessels was observed. Animal model study had revealed that complex **28** was capable of retarding the tumour growth in xenografted mice with effect as strong as the standard drug cisplatin while being better tolerated.



Scheme 13. Pt NHC complex 27 and addition of histidine to increase the bioavailability.

Schobert's group studied a series of different *cis* and *trans* configured Pt NHC complexes and their anticancer properties including *trans* complexes **29-33** bearing a (1,3-dibenzyl)imidazole-2-ylidene ligand with different leaving groups *trans* to it, as well as *cis* complexes **34** and **35** with two different NHC ligands on the structure (**Scheme 14**) (Muenzner *et al.*, 2015, Rehm *et al.*, 2016). All these Pt NHC complexes have shown remarkable efficacies with low micromolar IC_{50} against the test cell lines, including cisplatin resistant cancer cells. Notably, the cytotoxicity of **29-31** towards cancer cells increased with the steric shielding of their leaving chloride ligand by the two spectator ligands when going from **29** (spectator ligands: chloride and DMSO) to **30**

(chloride and PPh₃) to **31** (two PPh₃), i.e. lowest IC₅₀ values were recorded for complex **31**. The increment of steric bulkiness was contributed by PPh₃ which have a Tolman cone angle of 145°. Mechanistic study showed that, instead of intercalative binding with DNA, the cationic complex **31** caused DNA aggregation, which is a damage beyond repair. It was also reported that the complex **29** and **31** caused cell cycle arrest at G2/M phase and G1 phase, respectively. Meanwhile, DNA appears to be the main target for Pt NHC complexes **34** and **35**, albeit in a more differentiated way than cisplatin. The neutral *cis*-biscarbene complex **34b** and **35b** were shown to act via DNA aggregation, but not the case for *trans*-biscarbene complex **33**, suggesting that interaction of these Pt NHC complexes is correlated to the replaceability and sterical accessibility of the leaving ligand, and the overall charge of the complex. One of the key findings of Schobert's group was the retention of intrinsic ligand bioactivity in the metal NHC complexes (Rehm et al., 2016). Following this lead, it allows high degree of liberty in designing novel anticancer metal NHC complexes with numerous combinations of NHC ligands, ancillary ligands and leaving groups that contribute their inherent activity and thereby affecting the overall pharmacological properties. Besides, these works have also shown the fundamental importance of isomerism of various ligands revolving around the metal center in metal NHC complexes, where different biological activities may be achieved by altering the configurations.

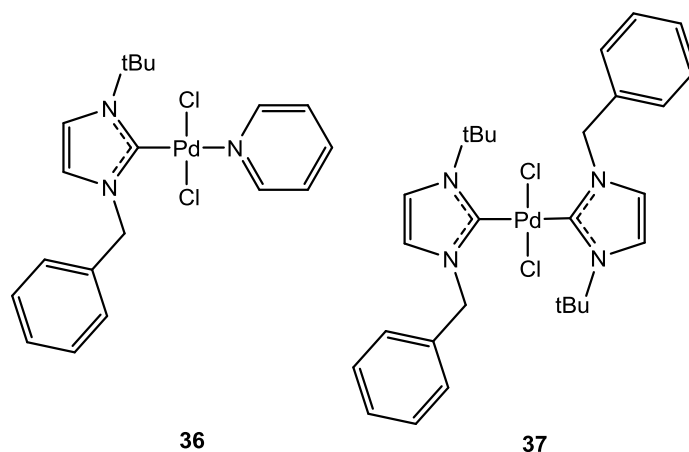


Scheme 14. Selected Pt NHC complexes with different *cis* and *trans* configurations exhibiting anticancer activities as reported by Schobert et al.

1.5.2. Palladium N-Heterocyclic carbene (Pd NHC) complexes

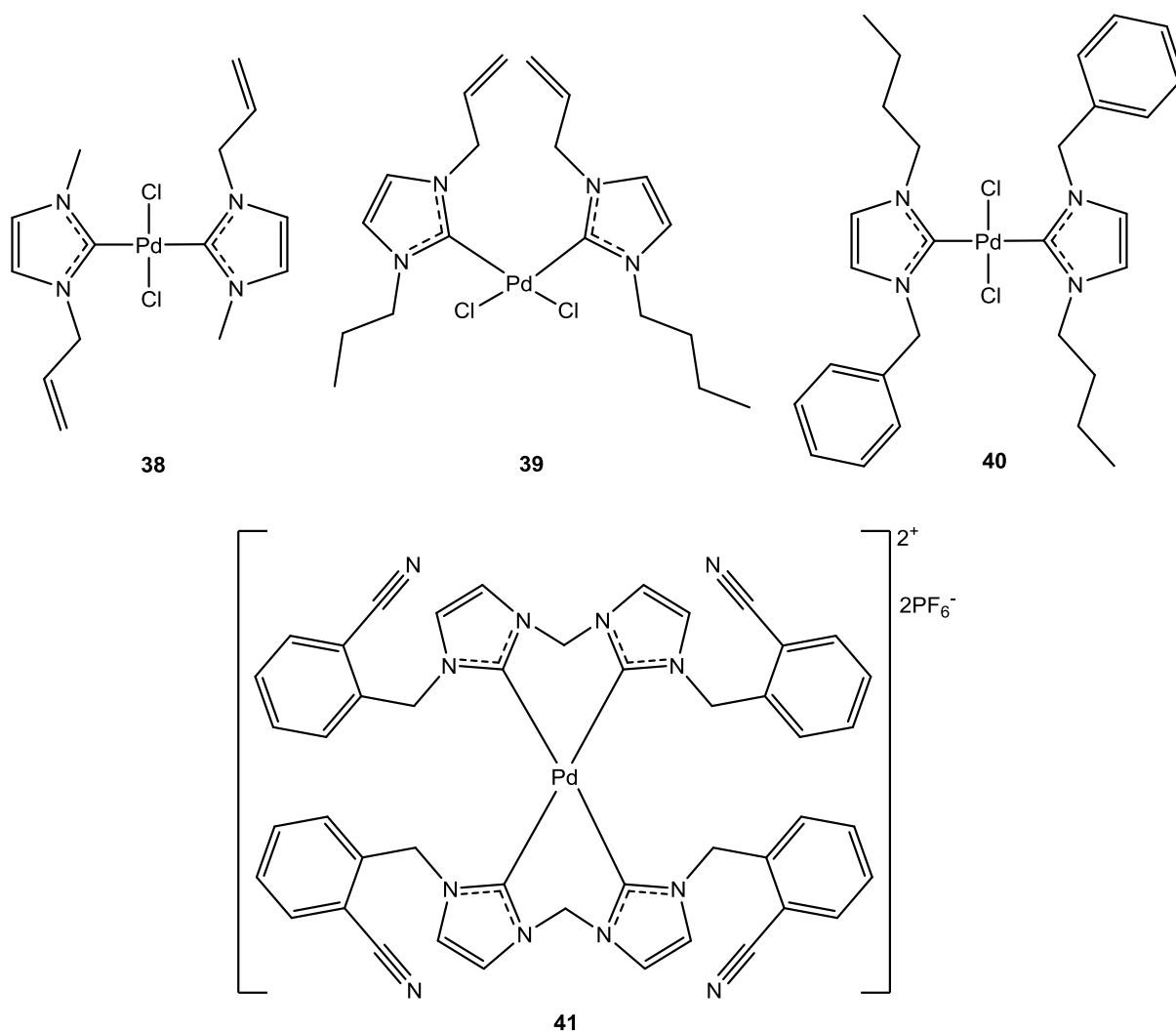
As a member of Group 10 metal, the coordination chemistry of palladium is very much similar to that of platinum, hence the adaptation of palladium for development of new chemotherapeutics to replace cisplatin is pretty straightforward. Despite the catalytic application of Pd NHC complexes is well established, the interest in palladium as therapeutic agents only started less than two decades ago. Since then, there are a number of novel mononuclear, dinuclear and multinuclear palladium NHC complexes with reduced cross-resistance to cisplatin, decreased toxicity and high specificity that have been developed (Teysot et al., 2009, Hindi et al., 2009b, Gao et al., 2009). In addition to the advantages as aforementioned, the potential of palladium complexes as anticancer agents were further supported by the findings of a hydrolytic and DNA-binding study, where the kinetically labile palladium complexes were found to be able to produce new charged species to interact with DNA, and also bind to DNA at a faster rate compared to the platinum complex, making it an attractive choice to look for replacement of platinum drugs (González et al., 1997).

A comprehensive work on synthesis, characterisation and biomedical studies of Pd NHC complexes as effective metallopharmaceutical agents was first reported by Ray *et al.* in 2007 (Ray et al., 2007). The Pd NHC complexes included one mixed complex with NHC and pyridine ligand [PdCl₂(NHC)(pyridine)] (**36**) and one bis(NHC) complex [PdCl₂(NHC)₂] (**37**) (**Scheme 15**). Both Pd NHC complexes **36** and **37** demonstrated potent cytotoxic activity against HeLa (cervical cancer), MCF7 (breast cancer) and HCT116 (colon adenocarcinoma) cell lines in micromolar range. Pd NHC complex **36** was able to moderately inhibit 35 (±3) % of HeLa cell proliferation at 10 μM after one cell cycle. On the other hand, Pd-bis(NHC) complex **37** displayed a higher cytotoxicity (2 to 20-fold) to the tested cell lines compared to cisplatin, in a concentration dependent manner, under analogous experimental condition. Higher toxicity observed in **37**, as compared to **36**, may be correlated with the higher electron density around the metal centre which is contributed by the two NHC ligands with strong electron donating abilities. Further studies revealed that Pd NHC complex **37** inhibited the HeLa cell proliferation by arresting cell cycle progression at the M-G2 transition phase and stopping the mitotic entry of the cell. Besides, authors also suggested that Pd NHC complex **37** played a part in leading the treated HCT116 cells into programmed cell death through a p53-dependent pathway.



Scheme 15. Pd-mono(NHC) complex 36 and Pd-bis(NHC) complex 37 with potent anticancer activities developed by Ray et al.

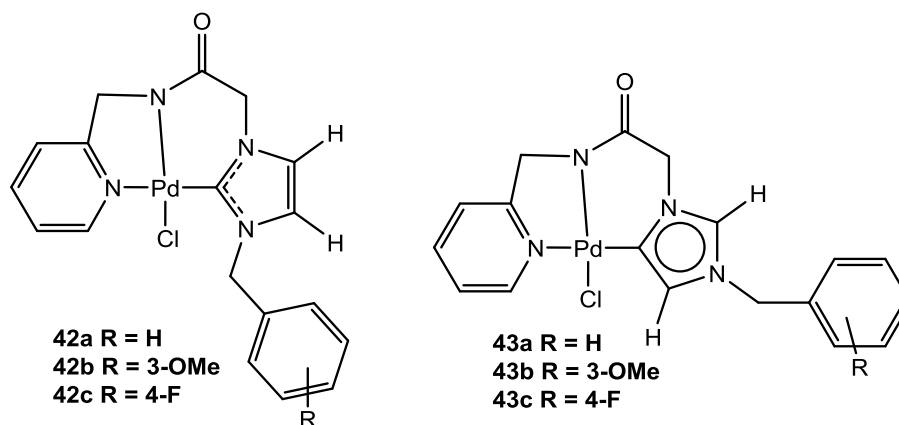
Haque and co-workers have synthesized a series of Pd NHC complexes with anticancer properties (Haque et al., 2013). These Pd NHC complexes were sterically-tuned as such that Pd NHC complexes **38** and **40** adopted a *trans-anti* arrangement of the NHC ligands, whereas Pd NHC complex **39** adopted a *cis-syn* arrangement (**Scheme 16**). These Pd NHC complexes **38-40** were evaluated for their cytotoxicity against human colorectal cancer cell line HCT116 using MTT assay. Only Pd NHC complexes **39** and **40** showed anticancer activities against HCT116 while complex **38** displayed no activity at all. Surprisingly, the *cis*-complex **39** (IC_{50} value of 26.5 μ M) showed less cytotoxicity as compared *trans*-complex **40** (IC_{50} value of 6.6 μ M). Further test has suggested that the mechanism of anticancer action could be due to an apoptotic cell death. Comparison between Pd NHC complexes **38-40** have raised the speculation that the anticancer properties of the complexes relied on the geometry around the Pd centre within the complex molecule as well as the substitutions on the ligand backbone. In a recent study by Haque *et al.*, a new Pd NHC complex **41** derived from a binuclear Ag-NHC complex was shown to exhibit significant antiproliferative activity against MCF7 cells with IC_{50} of 2.5 μ M, a value comparable with those of the standard drug used in the study, tamoxifen (IC_{50} = 2.4 μ M) (Haque et al., 2016b).



Scheme 16. A series of Pd NHC complexes with different *cis* and *trans* arrangement developed by Haque's group.

Lee *et al.* reported a series of interesting Pd NHC complexes bearing the tridentate ligands of NHC, amidate and pyridine donor moieties in either “normal” (**42**) or “abnormal” (**43**) binding modes (**Scheme 16**) (Lee et al., 2015). The Pd NHC complexes **42-43** were evaluated against a panel of human tumour cells including ovarian cancer (TOV21G), colon adenocarcinoma (SW620) and small-cell lung carcinoma (NCI-H1688) using MTT assay. Among all, Pd NHC complex **42b** displayed highest cytotoxicity against the cancer cells with high selectivity towards the TOV21G cell line (IC₅₀ value of 6.05 μM). Besides that, the cytotoxicity is highly dependent on the structure of the Pd NHC complexes. For instance, the “normal” Pd NHC complex **42b** was highly potent against TOV21G cells while its isomeric “abnormal” Pd NHC complex **43b** did not display any activity toward TOV21G cells. Besides that, replacement of

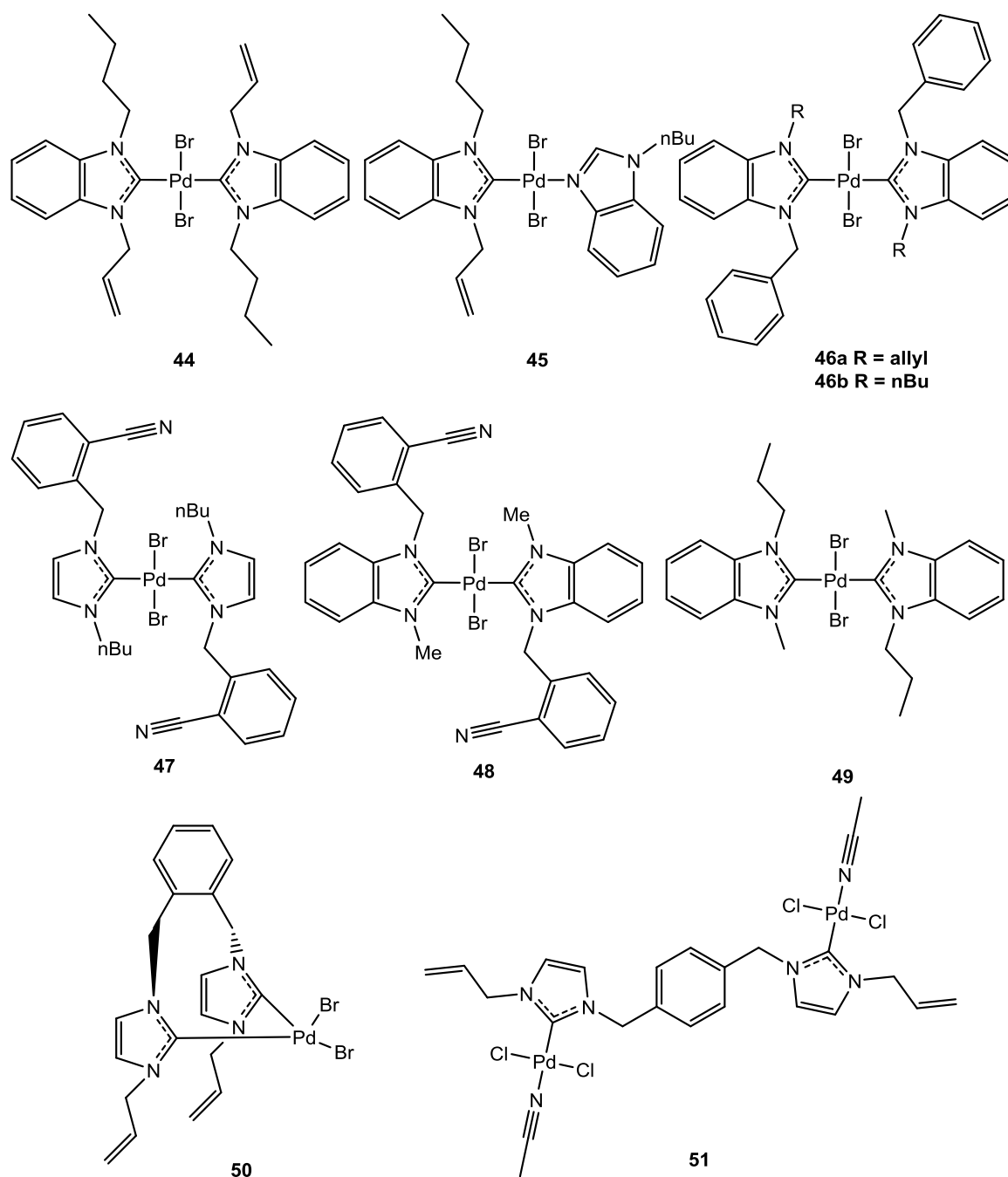
the R group into *H* (**42a**) or *N*-3-methoxy group (**42b**) led to poorer cytotoxicity as evident by increased half inhibitory concentration values (IC₅₀ value of 23.43 μM and 49.55 μM, respectively). The comparable half inhibitory concentration value of **42b** with cisplatin reflected the potential of this complex as anticancer drug candidate.



Scheme 17. Tridendate Pd NHC complexes with potent anticancer activities.

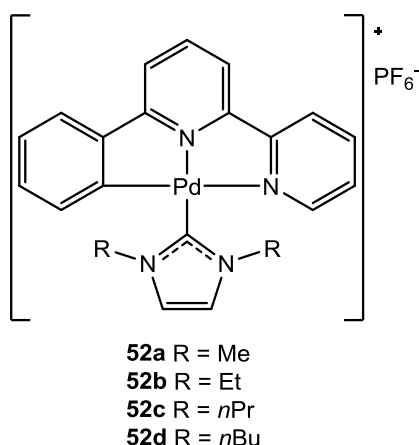
Recently, Ghdhayeb *et al.* had synthesized a panel of mono- and bis-NHC palladium complexes (**44-46**) from corresponding silver NHC complexes, and performed a preliminary study on their anticancer properties against human colorectal carcinoma HCT116 (**Scheme 18**) (Ghdhayeb *et al.*, 2017a). The Pd-mono(NHC) complex **45** was shown to be two times more potent than its bis(NHC) counterpart (**44**), which could be attributed to the ease of liberation of the metal ions in the case of Pd NHC complex **45**. Besides that, it was observed that Pd NHC complexes with benzyl substituents (**46**) displayed higher cytotoxicity against HCT116 as compared to the allyl derivatives (**44** and **45**), which is three to six times more effective. The HCT116 cells treated with these Pd NHC complexes have shown distortion of normal cell morphology, which caused the cancer cells to lose viability. In addition to that, the same research group have also synthesized a series of monometallic and bimetallic Pd NHC complexes **47-51** and evaluated their cytotoxicity against HCT116 (Ghdhayeb *et al.*, 2017b). The monometallic Pd NHC complexes **47-49** was shown to be displaying its toxicity similar to the previously discussed Pd NHC complexes **44-46** with half inhibitory concentration of 16.3 μM to 117.9 μM. Meanwhile, the monometallic and bimetallic Pd NHC complexes with xylyl-spacers, **50** and **51**, respectively demonstrated high potency towards HCT116 at single-digit micromolar range of 1.3 μM and 5.4 μM. Apart from this, difference in bioactivity was observed for different NHC ligands. This is demonstrated by the 3-fold increase in cytotoxicity observed in complex **47** bearing the

imidazolium-based ligand as compared to complex **48** which contain benzimidazolium-based ligand), albeit the difference in cytotoxicity could be contributed by different R group (R = Me or nBu) at the *N* wing tip of imidazolium ring at the same time. Similarly, these Pd NHC complexes acted by affecting the normal morphology of almost all the HCT116 cells, which instigated the cells to lose its viability and forms autophagic vacuoles after 72 hours of incubation. Nevertheless, the exact mechanism of action is yet to be discovered.



Scheme 18. A series of Pd NHC complexes with varying NHC ligands and metal multiplicity developed by Ghdayeb et al.

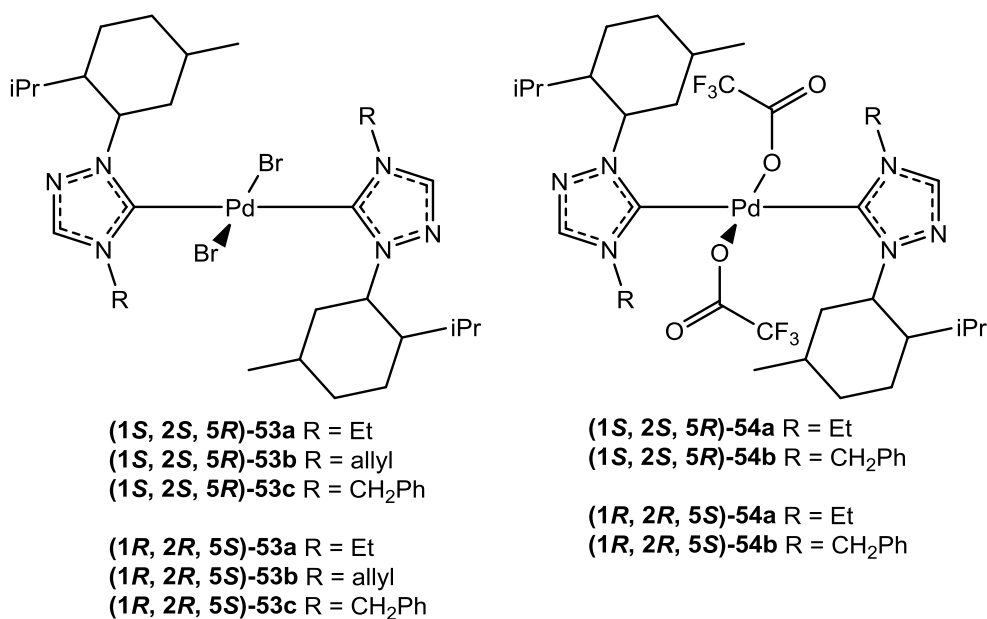
Apart from the luminescent cyclometalated Pt NHC complexes which shown significant anticancer activities which we discussed earlier, Che's group have also synthesized the corresponding cyclometalated Pd complexes **52** containing NHC ligands with different alkyl chain lengths as shown in **Scheme 19** (Fong et al., 2016). Among all, the Pd NHC complex **52d** displayed significant and selective cytotoxicity towards the tested cancer cell lines as compared to a normal human fibroblast cell line. The IC₅₀ obtained was in the single digit micromolar range that were up to 172-fold more cytotoxic than the benchmark cisplatin. Besides that, the *in vivo* anticancer potential of complex **52** was further exemplified by the significant inhibition of tumour growth in a nude mice model with no obvious body weight loss and no death. Mechanistic studies suggested that the anticancer effects of complex **52** was exerted via induction of mitochondrial dysfunction, antiangiogenic activity of endothelial cells, and inhibition of the epidermal growth factor receptor (EGFR) pathway in association with programmed cell death of cancer cells. This work, in particular, had highlighted the promising prospects of cyclometalated palladium NHC complexes for treatment of cancers.



Scheme 19. Cyclometalated Pd NHC complexes with anticancer activities developed by Che's group.

Based on the fact that the speculated target of Pd NHC complexes, DNA, is a chiral molecule, Kumar *et al.* have synthesized five enantiomeric pairs of chiral palladium complexes, **53** and **54**, of 1,2,4-triazole-derived chiral *N*-heterocyclic carbene ligands to study the effect of chirality on the anticancer potential of Pd NHC complexes (**Scheme 20**) (Kumar et al., 2017). They were first screened for antitumor property against the human breast cancer cell MCF7 using sulphonamide B assay. Only the enantiomeric pairs of **53a** and **54a** displayed cytotoxicity against MCF7 at single-digit micromolar range. Among these, the enantiomeric pair of chiral

Pd NHC complexes **54a** (**(1S, 2S, 5R)-54a** and **(1R, 2R, 5S)-54a**) bearing two polar CF₃CO₂ moieties, which improved its aqueous solubility, have showed extremely low IC₅₀ values (700 nM and 540 nM, respectively) compared to complexes **53a** and it is about 27-fold more effective than the benchmark cisplatin. Nevertheless, no influence on the cytotoxicity was observed with regards to the chirality as both enantiomers of all five enantiomeric pairs of Pd NHC complexes exhibited near-equal activities. The lack of difference in anticancer activities could be due to the larger dimensions of the chiral major (ca. 22 Å) and minor (ca. 12 Å) grooves of DNA with respect to the chiral menthyl moieties (ca. 8 Å) in the chiral Pd NHC complexes, as well as presence of different species interacting with the DNA strands other than the native form of chiral Pd NHC complexes. The most potent complex **(1R, 2R, 5S)-54a** was further studied for its anticancer activities against human cervical cancer (HeLa), human lung cancer (A549), mouse skin cancer (B16F10), and a multidrug resistant EMT6-AR1 cancer cells. The chiral Pd NHC complex **(1R, 2R, 5S)-54a** was highly cytotoxic towards the tested cell lines with half inhibitory concentration ranging from 1.6 μM to 10.5 μM. The good anticancer activity observed in multidrug resistant EMT6-AR1 cell line have suggested broad spectrum application of this chiral Pd NHC complex **(1R, 2R, 5S)-54a** as anticancer drug. The selectivity of complex **(1R, 2R, 5S)-54a** was determined by comparing its cytotoxicity towards non-tumour cell lines, mouse fibroblast skin cells (L929) and human epithelial breast cells (MCF10A), with respect to their cancerous cells, mouse skin cancer (B16F10) and human breast cancer cells (MCF7). Results have showed that **(1R, 2R, 5S)-54a** was roughly 8-fold more potent towards B16F10 relative to L929, and about 16-fold more potent towards MCF7 compared to MCF10A. Mechanistic studies on chiral Pd NHC complex **(1R, 2R, 5S)-54a** revealed that it stopped cancer cell proliferation by arresting the cells at the G2 phase, preventing them from entering the mitotic stage. It led to DNA damage in the MCF7 cells, causing production of reactive oxygen species (ROS) in the mitochondria and subsequently cell death. The chiral Pd NHC complex **(1R, 2R, 5S)-54a** was also shown to be involved in inducing p53-dependent programmed cell death in MCF7 cells.



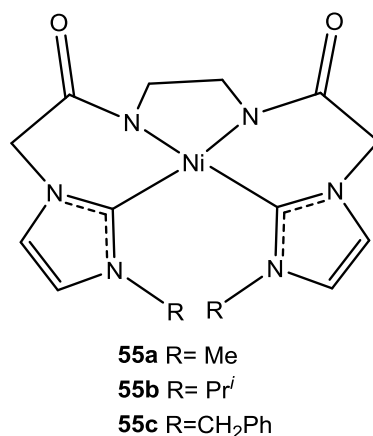
Scheme 20. Enantiomeric pairs of Pd NHC complexes with anticancer activities.

1.5.3. Nickel N-Heterocyclic carbene (Ni NHC) complexes

Nickel is an essential component in several metallozymes including urease, carbon monoxide dehydrogenase, and hydrogenase (Abu-Surrah and Kettunen, 2006). The chemistry of nickel complexes now stands at an important position in useful organic catalytic reactions (McGuinness et al., 1999, Terao et al., 2002, Zhou and Fu, 2003, González-Bobes and Fu, 2006, Tobisu et al., 2008). Although some toxicity of nickel compounds has been pointed out, they are relatively inexpensive in comparison with corresponding palladium and platinum analogues.

Although the study on Ni NHC complexes and their biomedical application is relatively scarce compared to Pt NHC and Pd NHC complexes, but the apparent potential of nickel complexes in antitumour studies has been reported recently. Ray and co-workers have designed three tetradentate Ni NHC complexes **55** with the intention to use them as agents for developing resistance to nickel toxicity (**Scheme 21**) (Ray et al., 2009). These Ni NHC complexes were tested against a combination of human cancer cell lines and mouse normal cells. These Ni NHC complexes **55** have shown less cytotoxicity than NiCl₂·6H₂O against HeLa and MCF7 cell lines under analogous condition. In addition, Ni NHC complex **55c** displayed only half the toxicity than that of cisplatin against the non-tumorigenic CHO cell line with minimal cell surface distortion (Ray et al., 2009). It is important to point out that while the cytotoxicity results showed no difference in selectivity of these Ni NHC complexes towards tumorigenic and non-tumorigenic cells (represented by complex **55c**), the cytotoxicity effect of Ni NHC is weaker

than that of $\text{NiCl}_2 \cdot 6\text{H}_2\text{O}$. These observations supported that the drastic reduction in cytotoxic activity of nickel was successfully achieved by chelation of the nickel ion through the powerful σ -donating tetradentate N/O-functionalized NHC ligands in Ni NHC complex (Ray et al., 2009). These Ni NHC σ -bonding molecular orbitals are deeply buried in the cyclometallated configuration, ultimately contributing to the inert nature of NHC-nickel interaction, which in turn leads to exceptional stability of these Ni NHC complexes. This is highly desirable in drug design as it can ensure the stability of the complexes during drug delivery.



Scheme 21. Nickel NHC complexes reported by Ray *et al.* (2009) that showed anticancer potential.

1.6. Group 10 metal NHC complexes with antimicrobial activities

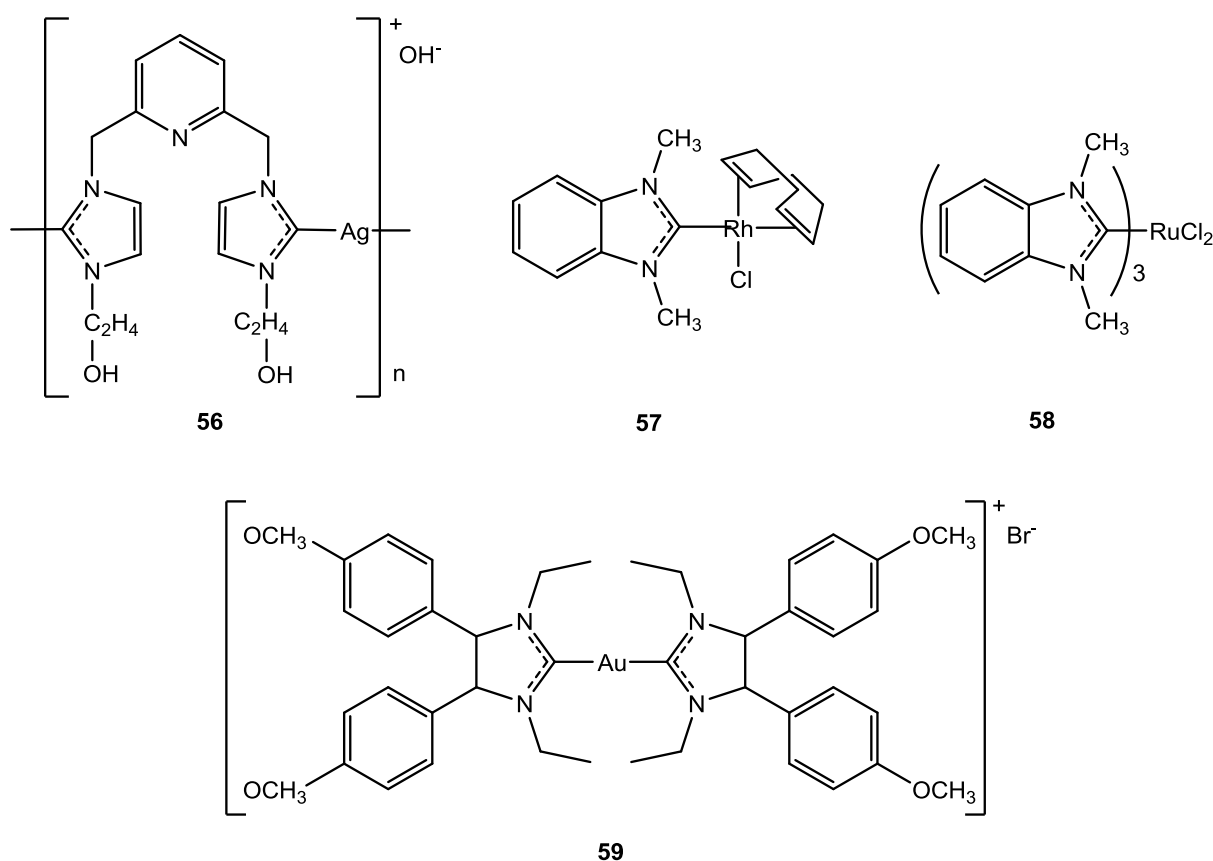
The search for novel drugs is especially crucial in this post-antimicrobial era due to the rapid emergence of antimicrobial resistant pathogens. The development of antimicrobial resistance (AMR) have been a global threat to the effective treatment of infections caused by bacteria, parasites, viruses and fungi. Antimicrobial is an agent capable of killing microorganisms or suppressing their growth. AMR arises when the microorganisms (bacteria, fungi, viruses, parasites) mutate or change upon exposure to antimicrobial agents (Wise et al., 1998). The microorganisms that developed AMR are usually being referred as “superbugs”. Although the development of AMR happens naturally over time as an evolution agenda, this problem have also been exacerbated by the over-prescription and misuse of antibiotics in both human and animals (Costelloe et al., 2010). Development of AMR results in reduced efficacy of antibacterial, antiparasitic, antiviral and antifungal drugs, making the treatment of patients costly, difficult or even impossible (WHO, 2014, Cosgrove, 2006). Most importantly, common medical procedures like organ transplantation, cancer chemotherapy, diabetes management and

major surgery become very high risk without effective antimicrobials for prevention and treatment of infections.

This issue of AMR is further complicated that by the ability of microorganisms to form biofilms. Microorganism do not exist as pure culture of dispersed single cells in real life. Instead, biofilms are formed when microorganisms come together to form a community that is attached to a solid surface and embedded in a self-produced slimy matrix of extracellular polymeric substances (EPS) (Flemming and Wingender, 2010, Islam et al., 2012). In biofilms, the EPS behaves as a physical barrier to antimicrobial agents which resulted in 100-1000 times of increased resistance to antimicrobial agents as compared to their planktonic forms (Bordi and de Bentzmann, 2011, Mah and O'Toole, 2001). Biofilms can form on a variety of biotic and abiotic surfaces including living tissues, medical devices, industrial or potable water piping system, or natural aquatic system (Donlan, 2002). Although multiple microbial species biofilms predominate in most environments, single species biofilms also exist in a variety of infections and on the surface of medical implants (O'Toole et al., 2000). In fact, biofilms have a massive impact on medicine as they can develop on many medical implants and, due to their enhanced resistance to antimicrobial agents, these infections can often only be treated by removal of the implant, thereby increasing the trauma to the patient and the treatment cost.

In spite of the rapid emergence of antimicrobial resistance pathogens and biofilm infections, there are relatively few antimicrobials being discovered and developed in the past decades. As a result, there is a lack of effective antimicrobial agent, especially those that can penetrate through the biofilms, to bring therapeutic benefits. This highlights the importance of novel drug discovery to combat antimicrobial resistant pathogens and biofilms.

The impetus for the antimicrobial study came from the knowledge that a number of elemental metals are well known for their antimicrobial activities, such as silver. In addition to that, numerous metal NHC complexes were reported to display significant antimicrobial activities against Gram-positive and/or Gram negative bacteria with minimum inhibitory concentration (MIC) below 10 $\mu\text{g}/\text{mL}$, including silver, gold, rhodium and ruthenium NHC complexes among others, with selected examples illustrated in **Scheme 22** (Cetinkaya et al., 1996, Cetinkaya et al., 1999, Melaiye et al., 2004, Özdemir et al., 2004, Melaiye et al., 2005, Baker et al., 2006, Kascatan-Nebioglu et al., 2006, Kascatan-Nebioglu et al., 2007, Ray et al., 2007, Hindi et al., 2008, Özdemir et al., 2010, Roland et al., 2011, Liu et al., 2012, Haque et al., 2016c, Karatas et al., 2016).

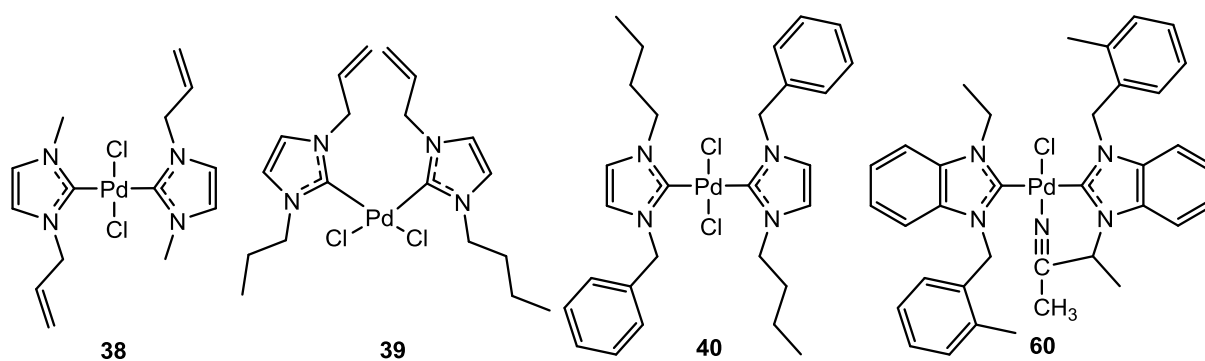


Scheme 22. Selected metal NHC complexes with significant minimum inhibitory concentration (MIC) below 10 $\mu\text{g/mL}$: pyridine-linked pincer silver(I) NHC complex (56), rhodium NHC complex (57), ruthenium NHC complex (58) and cationic bis(NHC)gold(I) complex (59).

1.6.1. Palladium N-Heterocyclic carbene (Pd NHC) complexes

Although plenty of impressive anticancer properties have been reported for Group 10 metal-NHC complexes, the information on the antimicrobial properties of these metal complexes are limited. However, Haque and co-workers have synthesized a series of Pd NHC complexes with antimicrobial properties, which were also potent anticancer agents as described earlier (**Scheme 23**) (Haque et al., 2013). Preliminary antimicrobial potential screening was performed against two representative Gram positive and Gram negative, namely *Staphylococcus aureus* (ATCC 29213) and *Escherichia coli* (ATCC 25922), by using disc diffusion assay. All Pd NHC complexes **38-40** showed satisfactory concentration-dependent antimicrobial activity with small volume of samples used (stock solution concentration of 800 $\mu\text{g/mL}$). In general, antimicrobial activities of Pd NHC complexes **38-40** were higher against the Gram-positive *S. aureus* compared to the Gram negative *E. coli*. To the best of our knowledge, this is the first report on the antimicrobial activity of Pd NHC complexes, which envisions another possible

biomedical application for Group 10 metal NHC complexes. With their previous discovery on the antimicrobial activities of Pd NHC complexes, Haque *et al.* have recently synthesized Pd NHC complex **60** and studied its antimicrobial property against *Staphylococcus aureus* (ATCC 29213) and *Escherichia coli* (ATCC 25922) using disc diffusion assay and broth dilution assay (**Scheme 23**) (Haque *et al.*, 2016d). Unfortunately, Pd NHC complex **60** only showed antibacterial activity towards Gram positive *S. aureus*, with no inhibition zone observed for the Gram negative *E. coli*. This result was further supported by the broth dilution assay where complex **60** showed antimicrobial activity against *S. aureus* with minimum inhibitory concentration (MIC) and minimum bactericidal concentration (MBC) of 50 and 100 $\mu\text{g/mL}$, respectively, while the growth of *E. coli* was not affected at all. Nonetheless, the reason and mechanism behind the observed selective antimicrobial activities of these Pd NHC complexes towards *S. aureus* is yet to be known.



Scheme 23 Palladium NHC complexes that shown significant antimicrobial activity with minimum inhibitory concentration (MIC) in $\mu\text{g/mL}$ range.

1.7. Summary and Research Gaps

From a transient intermediate to a main character in synthesis, metal NHC complexes have emerged as an important highlight in catalysis and biomedicine owing to its beneficial properties. There are many research that have been dedicated to the search of novel and efficient synthesis pathway of metal NHC complexes and their applications in various fields.

The reports on the anticancer properties of Group 10 metal NHC complexes have confirmed their potential in development of new chemotherapeutics to replace the current platinum-based drugs. Efforts have been made to circumvent the limitation of platinum-based chemotherapeutic drugs including, but not limited to, modification of NHC ligands or addition of less toxic conjugates to the metal NHC complexes to reduce to overall toxicity, as well as conjugation

with biological relevant molecules to increase the bioavailability of these metal NHC complexes. The Group 10 metal NHC complexes are thought to be targeting the DNA like cisplatin, but based on the mechanistic studies so far, it is impossible to have a unique target for the metal NHC complexes to exert their anticancer or antimicrobial activities. This is largely due to the vast chemical diversities of metal complexes with NHC ligands. In addition to that, the anticancer and antimicrobial effects could be affected by a variety of factors including the choice of metals, choice of NHC ligands, change of moieties on the metal NHC complexes, conjugation with other molecules or polymers, chirality of the metal NHC complexes, and others.

Among the Group 10 metal NHC complex, platinum NHC complexes, in particular, have been extensively studied for their anticancer properties. In this recent five years, palladium NHC have been a rising platform to look for new anticancer drugs owing to their similar properties with platinum. There were reports on Pt and Pd NHC complexes with anticancer activities comparable or exceeded that of the benchmark drug cisplatin, thereby highlighting the potential of Pt and Pd NHC complexes as new chemotherapeutic agents. In addition to that, research has also shown that palladium NHC complexes displayed antibacterial activities as well. Unfortunately, there is only less than a handful of report on the antimicrobial potential of Pd NHC complexes, which hopefully this will provide a guide to open up the exploration of Pd NHC complexes as potential antimicrobial agents. On the other hand, there is still a considerable large gap present pertaining Ni NHC complexes. With the highly toxic characteristic of Ni ions, nickel complexes with organic and inorganic ligands have been studied extensively for their antimicrobial properties but not the case for Ni NHC complexes. Hence, more analogues of metal NHC complexes with incorporation of nickel can be synthesized and studied for their potential biomedical applications. Nevertheless, systematic study on the mechanism of anticancer and antimicrobial actions of these Group 10 metal NHC complexes are required to reveal the exact mechanism before they could be disseminated as anticancer or antimicrobial drugs. Overall, these preliminary achievements in this rather new area of research may guide the future anticancer and antimicrobial drug development.

1.8. Research Objectives

Previously, Leung's group reported the synthesis and characterization of a series of novel cyclopalladated pyridine-functionalized NHC dichloride complexes showing interesting conformational behaviour and exhibiting remarkable activities in catalytic allylic alkylation reaction (Chiang, 2011, Chiang et al., 2010, Ng et al., 2013). In this study, the synthesis of a series of racemic pyridine-functionalised Group 10 metal NHC complexes, including nickel, palladium and platinum, will be exemplified. Although the catalytic properties of the Pd NHC complexes were previously known, there is a vast gap for the biological potential of these complexes to act as anticancer and antimicrobial agents. Also, the synthesis of the novel Pt and Ni NHC complexes which are analogous to the Pd NHC complexes would be an interesting starting point to study the effect of different metals on the biological activities of these metal NHC complexes. As literature implies, the metal center plays an important role in interacting with biological targets while lipophilicity is maintained at optimum level by adjusting the side chain in the metal NHC complex (Aher et al., 2017). Besides that, other main focuses include the influence of optical isomerism and different *N* wingtip substituents on the structure of respective Group 10 metal NHC complexes on the antimicrobial activities and cytotoxicity against cancer cells. Hence, the objectives of this research are:

- i. To synthesise racemic nickel, palladium and platinum NHC complexes;
- ii. To optically resolve racemic nickel, palladium and platinum NHC complexes;
- iii. To characterise the synthesized precedent compounds, imidazolium salts and, nickel, palladium and platinum NHC complexes with various spectroscopic techniques;
- iv. To evaluate the antimicrobial activities of these metal NHC complexes against selected strains of Gram positive and Gram negative bacteria, as well as yeast; and
- v. To evaluate the cell cytotoxicity effects of these metal NHC complexes against selected human carcinoma cell lines including colon carcinoma (HCT116), oral carcinoma (H103) and breast carcinoma (MCF7).

In this thesis, objectives (i) to (iii) will be discussed in **Chapter 2**, followed by **Chapter 3** which answer objective (iv), and lastly, objective (v) will be deliberated in **Chapter 4**.

CHAPTER 2 SYNTHESIS, CHARACTERISATION AND OPTICAL RESOLUTION OF PALLADIUM, PLATINUM AND NICKEL *N*-HETEROCYCLIC CARBENE (NHC) COMPLEXES

2.1. Introduction

As mentioned in Chapter 1, metal NHC complexes had been a prodigious field of research that came into the spotlights since three decades ago. Thus far, numerous metal NHC complexes with different metals, NHC ligands, denticity, chirality etc. that been synthesized for various applications especially catalysis and biomedicine applications. Nonetheless, the search for synthesis routes to create novel metal NHC complexes is infinite due to the great versatility of these NHC ligands.

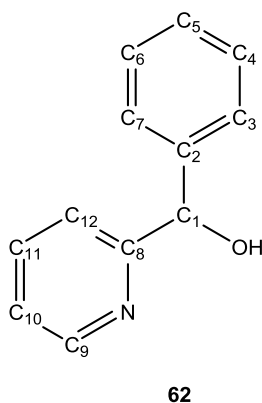
One of the main focuses of metal NHC complexes in biomedical applications had been placed on the Group 10 metals including nickel, palladium and platinum. This is owing to the therapeutic successes of platinum based drugs, especially cisplatin, as standard chemotherapeutic regimens to treat a number of cancers for more than thirty years. Following this lead, a series of nickel, palladium and platinum *N*-heterocyclic carbene complexes was synthesized in this study and studied for their in vitro biological activities.

In this chapter, the synthesis and characterization of these Group 10 metal (including nickel, palladium and platinum) NHC complexes will be discussed. This series of metal NHC complexes were made up of a five-membered imidazolylidenes NHC ligands functionalized with a pyridine group, a metal centre, and two ancillary ligands (i.e. Cl) in *cis* configurations. The NHC ligands were prepared from the deprotonation of imidazolium salts, where they have different R substituents at the *N* wingtip of the imidazolium ring namely the aliphatic methyl (Me) group, the aromatic phenyl (Ph) group and the bulky tert-butyl (*t*Bu) group. Notably, these metal NHC complexes the complex are bidentate, meaning that the metal centre is bound with two ligands. This also contributes to the formation of a six-membered ring in a structurally rigid cyclometalated fashion, making them a complex with high stability, which is a highly desirable property. Apart from that, one of the key characteristics of our series of group 10 metal NHC complexes is the presence of a chiral centre in the structure. This gives rise to the acquisition of racemic metal NHC complexes, where the optically active enantiomers can be separated via optical resolution from the racemates.

2.2. Results and Discussion

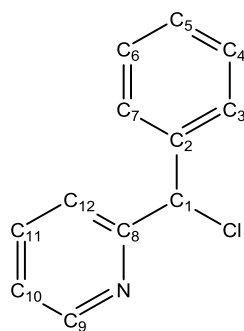
2.2.1. Synthesis and characterisation of imidazolium salts (or NHC precursors) **64**

As shown in the **Scheme 24** above, the synthesis of pyridine functionalized imidazolium salt **64** was achieved by initial reduction of the commercially available 2-benzoylpyridine (**61**) into phenyl(pyridine-2-yl)methanol **62**, followed by halogenation to give 2-(chloro(phenyl)methyl)pyridine **63**. Subsequent reaction of compound **63** with imidazoles (1-methylimidazole, 1-phenylimidazole and 1-*tert*-butylimidazole) yielded the target pyridine functionalized imidazolium salt **64a**, **64b** and **64c**, respectively. The intermediate compound **62** was prepared according to literature method (Kim and Kang, 2014). Compound **62** was isolated as a pale green oil after extraction and solidified into clear crystal upon recrystallization in ethanol solution (96 % yield). The purity and identity of compound **62** was determined by ^1H and ^{13}C NMR, in which both are in agreement with literature (Frassoldati et al., 2013).



Scheme 25. Chemical structure of compound phenyl(pyridine-2-yl)methanol, **62.**

Next, phenyl(pyridine-2-yl)methanol **62** was reacted with methane sulfonyl chloride in the presence of triethylamine in dichloromethane to give compound **63**, 2-(chloro(phenyl)methyl)pyridine. After running through gravitational column chromatography with hexane/ethyl acetate (80:20 v/v), it was isolated as yellow oil in 74 % yield. Identity of compound **63** was confirmed by the presence of its molecular ion peak $[\text{M}-\text{Cl}]^+$ at m/z 168.0804 (calculated 168.0813 for $\text{C}_{12}\text{H}_{10}\text{N}$). However, the ^1H NMR chemical shifts for compound **62** and **63** were not distinguishable due to high similarity, therefore ^{13}C NMR was utilised to confirm the conversion of OH into Cl. This is observed in the characteristic upfield shift of the carbon (C1) from $\delta = 75.00$ ppm (compound **62**) to 64.54 ppm (compound **63**). The spectral data for this compound are consistent with those reported in the literature (Chiang et al., 2010).

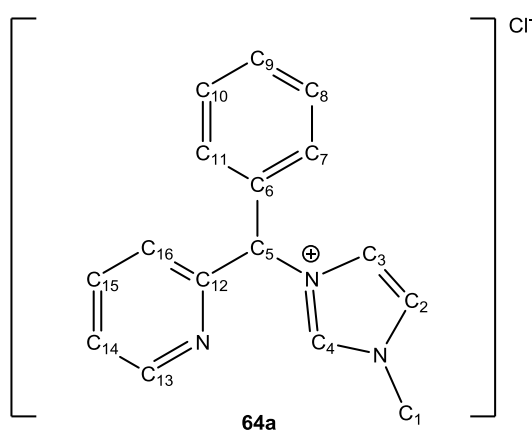


63

Scheme 26. Chemical structure of compound 2-(chloro(phenyl)methyl)pyridine, 63.

2.2.1.1. Synthesis and characterisation of 1-methyl-3-[phenyl(pyridin-2-yl)methyl]-1*H*-imidazolium chloride, 64a

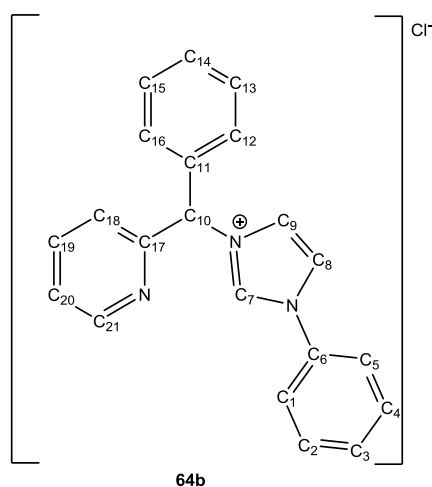
Imidazolium salts (or NHC precursors) **64a** was isolated as a hygroscopic off-white solid (yield 46%) after 48 hours of reflux and three successive precipitation from chloroform and diethyl ether. The characteristic imidazolium proton peak (H4) can be seen in ^1H NMR at $\delta = 10.39$ ppm. The wingtip methyl group on the imidazole ring revealed to be a singlet in the ^1H NMR at $\delta = 4.03$ ppm. The proton on the chiral centre of the compound (position H5) has a downfield shift that showed up in the aromatic proton region and was indistinguishable from other aromatic protons. The spectral data for this compound are consistent with those reported in the literature (Chiang et al., 2010). The molecular ion peak $[\text{M-H}]^+$ at m/z can be observed at 284.2074 (calcd. 284.0954) by mass spectrometry.



Scheme 27. Structure of imidazolium salt (R = Me), 64a.

2.2.1.2. Synthesis and characterisation of 1-phenyl-3-[phenyl(pyridin-2-yl)methyl]-1*H*-imidazolium chloride, **64b**

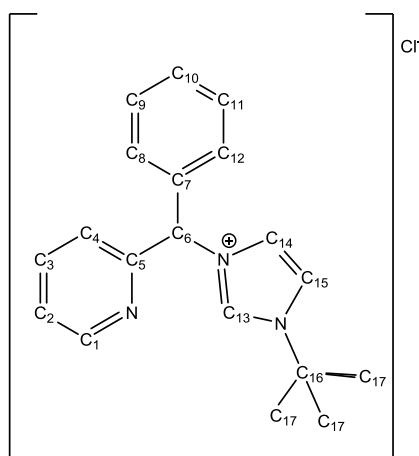
After 48 hours of reflux, imidazolium salts (or NHC precursors) **64b** was obtained in the form of brown oil in 2.9% yield. The characteristic imidazolium proton peak (H7) can be observed as a singlet at $\delta = 11.30$ ppm in ^1H NMR. Similar to **64a**, the proton on the chiral centre (H10) cannot be identified as it has a downfield shift and showed up in the aromatic proton region. The spectral data for this compound are consistent with those reported in the literature (Chiang, 2011). The molecular peak $[\text{M}-\text{Cl}]^+$ can be observed at m/z 312.1508 by MS (calcd. 312.1501).



Scheme 28. Structure of imidazolium salt (R = Ph), **64b**.

2.2.1.3. Synthesis and characterisation of 1-*tert*-butyl-3-[phenyl(pyridin-2-yl)methyl]-1*H*-imidazolium chloride, **64c**

On the other hand, imidazolium salts (or NHC precursors) **64c** was isolated as a brown solid in 54% yield after 48 hours of reflux. The characteristic imidazolium proton peak (H13) can be seen in ^1H NMR at $\delta = 11.19$ (singlet). The wingtip *tert*-butyl group on the imidazole was observed as a singlet at $\delta = 1.70$ ppm in ^1H NMR. There was a downfield shift for the proton the chiral centre of the ligand (H6) that eventually showed up in the aromatic proton region and therefore cannot be identified. The spectral data for this compound are consistent with those reported in the literature (Ng et al., 2013). Via MS, the molecular ion peak $[\text{M}-\text{Cl}]^+$ can be observed at m/z 292.3259 (calcd. 292.1814).



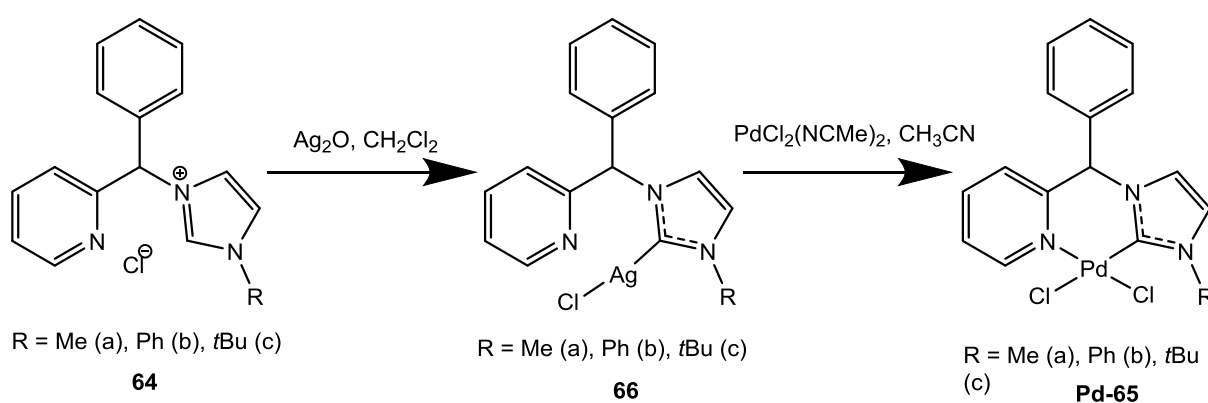
64c

Scheme 29. Structure of imidazolium salt (R = *t*Bu), 64c.

2.2.2. Synthesis and Characterisation of Racemic Metal NHC Complexes

2.2.2.1. Synthesis and characterization of racemic palladium NHC complexes

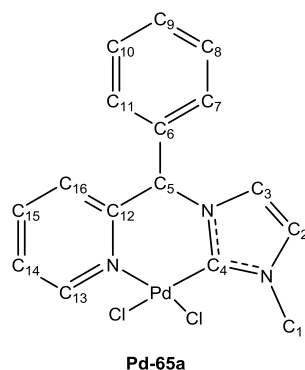
The imidazolium salts (NHC precursors **64**) were then subjected to transmetalation method adopted from Chiang (2011) to yield the racemic palladium NHC complexes as shown in **Scheme 30**. The crude silver(I) NHC complex (**66**) was generated *in situ*. After that, the crude silver complex was filtered through a short plug of celite in the dark and was immediately subjected to the subsequent reaction to yield the racemic palladium NHC complexes **65**.



Scheme 30. Two-steps transmetalation of imidazolium salts (or NHC precursors) (64**) into racemic palladium NHC complexes (Pd-**65**), with the generation of a silver NHC complex **66** *in situ*.**

2.2.2.1.1. Characterisation of racemic complex Pd-65a

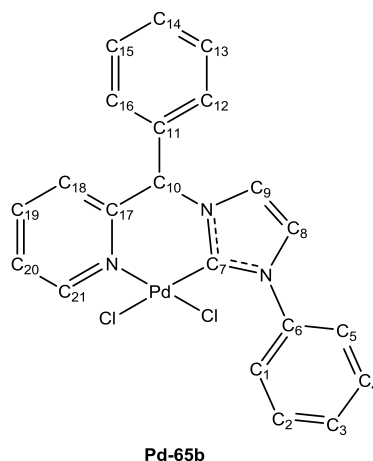
After transmetalation and precipitation from a concentrated reaction mixture in diethyl ether, the racemic complex **Pd-65a** was collected as an orange-yellow solid in 38% yield. The formation of racemic complex **Pd-65a** was confirmed by the disappearance of the characteristic imidazolium proton peak at $\delta = 10.39$ ppm. A general downfield shift was observed in the ^1H NMR upon metal coordination. The molecular peak $[\text{M-Cl}]^+$ can be observed at m/z 390.3347 via MS (calcd. 389.9989). The spectral data for this complex are consistent with those reported in the literature (Chiang et al., 2010). In most cases, no NCN resonance was observable the ^{13}C NMR spectrum of the synthesized Pd NHC complexes in $\text{DMSO-}d_6$. This is not unusual since metal NHC complexes with similar behaviour were reported. The reason for the absence of carbene signals is still unclear, nevertheless a fast dynamic behaviour combined with the poor relaxation of quaternary NCN could account for it (Garrison and Youngs, 2005).



Scheme 31. Structure of racemic complex Pd-65a.

2.2.2.1.2. Characterisation of racemic complex Pd-65b

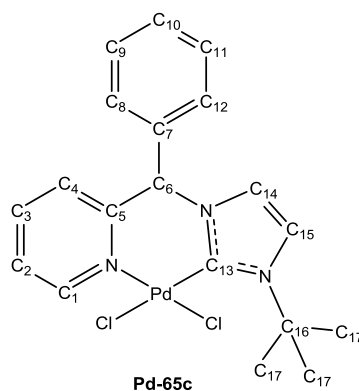
The racemic complex **Pd-65b** was collected as an orange-yellow solid in 40% yield after precipitation from a concentrated reaction mixture in diethyl ether. The formation of racemic complex **Pd-65b** was confirmed by the disappearance of the characteristic imidazolium proton peak at $\delta = 11.30$ ppm. Upon coordination, there is a general downfield shift in the ^1H NMR of racemic complex **Pd-65b** compared to imidazolium salts **64b**. The proton H10 experienced a downfield coordination shift and is indistinguishable from other aromatic protons. The molecular peak $[\text{M-Cl}]^+$ can be observed at m/z 451.9980 (calcd. 452.0146) via MS. The spectral data for this complex are consistent with those reported in the literature (Chiang, 2011).



Scheme 32. Structure of racemic complex Pd-65b.

2.2.2.1.3. Characterisation of racemic complex Pd-65c

Similar to racemic complex **Pd-65a** and **Pd-65b**, **Pd-65c** was isolated as an orange-yellow solid (60% yield) after precipitation from a concentrated reaction mixture in diethyl ether. The formation of racemic complex **Pd-65c** was identified by the disappearance of the characteristic imidazolium proton peak at $\delta = 11.19$ ppm. Upon coordination, a general downfield shift was observed in the ^1H NMR of racemic complex **Pd-65c** compared to imidazolium salts **64c**. The molecular peak $[\text{M}+\text{H}]^+$ can be found at m/z 468.0220 by MS (calcd. 468.0226). The spectral data for this complex are consistent with those reported in the literature (Ng et al., 2013).



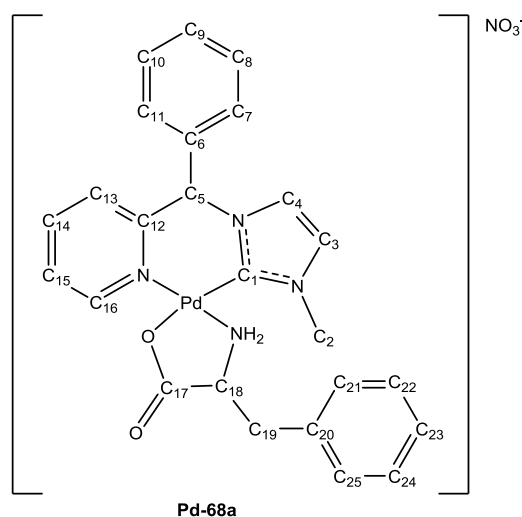
Scheme 33. Structure of racemic complex Pd-65c.

2.2.2.2. Optical resolution of racemic palladium NHC complexes

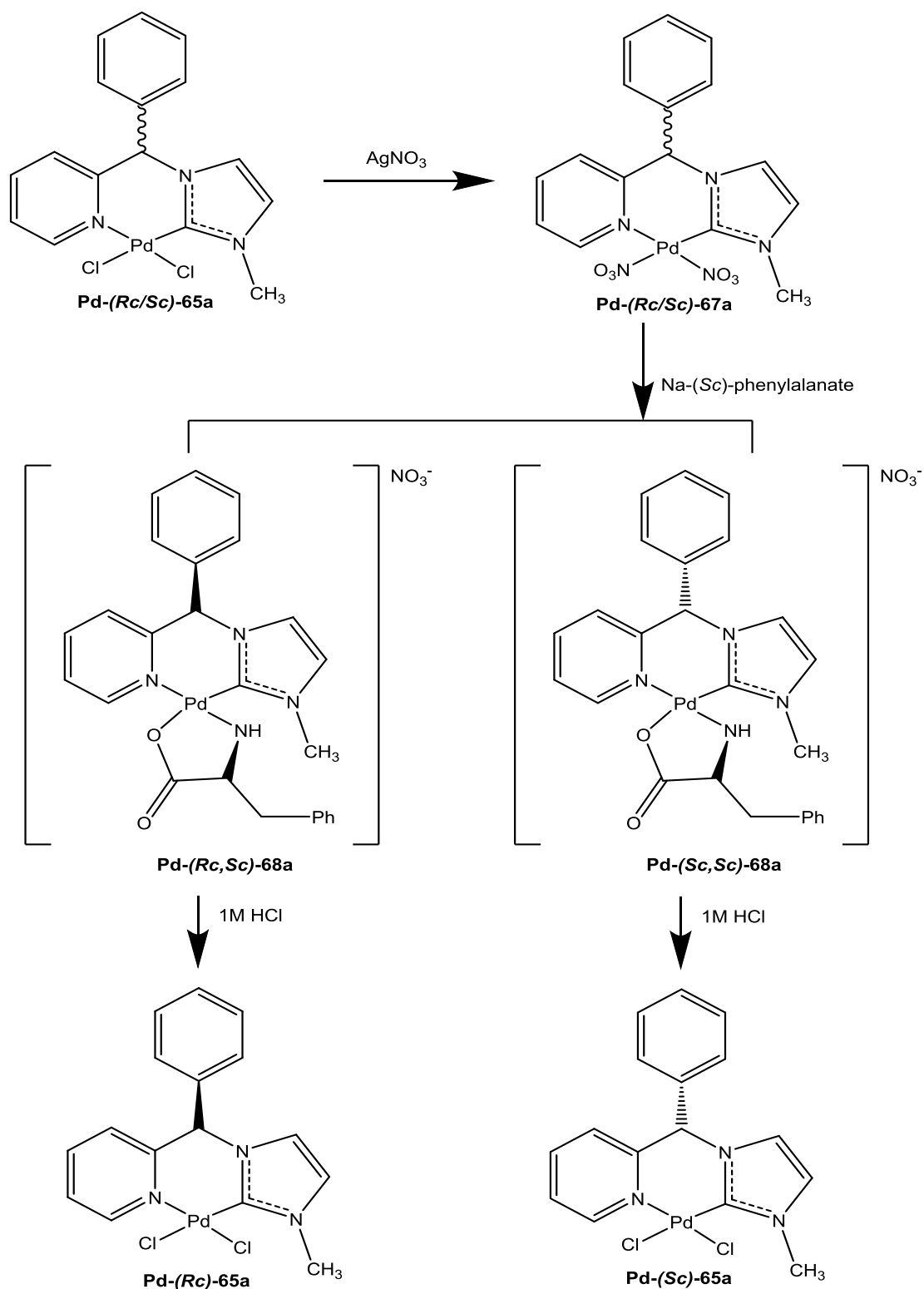
2.2.2.2.1. Optical resolution of racemic Pd-65a complex

Following a literature method, the optical resolution of the racemic **Pd-65a** was initiated by switching the counter ions present in the diastereomeric complexes from chloride into nitrate, and sodium-(*Sc*)-phenylalanate was used as the resolving reagent (**Scheme 35**) (Chiang et al., 2010). Fractional crystallization method was employed to yield the less soluble diastereomers (***Rc,Sc*-68a**) from methanol and diethyl ether. Whereas the optically active (***R*-65a**) was obtained by stirring a methanol solution of equal molar of diastereomers (***Rc,Sc*-68a**) with 1 M HCl. Their identities were confirmed with ^1H and ^{13}C NMR, which are also in agreement with a previous report (Chiang et al., 2010).

Slow diffusion of diethyl ether into the methanol solution of the **Pd-(*Sc,Sc*)-68a** enriched mother liquor is performed to allow the remaining **Pd-(*Rc,Sc*)-68a** to crystallize out. The **Pd-(*Rc,Sc*)-68a** and **Pd-(*Sc,Sc*)-68a** were distinguished with the presence of two distinct sets of proton resonances for each of the diastereomers. For examples, NH_2 in **Pd-(*Rc,Sc*)-68a** was characterised as a doublet and a multiplet at 4.99 ppm and 5.99-6.02 ppm respectively, while in **Pd-(*Sc,Sc*)-68a**, the NH_2 protons were presented around 7.00 ppm.



Scheme 34. Structure of diastereomeric complex Pd-68a.

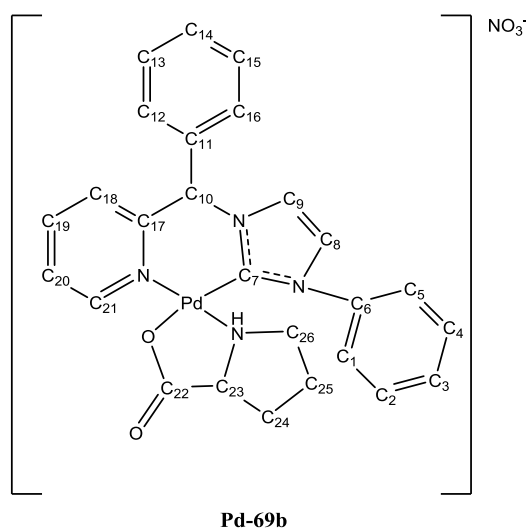


Scheme 35. Optical resolution for separation of racemic Pd-65a into their respective enantiomers (*Rc* or *Sc*) using sodium-(*Sc*)-phenylalanate.

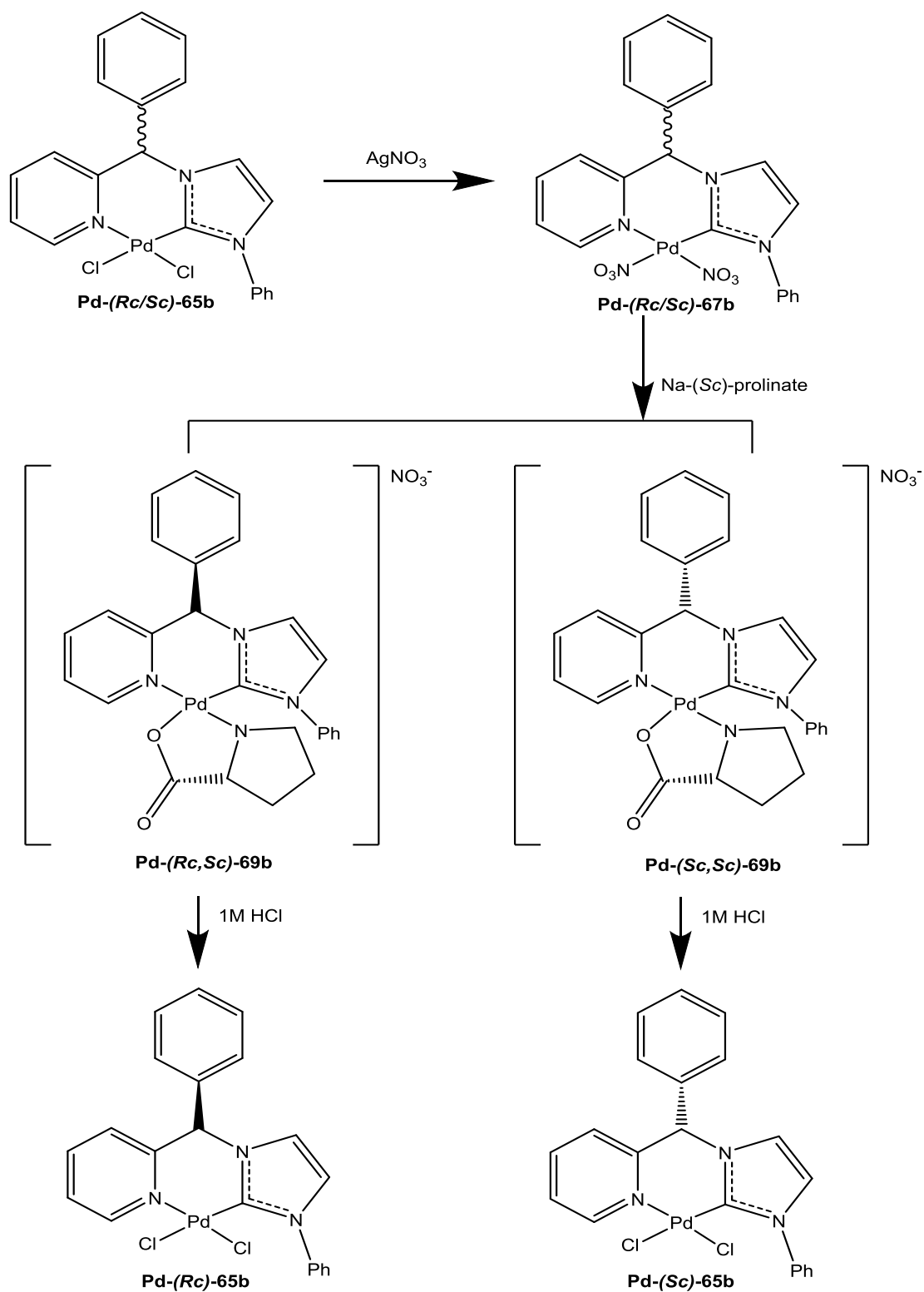
2.2.2.2.2. Optical resolution of racemic Pd-65b complex

Literature have reported the optical resolution of the racemic **Pd-65b** complex using sodium-(*Sc*)-prolinate without changing the counter anion present in the diastereomic complexes (Chiang, 2011) (**Scheme 37**). In our case, the two resulting diastereomers could not be separated resulting in several failed attempts of crystallisation. The problem was finally circumnavigated by changing the counter anion. After switching the counter anion from chloride to nitrate, successful optical resolution of racemic complex **Pd-65b** was achieved using sodium-(*Sc*)-prolinate as the auxiliary ligand. Fractional crystallisation from methanol and diethyl ether yielded the less soluble diastereomer **Pd-(*Sc,Sc*)-69b**. The identity of **Pd-(*Sc,Sc*)-69b** was confirmed through NMR and in agreement with literature. Slow diffusion of diethyl ether into the methanol solution of the **Pd-(*Rc,Sc*)-69b** enriched mother liquor is performed to allow the remaining **Pd-(*Sc,Sc*)-69b** to crystallise out.

The optically active **Pd-(*Sc*)-65b** was obtained by stirring a methanol solution of diastereomer **Pd-(*Sc,Sc*)-69b** with 1 M HCl. The optically active **Pd-(*Sc*)-65b** was isolated as a yellow powder in 79% yield. The identity was confirmed with ^1H NMR.



Scheme 36. Structure of diastereomeric complex Pd-69b.



Scheme 37. Optical resolution for separation of racemic Pd-65b into their respective enantiomers (*Rc* or *Sc*) using sodium-(*Sc*)-prolinate.

2.2.2.2.3. Optical resolution of racemic Pd-65c complex

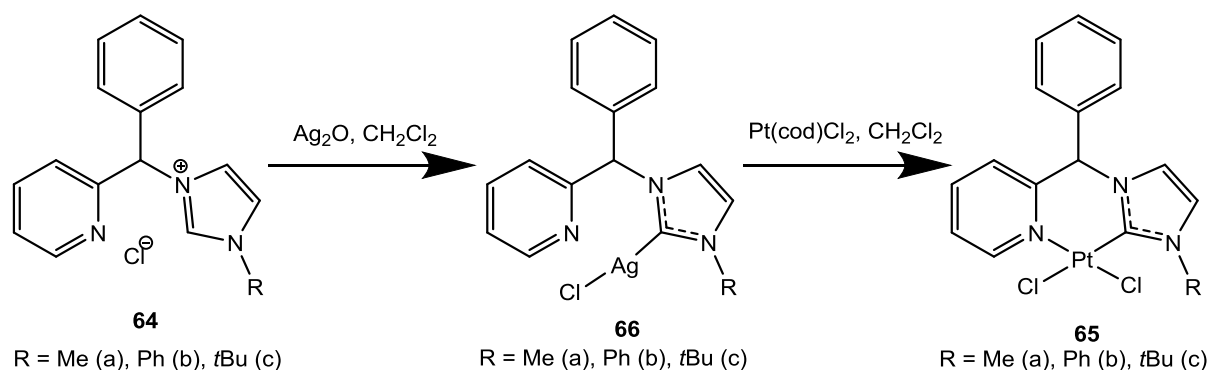
Based on the success of the optical resolution of racemic complexes **Pd-65a** and **Pd-65b** using chiral sodium-amino acid salts, we employed the method on complex **Pd-65c**. Likewise, the progress of diastereomers formation in optical resolution was monitor using ^1H NMR after addition of chiral sodium amino acid salt. Unfortunately, the optical resolution of **Pd-65c** was unsuccessful despite changing the ancillary chloride ligand and use of various sodium-amino acid salts. Those attempts to optimize the optical resolution of **Pd-65c** the optical resolution of **Pd-65c** were listed in **Table 1** below.

Table 1. List of parameters for the optical resolution of racemic complex Pd-65c.

Ancillary anion	Sodium amino acid salt	Resolved (Y/N)
Cl^-	sodium-(<i>Sc</i>)-phenylalanate	N
NO_3^-	sodium-(<i>Sc</i>)-phenylalanate	N
Cl^-	sodium-(<i>Sc</i>)-prolinate	N
NO_3^-	sodium-(<i>Sc</i>)-prolinate	N
Cl^-	sodium-(<i>Sc</i>)-tryptophan	N
NO_3^-	sodium-(<i>Sc</i>)-tryptophan	N
Cl^-	sodium-(<i>Sc</i>)-tyrosine	N
NO_3^-	sodium-(<i>Sc</i>)-tyrosine	N

2.2.2.3. Synthesis and characterisation of racemic platinum NHC complexes

Like the racemic palladium NHC complexes, the racemic platinum NHC complexes **Pt-65** were synthesized using the Ag_2O method. The imidazolium salts (NHC precursors **64**) were subjected to transmetalation and a crude silver NHC complex (**66**) were generated *in situ* (Scheme 38). After that, the crude silver complex was filtered through a short plug of celite in the dark and was immediately subjected to the subsequent reaction to yield the racemic platinum NHC complexes **65**, using dichloro(1,5-cyclooctadine)platinum(II) as the transmetalating agent.



Scheme 38. Two-steps transmetalation of the imidazolium salts (or NHC precursors) (**64**) into racemic platinum NHC complexes (**Pt-65**), with the generation of a silver NHC complex **66** *in situ*.

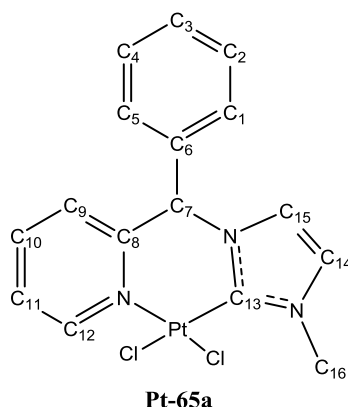
2.2.2.3.1. Characterisation of racemic complex **Pt-65a**

The racemic complex **Pt-65a** was isolated as an off white solid, 0.76 g, 35 %. MS m/z : $[\text{M}]^+$ calcd. for $\text{C}_{16}\text{H}_{15}\text{Cl}_2\text{N}_3\text{Pt}$ 514.0291, found 514.0169. The formation of racemic complex **Pt-65a** was confirmed by the disappearance of the characteristic imidazolium proton peak at $\delta = 10.39$ ppm, and the presence of the methyl peak at 3.90 ppm. A general downfield shift was observed in the ^1H NMR upon metal coordination. Due to the poor solubility of complex **Pt-65a** in wide array of solvents but DMSO, a few drops of DMSO was added to the MeOH solution of **Pt-65a** to solubilize it completely.

X-ray crystallography grade single crystals of racemic **Pt-65a** was obtained upon slow addition of diethyl ether into a methanol/DMSO solution of **Pt-65a**, which later isolated as a yellow crystal. An X-ray diffraction study was performed to elucidate the molecular structure of complex **Pt-65a**. Its molecular structure was depicted in **Figure 3**. The selected bond lengths and bond angles were listed in **Table 2**. The X-ray diffraction study of complex **Pt-65a** revealed that the six-membered ring is in the boat conformation, with the phenyl ring in the axial position.

A rotated view of the molecular structure is illustrated in **Figure 4** to best visualize the boat conformation. The platinum centre adopts a square planar geometry with the tetrahedral distortion angle $\theta = 5.7^\circ$ between the planes of [Cl(1)-Pt(1)-Cl(2)] and [C(13)-Pt(1)-N(1)]. Besides that, the Pt(1)-Cl(2) bond is 0.058 Å longer than the Pt(1)-Cl(1) bond. This may be due to the *trans* effect as Cl(2) is *trans* to a strong *trans* directing ligand NHC as compared to the Cl(1). In addition, the electron density of the double bond is equally shared among the two nitrogen atoms next to the carbene atom in the imidazole ring. This is observed through the similar bond length of N(2)-C(13) and N(3)-C(13), which both are approximately equal to 1.36 Å (an average of a C-N bond of 1.465 Å and a C=N bond of 1.279 Å).

Hereby we observed the similar interesting characteristics of complex **Pt-65a**, which was similar to complex **Pd-65a** which was reported previously (Chiang, 2011). Firstly, instead of the chair conformation, the six-membered ring preferably adopted a boat conformation. This is because in chair conformation, the angles in the pyridine and imidazole ring will be highly tensed owing to the presence of many sp^2 hybridized atoms in the six-membered ring as well as the planar pyridine and imidazole ring. Secondly, the bulkier phenyl ring is in the axial position rather than the usual equatorial position. In axial position, the phenyl group experienced minimal steric interaction with the pyridine and imidazole ring, which is highly favorable. Besides that, the square planar geometry in the platinum center reduced the flagpole interaction experienced by the bulky phenyl group as the chlorine atoms will be pointing away from the phenyl group, thereby avoiding unfavorable steric interactions.



Scheme 39. Structure of racemic complex Pt-65a.

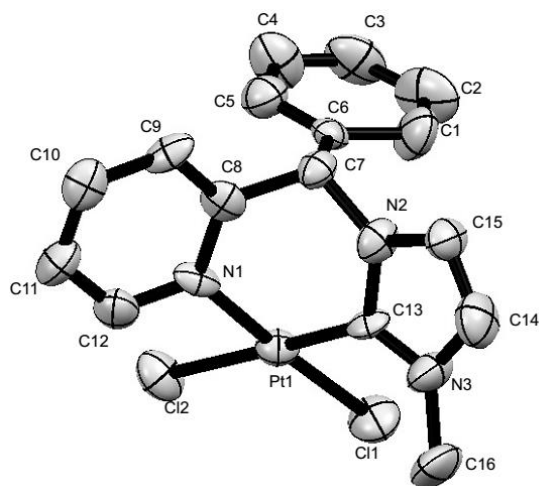


Figure 3. Molecular structure of racemic complex Pt-65a with thermal ellipsoids at 50% probability. DMSO solvent molecule and hydrogen atoms are omitted for clarity.

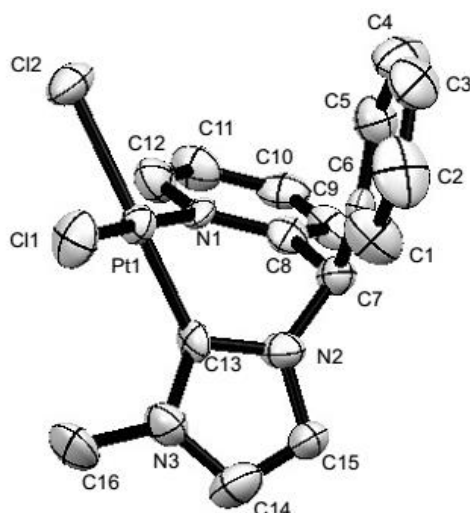


Figure 4. Rotated view of complex Pt-65a with thermal ellipsoids at 50% probability.

Table 2. Selected bond lengths (Å) and angles (°) for racemic complex Pt-65a.

Bond length (Å)	Pt(1)-Cl(1)	2.301(4)	N(2)-C(7)	1.47(2)
	Pt(1)-Cl(2)	2.359(4)	N(2)-C(13)	1.37(2)
	Pt(1)-N(1)	2.02(1)	N(2)-C(15)	1.41(2)
	Pt(1)-C(13)	1.95(1)	N(3)-C(13)	1.35(2)
	N(1)-C(8)	1.36(2)	N(3)-C(14)	1.40(2)
	N(1)-C(12)	1.33(2)	N(3)-C(16)	1.44(2)
	Bond angle (°)	Cl(1)-Pt(1)-Cl(2)	91.2(1)	Cl(2)-Pt(1)-C(13)
Cl(1)-Pt(1)-C(13)		92.4(4)	Cl(1)-Pt(1)-N(1)	176.8(3)
Cl(2)-Pt(1)-N(1)		90.8(3)	Pt(1)-C(13)-N(2)	119.9(9)
C(13)-Pt(1)-N(1)		85.8(5)	Pt(1)-N(1)-C(8)	120.1(9)
Pt(1)-C(13)-N(3)		136(1)	Pt(1)-N(1)-C(12)	120.0(9)

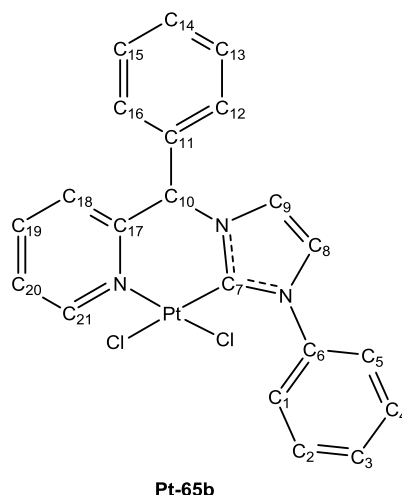
2.2.2.3.2. Characterisation of racemic complex Pt-65b

The racemic complex **Pt-65b** was obtained as an orange solid, 1.37 g, 45 %. MS (ESI) m/z : $[\text{MH-Cl}]^+$ calcd. for $\text{C}_{21}\text{H}_{18}\text{ClN}_3\text{Pt}$ 542.0837, found 542.0283. The formation of racemic complex **Pt-65b** was confirmed by the disappearance of the characteristic imidazolium proton peak at $\delta = 11.30$ ppm. Upon coordination, there is a general downfield shift in the ^1H NMR of racemic complex **Pt-65b** compared to imidazolium salt **64b**. The proton H10 have shifted downfield and is indistinguishable from other aromatic protons. Unlike **Pt-25a** and **Pt-25c**, there is no easily distinguishable proton, all appear in the aromatic region which was observed. Despite several attempts of recrystallization using different solvent system and different recrystallization method, we are unable to obtain crystals which are suitable for single crystal X-ray diffraction analysis to determine the absolute configuration of **Pt-65b**. Nevertheless, comparison was made to its counter complex **Pd-65b** via proton and carbon NMR (Table 3).

Table 3. ^1H and ^{13}C NMR spectral data for racemic complex Pt-65b in $\text{DMSO-}d_6$ and TMS as internal standard, with relative to racemic complex Pd-65b.

Pt-65b				Pd-65b			
δ ^1H , ppm ^a (m, integration, J in Hz)		δ ^{13}C , ppm ^b		δ ^1H , ppm ^a (m, integration, J in Hz)		δ ^{13}C , ppm ^b	
7.42 (s, 1H)	H10	67.53	C10	7.36-7.55 (m, 9 H)	arom.	67.08	C10
7.47-7.51 (m, 4 H)	arom.	121.83	C9			123.07	C9
7.55-7.61 (m, 4 H)	arom.	125.37	C8			123.90	C8
7.72-7.74 (m, 1 H)	H20	127.03	C20	7.66-7.71 (m, 1 H)	H20	124.83	C20
7.86-7.92 (m, 3 H)	arom.	127.45	C18	7.82-7.87 (m, 3 H)	arom.	125.13	C18
8.14-8.19 (m, 2 H)	H18, H9	128.89	arom.	8.03-8.10 (m, 2 H)	H18, H9	127.05	arom.
8.30-8.31 (m, 1 H)	H19	129.12	arom.	8.23 (m, 1 H)	H19	127.98	arom.
9.41 (dd, 1 H, $J_{\text{H,H}}$ = 1.2 Hz, 5.7 Hz)	H21	129.49	arom.	9.9.20-9.23 (m, 1 H)	H21	128.36	arom.
		129.82	arom.			128.57	arom.
		130.32	arom.			128.75	arom.
		139.04	arom.			137.73	arom.
		139.37	arom.			139.08	arom.
		140.76	C19			140.42	C19
		155.07	arom.			154.06	arom.
		155.58	C21			154.90	C21

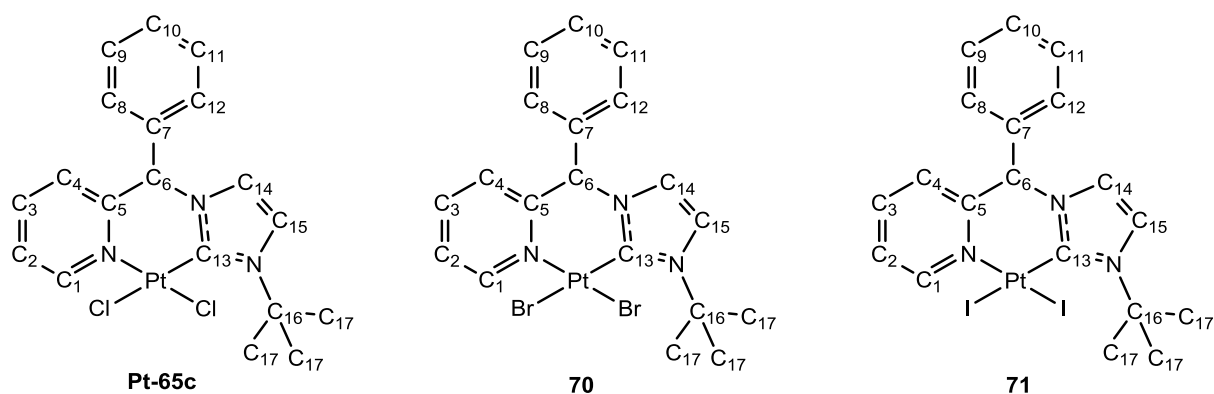
^aData were recorded at 300 MHz; ^bdata were recorded at 75 MHz.



Scheme 40. Structure of racemic complex Pt-65b.

2.2.2.3.3. Characterisation of racemic complex Pt-65c

Similarly, the racemic complex **Pt-65c** was isolated as a brown solid, 1.71 g (51 % yield). MS (ESI) m/z : $[M-H]^+$ calcd. for $C_{19}H_{20}Cl_2N_3Pt$ 555.0682, found 555.0453. The formation of racemic complex **Pt-65c** was identified by the disappearance of the characteristic imidazolium proton peak at $\delta = 11.19$ ppm and the proton at 1.61 ppm which contributed by *tert*-butyl (H17). A general downfield shift was observed in the 1H NMR of racemic complex **Pt-65c** compared to imidazolium salt **64c** upon coordination. We faced difficulties in obtaining crystallography grade crystals from recrystallization of racemic complex **Pt-65c**. Attempts to change the ancillary ligand from dichloro to dibromo and diiodo were performed since the dibromo complex **70** and diiodo complex **71** would have a poorer solubility in solvents as compared to dichloro complex, which may ease recrystallization (**Scheme 41**). The identities of these complex **70** and **71** were verified with the NMR and MS, which are both similar to the spectral data of complex **Pt-65c**. Unfortunately, both attempts failed to obtain the desired crystals of Pt NHC complexes. Nonetheless, comparison was made to its counter complex **Pd-65c** via 1H and ^{13}C NMR (**Table 4**) to confirm the structure of complex **Pt-65c**.



Scheme 41. Structure of racemic Pt NHC complexes Pt-65c, 70 and 71.

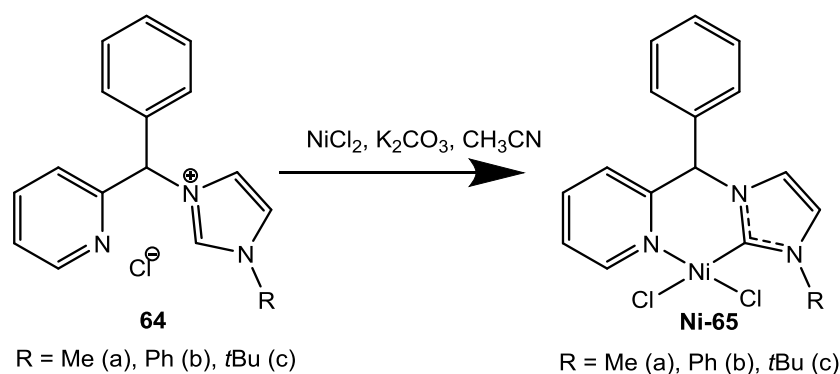
Table 4. ^1H and ^{13}C NMR spectral data for racemic complex Pt-65c in $\text{DMSO-}d_6$ and TMS as internal standard, with relative to racemic complex Pd-65c.

Pt-65c				Pd-65c			
δ ^1H , ppm ^a		δ ^{13}C , ppm ^b		δ ^1H , ppm ^a		δ ^{13}C , ppm ^b	
(m, integration, <i>J</i> in Hz)				(m, integration, <i>J</i> in Hz)			
1.61 (s, 9 H)	H17	30.88	C17	1.88 (s, 9 H)	H17	29.99	C17
7.21 (s, 1 H)	H6	60.38	C16	7.23 (s, 1 H)	H6	58.67	C16
7.34-7.48 (m, 6 H)	arom.	66.45	C6	7.36-7.46 (m, 5 H)	arom.	66.61	C6
		120.90	C15	7.58-7.62 (m, 1 H)	H2	120.27	C15
7.77-7.90 (m, 2 H)	H14, H15	123.02	C14	7.70 (s, 1 H)	H15	121.61	C14
7.94-7.96 (m, 1 H)	H4	123.89	C2	7.87 (s, 1 H)	H14	123.99	C2
8.07 (t, 1 H, $J_{\text{H,H}} = 2.1$ Hz)	H3	124.34	C4	7.99-8.02 (m, 1 H)	H4	124.98	C4
8.64-8.66 (m, 1 H)	H1	128.37	arom.	8.14-8.20 (m, 1 H)	H3	126.21	arom.
		128.96	arom.	9.96 (d, 1 H, $J_{\text{H,H}} = 5.1$ Hz)	H1	126.95	arom.
		129.56	arom.			127.43	arom.
		135.42	arom.			136.67	arom.
		137.43	arom.			139.06	arom.
		138.23	C3			149.64	C3
		150.09	arom.			153.86	arom.
		155.88	C1			153.98	C1

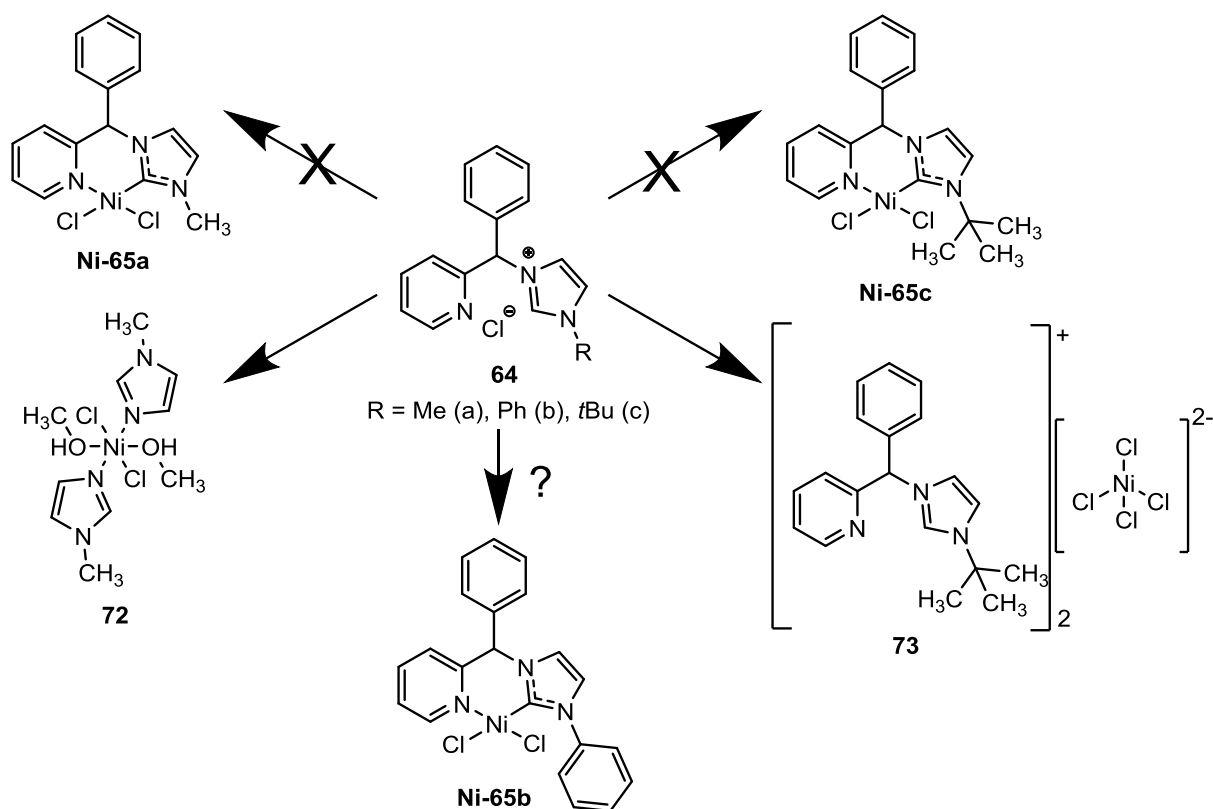
^aData were recorded at 300 MHz; ^b data were recorded at 75 MHz.

2.2.2.4. Synthesis and characterisation of racemic nickel NHC complexes

Unlike the palladium and platinum NHC complexes, we attempted another transmetalation method using NiCl₂, adapted from Ray et al. for synthesis of nickel NHC complexes (Ray et al., 2009). The imidazolium salts **64**, NiCl₂ and K₂CO₃ were stirred and refluxed for 24 hours in this one-pot synthesis method to obtain the crude Ni-NHC complexes (**Scheme 42**). Purification of the Ni-NHC complexes was performed using column chromatography, with CH₂Cl₂/MeOH (50:50 v/v) as the mobile phase, to yield the final complexes. The overall schematic representation for synthesis and characterisation of Ni NHC complexes in this project was illustrated in **Scheme 43**, with further discussion in the following sections.



Scheme 42. One-pot synthesis method for the transmetalation of the imidazolium salts (NHC precursors) (**64**) into racemic nickel NHC complexes (**Ni-65**).



Scheme 43. Overall schematic representation for synthesis and characterisation of Ni NHC complexes in this study.

Generally, it was observed that by using the NiCl_2 one-pot synthesis method, we were able to obtain the racemic Ni-NHC complexes **Ni-65** after purification with column chromatography, which were preliminarily confirmed by the proton NMR. However, different crystals structures were obtained upon recrystallisation: a nickel coordination complex **72** yielded from complex **Ni-65a** and a nickelate complex **73** yielded from complex **Ni-65c**. As a result, several attempts to optimize the synthesis of the designated Ni NHC complexes were performed as listed in **Table 5** below. Though none of the attempts successfully gave us the results similar to those of Pd NHC and Pt NHC complexes.

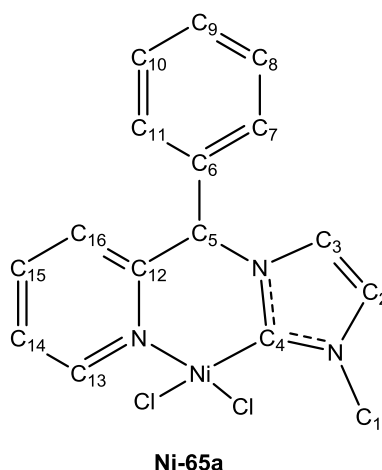
Table 5. List of synthesis parameters for optimizing the synthesis of Ni NHC complexes.

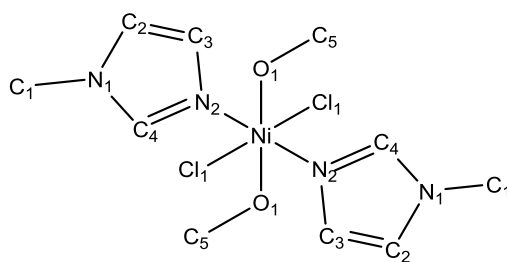
Method	Transmetalating agent	Solvent(s)	Temp. (°C)	Time (hrs)	Remarks ^a
One-pot synthesis	NiCl ₂	Acetonitrile	Reflux	24	Yes
One-pot synthesis	Ni(PPh ₃) ₂ Cl ₂	Acetonitrile	Reflux	24	No
Ag ₂ O-mediated	NiCl ₂	Dichloromethane	Room temp.	12	No
Ag ₂ O-mediated	Ni(PPh ₃) ₂ Cl ₂	Dichloromethane	Room temp.	12	No
Ag ₂ O-mediated	Ni(PPh ₃) ₂ Cl ₂	Dichloromethane	Reflux	24	No
Ag ₂ O-mediated	Ni(PPh ₃) ₂ Cl ₂	Dichloromethane	Reflux	8	No
Ag ₂ O-mediated	NiCl ₂	Dichloromethane	Reflux	24	No
Ag ₂ O-mediated	NiCl ₂	Dichloromethane, ethanol	Reflux	24	No
Ag ₂ O-mediated	NiCl ₂	Methanol	80	8	No
Ag ₂ O-mediated	NiCl ₂	Dichloromethane, methanol	65	8	No
Ag ₂ O-mediated	NiCl ₂	Dichloromethane, methanol	80	24	No
Ag ₂ O-mediated	NiCl ₂	Dichloromethane, methanol	50	24	No
Ag ₂ O-mediated	NiCl ₂	Tetrahydrofuran	Reflux	24	No

^a denotes that the reaction's final product was verified with proton NMR, compared and confirmed with the desired structures.

2.2.2.4.1. Characterisation of racemic complex Ni-65a

After purification, the racemic **Ni-65a** complex was isolated as a hygroscopic greenish brown solid, 3.30 g, 39 %. The identity of racemic complex **Ni-65a** was first confirmed using ¹H NMR before recrystallisation. Light green crystals were obtained from slow diffusion of diethyl ether into a methanol solution of racemic complex **Ni-65a**. Characterisation of the crystals using single crystal XRD analysis confirmed it to be an unexpected nickel coordination complex **72** with molecular formula of C₁₀H₂₁Cl₂N₄O₂Ni. The molecular ion peak for [MH-Cl]⁺ can be found at 322.0707 (calcd. 322.4378) in MS. Its molecular structure was depicted in **Figure 5**. The selected bond lengths and bond angles were listed in **Table 6**.

**Scheme 44. Structure of racemic complex Ni-65a.**



72

Scheme 45. Structure of unexpected crystal, nickel complex 72, obtained from recrystallization of racemic complex Ni-65a.

Table 6. Selected bond lengths (Å) and angles (°) for unexpected nickel complex 72.

Bond length (Å)	Ni(1)-Cl(1)	2.4502	Ni(1)-Cl(1)	2.4502
	Ni(1)-O(1)	2.1	Ni(1)-O(1)	2.1
	Ni(1)-N(2)	2.076	Ni(1)-N(2)	2.076
	O(1)-H(1)	0.85(2)	O(1)-H(1)	0.85(2)
	O(1)-C(5)	1.418(3)	O(1)-C(5)	1.418(3)
	N(2)-C(4)	1.315(4)	N(2)-C(4)	1.315(4)
	N(2)-C(3)	1.373(3)	N(2)-C(3)	1.373(3)
	N(1)-C(4)	1.344(3)	N(1)-C(4)	1.344(3)
	N(1)-C(2)	1.359(4)	N(1)-C(2)	1.359(4)
	N(1)-C(1)	1.467(5)	N(1)-C(1)	1.467(5)
	C(3)-C(2)	1.350(4)	C(3)-C(2)	1.350(4)
Bond angle (°)	N(2)-Ni(1)-Cl(1)	90.72	Cl(5)-Ni(1)-O(1)	89.59
	N(2)-Ni(1)-O(1)	90.79	Cl(4)-Ni(1)-O(1)	90.41
	N(2)-Ni(1)-Cl(1)	89.28	Cl(5)-Ni(1)-O(1)	89.59
	N(2)-Ni(1)-O(1)	89.21	Cl(4)-Ni(1)-O(1)	90.41
	O(7)-Ni(1)-N(1)	90.79	Cl(1)-Ni(1)-Cl(1)	180
	O(2)-Ni(1)-N(1)	89.21	O(1)-Ni(1)-O(1)	180
	Cl(2)-Ni(1)-N(1)	89.28	N(1)-Ni(1)-N(1)	180
	N(7)-Ni(1)-Cl(1)	90.72		

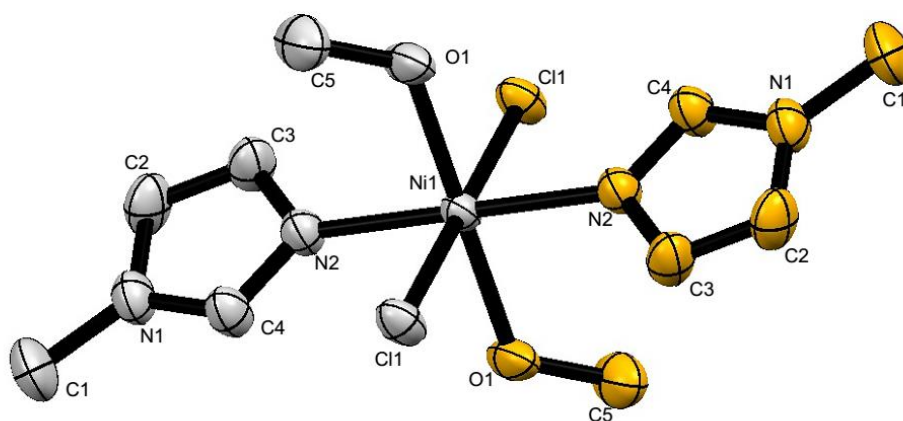


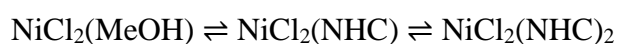
Figure 5. Molecular structure of unexpected nickel complex **72 with thermal ellipsoids at 50% probability. Hydrogen atoms are omitted for clarity.**

Based on the results, the crystal structure had a plane of inversion with a nickel centre. The nickel atom was coordinated to three different ligands including methanol, methylimidazole and chloride. The nickel centre adopted a standard octahedral conformation with six bonding atoms positioned at approximately 90° to each other. The incorporation of solvent molecule into a chemical structure as observed in complex **72** was not surprising. Zhang *et al.* had reported nickel NHC complexes that have solvent molecules incorporated into the structure apart of the NHC ring, where the solvent molecule is always located at the equatorial plane and arranged *trans* to a NHC ring (Zhang *et al.*, 2009).

Proton NMR was unable to resolve the peaks of complex **72**, regardless of whether DMSO- d_6 or CDCl₃ was used. Essentially, the unexpected complex **72** obtained from the recrystallization of **Ni-65a** was a high spin paramagnetic species (d^8 octahedral), which prevent NMR spectroscopic characterisation and hence their structures were only determined by X-ray diffraction studies. In the proton NMR spectra obtained for complex **72**, the signals are broad and unsatisfactory due to the different sets of ligand signals which indicates the different magnetically inequivalent ligands coordinated to the nickel center. This will be further accentuated if there are coordinating solvents, for example DMSO, that will coordinate to the metal centre and induce octahedral broadening. Also, the analysis of NMR spectrum is further complicated by the effect of the paramagnetic nickel center on chemical shifts.

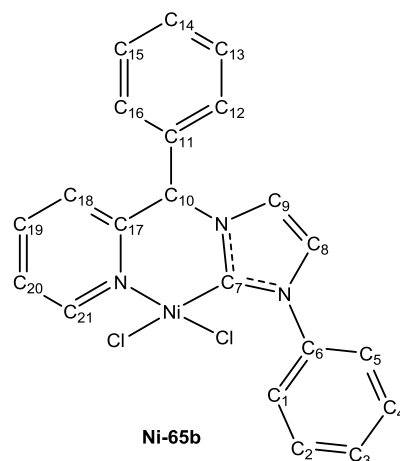
Previous literature reported different nickel NHC complexes with C-N bond cleavage which resulted in different Ni complexes as well as cleavage of a pyridine ligand around the metal organometallic center, which does not make our observation on C₅-N cleavage and attainment of complex **72** surprising (Zhong et al., 2016, Huertos et al., 2008). Zhong et al. had proposed that a complicated reaction took place during transmetalation, especially in methanol or other alcohol with the presence of a base, which resulted in the cleavage of the C-N bond of the adjacent bridge to the imidazolium ring though the exact mechanism is yet to be elucidated (Zhong et al., 2016).

Also, previously Winston et al. (2004) reported a series of Ni NHC complexes with varying coordination geometries, where they encountered the problems in obtaining pure crystals from Ni NHC complexes reaction mixture due to formation of co-crystals. This is similar to our observation on the selective isolation of complex **72** from complex **Ni-65a**, where the reason was not clear as well. It is characteristic of nickel(II) complexes that complicated equilibria, which are generally temperature dependent and sometimes concentration dependent, exist between the various structural types. Nevertheless, the formation of co-crystals can be rationalised by postulating the establishment of an equilibrium involving mono- and di-substituted Ni containing species. The equilibrium proposed below is thereby plausible and has been suggested for other Ni(II)/bidendate ligand system (Winston et al., 2004, Handley et al., 2001).



2.2.2.4.2. Characterisation of racemic complex **Ni-65b**

After purification using column chromatography, the racemic **Ni-65b** complex was isolated as a brown solid, 0.43 g, 34 %. The ¹H NMR was performed to preliminarily determine the identity of racemic complex **Ni-65b** before recrystallisation. Unfortunately, despite several attempts of recrystallization using different solvent systems and different recrystallization methods, we are unable to obtain crystals which are suitable for single crystal X-ray diffraction analysis to determine the absolute configuration of **Ni-65b**.



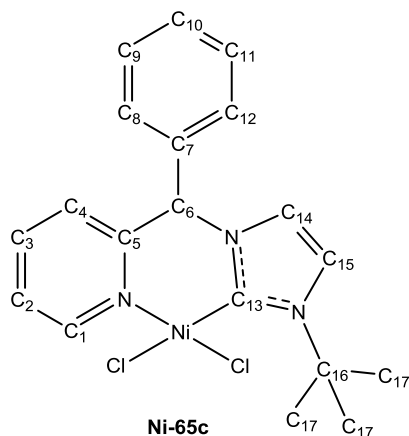
Scheme 46. Structure of racemic complex Ni-65b.

2.2.2.4.3. Characterisation of racemic complex Ni-65c

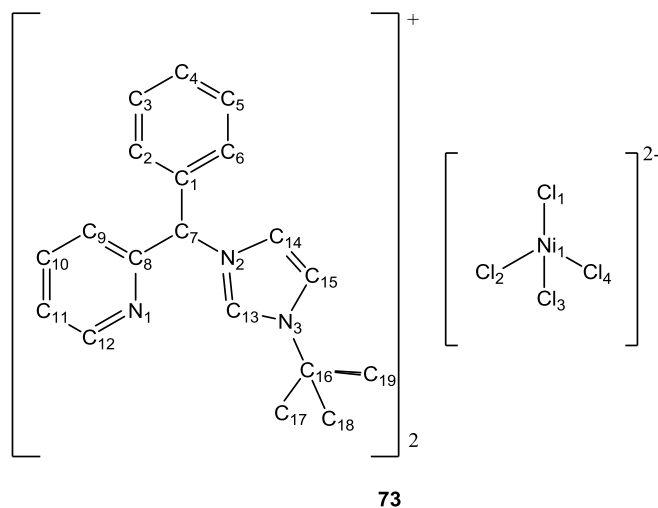
After purified with column chromatography, the racemic **Ni-65c** complex was isolated as a hygroscopic green solid, 1.53 g, 73 %. The preliminary identification of racemic complex **Ni-65c** was performed using ^1H NMR before proceeded to recrystallisation. Blue green crystals were obtained from slow diffusion of diethyl ether into a methanol solution of racemic complex **Ni-65c**. Characterisation of the crystals using single crystal XRD analysis confirmed it to be an unexpected nickelate complex **73** with molecular formula of $(\text{C}_{19}\text{H}_{22}\text{N}_3)_2\text{NiCl}_4$ (**Figure 6**). The molecular ion peak for $[\text{M-NiCl}_4]^+$ can be found at 291.1700 (calcd. 292..1814) in MS. The selected bond lengths and angles were presented in **Table 7**. Based on the results, the crystal was made up of two units of positively-charged pyridine-functionalised imidazole ring with *tert*-butyl, and a negatively-charged NiCl_4^{2-} ion. The negatively-charged NiCl_4^{2-} ion was in an expected tetrahedral coordination geometry with an average angle of 109.5° . From the bond length of N(3)-C(13), N(2)-C(13) and C(15)-C(14), also corresponded to N(5)-C(32), N(6)-C(32) and C(33)-C(34), which are all approximately 1.33 Å, it is evident that the positive charge delocalised over the entire five-membered imidazole ring, thereby offering the cationic ligand additional stability.

Zhang et al. had suggested that it is impossible to host two ligands around nickel ions due to large steric hindrance, hence the failure in incorporation of large and bulky group to create Ni NHC complexes (Zhang et al., 2009). In addition to that, weaker M-C bonds are being formed in Ni case as compared to Pd and Pt. Therefore, it is speculated that the separation of the bulky

phenyl group and pyridine group from the overall structure of complex **Ni-65c**, which yielded complex **73** upon recrystallization, could be due to their large steric repulsion pressure that force the complex to restructure. It was previously reported in literature that reprotonation of the carbene moieties had occurred upon transmetalation, instead of transfer to nickel, with formation of a mixed tetrachloronickelate/chloride imidazolium salt (Hameury et al., 2014b, Hameury et al., 2014a). It was reasoned that the formation of stable $[\text{NiCl}_4]^{2-}$ was more kinetically favoured as compared to transmetalation to Ni, thus preventing transmetalation.



Scheme 47. Structure of racemic complex Ni-65c.



Scheme 48. Structure of unexpected crystal, nickel complex 73, obtained from recrystallization of racemic complex Ni-65c.

Table 7. Selected bond lengths (Å) and angles (°) for unexpected nickel complex 73.

	Ni(1)-Cl(2)	2.268(2)	Ni(1)-Cl(3)	2.238(2)
	Ni(1)-Cl(1)	2.253(2)	Ni(1)-Cl(4)	2.253(2)
	N(5)-C(26)	1.483(8)	N(3)-C(13)	1.342(8)
	N(5)-C(32)	1.331(5)	N(3)-C(15)	1.359(8)
	N(5)-C(33)	1.366(9)	N(3)-C(16)	1.496(6)
	N(6)-C(32)	1.33(1)	N(2)-C(13)	1.323(6)
	N(6)-C(34)	1.370(7)	N(2)-C(7)	1.488(7)
	N(6)-C(35)	1.496(8)	N(2)-C(14)	1.365(9)
	N(4)-C(27)	1.347(8)	C(1)-C(6)	1.382(7)
	N(4)-C(31)	1.338(9)	C(1)-C(7)	1.517(6)
	C(26)-C(27)	1.513(7)	C(1)-C(2)	1.39(1)
	C(26)-C(20)	1.514(5)	N(1)-C(8)	1.315(7)
	C(27)-C(28)	1.38(1)	N(1)-C(12)	1.34(1)
Bond length (Å)	C(20)-C(25)	1.393(8)	C(8)-C(7)	1.508(9)
	C(20)-C(21)	1.379(8)	C(8)-C(9)	1.41(1)
	C(28)-C(29)	1.39(1)	C(6)-C(5)	1.380(7)
	C(25)-C(24)	1.368(8)	C(15)-C(14)	1.35(1)
	C(33)-C(34)	1.35(1)	C(16)-C(17)	1.52(1)
	C(29)-C(30)	1.39(1)	C(16)-C(18)	1.53(1)
	C(21)-C(22)	1.393(9)	C(16)-C(19)	1.52(1)
	C(31)-C(30)	1.38(2)	C(9)-C(10)	1.38(2)
	C(35)-C(37)	1.50(1)	C(5)-C(4)	1.37(1)
	C(35)-C(38)	1.52(1)	C(2)-C(3)	1.375(9)
	C(35)-C(36)	1.54(1)	C(10)-C(11)	1.33(1)
	C(24)-C(23)	1.36(1)	C(4)-C(3)	1.38(1)
	C(22)-C(23)	1.36(1)	C(12)-C(11)	1.37(2)
	Cl(1)-Ni(1)-Cl(2)	116.54(7)	Cl(1)-Ni(1)-Cl(2)	105.02(7)
Bond angle (°)	Cl(1)-Ni(1)-Cl(3)	106.88(7)	Cl(1)-Ni(1)-Cl(3)	112.82(7)
	Cl(1)-Ni(1)-Cl(4)	107.64(7)	Cl(1)-Ni(1)-Cl(2)	108.12(7)

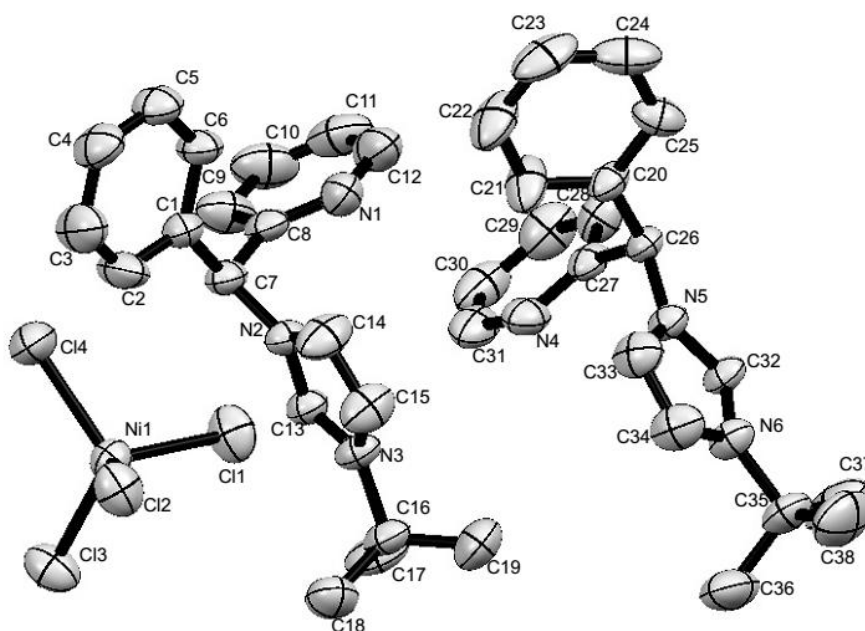


Figure 6. Molecular structure of unexpected nickel complex 73 with thermal ellipsoids at 50% probability. Hydrogen atoms are omitted for clarity.

2.3. Conclusion

In this chapter, a series of precursors, imidazolium salts (NHC precursors), and Group 10 metal NHC complexes were successfully synthesized. The structures and identities of the synthesized complexes have been investigated and confirmed by using different spectroscopy techniques including proton (^1H) and carbon (^{13}C) nuclear magnetic resonance (NMR) spectroscopy as well as mass spectrometry. Following recrystallisation, the absolute configuration of a platinum NHC complex in solid state had been successfully elucidated via single crystal X ray crystallography. The six-membered ring of the platinum NHC complex adopted a boat conformation with the phenyl ring arranged at the axial position. Meanwhile, two unexpected nickel complexes, i.e. simple nickel coordination complex and nickelate complex, were obtained upon recrystallisation from Ni NHC complexes and studied using X ray crystallography. Apart from that, two racemic palladium NHC complexes were separated into their respective enantiomers via optical resolution approach. The stability of these metal NHC complexes in both solid and liquid state at room temperature is highly desirable characteristics of drug candidates, thereby their biological activities will be studied.

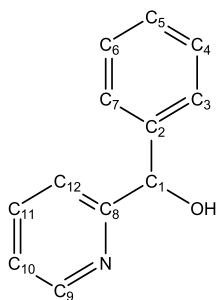
2.4. Experimental

2.4.1. General procedures

All the commercially available chemicals and solvents were used without prior drying or purification. Reactions involving air-sensitive compounds were performed under a positive pressure of nitrogen. Bis(acetonitrile)palladium chloride $\text{PdCl}_2(\text{CH}_3\text{CN})_2$, dichloro(1, 5-cyclooctadiene)platinum(II) $\text{Pt}(\text{cod})\text{Cl}_2$, 1-phenylimidazole and 1-*tert*-butylimidazole were prepared according to literature methods with some modifications (Cowley et al., 2006, Mathews et al., 2004, McDermott et al., 1976, Rout et al., 2007). Melting point determination was carried out using Stuart Digital Melting Point Apparatus SMP10 with 1 °C resolution. Mass spectra were recorded on Agilent 1290 Infinity LC system coupled to Agilent 6520 Accurate-Mass Q-TOF mass spectrometer with dual ESI source. Optical activity of the diastereomers and enantiomers were determined by using Rudolph AUTOPOL VI automatic polarimeter at 436nm. Proton nuclear magnetic resonance (^1H NMR) and carbon nuclear magnetic resonance (^{13}C NMR) spectroscopy were performed on a Bruker Advance 300 NMR spectrometer. The number of protons (n) for a given resonance is indicated by n H. Coupling constants are reported as a *J* value in Hz. Proton nuclear magnetic resonance spectra ^1H NMR are reported as δ in units of parts per million (ppm) downfield from SiMe_4 (δ 0.00). Carbon nuclear magnetic resonance spectra ^{13}C NMR are reported as δ in units of parts per million (ppm) relative to the signal of chloroform-*d* (δ 77.16 ppm, triplet) and DMSO-*d*₆ (δ 39.52 ppm, septet). All chemical shifts reported are referenced to the chemical shifts of their respective residual solvent resonances. Unless stated otherwise, all NMR experiments are carried out at 300 K. The single crystal X ray diffraction studies were performed by X ray crystallography facilities in University Malaya (UM) and Universiti Kebangsaan Malaysia (UKM), Malaysia.

2.4.2. Synthesis and characterisation of imidazolium salts (NHC precursors) 64

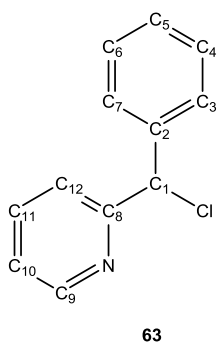
2.4.2.1. Synthesis of phenyl(pyridine-2-yl)methanol, 62



62

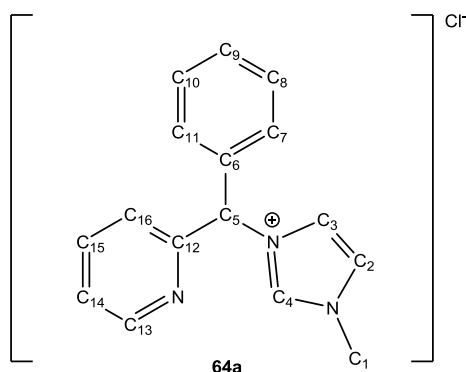
The method for reduction of 2-benzoylpyridine into phenyl(pyridin-2-yl)methanol was modified from literature (Kim and Kang, 2014). Sodium borohydride (2.04 g, 53.9 mmol) in 50 mL 95 % ethanol was added dropwise into a solution of 2-benzoylpyridine (5.00 g, 27.3 mmol) in 50.0 mL 95% ethanol on an ice bath. The reaction mixture was stirred continuously for 1 hour until reaction is completed. Then, 100 mL of water was added to the reaction mixture and the solution was heated at 90 °C for 15 minutes. Then, the solution was extracted with ethyl acetate thrice and the solvent was evaporated under reduced pressure to obtain a pale green oil. Slow evaporation of a solution in ethanol at room temperature yielded the clear crystal solid, 5.01 g, 96.4 %. M.p. = 88 – 90 °C. ¹H NMR (300 MHz, CDCl₃): δ = 5.29 (d, 1 H, *J*_{H,H} = 4.5 Hz, OH), 5.75 (d, 1 H, *J*_{H,H} = 4.5 Hz, H1), 7.13-7.39 (m, 7 H, arom.), 7.60-7.61 (m, 1 H, arom.) and 8.55 (ddd, 1 H, *J*_{H,H} = 5.1 Hz, *J*_{H,H} = 1.2 Hz, *J*_{H,H} = 0.9 Hz, arom.) ppm. ¹³C NMR (75 MHz, CDCl₃): δ = 75.00 (C1), 121.35, 122.42, 127.07, 127.82, 128.56, 136.83, 143.23, 147.83 and 160.91 (arom.) ppm. MS (ESI) *m/z*: [M+H]⁺ calcd. for C₁₂H₁₂NO 186.0919, found 186.0912.

2.4.2.2. Synthesis of 2-(chloro(phenyl)methyl)pyridine, **63**



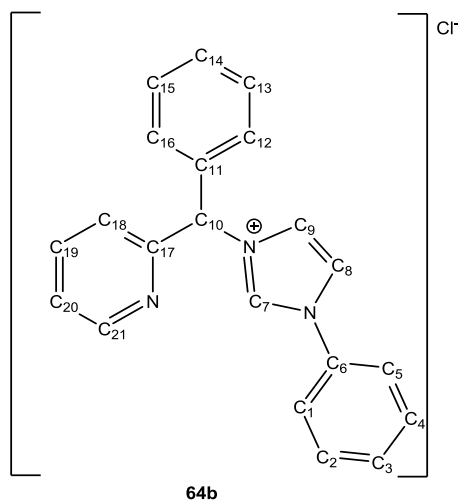
Phenyl(pyridin-2-yl)methanol **62** (1.85 g, 10.5 mmol) and triethylamine (3.40 mL, 24.4 mmol) in 32.0 mL of CH_2Cl_2 was stirred in an ice bath. Methanesulfonyl chloride (1.20 mL, 15.8 mmol) was added dropwise into the stirring solution. The reaction mixture was left to warm up slowly to room temperature. The reaction mixture was allowed to stir overnight and then poured into a saturated aqueous NaHCO_3 solution. The aqueous layer was extracted with chloroform thrice. The combined organic layers were washed with H_2O , dried over anhydrous MgSO_4 and evaporated *in vacuo* to give a red liquid. The resultant red liquid was subjected to column chromatography (ethyl acetate/hexane 1:4 v/v) to give yellow oil, 1.52 g, 74.3 %. The spectral data for this compound are consistent with those reported in the literature (Chiang et al., 2010). ^1H NMR (300 MHz, CDCl_3): δ = 6.16 (s, 1 H, H1), 7.20 (ddd, 1 H, $J_{\text{H,H}} = 7.5$ Hz, $J_{\text{H,H}} = 4.8$ Hz, $J_{\text{H,H}} = 1.2$ Hz, arom.), 7.25-7.37 (m, 3 H, arom.), 7.45-7.56 (m, 3 H, arom.), 7.67-7.73 (m, 1 H, arom.) and 8.57 (ddd, 1 H, $J_{\text{H,H}} = 4.8$, $J_{\text{H,H}} = 1.8$, $J_{\text{H,H}} = 0.9$ Hz, H9) ppm. ^{13}C NMR (75 MHz, CDCl_3): δ = 64.54 (C1), 122.09 and 122.81 (arom.), 127.78 (C10), 128.28 (C12), 128.64 and 137.05 (arom.), 139.96 (C12), 149.19 (C8) and 159.75 (C9) ppm. MS (ESI) m/z : $[\text{M}-\text{Cl}]^+$ calcd. for $\text{C}_{12}\text{H}_{10}\text{N}$ 168.0813, found 168.0804.

2.4.2.3. Synthesis of 1-methyl-3-[phenyl(pyridin-2-yl)methyl]-1*H*-imidazolium chloride, **64a**



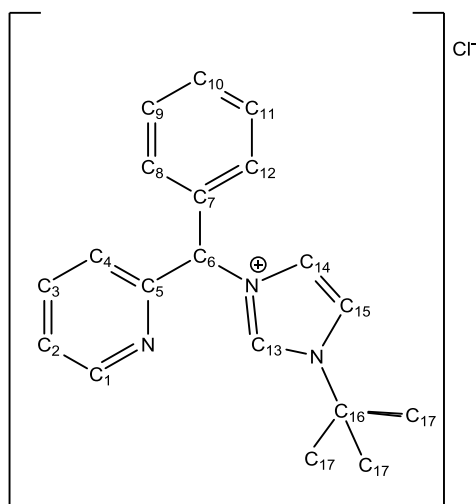
Liquid 1-methylimidazole (1.80 mL, 22.6 mmol) was added to a stirring solution of compound **63** (4.60 g, 22.6 mmol) in 50.0 mL of CH₃CN. The reaction mixture was heated at refluxing temperature for 48 hours. The reaction mixture was reduced *in vacuo* and the resulting oil was stirred in diethyl ether. The diethyl ether layer was decanted away to give a hygroscopic off white solid, 2.97 g, 45.8 %. The spectral data for the compound are consistent with those reported in the literature (Chiang et al., 2010). ¹H NMR (300 MHz, CDCl₃): δ = 4.03 (s, 3 H, CH₃), 7.26-7.37 (m, 4 H, arom.) 7.41-7.46 (m, 3 H, arom.), 7.63-7.76 (m, 4 H, arom.), 8.57-8.60 (m, 1 H, H13) and 10.39 (s, 1 H, H4) ppm. ¹³C NMR (75 MHz, CDCl₃): δ = 36.63 (C1), 65.98 (C5), 122.48 (C2), 122.58 (C3), 123.78 (C14), 124.36 (C16), 128.84, 129.24, 129.34, 136.43 and 137.61 (arom.), 137.85 (C15), 149.52 (arom.) and 155.09 (C13) ppm. MS (ESI) *m/z*: [M-H]⁺ calcd. for C₁₆H₁₅N₃Cl 284.0954, found 284.2074.

2.4.2.4. Synthesis of 1-phenyl-3-[phenyl(pyridin-2-yl)methyl]-1*H*-imidazolium chloride, **64b**



Liquid 1-phenylimidazole (3.24 g, 24.5 mmol) was added to a stirring solution of compound **63** (5.00 g, 24.5 mmol) in 50.0 mL of CH₃CN. The reaction mixture was heated at refluxing temperature for 48 hours. The reaction mixture was reduced *in vacuo* and the resulting oil was stirred in diethyl ether. The diethyl ether layer was decanted away to give a brown oil, 2.71g, 28.8%. The spectral data for the compound are consistent with those reported in the literature (Chiang, 2011). ¹H NMR (300 MHz, CDCl₃): δ = 7.34-7.39 (m, 3 H, arom.), 7.49-7.61 (m, 5 H, arom.), 7.67-7.79 (m, 5 H, arom.), 7.96 (t, 1 H, *J*_{H,H} = 1.8 Hz, arom.), 8.23 (s, 1H, H10), 8.60 (ddd, 1 H, *J*_{H,H} = 0.9 Hz, *J*_{H,H} = 1.8 Hz, *J*_{H,H} = 4.8 Hz, H21) and 11.30 (s, 1 H, H7) ppm. ¹³C NMR (75 MHz, CDCl₃): δ = 65.82 (C10), 119.47 (C8), 121.71 (C20), 123.44 (C18), 123.80, 124.81, 129.10, 129.25, 129.41, 130.19, 130.56, 134.54, 136.28, 136.42, 137.71 and 149.34 (arom.), 155.02 (C17) ppm. MS (ESI) *m/z*: [M-Cl]⁺ calcd. for C₂₁H₁₈N₃ 312.1501, found 312.1508.

2.4.2.5. Synthesis of 1-*tert*-butyl-3-[phenyl(pyridin-2-yl)methyl]-1*H*-imidazolium chloride, **64c**

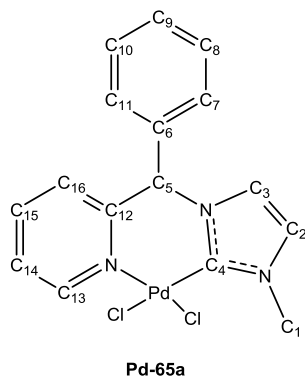


64c

Liquid 1-*tert*-butylimidazole (5.00 g, 40.3 mmol) was added to a stirring solution of compound **63** (8.21 g, 40.3 mmol) in 100 mL of CH₃CN. The reaction mixture was heated at refluxing temperature for 48 hours. The reaction mixture was reduced *in vacuo* and the resulting oil was stirred in diethyl ether. The diethyl ether layer was decanted away to give a brown solid, 8.24 g, 54.0 %. The spectral data for the compound are consistent with those reported in the literature (Ng et al., 2013). ¹H NMR (300 MHz, CDCl₃): δ = 1.70 (s, 9 H, H17), 7.27-7.37 (m, 5 H, arom.), 7.50-7.55 (m, 2H, arom.), 7.69-7.75 (m, 1 H, arom.), 7.81-7.83 (m, 1 H, arom.), 8.14 (s, 1 H, arom.), 8.59 (ddd, 1 H, *J*_{H,H} = 0.9 Hz, *J*_{H,H} = 1.8 Hz, *J*_{H,H} = 4.8 Hz, H1) and 11.19 (s, 1 H, H13) ppm. ¹³C NMR (75 MHz, CDCl₃): δ = 30.05 (C17), 60.13 (C16), 65.26 (C6), 117.97 (C15), 122.50 (C14), 123.60 (C2), 124.87 (C4), 128.91, 129.07, 136.53 and 136.96 (arom.), 137.55 (C3), 149.30 (arom.) and 155.44 (C1) ppm. MS (ESI) *m/z*: [M-Cl]⁺ calcd. for C₁₉H₂₂N₃ 292.1814, found 292.3259.

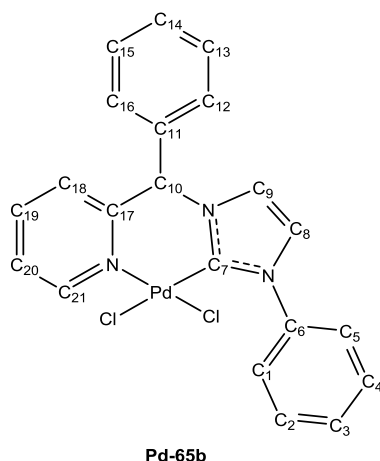
2.4.3. Synthesis of racemic palladium NHC complexes

2.4.3.1. Synthesis of racemic complex (\pm)-Pd-65a



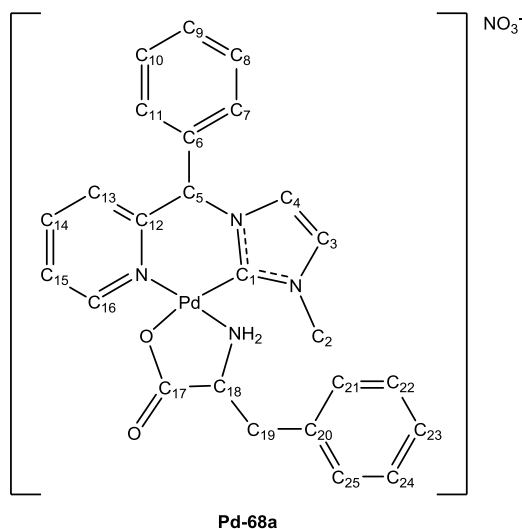
To a solution of compound **64a** (3.57 g, 12.5 mmol) in 30.0 mL of CH₂Cl₂, Ag₂O (1.58 g, 6.81 mmol) was added in the dark. The reaction mixture was stirred at room temperature overnight and was filtered through a short plug of celite. A PdCl₂(CH₃CN)₂ suspension (3.24 g, 12.5 mmol in 100 mL CH₃CN) was added to the filtrate in the dark. The reaction mixture was then allowed to stir overnight at room temperature and was filtered through celite the next day. The filtrate was reduced *in vacuo* to approximately 50.0 mL and then 200 mL of diethyl ether was added which resulted in the precipitation of orange-yellow solid 2.10 g, 37.6 %. The spectral data for the compound are consistent with those reported in the literature (Chiang et al., 2010). M.p. = 245 – 247 °C (decomposed). ¹H NMR (300 MHz, DMSO-*d*₆): δ = 3.96 (s, 3 H, H1), 7.26 (s, 1 H, H5), 7.35-7.50 (m, 5 H, arom.), 7.60-7.65 (m, 1 H, H14), 7.81 (d, 1 H, *J*_{H,H} = 1.8 Hz, H3), 8.00-8.02 (m, 1 H, H16), 8.20 (td, 1 H, *J*_{H,H} = 1.5 Hz, *J*_{H,H} = 7.8 Hz, H15) and 9.10-9.16 (m, 1 H, H13) ppm. ¹³C NMR (75 MHz, DMSO-*d*₆): δ = 38.35 (C1), 67.07 (C5), 122.89 (C2), 124.62 (C3), 125.60 (C14), 126.81 (C16), 127.45, 128.81, 129.28 and 140.94 (arom.), 152.08 (C15), and 155.06 (C13) ppm. MS (ESI) *m/z*: [M-Cl]⁺ calcd. for C₁₆H₁₅ClN₃Pd 389.9989, found 390.3347.

2.4.3.2. Synthesis of racemic complex (\pm)-Pd-65b



To a solution of compound **64b** (4.50 g, 13.4 mmol) in 30.0 mL of CH_2Cl_2 , Ag_2O (1.70 g, 7.34 mmol) was added in the dark. The reaction mixture was stirred at room temperature overnight and was filtered through a short plug of celite. A $\text{PdCl}_2(\text{CH}_3\text{CN})_2$ suspension (3.48 g, 13.4 mmol in 100 mL CH_3CN) was added to the filtrate in the dark. The reaction mixture was then allowed to stir overnight at room temperature and was filtered through celite the next day. The filtrate was reduced *in vacuo* to approximately 50.0 mL and then 200 mL of diethyl ether was added which resulted in the precipitation of orange-yellow solid 1.50 g, 39.9 %. M.p. = 288 – 289 °C (decomposed). The spectral data for the compound are consistent with those reported in the literature (Chiang, 2011). ^1H NMR (300 MHz, $\text{DMSO}-d_6$): δ = 7.36-7.55 (m, 9 H, arom.), 7.66-7.71 (m, 1 H, H20), 7.82-7.87 (m, 3 H, arom.), 8.03-8.10 (m, 2 H, H18 and H9), 8.17-8.22 (m, 1 H, H19) and 9.9.20-9.23 (m, 1 H, H21) ppm. ^{13}C NMR (75 MHz, $\text{DMSO}-d_6$): δ = 67.08 (C10), 123.07 (C9), 123.90 (C8), 124.83 (C20), 125.13 (C18), 127.05, 127.98, 128.36, 128.57, 128.75, 137.73 and 139.08 (arom.) 140.42 (C19), 154.06 (arom.) and 154.90 (C21) ppm. MS (ESI) m/z : $[\text{M}-\text{Cl}]^+$ calcd. for $\text{C}_{21}\text{H}_{17}\text{ClN}_3\text{Pd}$ 452.0146, found 451.9980.

left to stand overnight. From the diastereomeric mixture, only complex **Pd-(Rc,Sc)-68a** crystallized out as off-white crystals the next day and was isolated and washed with MeOH. The mother liquor was enriched with **Pd-(Sc,Sc)-68a**. The spectral data for the diastereomer is consistent with previous literature (Chiang et al., 2010).

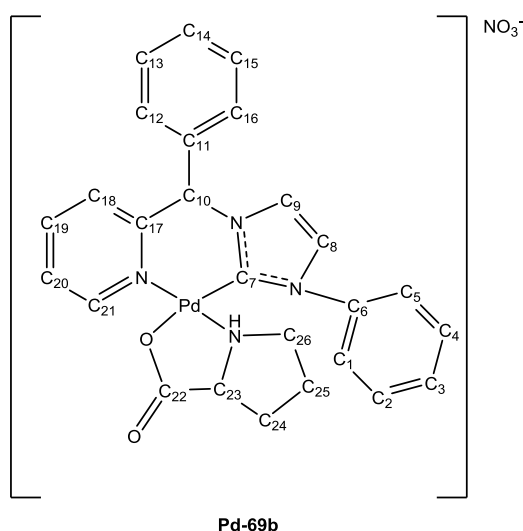


Diastereomer **Pd-(Rc,Sc)-68a**: Off white solid. $[\alpha]_{436} +78.6$ (*c* 0.05, DMSO), lit.(Chiang et al., 2010) $[\alpha]_{436} +83.3$ (*c* 0.5, DMSO). M.p. = 133 – 135 °C (decomposed). ^1H NMR (300 MHz, DMSO-*d*₆): δ = 2.63 (dd, 1 H, $J_{\text{H,H}} = 6.0$ Hz, $J_{\text{H,H}} = 14.4$ Hz, H18), 3.17 (d, 1 H, $J_{\text{H,H}} = 5.4$ Hz, H19), 3.47-3.54 (m, 1 H, H19), 3.75 (s, 3 H, H2), 4.99 (d, 1 H, $J_{\text{H,H}} = 9.9$ Hz, NH), 5.99-6.02 (m, 1 H, NH), 6.94-6.98 (d, 2 H, arom.), 7.17-7.26 (m, 4 H, arom.), 7.34-7.42 (m, 3 H, arom.), 7.47-7.52 (m, 2 H, arom.), 7.60 (d, 1 H, $J_{\text{H,H}} = 1.8$ Hz, arom.), 7.75-7.80 (m, 1 H, arom.), 7.91 (d, 1 H, $J_{\text{H,H}} = 1.8$ Hz, arom.), 8.15-8.18 (m, 1 H, arom.), 8.32-8.38 (m, 1 H, arom.) and 8.72 (dd, 1 H, $J_{\text{H,H}} = 1.5$ Hz, $J_{\text{H,H}} = 5.7$ Hz, H16) ppm. ^{13}C NMR (75 MHz, DMSO-*d*₆): δ = 36.66 (C2), 48.48 (C19), 62.13 (C5), 65.80 (C18), 123.02 (C3), 124.04 (C4), 126.06 (C15), 126.23 (C13), 126.50, 127.08, 127.98, 128.36, 128.71, 129.00, 136.73, 139.14, 141.54, 151.14 and 152.52 (Ph), 154.15 (C16) and 178.64 (C17) ppm. MS (ESI) *m/z*: $[\text{M}-\text{NO}_3]^+$ calcd. for C₂₅H₂₅N₄O₂Pd 519.1012, found 519.1048.

The optically active **Pd-(Rc)-65a** was obtained by stirring a methanol solution of diastereomer **Pd-(Rc,Sc)-68a** with 1 M HCl. The optically active **Pd-(Rc)-65a** was isolated as a yellow powder, 59.0 %. $[\alpha]_{436} +87.4$ (*c* 0.05, DMSO), lit.(Chiang et al., 2010) $[\alpha]_{436} -12.5$ (*c* 0.5, DMSO). MS (ESI) *m/z*: $[\text{M}-\text{Cl}]^+$ calcd. for C₁₆H₁₅ClN₃Pd 389.9989, found 390.3345.

2.4.4.2. Optical resolution of racemic complex Pd-65b

To a suspension of the racemic complex **Pd-65b** (0.260 g, 0.530 mmol) in 20.0 mL of MeOH, AgNO₃ (0.180 g, 1.06mmol) was added. The reaction mixture was allowed to stir in the dark at room temperature for 3 hours and was filtered through celite. The orange filtrate was treated with sodium (*Sc*)-prolinate (0.070 g, 0.530 mmol) in 100 mL MeOH. The reaction was then stirred for 2 hours and was concentrated to approximately 50.0 mL and was left to stand overnight. From the diastereomic mixture, only complex **Pd-(*Sc,Sc*)-69b** crystallized out as off-white crystals the next day and was isolated and washed with MeOH. The mother liquor was enriched with **Pd-(*Rc,Sc*)-69b**. The spectral data for the diastereomer is consistent with previous literature (Ng et al., 2013).

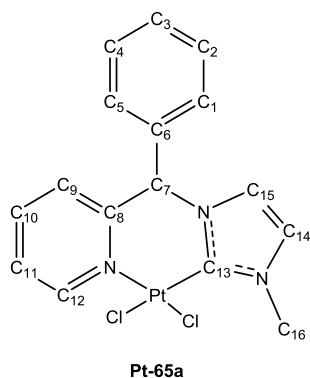


Diastereomer **Pd-(*Sc,Sc*)-69b**: Off-white solid. [α]₄₃₆ -153.2 (*c* 0.05, DMSO), lit.(Ng et al., 2013) [α]₄₃₆ -167 (*c* 0.5, DMSO). M.p. = 222 – 223 °C (decomposed). ¹H NMR (300 MHz, DMSO-*d*₆): δ = 1.07-1.12 (m, 1 H, H24), 1.20-1.26 (m, 1 H, H25), 1.46-1.50 (m, 1 H, H25), 1.69-1.75 (m, 1 H, H26), 2.15-2.18 (m, 1 H, H26), 7.39-7.49 (m, 6 H, arom.), 7.62-7.64 (m, 1 H, arom.), 7.67-7.72 (m, 2 H, arom.), 7.75-7.79 (m, 1 H, arom.), 7.87-7.90 (m, 2 H, arom.), 7.93-7.94 (m, 1 H, arom.), 8.13 (d, 1 H, $J_{H,H}$ = 2.1 Hz, arom.), 8.22 (dd, 1 H, $J_{H,H}$ = 7.8 Hz, $J_{H,H}$ = 1.5 Hz, arom.), 8.32-8.37 (m, 1 H, H19) and 8.75 (dd, 1 H, $J_{H,H}$ = 6.0 Hz, $J_{H,H}$ = 1.8 Hz, H21) ppm. ¹³C NMR (75 MHz, DMSO-*d*₆): δ = 22.90 (C24), 28.27 (C25), 49.36 (C26), 66.80 (C10), 67.07 (C23), 124.47 (C9), 124.82 (C8), 126.40 (C20), 126.62 (C18), 127.14, 127.32, 129.02, 129.47, 130.20, 130.35, 153.31 and 153.45 (Ph), 154.96 (C21) and 178.13 (C22) ppm. MS (ESI) *m/z*: [M-HNO₃]⁺ calcd. for C₂₉H₂₆N₄O₂Pd 568.1091, found 568.1928.

The optically active **Pd-(Sc)-65b** was obtained by stirring a methanol solution of diastereomer **Pd-(Sc,Sc)-69b** with 1 M HCl. The optically active **Pd-(Sc)-65b** was isolated as a yellow powder in 50.0 % yield. $[\alpha]_{436} -45.7$ (c 0.05, DMSO), lit. (Ng et al., 2013) $[\alpha]_{436} -27.8$ (c 0.2, MeOH). MS (ESI) m/z : $[M-Cl]^+$ calcd. for $C_{21}H_{17}ClN_3Pd$ 452.0146, found 452.0022.

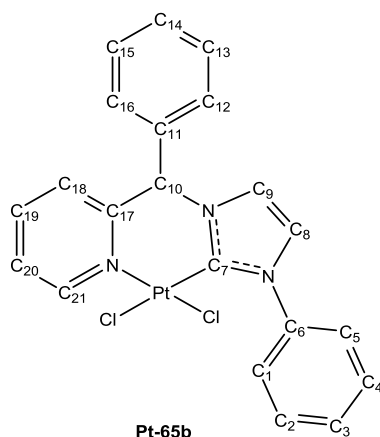
2.4.5. Synthesis of racemic platinum NHC complexes

2.4.5.1. Synthesis of racemic complex (\pm)-Pt-65a



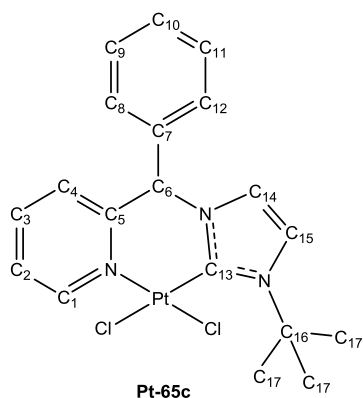
To a solution of compound **64a** (1.20 g, 4.20 mmol) in 30.0 mL of CH_2Cl_2 , Ag_2O (0.590 g, 2.52 mmol) was added in the dark. The reaction mixture was stirred at room temperature overnight and was filtered through a short plug of celite. The $Pt(cod)Cl_2$ (1.57 g, 4.19 mmol) was added to the orange filtrate in the dark. The reaction mixture was then allowed to stir at room temperature for two weeks and was filtered through celite. The orange yellow filtrate was reduced under vacuo and Et_2O was added to obtain an off white solid, 0.760 g, 35.0 %. M.p. = 236 – 238 °C (decomposed). Light yellow crystals were obtained from slow diffusion of diethyl ether into a methanol/DMSO solution of (\pm)-**Pt-65a**. 1H NMR (300 MHz, $DMSO-d_6$): δ = 3.90 (s, 3 H, H16), 7.05 (s, 1 H, H7), 7.26-7.45 (m, 6 H, arom.), 7.54-7.60 (m, 1 H, H11), 7.75 (d, 1 H, $J_{H,H}$ = 2.1 Hz, H15), 7.97-7.99 (m, 1 H, H12), 8.20-8.26 (m, 1 H, H10) and 9.31 (dd, 1 H, $J_{H,H}$ = 1.5 Hz, $J_{H,H}$ = 6.0 Hz, H9) ppm. ^{13}C NMR (75 MHz, $DMSO-d_6$): δ = 37.60 (C16), 66.95 (C7), 122.09 (C14), 123.90 (C15), 126.32 (C11), 127.22 (C9), 128.49, 129.07, 129.48, 138.15 and 139.84 (arom.), 140.29 (C10), 154.57 (arom.), 155.57 (C12) ppm. MS (ESI) m/z : $[M]^+$ calcd. for $C_{16}H_{15}Cl_2N_3Pt$ 514.0291, found 514.0169.

2.4.5.2. Synthesis of racemic complex (\pm)-Pt-65b



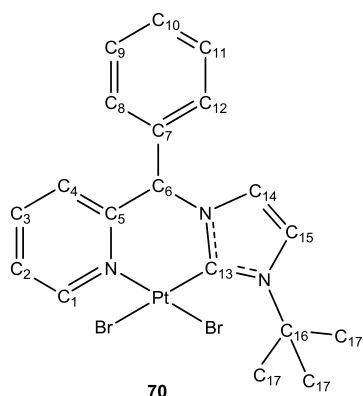
To a solution of compound **64b** (1.86 g, 5.35 mmol) in 30.0 mL of CH_2Cl_2 , Ag_2O (0.620 g, 2.67 mmol) was added in the dark. The reaction mixture was stirred at room temperature overnight and was filtered through a short plug of celite. The $\text{Pt}(\text{cod})\text{Cl}_2$ (1.99 g, 5.32 mmol) was added to the orange filtrate in the dark. The reaction mixture was then allowed to stir at room temperature for two weeks and was filtered through celite. The orange yellow filtrate was reduced under reduced pressure to yield orange solid, 1.37 g, 44.5 %. M.p. = 241 – 243 °C (decomposed). ^1H NMR (300 MHz, $\text{DMSO}-d_6$): δ = 7.42 (s, 1 H, H10), 7.47-7.51 (m, 4 H, arom.), 7.55-7.61 (m, 4 H, arom.), 7.72-7.74 (m, 1 H, H20), 7.86-7.92 (m, 3 H, arom.), 8.14-8.19 (m, 2 H, H18, H9), 8.30-8.31 (m, 1 H, H19), 9.41 (dd, 1 H, $J_{\text{H,H}} = 1.2 \text{ Hz}, 5.7 \text{ Hz}$, H21) ppm. ^{13}C NMR (75 MHz, $\text{DMSO}-d_6$): δ = 67.53 (C10), 121.83 (C9), 125.37 (C8), 127.03 (C20), 127.45 (C18), 128.89, 129.12, 129.49, 129.82, 130.32, 139.04 and 139.37 (arom.), 140.76 (C19), 155.07 (arom.) and 155.58 (C21) ppm. MS (ESI) m/z : $[\text{MH}-\text{Cl}]^+$ calcd. for $\text{C}_{21}\text{H}_{18}\text{ClN}_3\text{Pt}$ 542.0837, found 542.0283.

2.4.5.3. Synthesis of racemic complex (\pm)-Pt-65c



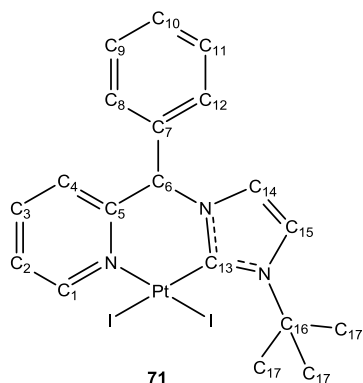
To a solution of compound **64c** (1.98 g, 6.03 mmol) in 30.0 mL of CH_2Cl_2 , Ag_2O (0.700 g, 3.02 mmol) was added in the dark. The reaction mixture was stirred at room temperature overnight and was filtered through celite and removed the solvent *in vacuo*. The intermediate Ag-NHC complex (1.18 g, 2.50 mmol) was then added with $\text{Pt}(\text{cod})\text{Cl}_2$ (0.940 g, 2.50 mmol) in the dark. The reaction mixture was then allowed to stir at room temperature for 2 weeks and was filtered through celite. The orange yellow filtrate was reduced under reduced pressure to yield brown solid, 1.71g, 51.0%. M.p. = 227 – 228 °C (decomposed). ^1H NMR (300 MHz, $\text{DMSO}-d_6$): δ = 1.61 (s, 9 H, H17), 7.21 (s, 1 H, H6), 7.34-7.48 (m, 6 H, arom.), 7.77-7.90 (m, 2 H, H14, H15), 7.94-7.96 (m, 1 H, H4), 8.07 (t, 1 H, $J_{\text{H,H}} = 2.1$ Hz, H3) and 8.64-8.66 (m, 1 H, H1) ppm. ^{13}C NMR (75 MHz, $\text{DMSO}-d_6$): δ = 30.88 (C17), 60.38 (C16), 66.45 (C6), 120.90 (C15), 123.02 (C14), 123.89 (C2), 124.34 (C4), 128.37, 128.96, 129.56, 135.42 and 137.43 (arom.), 138.23 (C3), 150.09 (arom.) and 155.88 (C1) ppm. MS (ESI) m/z : $[\text{M}-\text{H}]^+$ calcd. for $\text{C}_{19}\text{H}_{20}\text{Cl}_2\text{N}_3\text{Pt}$ 555.0682, found 555.0453.

2.4.5.4. Preparation of racemic dibromide complex (\pm)-70



The solution of racemic complex (\pm)-**Pt-65c** (1.64 g, 2.94 mmol) in 50.0 mL dichloromethane was added to potassium bromide (3.53 g, 29.7 mmol) in acetone (50.0 mL) and water (10.0 mL). The mixture was then stirred vigorously for 15 minutes. The solvents were removed *in vacuo* and the residue was extracted with dichloromethane and water. Then, the organic layer was dried by using anhydrous magnesium sulphate. Removal of solvent gave (\pm)-**70** as a brown solid, 1.04 g, 54.7 %. M.p. = 205 – 207 °C (decomposed). ^1H NMR (300 MHz, $\text{DMSO-}d_6$): δ = 1.61 (s, 9 H, H17), 7.18 (s, 1 H, H6), 7.41-7.49 (m, 5 H, arom.), 7.65-7.70 (m, 1 H, H2), 7.88-7.96 (m, 3 H, arom.), 8.07 (t, 1 H, $J_{\text{H,H}} = 1.8$ Hz, H3) and 8.65 (ddd, 1 H, $J_{\text{H,H}} = 0.9$ Hz, $J_{\text{H,H}} = 1.8$ Hz, $J_{\text{H,H}} = 4.8$ Hz, H1) ppm. ^{13}C NMR (75 MHz, $\text{DMSO-}d_6$): δ = 30.36 (C17), 59.64 (C16), 65.70 (C6), 120.12 (C15), 122.26 (C14), 123.10 (C2), 123.59 (C4), 127.92, 128.18, 128.79, 134.56 and 136.61 (arom.), 137.47 (C3), 149.32 (arom.) and 155.06 (C1) ppm. MS (ESI) m/z : $[\text{M}]^+$ calcd. for $\text{C}_{19}\text{H}_{21}\text{Br}_2\text{N}_3\text{Pt}$ 643.9750, found 644.0705.

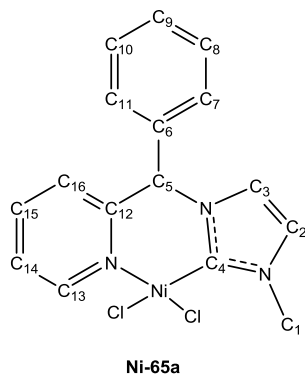
2.4.5.5. Preparation of racemic diiodo complex (\pm)-71



The solution of racemic complex (\pm)-**Pt-65c** (1.01 g, 1.81 mmol) in 100 mL dichloromethane was mixed with sodium iodide (2.00 g, 13.3 mmol) in acetone (100 mL). The mixture was then stirred vigorously for 15 minutes. The solvents were removed *in vacuo* and the residue was extracted with dichloromethane. Then, the solvent was removed under reduced pressure and diethyl ether was added to obtain (\pm)-**71** as a brown solid, 1.05 g, 78.4 %. M.p. = 213 – 216 °C (decomposed). ^1H NMR (300 MHz, $\text{DMSO-}d_6$): δ = 1.61 (s, 9 H, H17), 7.16 (s, 1 H, H6), 7.34-7.48 (m, 5 H, arom.), 7.88-7.95 (m, 3 H, arom.), 8.07 (t, 1 H, $J_{\text{H,H}} = 2.1$ Hz, H3) and 8.65 (ddd, 1 H, $J_{\text{H,H}} = 0.9$ Hz, $J_{\text{H,H}} = 1.8$ Hz, $J_{\text{H,H}} = 4.8$ Hz, H1) ppm. ^{13}C NMR (75 MHz, $\text{DMSO-}d_6$): δ = 31.07 (C17), 59.92 (C16), 66.06 (C6), 120.38 (C15), 122.54 (C14), 123.35 (C2), 123.86 (C4), 128.44, 129.06, 129.71, 134.77 and 136.82 (arom.), 137.74 (C3), 149.58 (arom.) and 155.30 (C1) ppm. MS (ESI) m/z : $[\text{M}]^+$ calcd. for $\text{C}_{19}\text{H}_{21}\text{I}_2\text{N}_3\text{Pt}$ 739.9437, found 740.1476.

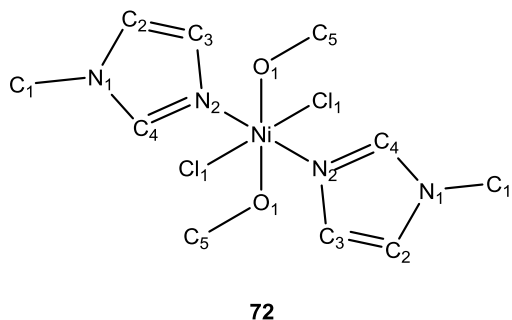
2.4.6. Synthesis of racemic nickel NHC complexes

2.4.6.1. Synthesis of racemic complex (\pm)-Ni-65a

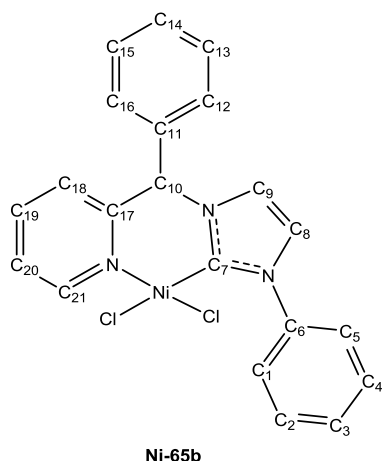


Compound **64a** (6.34 g, 22.2 mmol), NiCl₂ (4.05 g, 31.2 mmol) and K₂CO₃ (13.0 g, 93.7 mmol) were taken in 50.0 mL of acetonitrile. The reaction mixture was refluxed for 24 hours, filtered and the solvent was removed. The dark purple residue was extracted in CH₂Cl₂, which was filtered and evaporated under vacuum to obtain the purple oil. The crude purple oil was subjected to purification using column chromatography with CH₂Cl₂/MeOH (50:50 v/v) as the mobile phase. The racemic **Ni-65a** complex was isolated as a hygroscopic greenish brown solid, 3.30 g, 39.2 %. ¹H NMR (300 MHz, DMSO-*d*₆): δ = 4.05 (s, 3 H, H2), 7.21 (s, 1 H, H5), 7.27-7.37 (m, 5 H, arom.), 7.45-7.48 (m, 3 H, arom.), 7.70-7.76 (m, 2 H, H13, H14) and 8.59 (d, 1 H, J_{H,H} = 4.5 Hz, H16) ppm.

Light green crystals were obtained from slow diffusion of diethyl ether into a methanol solution of (\pm)-**Ni-65a**. Characterisation of the crystals using single crystal XRD analysis confirmed it to be an unexpected nickel coordination complex **72** with molecular formula of C₁₀H₂₀Cl₂N₄O₂Ni. MS (ESI) *m/z*: [MH-Cl]⁺ calcd. for C₁₀H₂₁ClN₄O₂Ni 322.0707, found 322.1890. M.p. = 130 – 131 °C.



2.4.6.2. Synthesis of racemic complex (\pm)-Ni-65b



Compound **64b** (1.81 g, 5.20 mmol), NiCl₂ (0.680 g, 5.25 mmol) and K₂CO₃ (2.18 g, 15.8 mmol) were dissolved in 50.0 mL of acetonitrile. The reaction mixture was refluxed for 24 hours, filtered and the solvent was removed. The dark brown residue was extracted in CH₂Cl₂, which was filtered and evaporated under vacuum to obtain the brown oil. The crude brown oil was subjected to purification using column chromatography with CH₂Cl₂/MeOH (50:50 v/v) as the mobile phase. The racemic **Ni-65b** complex was isolated as a hygroscopic brown solid, 0.590 g, 25.7%. ¹H NMR (300 MHz, DMSO-*d*₆): δ = 7.25-7.90 (m, 11 H, arom.), 7.87-7.93 (m, 1 H, arom.), 8.03-8.06 (m, 2 H, H18 and H9), 8.08 (t, 1 H, J_{H,H} = 11.5 Hz, H19) and 8.72-8.73 (m, 1 H, H21) ppm.

CHAPTER 3 ANTIMICROBIAL STUDIES OF PALLADIUM, PLATINUM AND NICKEL N-HETEROCYCLIC CARBENE (NHC) COMPLEXES

3.1. Introduction

Antimicrobials are agents capable of killing microorganisms or suppressing their growth. Nevertheless, in this post-antimicrobial era, currently available antimicrobials are slowly losing their effectiveness against the microorganisms. An important factor for this decreasing effectiveness are the emergence of antimicrobial resistant pathogens. Further complicating the matter is the fact that a lot of pathogens are capable of producing biofilms. Biofilms are aggregation of bacteria embedded in a self-produced slimy matrix of extracellular polymeric substances (EPS), which make it difficult for the antimicrobials to reach and kill the bacteria effectively. Despite the rapid emergence of antimicrobial resistance phenomena and biofilm infections, there are relatively few antimicrobials being discovered and developed in the past decades. This highlights the importance of discovering novel antimicrobials to combat antimicrobial resistant pathogens and biofilms.

The impetus for the antimicrobial study came from the knowledge that a number of elemental metals are well known for their antimicrobial activities, such as silver, mercury, copper and others. Besides that, a number of metal NHC complexes displayed significant antimicrobial activities against bacteria with minimum inhibitory concentration (MIC) below 10 $\mu\text{g/mL}$, including some silver, gold, rhodium and ruthenium NHC complexes as described previously in Chapter 1. Especially for Ag NHC complexes, they have been extensively studied for their antimicrobial properties and were treated as the “benchmark” of metal NHC complexes with significant antimicrobial activities.

Although there is no literature available on the antimicrobial activities of nickel and platinum NHC complexes, some palladium NHC complexes were reported to exhibit antimicrobial activities with MIC and MBC values of 50 and 100 $\mu\text{g/mL}$, respectively (Haque et al., 2013, Haque et al., 2016d). Nonetheless, these reports on the antimicrobial potential of Pd NHC complexes are rather preliminary as they were only tested against two bacteria i.e. *Staphylococcus aureus* and *Escherichia coli*. This is because *S. aureus* and *E. coli* are examples for Gram positive bacteria and Gram negative bacteria, respectively, yet there are a numbers of pathogenic bacteria which should be taken into consideration for evaluation of these Pd NHC complexes as effective antimicrobial agents.

In this chapter, the previously synthesized compounds from Chapter 2, inclusive but not limited to the precursors, imidazolium salts (NHC precursors), and Group 10 metal NHC complexes will be subjected to broth microdilution assay (BMD) to determine their antimicrobial activities. They will be tested against a panel of clinically relevant microorganisms including Gram positive and Gram negative bacteria, as well as *Candida spp.* (yeasts). Apart from those pathogenic bacteria, the rationale behind the inclusion of yeasts into the panel of microorganism tested was the capability of *Candida spp.* to cause opportunistic yeast infection, also known as candidiasis, which affects mouth, genitals and even blood. Some of common bacterial susceptibility tests for antimicrobial activities determination include broth dilution assay, broth microdilution assay, antimicrobial gradient diffusion method, well diffusion test, disk diffusion test and others. The main advantages for utilizing the broth microdilution method in this study comprises the generation of quantitative results (i.e. MICs), reproducibility and convenience of the method, as well as the economy of reagents and space that occurs due to the miniaturization of the test (Reller et al., 2009).

3.2. Results and Discussion

Broth microdilution assay was conducted in this study to determine the antimicrobial activities of the synthesized complexes and other compounds against 16 strains of microorganisms including nine strains of Gram positive bacteria, four strains of Gram negative bacteria, and three strains of *Candida sp.* (**Table 13**). Their antimicrobial activities were quantitatively expressed in terms of minimum inhibitory concentration (MIC) and minimum bactericidal concentration (MBC). MIC is the minimum concentration of a compound to inhibit the growth of the microorganisms, whereas MBC is referring to the minimum concentration of a compound to kill the microorganisms tested. The compounds tested and their respective MIC and MBC values were tabulated in **Table 9-12** as listed in **Table 8** below, which also showed the highest final concentration tested for each compound. The difference in final concentrations was due to the limited solubility of metal NHC complexes in a wide array of solvents but DMSO. Metal NHC complexes were prepared at 20 mM in 100% DMSO, the highest concentration possible with complete dissolution, whereas the precursors and imidazolium salts **64** were prepared at 200 mM (stock concentration). Following this, the final concentration of DMSO in the broth microdilution assay was 2.5 %. Solvent control (2.5 % DMSO) have been tested against the panel of microorganisms, and it showed that the solvent control have no effect against the microorganism tested.

Table 8. List of compounds tested in antimicrobial assay.

Table	Group	Compounds tested	Highest final concentration tested (mM)
Table 9	Precursors	Compound 62, 63	5.000
	Imidazolium salts	64a, 64b, 64c	5.000
	Imidazoles	Imidazole (im), methylimidazole [Me(im)], phenylimidazole [Ph(im)], <i>tert</i> -butylimidazole [<i>t</i> Bu(im)]	5.000
Table 10	Metal salts	PdCl ₂ , K ₂ PtCl ₄ , NiCl ₂	0.500
	Transmetalating agent	Pd(CH ₃ CN) ₂ Cl ₂ , Pt(cod)Cl ₂ , NiCl ₂	0.500
	Antibiotics	Chloramphenicol (CHL), cefotaxime (CTX), cycloheximide (CHX)	0.050
Table 11	Pd NHC complexes	Pd-65a, Pd-65b, Pd-65c, Pd-(<i>Rc</i>)-65a, Pd-(<i>Sc</i>)-65b	0.500
	Diastereomers	Pd-(<i>Rc,Sc</i>)-68a, Pd-(<i>Sc,Sc</i>)-69b	0.500
Table 12	Pt NHC complexes	Pt-65a, Pt-65b, Pt-65c, 70, 71	0.500
	Ni complexes	72,73	0.500

In this study, three antibiotics were utilised as the reference drugs in the antimicrobial assay includes chloramphenicol (CHL), cefotaxime (CTX) and cycloheximide (CHX) (**Table 10**). Chloramphenicol is a type of broad spectrum antibiotic that exerts antimicrobial effect through protein synthesis inhibition by binding to the 50S ribosomal subunit, whereas cefotaxime is a broad spectrum bactericidal β -lactam antibiotic which interferes bacterial cell wall synthesis by binding to one or more of the penicillin-binding proteins). On the other hand, cycloheximide is an effective antifungal agent that exerts its antimicrobial function via inhibition of protein synthesis and apoptosis in eukaryotes, such as mold, yeast, phytopathogenic fungi.

Table 9. Antimicrobial activity of precursors, imidazolium salts and imidazoles reported as MIC and MBC in mM.^a

Microorganisms tested	MIC (mM)								
	62	63	64a	64b	64c	im	Me(im)	Ph(im)	tBu(im)
<i>Bacillus cereus</i> ATCC 14579 ⁺	> 5.000	> 5.000	5.000	2.500	5.000	> 5.000	> 5.000	5.000	> 5.000
<i>Bacillus subtilis</i> ATCC 8188 ⁺	> 5.000	> 5.000	5.000	2.500	5.000	> 5.000	> 5.000	5.000	> 5.000
<i>Staphylococcus aureus</i> ATCC 29213 ⁺	> 5.000	> 5.000	2.500	1.250	2.500	> 5.000	> 5.000	5.000	> 5.000
<i>Staphylococcus aureus</i> ATCC 6538P ⁺	> 5.000	> 5.000	2.500	1.250	2.500	> 5.000	> 5.000	> 5.000	> 5.000
<i>Staphylococcus aureus</i> ATCC 700699 ^{b+}	> 5.000	> 5.000	5.000	1.250	5.000	> 5.000	> 5.000	5.000	> 5.000
<i>Staphylococcus aureus</i> ATCC 43300 ^{b+}	> 5.000	> 5.000	5.000	1.250	2.500	> 5.000	> 5.000	5.000	> 5.000
<i>Staphylococcus aureus</i> ATCC 33591 ^{b+}	> 5.000	> 5.000	5.000	1.250	5.000	> 5.000	> 5.000	5.000	> 5.000
<i>Enterococcus faecalis</i> ATCC 29212 ⁺	> 5.000	> 5.000	> 5.000	5.000	> 5.000	> 5.000	> 5.000	> 5.000	> 5.000
<i>Enterococcus faecalis</i> ATCC 700802 ^{ca}	> 5.000	> 5.000	> 5.000	> 5.000	> 5.000	> 5.000	> 5.000	> 5.000	> 5.000
<i>Escherichia coli</i> ATCC 25922 ⁻	> 5.000	> 5.000	> 5.000	5.000	> 5.000	> 5.000	> 5.000	5.000	> 5.000
<i>Klebsiella pneumoniae</i> ATCC 10031 ⁻	> 5.000	> 5.000	> 5.000	2.500	> 5.000	> 5.000	> 5.000	5.000	> 5.000
<i>Pseudomonas aeruginosa</i> ATCC 10145 ⁻	> 5.000	> 5.000	> 5.000	> 5.000	> 5.000	> 5.000	> 5.000	> 5.000	> 5.000
<i>Shigella flexneri</i> ATCC 12022 ⁻	> 5.000	> 5.000	5.000	1.250	5.000	> 5.000	> 5.000	> 5.000	> 5.000
<i>Candida albicans</i> IMR ^Y	> 5.000	> 5.000	2.500	1.250	5.000	> 5.000	> 5.000	2.500	> 5.000
<i>Candida albicans</i> Clinical isolate ^Y	> 5.000	> 5.000	5.000	1.250	5.000	> 5.000	> 5.000	5.000	> 5.000
<i>Candida tropicalis</i> Clinical isolate ^Y	> 5.000	> 5.000	5.000	2.500	> 5.000	> 5.000	> 5.000	5.000	> 5.000

Microorganisms tested	MBC (mM)								
	62	63	64a	64b	64c	im	Me(im)	Ph(im)	tBu(im)
<i>Bacillus cereus</i> ATCC 14579 ⁺	> 5.000	> 5.000	5.000	2.500	5.000	> 5.000	> 5.000	5.000	> 5.000
<i>Bacillus subtilis</i> ATCC 8188 ⁺	> 5.000	> 5.000	> 5.000	2.500	> 5.000	> 5.000	> 5.000	> 5.000	> 5.000
<i>Staphylococcus aureus</i> ATCC 29213 ⁺	> 5.000	> 5.000	5.000	5.000	5.000	> 5.000	> 5.000	> 5.000	> 5.000
<i>Staphylococcus aureus</i> ATCC 6538P ⁺	> 5.000	> 5.000	5.000	5.000	5.000	> 5.000	> 5.000	> 5.000	> 5.000
<i>Staphylococcus aureus</i> ATCC 700699 ^{b+}	> 5.000	> 5.000	> 5.000	5.000	> 5.000	> 5.000	> 5.000	> 5.000	> 5.000
<i>Staphylococcus aureus</i> ATCC 43300 ^{b+}	> 5.000	> 5.000	5.000	2.500	5.000	> 5.000	> 5.000	> 5.000	> 5.000
<i>Staphylococcus aureus</i> ATCC 33591 ^{b+}	> 5.000	> 5.000	> 5.000	> 5.000	> 5.000	> 5.000	> 5.000	> 5.000	> 5.000
<i>Enterococcus faecalis</i> ATCC 29212 ⁺	> 5.000	> 5.000	> 5.000	> 5.000	> 5.000	> 5.000	> 5.000	> 5.000	> 5.000
<i>Enterococcus faecalis</i> ATCC 700802 ^{ca}	> 5.000	> 5.000	> 5.000	> 5.000	> 5.000	> 5.000	> 5.000	> 5.000	> 5.000
<i>Escherichia coli</i> ATCC 25922 ⁻	> 5.000	> 5.000	> 5.000	5.000	> 5.000	> 5.000	> 5.000	> 5.000	> 5.000
<i>Klebsiella pneumoniae</i> ATCC 10031 ⁻	> 5.000	> 5.000	> 5.000	5.000	> 5.000	> 5.000	> 5.000	> 5.000	> 5.000
<i>Pseudomonas aeruginosa</i> ATCC 10145 ⁻	> 5.000	> 5.000	> 5.000	> 5.000	> 5.000	> 5.000	> 5.000	> 5.000	> 5.000
<i>Shigella flexneri</i> ATCC 12022 ⁻	> 5.000	> 5.000	5.000	5.000	> 5.000	> 5.000	> 5.000	> 5.000	> 5.000
<i>Candida albicans</i> IMR ^Y	> 5.000	> 5.000	5.000	2.500	5.000	> 5.000	> 5.000	> 5.000	> 5.000
<i>Candida albicans</i> Clinical isolate ^Y	> 5.000	> 5.000	> 5.000	2.500	5.000	> 5.000	> 5.000	> 5.000	> 5.000
<i>Candida tropicalis</i> Clinical isolate ^Y	> 5.000	> 5.000	> 5.000	5.000	> 5.000	> 5.000	> 5.000	5.000	> 5.000

^aThe antimicrobial assay was performed in triplicates. The compounds with no antimicrobial activity were reported as more than the maximum working concentration tested in mM. Antibiotic resistant microorganisms: ^bMethicillin-resistant *Staphylococcus aureus* (MRSA); ^cVancomycin-resistant *Enterococci* (VRE) Microorganisms in group: ⁺Gram positive bacteria; ⁻ Gram negative bacteria; ^Y Yeast.

Table 10. Antimicrobial activity of metal salts, transmetalating agents and antibiotics, reported as MIC and MBC in mM.^a

Microorganisms tested	MIC (mM)							
	PdCl ₂	K ₂ PtCl ₄	NiCl ₂	Pd(CH ₃ CN) ₂ Cl ₂	Pt(cod)Cl ₂	CHL	CTX	CHX
<i>Bacillus cereus</i> ATCC 14579 ⁺	> 0.500	> 0.500	> 0.500	> 0.500	0.004	0.006	> 0.050	> 0.050
<i>Bacillus subtilis</i> ATCC 8188 ⁺	> 0.500	> 0.500	> 0.500	> 0.500	0.004	0.006	0.050	> 0.050
<i>Staphylococcus aureus</i> ATCC 29213 ⁺	> 0.500	> 0.500	> 0.500	> 0.500	0.004	0.025	0.006	> 0.050
<i>Staphylococcus aureus</i> ATCC 6538P ⁺	> 0.500	> 0.500	> 0.500	> 0.500	0.004	0.025	0.003	> 0.050
<i>Staphylococcus aureus</i> ATCC 700699 ^{b+}	> 0.500	> 0.500	> 0.500	> 0.500	0.004	0.025	> 0.050	> 0.050
<i>Staphylococcus aureus</i> ATCC 43300 ^{b+}	> 0.500	> 0.500	> 0.500	> 0.500	0.004	0.025	0.013	> 0.050
<i>Staphylococcus aureus</i> ATCC 33591 ^{b+}	> 0.500	> 0.500	> 0.500	> 0.500	0.004	0.025	> 0.050	> 0.050
<i>Enterococcus faecalis</i> ATCC 29212 ⁺	> 0.500	> 0.500	> 0.500	> 0.500	0.031	0.050	> 0.050	> 0.050
<i>Enterococcus faecalis</i> ATCC 700802 ^{c+}	> 0.500	> 0.500	> 0.500	> 0.500	0.063	0.050	> 0.050	> 0.050
<i>Escherichia coli</i> ATCC 25922 ⁻	> 0.500	> 0.500	> 0.500	> 0.500	0.250	0.025	1.950×10 ⁻⁴	> 0.050
<i>Klebsiella pneumoniae</i> ATCC 10031 ⁻	> 0.500	> 0.500	> 0.500	> 0.500	0.250	0.003	2.440×10 ⁻⁵	> 0.050
<i>Pseudomonas aeruginosa</i> ATCC 10145 ⁻	> 0.500	> 0.500	> 0.500	> 0.500	0.500	> 0.050	0.050	> 0.050
<i>Shigella flexneri</i> ATCC 12022 ⁻	> 0.500	> 0.500	> 0.500	> 0.500	0.250	0.006	4.880×10 ⁻⁵	> 0.050
<i>Candida albicans</i> IMR ^Y	> 0.500	> 0.500	> 0.500	> 0.500	> 0.500	> 0.050	0.050	0.050
<i>Candida albicans</i> Clinical isolate ^Y	> 0.500	> 0.500	> 0.500	> 0.500	> 0.500	> 0.050	> 0.050	0.050
<i>Candida tropicalis</i> Clinical isolate ^Y	> 0.500	> 0.500	> 0.500	> 0.500	> 0.500	> 0.050	> 0.050	0.050

Microorganisms tested	MBC (mM)							
	PdCl ₂	K ₂ PtCl ₄	NiCl ₂	Pd(CH ₃ CN) ₂ Cl ₂	Pt(cod)Cl ₂	CHL	CTX	CHX
<i>Bacillus cereus</i> ATCC 14579 ⁺	> 0.500	> 0.500	> 0.500	> 0.500	0.500	> 0.050	> 0.050	> 0.050
<i>Bacillus subtilis</i> ATCC 8188 ⁺	> 0.500	> 0.500	> 0.500	> 0.500	0.500	> 0.050	> 0.050	> 0.050
<i>Staphylococcus aureus</i> ATCC 29213 ⁺	> 0.500	> 0.500	> 0.500	> 0.500	0.500	> 0.050	> 0.050	> 0.050
<i>Staphylococcus aureus</i> ATCC 6538P ⁺	> 0.500	> 0.500	> 0.500	> 0.500	0.500	> 0.050	> 0.050	> 0.050
<i>Staphylococcus aureus</i> ATCC 700699 ^{b+}	> 0.500	> 0.500	> 0.500	> 0.500	0.500	> 0.050	> 0.050	> 0.050
<i>Staphylococcus aureus</i> ATCC 43300 ^{b+}	> 0.500	> 0.500	> 0.500	> 0.500	0.250	> 0.050	> 0.050	> 0.050
<i>Staphylococcus aureus</i> ATCC 33591 ^{b+}	> 0.500	> 0.500	> 0.500	> 0.500	0.500	> 0.050	> 0.050	> 0.050
<i>Enterococcus faecalis</i> ATCC 29212 ⁺	> 0.500	> 0.500	> 0.500	> 0.500	0.500	> 0.050	> 0.050	> 0.050
<i>Enterococcus faecalis</i> ATCC 700802 ^{c+}	> 0.500	> 0.500	> 0.500	> 0.500	0.500	> 0.050	> 0.050	> 0.050
<i>Escherichia coli</i> ATCC 25922 ⁻	> 0.500	> 0.500	> 0.500	> 0.500	0.500	> 0.050	0.002	> 0.050
<i>Klebsiella pneumoniae</i> ATCC 10031 ⁻	> 0.500	> 0.500	> 0.500	> 0.500	0.500	0.003	2.440×10 ⁻⁵	> 0.050
<i>Pseudomonas aeruginosa</i> ATCC 10145 ⁻	> 0.500	> 0.500	> 0.500	> 0.500	> 0.500	> 0.050	> 0.050	> 0.050
<i>Shigella flexneri</i> ATCC 12022 ⁻	> 0.500	> 0.500	> 0.500	> 0.500	0.500	0.050	4.880×10 ⁻⁵	> 0.050
<i>Candida albicans</i> IMR ^Y	> 0.500	> 0.500	> 0.500	> 0.500	> 0.500	> 0.050	0.050	0.050
<i>Candida albicans</i> Clinical isolate ^Y	> 0.500	> 0.500	> 0.500	> 0.500	> 0.500	> 0.050	> 0.050	0.050
<i>Candida tropicalis</i> Clinical isolate ^Y	> 0.500	> 0.500	> 0.500	> 0.500	> 0.500	> 0.050	> 0.050	0.050

^aThe antimicrobial assay was performed in triplicates. The compounds with no antimicrobial activity were reported as more than the maximum working concentration tested in mM.

Antibiotic resistant microorganisms: ^bMethicillin-resistant *Staphylococcus aureus* (MRSA); ^cVancomycin-resistant *Enterococci* (VRE)

Microorganisms in group: ⁺Gram positive bacteria; ⁻ Gram negative bacteria; ^Y Yeast.

Table 11. Antimicrobial activity of synthesized palladium complexes, reported as MIC and MBC in mM.^a

Microorganisms tested	MIC (mM)						
	Pd-65a	Pd-(Rc,Sc)-68a	Pd-(Rc)-65a	Pd-65b	Pd-(Sc,Sc)-69b	Pd-(Sc)-65b	Pd-65c
<i>Bacillus cereus</i> ATCC 14579 ⁺	> 0.500	> 0.500	0.125	0.250	> 0.500	> 0.500	0.063
<i>Bacillus subtilis</i> ATCC 8188 ⁺	> 0.500	> 0.500	0.250	0.063	> 0.500	> 0.500	0.016
<i>Staphylococcus aureus</i> ATCC 29213 ⁺	> 0.500	> 0.500	0.250	0.125	> 0.500	> 0.500	0.125
<i>Staphylococcus aureus</i> ATCC 6538P ⁺	> 0.500	0.125	0.031	0.250	> 0.500	> 0.500	0.031
<i>Staphylococcus aureus</i> ATCC 700699 ^{b+}	> 0.500	0.125	0.031	0.250	> 0.500	> 0.500	0.063
<i>Staphylococcus aureus</i> ATCC 43300 ^{b+}	> 0.500	> 0.500	0.250	0.250	> 0.500	> 0.500	0.125
<i>Staphylococcus aureus</i> ATCC 33591 ^{b+}	> 0.500	0.125	0.031	0.500	> 0.500	> 0.500	0.063
<i>Enterococcus faecalis</i> ATCC 29212 ⁺	> 0.500	> 0.500	0.250	0.250	> 0.500	> 0.500	0.125
<i>Enterococcus faecalis</i> ATCC 700802 ^{c+}	> 0.500	> 0.500	0.250	0.250	> 0.500	> 0.500	0.125
<i>Escherichia coli</i> ATCC 25922 ⁻	> 0.500	0.500	0.125	0.500	> 0.500	> 0.500	0.125
<i>Klebsiella pneumoniae</i> ATCC 10031 ⁻	> 0.500	0.500	0.125	> 0.500	> 0.500	> 0.500	0.250
<i>Pseudomonas aeruginosa</i> ATCC 10145 ⁻	> 0.500	0.500	0.125	> 0.500	> 0.500	> 0.500	0.250
<i>Shigella flexneri</i> ATCC 12022 ⁻	> 0.500	0.500	0.125	0.500	> 0.500	> 0.500	0.250
<i>Candida albicans</i> IMR ^Y	> 0.500	> 0.500	0.250	0.500	> 0.500	> 0.500	0.250
<i>Candida albicans</i> Clinical isolate ^Y	> 0.500	0.125	0.063	> 0.500	> 0.500	> 0.500	0.125
<i>Candida tropicalis</i> Clinical isolate ^Y	> 0.500	0.250	0.125	> 0.500	> 0.500	> 0.500	0.250

Microorganisms tested	MBC (mM)						
	Pd-65a	Pd-(Rc,Sc)-68a	Pd-(Rc)-65a	Pd-65b	Pd-(Sc,Sc)-69b	Pd-(Sc)-65b	Pd-65c
<i>Bacillus cereus</i> ATCC 14579 ⁺	> 0.500	> 0.500	0.250	0.500	> 0.500	> 0.500	0.250
<i>Bacillus subtilis</i> ATCC 8188 ⁺	> 0.500	> 0.500	0.250	> 0.500	> 0.500	> 0.500	0.250
<i>Staphylococcus aureus</i> ATCC 29213 ⁺	> 0.500	> 0.500	> 0.500	0.500	> 0.500	> 0.500	0.500
<i>Staphylococcus aureus</i> ATCC 6538P ⁺	> 0.500	> 0.500	> 0.500	> 0.500	> 0.500	> 0.500	0.125
<i>Staphylococcus aureus</i> ATCC 700699 ^{b+}	> 0.500	0.500	> 0.500	> 0.500	> 0.500	> 0.500	0.500
<i>Staphylococcus aureus</i> ATCC 43300 ^{b+}	> 0.500	> 0.500	> 0.500	> 0.500	> 0.500	> 0.500	0.500
<i>Staphylococcus aureus</i> ATCC 33591 ^{b+}	> 0.500	> 0.500	0.500	> 0.500	> 0.500	> 0.500	0.125
<i>Enterococcus faecalis</i> ATCC 29212 ⁺	> 0.500	> 0.500	0.500	> 0.500	> 0.500	> 0.500	0.500
<i>Enterococcus faecalis</i> ATCC 700802 ^{c+}	> 0.500	> 0.500	0.500	> 0.500	> 0.500	> 0.500	0.500
<i>Escherichia coli</i> ATCC 25922 ⁻	> 0.500	0.500	0.250	0.500	> 0.500	> 0.500	0.500
<i>Klebsiella pneumoniae</i> ATCC 10031 ⁻	> 0.500	0.500	0.125	> 0.500	> 0.500	> 0.500	0.500
<i>Pseudomonas aeruginosa</i> ATCC 10145 ⁻	> 0.500	> 0.500	0.250	> 0.500	> 0.500	> 0.500	0.500
<i>Shigella flexneri</i> ATCC 12022 ⁻	> 0.500	0.500	0.250	0.500	> 0.500	> 0.500	0.250
<i>Candida albicans</i> IMR ^Y	> 0.500	> 0.500	0.500	> 0.500	> 0.500	> 0.500	0.500
<i>Candida albicans</i> Clinical isolate ^Y	> 0.500	0.250	0.250	> 0.500	> 0.500	> 0.500	0.500
<i>Candida tropicalis</i> Clinical isolate ^Y	> 0.500	0.500	0.125	> 0.500	> 0.500	> 0.500	0.500

^aThe antimicrobial assay was performed in triplicates. The compounds with no antimicrobial activity were reported as more than the maximum working concentration tested in mM. Antibiotic resistant microorganisms: ^bMethicillin-resistant *Staphylococcus aureus* (MRSA); ^c Vancomycin-resistant *Enterococci* (VRE) Microorganisms in group: ⁺ Gram positive bacteria; ⁻ Gram negative bacteria; ^Y Yeast.

Table 12. Antimicrobial activity of synthesized platinum and nickel complexes, reported as MIC and MBC in mM.^a

Microorganisms tested	MIC (mM)						
	Pt-65a	Pt-65b	Pt-65c	70	71	72	73
<i>Bacillus cereus</i> ATCC 14579 ⁺	0.500	0.002	0.002	0.008	0.002	> 0.500	> 0.500
<i>Bacillus subtilis</i> ATCC 8188 ⁺	0.500	0.004	0.002	0.016	0.002	> 0.500	> 0.500
<i>Staphylococcus aureus</i> ATCC 29213 ⁺	0.500	0.002	0.004	0.008	0.004	> 0.500	> 0.500
<i>Staphylococcus aureus</i> ATCC 6538P ⁺	0.500	0.008	0.004	0.031	0.004	> 0.500	> 0.500
<i>Staphylococcus aureus</i> ATCC 700699 ^{b+}	0.500	0.001	0.004	0.004	0.002	> 0.500	> 0.500
<i>Staphylococcus aureus</i> ATCC 43300 ^{b+}	0.500	0.001	0.002	0.004	0.002	> 0.500	> 0.500
<i>Staphylococcus aureus</i> ATCC 33591 ^{b+}	0.500	0.004	0.004	0.016	0.004	> 0.500	> 0.500
<i>Enterococcus faecalis</i> ATCC 29212 ⁺	0.500	0.031	0.031	0.125	0.031	> 0.500	> 0.500
<i>Enterococcus faecalis</i> ATCC 700802 ^{c+}	0.500	0.063	0.031	0.125	0.031	> 0.500	> 0.500
<i>Escherichia coli</i> ATCC 25922 ⁻	0.500	0.125	0.063	0.500	0.125	> 0.500	> 0.500
<i>Klebsiella pneumoniae</i> ATCC 10031 ⁻	0.500	0.125	0.016	0.250	0.031	> 0.500	> 0.500
<i>Pseudomonas aeruginosa</i> ATCC 10145 ⁻	0.500	0.063	0.013	0.250	0.500	> 0.500	> 0.500
<i>Shigella flexneri</i> ATCC 12022 ⁻	0.500	0.063	0.625	0.250	0.063	> 0.500	> 0.500
<i>Candida albicans</i> IMR ^Y	0.500	0.063	0.008	0.063	0.008	> 0.500	> 0.500
<i>Candida albicans</i> Clinical isolate ^Y	0.500	0.063	0.016	0.125	0.031	> 0.500	> 0.500
<i>Candida tropicalis</i> Clinical isolate ^Y	0.500	0.016	0.125	0.250	0.016	> 0.500	> 0.500

Microorganisms tested	MBC (mM)						
	Pt-65a	Pt-65b	Pt-65c	70	71	72	73
<i>Bacillus cereus</i> ATCC 14579 ⁺	> 0.500	0.250	0.125	0.125	0.125	> 0.500	> 0.500
<i>Bacillus subtilis</i> ATCC 8188 ⁺	> 0.500	0.125	0.016	0.031	0.002	> 0.500	> 0.500
<i>Staphylococcus aureus</i> ATCC 29213 ⁺	> 0.500	0.125	0.031	0.250	0.500	> 0.500	> 0.500
<i>Staphylococcus aureus</i> ATCC 6538P ⁺	> 0.500	0.125	0.063	0.031	0.125	> 0.500	> 0.500
<i>Staphylococcus aureus</i> ATCC 700699 ^{b+}	> 0.500	0.125	0.063	0.063	0.125	> 0.500	> 0.500
<i>Staphylococcus aureus</i> ATCC 43300 ^{b+}	> 0.500	0.031	0.031	0.063	0.063	> 0.500	> 0.500
<i>Staphylococcus aureus</i> ATCC 33591 ^{b+}	> 0.500	0.063	0.008	0.063	0.063	> 0.500	> 0.500
<i>Enterococcus faecalis</i> ATCC 29212 ⁺	> 0.500	0.250	0.250	0.250	0.250	> 0.500	> 0.500
<i>Enterococcus faecalis</i> ATCC 700802 ^{c+}	> 0.500	0.250	0.125	0.250	0.063	> 0.500	> 0.500
<i>Escherichia coli</i> ATCC 25922 ⁻	> 0.500	0.250	0.125	> 0.500	0.500	> 0.500	> 0.500
<i>Klebsiella pneumoniae</i> ATCC 10031 ⁻	> 0.500	0.250	0.031	0.250	0.250	> 0.500	> 0.500
<i>Pseudomonas aeruginosa</i> ATCC 10145 ⁻	> 0.500	0.500	0.500	0.500	> 0.500	> 0.500	> 0.500
<i>Shigella flexneri</i> ATCC 12022 ⁻	> 0.500	0.250	0.250	0.250	0.250	> 0.500	> 0.500
<i>Candida albicans</i> IMR ^Y	> 0.500	0.250	0.063	0.125	0.031	> 0.500	> 0.500
<i>Candida albicans</i> Clinical isolate ^Y	> 0.500	0.250	0.063	> 0.500	0.125	> 0.500	> 0.500
<i>Candida tropicalis</i> Clinical isolate ^Y	> 0.500	0.250	0.125	0.500	0.063	> 0.500	> 0.500

^aThe antimicrobial assay was performed in triplicates. The compounds with no antimicrobial activity were reported as more than the maximum working concentration tested in mM. Antibiotic resistant microorganisms: ^bMethicillin-resistant *Staphylococcus aureus* (MRSA); ^cVancomycin-resistant *Enterococci* (VRE) Microorganisms in group: ⁺ Gram positive bacteria; ⁻ Gram negative bacteria; ^Y Yeast.

Overall, the Gram positive bacterial strains were inhibited by low micromolar concentrations of the synthesized complexes, whereas substantially lower efficacies against Gram negative bacterial strains were observed. The different susceptibility of Gram positive and Gram negative bacteria can be attributed to their morphological differences (Jiang et al., 2004). The outer peptidoglycan layer of Gram positive bacteria is an effective permeability layer. On the other hand, the outer membrane of Gram negative bacteria contained structural lipopolysaccharide components, thereby making the cell wall impermeable to lipophilic solutes while porins, a membrane transport protein, constitute a selective barrier to the hydrophilic solutes. The compounds synthesized were not soluble in a wide array of solvents but DMSO, and they were made up of several conjugated rings, which give rise their hydrophobicity (i.e. lipophilicity). Therefore, the lack of efficacy against Gram negative bacteria was not surprising.

In this study, we have tested multiple strains of the same bacteria. For examples, the *Staphylococcus aureus* strains which are sensitive to methicillin (MSSA) and those which are resistant to methicillin (MRSA), as well as *Enterococcus faecalis* and its antibiotic-resistant strain (vancomycin-resistant Enterococci, VRE). This is because certain compounds may have different degree of antimicrobial activities against different strains of bacteria, especially against the antibiotic-resistant strains (Beceiro et al., 2013). The strain variation effect would render the antimicrobial compound to be effective against some strains but not the other, which in turn would make the antimicrobial compounds less viable to be used as an antimicrobial drug. Notably, the antimicrobial activities of the metal NHC complexes against *S. aureus* was observed to be strain dependent. For instance, there was an eight-fold difference in the MIC values of the **Pd-(Rc)-65a** against MSSA ATCC 29213 and MRSA ATCC 33591 (**Table 11**). CLSI (2012) had proposed that two treatments with MIC values within two-fold difference is not significantly different from each other. The strain dependent activity observed could be due to differences in the cell wall compositions, such as presence of membrane-bound penicillin-binding proteins in MRSA (Oliveira et al., 2002, Crisóstomo et al., 2001). Majority of the antimicrobial studies of metal NHC complexes focused only on a single strain of each bacterial species and concluded that they are effective against the bacterial species (Haque et al., 2013, Haque et al., 2016d, Ray et al., 2007, Gümüş et al., 2003, Onar et al., 2018, Karatas et al., 2016, Schmidt et al., 2017). However, our results suggested otherwise, which implies the importance of testing the complexes against several strains of a same bacterium before such conclusion can be made.

Imidazolium salts or NHC precursors **64** have showed antimicrobial activities at 5 mM or below against the microorganisms tested. The results are in agreement with other imidazolium-based salts that displayed antimicrobial properties as reported by literature (Mumtaz et al., 2016, Dembereinyamba et al., 2004, Riduan and Zhang, 2013, Borowiecki et al., 2013, Gravel and Schmitzer, 2017). Nevertheless, the activities were not comparable to some imidazolium salts which were reported to have MIC values in μM range (Riduan and Zhang 2013). This could be due to the structure of the synthesized imidazolium salts **64** were lack of effectively long alkyl chain. Literature have suggested that the antimicrobial activity is often dependent on the chain length of the *N*-substituted imidazolium salts, in which the lowest MIC were achieved by compounds with long alkyl chains (C_8 to C_{16}) while alkyl chains of less than six carbons are generally not active (Dembereinyamba *et al.* 2011; Borowiecki *et al.* 2013). Longer alkyl chain is thought to be associated with disruption of bacterial membrane, probably due to the integration of the long hydrocarbon chain with the lipid bilayer of the cell membrane, leading to leakage of the cell content (Birnie et al., 2000). Nonetheless, the optimum antimicrobial activities of an imidazolium salts can be postulated to several factors including hydrophobicity, adsorption, critical micellar concentrations, aqueous solubility and transport in the assay medium, with solubility in the assay medium being the limiting factor for transport (Cornellas et al., 2011, Garcia et al., 2013, Kanjilal et al., 2009, Morán et al., 2001).

The mechanism of antimicrobial action of imidazolium salts is proposed to be similar to that of quaternary ammonium surfactants. The bacterial cell walls are negatively charged at physiological pH. Meanwhile, the cationic nature of imidazolium salts will be attracted to the bacterial cell wall electrostatically, whereby their hydrophobic components will disrupt the bacterial cell membrane which leads to leakage of intercellular components and ultimately cell death (Riduan and Zhang, 2013). Gram negative bacteria have an additional outer membrane that prevent adsorption, hence the Gram positive bacteria are generally more susceptible to treatment with surfactants.

As shown in **Table 9** above, the precursor compounds **62** and **63** did not show any antimicrobial activities at the highest concentration tested (5 mM). On the other hand, the 1-methylimidazole, 1-phenylimidazole, 1-*tert*-butylimidazole and imidazole, which are the basic azoles used for preparation of imidazolium salts **64** were also tested for their antimicrobial potential. However, they also did not display any antimicrobial activities, except for 1-phenylimidazole which was able to inhibit microorganism at 5 mM (**Table 9**). Together with the previous results, it is speculated that basic backbone structure of the imidazolium salts **64**, which comprises of a

chiral carbon bonded to a phenyl ring and a pyridine group, does not have antimicrobial property, as illustrated by the absence of antimicrobial activities in compound **62** and **63**. Instead, the antimicrobial activities improved after alkylation with the 1-methylimidazole, 1-phenylimidazole and 1-*tert*-butylimidazole to yield the targeted imidazolium salts **64**.

On top of that, it is interesting to know if the free metal ions (nickel, palladium and platinum ions in this case) and the transmetalating agents exhibit any antimicrobial activities, hence they are subjected to the BMD assay under the same experimental conditions. Based on the results, the NiCl₂, PdCl₂ and K₂PtCl₄ did not show antimicrobial activities at the highest concentration tested (0.5 mM) (**Table 10**). This is in agreement with other literature reported MIC values: NiCl₂ exhibited antimicrobial activities with MIC of 2 mM and above (Drašković et al., 2017, Sheikhshoaie et al., 2018), PdCl₂ was reported to have MIC values of more than 2.82 mM (Burgos et al., 2014), whereas K₂PtCl₄ was reported with MIC values of 1.45 mM and above (Radulović et al., 2006) against a series of microorganisms consisting of different Gram positive and Gram negative bacteria, and yeasts.

Interestingly, the transmetalating agent Pt(cod)Cl₂ displayed significant antimicrobial activities while Pd(CH₃CN)₂Cl₂ did not exhibit antimicrobial activities at the highest concentration tested (0.5 mM) (**Table 10**). It was effective against Gram-positive and Gram negative bacteria with MIC as low as 4 μM, but it is ineffective against the *Candida* sp. with MIC values above 0.5 mM (**Table 10**). Bacteriostatic activity (i.e. it keeps the bacteria in the stationary phase of growth) is defined as a ratio of MBC to MIC of more than four (Pankey and Sabath, 2004). Therefore, Pt(cod)Cl₂ is considered strongly bacteriostatic towards Gram-positive bacteria because there is more than 4-fold difference between the MIC and MBC values. The Therefore, the lack of antimicrobial activities against the Gram negative bacteria was not unexpected. Notably, this is the first report of antimicrobial activities of Pt(cod)Cl₂ as there have been, to the best of our knowledge, no previous literature on the antimicrobial activity of Pt(cod)Cl₂ complex but with only cytotoxicity study of modified derivatives of Pt(cod)Cl₂ available (Enders et al., 2014).

As mentioned earlier, although **64** showed antimicrobial activities in 5 mM or below against some pathogens, which are not comparable to other imidazolium salts which were reported to have MIC values in μM range. Nonetheless, it was observed that the antimicrobial activities increase remarkably upon coordination to the metals, including palladium (**Pd-65**) and platinum (**Pt-65**). Among the racemic **Pd-65** complexes tested, **Pd-65c** displayed the best

antimicrobial activities against all the microorganism strains tested, with the lowest MIC value of 0.016 mM (or 7 µg/mL) against *B. subtilis* (**Table 11**). Direct comparison with the findings of Haque's group is not possible. This is because different antimicrobial assays were utilised, where they studied a series of Pd NHC complexes with disc diffusion assay and broth dilution assay against *S. aureus* ATCC 29213 and *E. coli* ATCC 25922 only (Haque et al., 2013, Haque et al., 2016d). One of the major drawbacks of using disc diffusion assay is the antimicrobial activities were highly dependent on the capability of the compound to diffuse through the agar medium, where the overall lipophilicity of the structures will be the limiting factor to accurately determine the antimicrobial activities in this case. Nonetheless, it is suggested that the antimicrobial activities of **Pd-65b** and **Pd-65c** were better as compared to those reported, as their Pd NHC complexes are effective against *S. aureus* only with MIC of 50 µg/mL. In addition to that, the lack of antimicrobial activity observed for **Pd-65a** with the aliphatic methyl group *N*-tip compared to the **Pd-65b** with the aromatic phenyl *N*-tip and the **Pd-65c** with the bulky *tert*-butyl *N*-tip was not surprising. This could be due to the overall lipophilicity of the entire structure. The complex **Pd-65a** only made up of a single carbon unit alkyl chain while longer chain length would be expected for better antimicrobial activities. Whereas the respective aromatic phenyl group and bulky *tert*-butyl group in Pd NHC complex **Pd-65b** and **Pd-65c** would give the intrinsic lipophilicity to the structures resulting in better antimicrobial activities of those two complexes.

Furthermore, the **Pt-65** complexes displayed significant antimicrobial activities as compared to the **Pd-65** complexes (**Table 12**). Similarly, the **Pt-65b** and **Pt-65c** complexes, which bear the aromatic phenyl ring and the bulky *tert*-butyl group at the *N* tip of the imidazole ring respectively, were more capable of inhibiting the growth of microorganisms at a lower concentration as compared to the **Pt-65a** complex which bears the aliphatic CH₃ group. The **Pt-65b** and **Pt-65c** complexes displayed similar pattern of antimicrobial activities against the microorganisms tested, with MIC at the micromolar range being reported. The most substantial antimicrobial activities were observed against Gram positive bacteria with MIC below 10 µM (or below 5 µg/mL). There is no available literature reported on the antimicrobial activities of Pt NHC complexes. Nevertheless, the antimicrobial activities of **Pt-65** complexes were comparable to those Ag and Au NHC complexes which are widely known for their antimicrobial properties. For examples, Young's group reported a series of Ag NHC complexes with MIC lower than 10 µg/mL (Hindi et al., 2008, Kascatan-Nebioglu et al., 2006). Ray *et al.* also reported two antimicrobial gold and silver NHC complexes with MIC values at 15 µM and

25 μM , respectively (Ray et al., 2007). Also, it is observed that the complexes **Pt-65c**, **70** and **71**, which have different ancillary ligands (chloride, bromide and iodide, respectively), exhibited similar antimicrobial activities. This suggested that the change of ancillary ligands does not have significant effect on the complexes' antimicrobial activities in this case.

In general, the findings suggested that the antimicrobial activity arises from a synergy between the metal and the ligand. Based on Tweedy's chelation theory, the ion polarity of the metal centre is reduced by overlapping of the ligand orbitals and the exchange of the partial positive charge of the metal ion to the donor atoms of the ligands; thereby the delocalization of π -electrons on the chelate ring increases and improves the lipophilicity of the complexes (Neelakantan *et al.* 2010; Burgos *et al.* 2014). The increased lipophilicity allows the complex to penetrate the lipid membrane and block the metal binding sites on the enzymes, which might result in the disturbance of cellular respiration and protein synthesis, thereby inhibiting the growth (Prabhakaran *et al.* 2008). Generally, the nucleic acids, especially the deoxyribonucleic acid (DNA), is commonly considered to be the main target of group 10 metallodrugs through the formation of intra- and inter-strand adducts, while metal-bonding to sulphur-containing groups in proteins and interference with mitochondria functions were also reported (Sava *et al.* 2011).

Remarkably, while the racemic complex **Pd-65a** did not show any antimicrobial activity at the highest concentration tested (0.5 mM), its corresponding purified enantiomer **Pd-(Rc)-65a** was shown to inhibit the microorganisms tested. In contrast, this is not the same for Pd NHC complex **65b**, where both the racemic complex **Pd-65b** and the optically pure **Pd-(Sc)-65b** did not show any antimicrobial activity at the highest concentration tested (0.5 mM). This may be attributed to the antimicrobial property of Pd NHC complexes is more prominent in the *R* enantiomers instead of *S* enantiomers, and the antimicrobial property of **Pd-(Rc)-65** may be masked by **Pd-(Sc)-65** when they coexisted in the racemic complex **Pd-65**. It is not uncommon that there is only one major bioactive enantiomer out of two in racemic drugs (Asmus and Hendeles, 2000, Marzo and Heftmann, 2002). The most famous example would be thalidomide, where (*R*)-thalidomide is effective against morning sickness while (*S*)-thalidomide is teratogenic (Chhabra et al., 2013, Mauro and Giovanni, 2007). Therefore, optical resolution is important so that the respective enantiomers can be evaluated for their respective bioactive potentials.

Last but not least, the unexpected nickel coordination complex **72** and nickelate complex **73** did not display antimicrobial activities at the highest concentration tested (0.5 mM). However,

nickelate complexes were known to have antimicrobial activities towards both Gram positive and Gram negative bacteria though comparison cannot be made in this case as the antimicrobial activities were reported in terms of zone of inhibition obtained from disk diffusion assay and well diffusion assay (Çolak et al., 2010, Mohamed et al., 2014, Khojasteh and Matin, 2015). It is speculated that the lack of antimicrobial activities of the nickelate complex **73** was due to the low final concentration tested. Therefore, antimicrobial activities are expected in case of increment of the final concentration tested of this nickelate complex **73**.

3.3. Conclusion

In this chapter, a series of compounds but not limited to those precursors, imidazolium salts (or NHC precursors), and Group 10 metal NHC complexes synthesized in Chapter 2 were tested against a panel of microorganisms including Gram positive and Gram bacteria, as well as yeasts by using broth microdilution assays. The experimental results revealed that the imidazolium salts (or NHC precursors) **64** exhibited antimicrobial activities as suggested by the literatures. Besides that, it was observed that the palladium and platinum NHC complexes **Pd-65** and **Pt-65** exhibited improved antimicrobial activities upon coordination to metals, as compared to their corresponding imidazolium salts (NHC precursors), with minimum inhibitory concentration (MIC) values in the micromolar range. Notably, the antimicrobial activities of platinum NHC complexes **Pt-65b** and **Pt-65c** were determined to be as low as 2 μ M, which are comparable to silver NHC complexes with renowned antimicrobial profiles. Besides, the optically resolved *R* enantiomers of palladium NHC complexes have shown evident antimicrobial activities compared to *S* enantiomers, resembling chiral drugs with only one bioactive enantiomer out of two. Lastly, evidence for influence of the *N* wingtip substituents of imidazole ring on the antimicrobial properties of the metal NHC complexes was found.

3.4. Experimental

3.4.1. Microorganisms

The antimicrobial assay was conducted against thirteen strains of bacteria and three strains of *Candida sp.* as listed in **Table 13**.

Table 13. The list of microorganisms used in broth microdilution assay to determine the antimicrobial activity of the synthesized compounds.

Group	Strain	Microorganism
Gram positive bacteria	ATCC 14579	<i>Bacillus cereus</i>
	ATCC 8188	<i>Bacillus subtilis</i>
	ATCC 29213	Methicillin-sensitive <i>Staphylococcus aureus</i> (MSSA)
	ATCC 6538P	Methicillin-sensitive <i>Staphylococcus aureus</i> (MSSA)
	ATCC 700699	Methicillin-resistant <i>Staphylococcus aureus</i> (MRSA)
	ATCC 43300	Methicillin-resistant <i>Staphylococcus aureus</i> (MRSA)
	ATCC 33591	Methicillin-resistant <i>Staphylococcus aureus</i> (MRSA)
	ATCC 29212	<i>Enterococcus faecalis</i>
ATCC 700802	Vancomycin-resistant <i>Enterococcus faecalis</i> (VRE)	
Gram negative bacteria	ATCC 25922	<i>Escherichia coli</i>
	ATCC 10031	<i>Klebsiella pneumoniae</i>
	ATCC 10145	<i>Pseudomonas aeruginosa</i>
	ATCC 12022	<i>Shigella flexneri</i>
Yeast (Fungus)	IMR	<i>Candida albicans</i>
	Clinical isolate	<i>Candida albicans</i>
	Clinical isolate	<i>Candida tropicalis</i>

3.4.2. Broth microdilution assay (BMD)

The broth microdilution assay was conducted on 96-well microtiter plates according to protocol stated by Clinical and Laboratory Standards Institute (CLSI, 2012) with some amendments. The compounds tested were prepared in 10% DMSO in PBS solution. Positive controls utilised in this assay were chloramphenicol (0.250 mg/mL) for bacteria and cyclohexamine (1.00 mg/mL) for *Candida sp.*. Two negative controls were prepared: with MHB broth only, and with 10.0 % DMSO in PBS. Overnight bacteria culture in Mueller-Hinton broth (MHB) was adjusted to match 0.5 McFarland standard and diluted 1:100 in MHB. Into each well of the 96-well microtiter plate, the compounds of interest were serially diluted two-fold with MHB to obtain final working concentrations range between 0.500 mM and 391 μ M (for metal complexes) or 5.00 mM and 39.1 μ M (for compounds other than metal complexes) in 100 μ L broth. Then, 100 μ L of 1:100 diluted bacterial suspensions were added into each well prior to incubation at 37 °C for 24 hours. The well with the lowest concentration of compounds that has no observed growth was determined as the minimum inhibitory concentration (MIC). The content of clear wells was streaked on Mueller-Hinton agar (MHA) and incubated overnight. The minimum bactericidal concentration (MBC) was determined as the lowest concentration of compound in which the inoculum did not give bacterial broth on the MHA. The experiment was performed in triplicates.

CHAPTER 4 CYTOTOXICITY STUDIES OF PALLADIUM, PLATINUM AND NICKEL *N*-HETEROCYCLIC CARBENE (NHC) COMPLEXES

4.1. Introduction

Cancer is the second leading cause of death in the world, right after cardiovascular diseases, which affects people from all genders and age groups. It is class of diseases recognized by uncontrolled cell proliferation beyond their usual boundaries, invasion and destruction of neighbouring tissues, and dispersion to other body parts and organs through blood or lymph, or otherwise known as metastasis (Tandon et al., 2018). Cancer cells are capable of avoiding apoptosis and continue to divide uncontrollably, while the normal cells are usually eliminated by apoptosis or programmed cell death when they are damaged beyond repair (Domagoj, 2008).

The most common types of cancers around the world include lung, breast, colorectal, prostate, skin and stomach cancers, whereby the majority of cancer deaths is caused by lung, breast, colorectal, stomach and liver cancers (WHO, 2014). The number of new cancer cases is on the rise globally yet there are only limited choices of therapeutic options which can cure cancers. Notably, cisplatin and other platinum based metallodrugs have played an essential role in chemotherapy of cancer patients for more than 30 years to date. Nonetheless, the limitations of these platinum based chemotherapeutics, especially the severe side effects experienced by the patients, have posed a strict boundary on the applicability of these drugs. This highlights that there is an urgent need to search for novel anticancer complexes with improved therapeutic window and reduced toxicity.

Taking cisplatin as the starting point, platinum based complexes have been explored extensively as an anticancer drug candidate. Besides that, due to the high resemblance to the chemistry of platinum, there is a focus on studying the palladium complexes for their anticancer properties since more than a decade ago. One of the approaches to circumvent the drawbacks of these metal based drugs is to reduce the toxicity of a complex by varying the coordinated nitrogen ligand or changing the leaving groups (Edwards et al., 2005, Quirante et al., 2011). With regards to this, the *N*-heterocyclic carbene (NHC) ligands have been a prominent choice. A number of group 10 metal NHC complexes including platinum, palladium and nickel NHC complexes with excellent anticancer activities have been depicted previously in Chapter 1.

In this chapter, cytotoxicity studies are conducted by using the previously synthesized compounds from Chapter 2, inclusive but not limited to the precursors, imidazolium salts or NHC ligands, and Group 10 metal NHC complexes. MTT (3-(4,5-dimethylthiazol-2-yl)-2,5-diphenyltetrazolium bromide) cell viability assay will be carried out to determine the cytotoxicities of the tested compounds against a panel of human carcinoma cell lines including oral (H103), breast (MCF7) and colon (HCT116) cancer cells. On top of that, the compounds will also be tested against a series of normal cell lines such as skin keratinocytes (HACAT), lung epithelial cells (BEAS2B) and oral epithelial cells (OKF6) for selectivity index study.

4.2. Results and Discussion

4.2.1. Cytotoxicity study against human carcinoma cell lines

MTT cell viability assay was performed to determine cell cytotoxicity of the synthesized complexes on tested carcinoma and normal cell lines. The rationale behind MTT cell viability assay lies on the ability of mitochondrial dehydrogenase to reduce MTT tetrazolium dyes into blue formazan product. This reflects the normal functioning of mitochondria and thereby, the cell viability.

Three selected human carcinoma cell lines, including H103 (oral carcinoma), HCT116 (colon carcinoma) and MCF7 (breast carcinoma), were exposed to various concentrations of complexes, from 0 μM to 40 μM , for 48 hours before determination of their respective cell viabilities using the MTT cell viability assay. The absorbance values obtained based on the quantity of the blue formazan product were converted to their respective cell viability at different concentrations to generate a plot. Using these data, the cytotoxicity of the tested compounds was expressed in terms of IC_{50} or half maximal inhibitory concentration, which is the concentration where the compound inhibited 50 % of the seeded cells. The IC_{50} values of all the compounds tested were tabulated in **Table 14** below.

In this assay, cisplatin was utilised as a positive control as it is a clinically used antitumor drug. Cisplatin was known to exert its antitumor action via binding of cisplatin to DNA and non-DNA targets, which further induce cell death through apoptosis, necrosis or both within the heterogenous population of cells that forms a tumoral mass (Cepeda et al., 2007). It is a great reference drug for comparing the cell cytotoxicity of the synthesized metal NHC complexes to reflect the possible effectiveness and applicability of these metal NHC complexes as novel anticancer drugs in this preliminary screening stage.

Table 14. Cytotoxicity of all compounds against selected human carcinoma cell lines, reported as IC₅₀ (concentration required for 50% inhibition *in vitro*) in terms of μM.

Compound group	Cell lines**	IC ₅₀ of compound tested (μM)*		
		H103	HCT116	MCF7
Control	Cisplatin	6.16 ± 0.04 ^a	10.78 ± 0.21 ^a	19.78 ± 0.21 ^a
Precursors	62	> 40.00	> 40.00	> 40.00
	63	> 40.00	> 40.00	> 40.00
Imidazoles	Me(im)	> 40.00	> 40.00	> 40.00
	Ph(im)	> 40.00	> 40.00	> 40.00
	tBu(im)	> 40.00	> 40.00	> 40.00
	imidazole	> 40.00	> 40.00	> 40.00
Imidazolium salts	64a	> 40.00	> 40.00	> 40.00
	64b	> 40.00	> 40.00	> 40.00
	64c	> 40.00	> 40.00	> 40.00
Metal salts	PdCl ₂	> 40.00	> 40.00	> 40.00
	K ₂ PtCl ₄	> 40.00	> 40.00	> 40.00
	NiCl ₂	> 40.00	> 40.00	> 40.00
Transmetalating agent	Pd(CH ₃ CN) ₂ Cl ₂	> 40.00	> 40.00	> 40.00
	Pt(cod)Cl ₂	> 40.00	> 40.00	> 40.00
Pd NHC complexes	Pd-65a	> 40.00	> 40.00	> 40.00
	Pd-65b	13.90 ± 0.37 ^b	18.60 ± 0.39 ^b	36.69 ± 0.10 ^b
	Pd-65c	22.40 ± 1.01 ^{cd}	38.74 ± 0.51 ^c	> 40.00
	Pd-(Rc)-65a	34.77 ± 0.47 ^e	36.46 ± 0.34 ^d	26.27 ± 0.84 ^c
	Pd-(Sc)-65b	23.14 ± 0.25 ^c	> 40.00	> 40.00
Diastereomers	Pd-(Rc,Sc)-68a	> 40.00	> 40.00	> 40.00
	Pd-(Sc,Sc)-69b	> 40.00	> 40.00	> 40.00
Pt NHC complexes	Pt-65a	> 40.00	> 40.00	> 40.00
	Pt-65b	21.93 ± 0.50 ^d	15.19 ± 0.14 ^e	28.34 ± 0.26 ^d
	Pt-65c	6.18 ± 0.19 ^a	5.52 ± 0.03 ^f	7.33 ± 0.13 ^e
	70	16.90 ± 1.07 ^f	11.96 ± 0.65 ^g	25.98 ± 0.33 ^c
	71	11.28 ± 0.87 ^g	6.04 ± 0.07 ^h	15.91 ± 0.19 ^f
Ni complexes	72	> 40.00	> 40.00	> 40.00
	73	32.71 ± 1.12 ^h	> 40.00	> 40.00

* The IC₅₀ tabulated represents the average of four independent experiments ± SEM. Different letters (a – h) represent significant differences between different compounds tested for that particular cell line.

** Cell lines: H103 (human oral carcinoma), HCT116 (human colon carcinoma), MCF7 (human breast carcinoma)

In general, the results showed that the compounds tested had an inhibitory effect in a dose-dependent manner against the cancer cells tested (**Table 14**). This is expected as different cell lines would have different growth rates, drug sensitivities, oncogene expressions and other factors that might possibly causes the variations in the cells (Barretina et al., 2012, Johnson et al., 2001). Literatures have also demonstrated that those reported IC₅₀ values of metal NHC complexes may vary between different cell lines evaluated, therefore it is plausible that these metal NHC complexes would have different magnitudes of potency in other cell types.

Based on the results in **Table 14** above, it was observed that the imidazolium salts **64** did not display significant cytotoxicity against the three cancer cell lines tested with IC_{50} more than the highest concentration tested (40 μ M). In addition, similar to those observed in the antimicrobial assay, no cell cytotoxicity effect was observed for the precursors (compound **62** and **63**) at 40 mM, the highest concentration tested (**Table 14**). Combining these observations, it is reasoned that basic backbone structure of the imidazolium salts **64**, which comprises of a chiral carbon bonded to a pyridine group and a phenyl ring is not cytotoxic, as demonstrated by the lack of cell cytotoxicity in compound **62** and **63**. Besides that, the cell cytotoxicity study also revealed that the azoles, including 1-methylimidazole, 1-phenylimidazole, 1-*tert*-butylimidazole and imidazole, which were used for preparation of imidazolium salts **64** did not display any cell cytotoxicity effect at the highest concentration tested (**Table 14**). Nevertheless, literatures have suggested that heterocyclic compounds with imidazole moieties were known to exhibit anticancer activities that acted via different targets including DNA, VEGF, mitotic microtubules, histone deacetylases, receptor tyrosine kinases, topoisomerases, CYP26A1 enzyme, rapid accelerated fibrosarcoma (RAF) kinases and others (Ali et al., 2017, Chen et al., 2008, Ali et al., 2015).

The metal ions (nickel, palladium and platinum ions in the different metal salts used) and the transmetalating agents were also tested for their cell cytotoxicity effects against the selected cancer cells under similar experimental conditions. According to the results, the $NiCl_2$, $PdCl_2$ and K_2PtCl_4 salts did not exhibit cell cytotoxicity at the highest concentration tested (40 μ M) (**Table 14**). This is not unexpected as simple salts like these are generally known to be possessing antimicrobial feature but none have been known to be antiproliferative at such low concentrations. Similarly, the transmetalating agent $Pd(CH_3CN)_2Cl_2$ and $Pt(cod)Cl_2$ complex have an IC_{50} value of more than 40 μ M (**Table 14**). Though no literature that had reported the anticancer activity of $Pd(CH_3CN)_2Cl_2$ complex before, the $Pt(cod)Cl_2$ complex was shown to be fitting those described previously in literature. Studies have shown that the original $Pt(cod)Cl_2$ complex was not significantly active (with half-inhibitory concentration above 100 μ M) against the tested human cancer cell lines (MCF7 breast carcinoma and HT29 colon carcinoma), while replacement of at least one chlorine atom (R group) of the $Pd(cod)Cl_2$ complex will lead to the formation of distinctively bioactive complexes (Enders et al., 2014, Butsch et al., 2009). Despite that, the cisplatin exerts its cytotoxicity effect by DNA intercalation through the actions of their two chlorine atoms, the lack of cytotoxicity of $Pt(cod)Cl_2$ complex is not surprising. The hydrophobic organic 1,5-cyclooctadiene ligand,

which is replacing the two amine ligands in cisplatin, may act like a steric shield and hinder the ideal interaction between a compound and its binding site, hence this may explain the lack of cytotoxic effect of Pt(cod)Cl₂ complex compared to their modified platinum complexes with cyclooctadiene ligands (Moller et al., 2014, Patrick, 2013).

Previously we have showed that there is no cell cytotoxicity effect was observed for the imidazolium salts **64** up to 40 μM against the three carcinoma cell lines tested. Therefore, the cytotoxic effects observed in the racemic palladium and platinum complexes **65** is speculated to be mainly due to the metal-ligand interaction with cellular components (**Table 14**). The cell cytotoxicity effects of these active complexes were comparable to those of other reported organic anticancer agents, including noscapine (IC₅₀ of 20-35 μM) and estramustine (IC₅₀ of 0.5-17 μM) (Nicholson et al., 2002, Zhou et al., 2003). Also, the IC₅₀ values of metal NHC complexes have been previously reported to vary within different cell lines, hence it is conceivable that these metal NHC complexes could show greater potency in other cell types.

In general, the metal NHC complex **65b** (with aromatic phenyl *N*-tip) and **65c** (with bulky tert-butyl *N*-tip), regardless of palladium or platinum, have shown better cytotoxic effect compared to their analogue **65a** (with aliphatic methyl *N*-tip) against the tested carcinoma cell lines as evidenced by the low IC₅₀ values recorded (**Table 14**). This structure-activity relationship may be attributed to the central metal atom as explained by Tweedy's chelation theory and overall lipophilicity of the compounds (El-Tabl et al., 2015, Raman et al., 2009). Upon metal chelation to the ligand, the polarity of the metal ion will be reduced to a greater extent due to overlapping of the ligand orbital and partial sharing of the positive charge of metal ions with donor atoms of the ligand, which then increases the delocalization of the π-electrons over the entire chelate ring and enhances the lipophilicity of the metal NHC complexes (Neelakantan *et al.* 2010; Burgos *et al.* 2014). With the increased lipophilicity, the metal NHC complexes can now penetrate the lipid membrane with higher efficiency and block the metal binding sites on the enzymes, ultimately leading to growth inhibition of the organisms via disturbance of cellular respiration and protein synthesis (Prabhakaran *et al.* 2008). Besides that, it was known that the steric factors (bulk, size and shape) of drug can affect how easily it can approach and interact with a binding site. Bulky substituents may act like a steric shield and hinder the ideal interaction between a compound and its binding site, alternatively, it may help to orientate the compound properly for maximum binding and increase activity (Moller et al., 2014, Patrick, 2013).

Comparison between different metal centres of the metal NHC complexes have revealed that there are variations in their cytotoxicities against the cancer cells tested. Based on **Table 14** above, the **Pt-65** complexes displayed higher cytotoxicities against the carcinoma cell line tested as compared to the **Pd-65** complexes (IC₅₀ range of 13.90 to 38.74 μM) with IC₅₀ ranging from 5.52 to 28.34 μM. Among all, **Pt-65c** with the bulky *tert*-butyl *N* substituent was the most potent among all the metal NHC complexes tested, with IC₅₀ that are two to three times lower than that of the anticancer drug cisplatin. These results are not surprising as platinum NHC complexes were well known for their anticancer properties, as evident by the widespread applications of platinum based drugs as chemotherapeutics. Literature have reported a series of Pt NHC complexes with varying IC₅₀ compared to cisplatin, ranging from as low as 0.01 μM to more than 100 μM (Skander et al., 2010, Sun et al., 2011, Dahm et al., 2015, Adhikary et al., 2012, Zhang et al., 2015, Chekkat et al., 2016, Schmitt et al., 2016). Therefore, the synthesized Pt NHC complexes **Pt-65** were moderately cytotoxic towards the cancer cells tested, among others. Markedly, a *trans*-Pd NHC complex **36** (see page 20) with impressive cell cytotoxicity against HeLa, HCT116 and MCF7 carcinoma cells with IC₅₀ of 0.8 to 4 μM and was twice more effective than cisplatin have been reported (Ray et al., 2007). Complex **36** highly resembled our complex **Pd-65c**: a monometallic complex bearing a NHC ring with *tert*-butyl group at the *N* tip, functionalised with a phenyl ring and a pyridine group. Though the role of cyclometalated fashion of complex **Pd-65c** in cytotoxicities is yet to be confirmed, direct comparison should not be made with Pd NHC complex **36** as the bioassay, experimental conditions and cell lines used to study the complexes' cytotoxicity effects were dissimilar. Nonetheless, it is suggested that the racemic complex **Pd-65c** could potentially be a good cytotoxic agent, and could perform even better once it is resolved into its respective enantiomers.

Interestingly, the optically active enantiomer **Pd-(Rc)-65a** was shown to be cytotoxic with IC₅₀ around 26 to 34 μM against the three cell lines tested as compared to the racemic Pd NHC complex **Pd-65a** (**Table 14**). Inversely, as opposed to the enantiomer **Pd-(Rc)-65a** which have enhanced cell cytotoxicity against the carcinomas after optical resolution, the IC₅₀ values **Pd-(Sc)-65b** were higher than that of racemic Pd NHC complex **Pd-65b** with reduced cytotoxicity (**Table 14**). Similar to its antimicrobial properties, it is speculated the cell toxicity of *R* enantiomers is more evident compared to *S* enantiomers. As aforementioned, for the racemic complex **Pd-65**, which the enantiomers **Pd-(Rc)-65** and **Pd-(Sc)-65** coexisted, the cell cytotoxicity effect of **Pd-(Rc)-65** may be masked by **Pd-(Sc)-65**, a similar circumstance for other racemic drugs with one major bioactive enantiomers (Asmus and Hendeles, 2000, Marzo

and Heftmann, 2002). Nonetheless, in a recent study where Kumar et al. studied five enantiomeric pairs of Pd NHC complexes (**53** and **54**) derived from 1,2,4-triazole (see page 26), no influence on the cytotoxicity was observed in regards to the chirality as both enantiomers of all five enantiomeric pairs exhibited near-equal activities, whereby one of the enantiomeric pair was shown to be three- to 27-fold more active than the benchmark cisplatin against human carcinoma cell lines (Kumar et al., 2017). Nevertheless, it is known that for a racemic complex, in this case Pd NHC complexes **Pd-65**, each enantiomer possesses its own pharmacological activities that can be null, similar, different or opposite (Nguyen et al., 2006). Even though the Pd NHC complexes **65** showed lower cytotoxic effects compared to cisplatin, the racemic Pd NHC complexes **Pd-65b** and **Pd-65c** have exhibited substantial cell cytotoxicities against the carcinoma cells tested. Therefore, it is important to separate the enantiomers via optical resolution and evaluate their respective bioactivities.

The mode of action of platinum and palladium NHC complexes is generally due to covalent bonding at the minor groove of DNA causing crosslinking of the bases (especially with guanine), and the square planar configuration at the metal centre enabled intercalation of the compounds with the DNA involving a π - π stacking. Additionally, a mode of action involving interference of cancer cell proliferation by arresting the cells at the G2 phase; caused production of reactive oxygen species (ROS) in the mitochondria which led to cell death; and involved in inducing p53-dependent programmed cell death have also been proposed for palladium NHC complex (Ray et al., 2007, Kumar et al., 2017). There were also reports on the Pt NHC complexes accumulated in the nucleus, mitochondria or cytoplasm and play an important role in triggering cell apoptosis (Sun *et al.*, 2011, Chekkat *et al.*, 2016). Apart from the usual DNA target, platinum NHC complexes were recently shown to be interacting with G-quadruplex (G4) structures from telomeric sequence involved in oncogene promoters and thereby causing cell death (Betzer et al., 2016).

Lastly, it was observed that the unexpected nickel coordination complex **72** did not display cytotoxicity against the cancer cells at the highest concentration tested (40 μ M). While the unexpected nickelate complex **73** was not cytotoxic towards HCT116 and MCF7 at 40 μ M, it was cytotoxic towards the oral cancer cells (H103) with IC_{50} value of 32.71 μ M. There was a previous report on a sodium tris(aspartato)nickelate(II) complex which displayed LC_{50} (the concentration of a given compound which is lethal to 50% of the cell) values of 4.187-8.044 μ g/mL in an *in vivo* brine shrimp lethality bioassay (Aiyelabola et al., 2017). This thereby suggesting that nickelate complex could be a cytotoxic agent towards living cells. Nonetheless,

the low cytotoxicity of the nickelate complex **73** against cancer cells observed could be attributed the high final concentration used in the assay, and the cytotoxicity is expected to enhance with increment of the final concentration tested of this nickelate complex **73**.

4.2.2. Selectivity index study

Despite that the cytotoxic effects of the tested complexes **Pd-65** and **Pt-65** towards the selected cancer cells are promising, these metal NHC complexes should not harm the normal cells. Therefore, a selectivity index study was conducted to compare the cytotoxicity effects of these metal complexes against both cancer cells and normal cells. First and foremost, the synthesized complexes that were effective against the cancer cells were also tested against a panel of normal human cells including OKF6 (human oral epithelial cells), HACAT (human skin keratinocytes) and BEAS2B (human lung epithelial cells). The selection of these three human cell lines was to explore the prospect of possible drug delivery methods for future applications, i.e. oral administration of drug, dermal or transdermal drug delivery *via* skin, as well as pulmonary delivery *via* lung. Their respective cytotoxicities against OKF6, HACAT and BEAS2B were tabulated in **Table 15**. Likewise, a dose-dependent pattern was observed for the same compound against the normal cell lines tested. Besides, the IC₅₀ values obtained were neither significantly higher nor lower than that of against the cancer cells (as listed in **Table 14**).

Table 15. Cytotoxicity of selected compounds against selected human normal cell lines, reported as IC₅₀ (concentration required for 50% inhibition *in vitro*) in terms of μM.

Compound group	Cell lines**	IC ₅₀ of compound tested (μM)*		
		OKF6	HACAT	BEAS2B
Control	Cisplatin	ND	7.59 ± 0.62 ^a	9.64 ± 0.21 ^a
Pd NHC complexes	Pd-65b	8.17 ± 0.13 ^{ab}	15.86 ± 1.75 ^b	16.10 ± 0.56 ^b
	Pd-65c	5.89 ± 0.05 ^c	12.70 ± 0.77 ^c	7.60 ± 0.30 ^c
	Pd-(Rc)-65a	16.88 ± 3.27 ^d	> 40.00	33.37 ± 0.44 ^d
	Pd-(Sc)-65b	23.73 ± 0.56 ^e	> 40.00	> 40.00
Pt NHC complexes	Pt-65b	8.08 ± 0.03 ^a	24.26 ± 0.51 ^d	10.71 ± 0.24 ^e
	Pt-65c	5.20 ± 0.01 ^f	5.89 ± 0.07 ^e	5.46 ± 0.02 ^f
	70	8.45 ± 0.28 ^b	15.04 ± 0.78 ^b	6.40 ± 0.18 ^g
	71	5.98 ± 0.03 ^g	11.38 ± 0.49 ^f	5.50 ± 0.06 ^f
Ni complex	73	18.75 ± 1.61 ^h	> 40.00	32.91 ± 1.13 ^d

* The IC₅₀ tabulated represents the average of four independent experiments ± SEM. Different letters (a – h) represent significant differences between different compounds tested for that particular cell line.

** Cell lines: OKF6 (human oral epithelial cells), HACAT (human skin cells, keratinocytes), BEAS2B (human lung epithelial cells)
Abbreviation: ND, not determined.

The selectivity index (SI) indicates the cytotoxic selectivity of the compound against cancer cells and its safety towards normal cells. It was determined from the ratio of the IC₅₀ value obtained from the cell viability test on normal cells versus the IC₅₀ value obtained for the cancer cells. The compound with selectivity index value higher than 3 is suggested to have high selectivity towards a particular cell line while value above 1 indicates greater inhibition of cancer cells survival than normal cells (Haque et al., 2016a, Mahavorasirikul et al., 2010, Peña-Morán et al., 2016, Flis and Spławski, 2009). In this case, selectivity index was computed based on the IC₅₀ values of three cancer cell lines and a normal cell at a time. **Table 16**, **Table 17** and **Table 18** below presented the selectivity index of the active complexes for OKF6 (oral epithelial cells), HACAT (skin keratinocytes) and BEAS2B (lung epithelial cells), respectively.

In general, it was observed that the tested metal NHC complexes **Pd-65** and **Pt-65** were not selective against the cancer cells as the SI value obtained were below 2 and laid between the range of 0.15 to 1.60. Although some of the tested complexes have the SI values that are comparable or even surpassed that of cisplatin, the selectivity towards the cancer cells was unsatisfactory as it is less than three. Cisplatin is renowned for its high effectiveness in the treatment for ovarian and testicular cancers and is also widely employed for treatment of cervical, bladder, head and neck, oesophageal and small cell lung cancers (Cepeda et al., 2007). Cisplatin is traditionally administered through the vein intravenously as an infusion. Therefore, the low selectivity index of cisplatin calculated was not surprising as the cell lines utilised are oral, colon and breast cells. On top of that, the low selectivity of cisplatin towards the normal cells explained the toxicities of cisplatin towards the cancer patients, which are reflected by the side effects experienced after cisplatin treatment.

However, these low selectivity index obtained could be due to the fast doubling time of the normal oral epithelial cells (OKF6), normal skin keratinocytes (HACAT) and normal lung epithelial cells (BEAS2B), which are similar to that of the cancer cell lines. As a result, these fast-growing normal cells were also susceptible to the metal complexes at low concentration of compounds, as observed from their IC₅₀ values. Otherwise, literature have suggested that higher concentration of drug is required to inhibit slow-growing cells in relations with its higher doubling time in culture, and this would make the cell resistant to the cytotoxic agents tested (Haque et al., 2016a, Henriksson et al., 2011). Therefore, it is anticipated that the cytotoxicity of these synthesized complexes would reduce when it is tested against a slow-growing cell line, such as CCD841CON (a colorectal epithelial cell line), which resembled the growth rate of typical normal cells, thereby increase the selectivity index in such cases.

Table 16. Selectivity index (SI) of selected compounds for oral epithelial cells (OKF6) against oral cancer (H103), colon cancer (HCT116), and breast cancer (MCF7) cells.

Compound tested	Selectivity Index (SI) against OKF6 ^a		
	Oral	Colon	Breast
Cisplatin	ND	ND	ND
Pd-65b	0.59	0.44	0.22
Pd-65c	0.26	0.15	ND
Pd-(Rc)-65a	0.49	0.46	0.64
Pd-(Sc)-65b	1.03	ND	ND
Pt-65b	0.37	0.53	0.29
Pt-65c	0.84	0.94	0.71
70	0.50	0.71	0.33
71	0.53	0.99	0.38
73	0.57	ND	ND

^aSelectivity index (SI) was determined from the ratio of the IC₅₀ obtained from the test against normal cells versus the IC₅₀ for cancer cells. Abbreviation: ND, not determined.

Table 17. Selectivity index (SI) of selected compounds for skin keratinocytes (HACAT) against oral cancer (H103), colon cancer (HCT116), and breast cancer (MCF7) cells.

Compound tested	Selectivity Index (SI) against HACAT ^a		
	Oral	Colon	Breast
Cisplatin	1.23	0.70	0.38
Pd-65b	1.14	0.85	0.43
Pd-65c	0.57	0.33	ND
Pd-(Rc)-65a	ND	ND	ND
Pd-(Sc)-65b	ND	ND	ND
Pt-65b	1.11	1.60	0.86
Pt-65c	0.95	1.07	0.80
70	0.89	1.26	0.58
71	1.01	1.88	0.72
73	ND	ND	ND

^aSelectivity index (SI) was determined from the ratio of the IC₅₀ obtained from the test against normal cells versus the IC₅₀ for cancer cells. Abbreviation: ND, not determined.

Table 18. Selectivity index (SI) of selected compounds for lung epithelial cells (BEAS2B) against oral cancer (H103), colon cancer (HCT116), and breast cancer (MCF7) cells.

Compound tested	Selectivity Index (SI) against BEAS2B ^a		
	Oral	Colon	Breast
Cisplatin	1.57	0.89	0.49
Pd-65b	1.16	0.87	0.44
Pd-65c	0.34	0.20	ND
Pd-(Rc)-65a	0.96	0.92	1.27
Pd-(Sc)-65b	ND	ND	ND
Pt-65b	0.49	0.71	0.38
Pt-65c	0.88	0.99	0.75
70	0.38	0.54	0.25
71	0.49	0.91	0.35
73	1.01	ND	ND

^aSelectivity index (SI) was determined from the ratio of the IC₅₀ obtained from the test against normal cells versus the IC₅₀ for cancer cells. Abbreviation: ND, not determined.

4.3. Conclusion

This chapter discussed the anticancer activities of a series of compounds including but not limited to those precursors, imidazolium salts (or NHC precursors), and Group 10 metal NHC complexes synthesized in Chapter 2. Their respective cytotoxicity effects were evaluated against a panel of human carcinoma cell lines, including H103 (oral cancer), HCT116 (colon cancer) and MCF7 (breast cancer) by using MTT cell viability assay. The experimental results showed that upon coordination to metals, the cytotoxicity effects of the Pd and Pt NHC complexes **65** increased significantly as compared to the imidazolium salts **64**. Based on the comparison of IC₅₀ with literature values, these metal NHC complexes **65** had moderate cytotoxicities against the cancer cells tested. Remarkably, the complex **Pt-65c** displayed significant cytotoxicities towards the cancer cells with IC₅₀ values that are two to three times lower than that of the anticancer benchmark cisplatin. Variable cytotoxicities were also observed for the *R* and *S* enantiomer of palladium NHC complexes, in which latter was less cytotoxic towards the cancer cells tested. In addition to that, evidence for influence of the *N* wingtip substituents of imidazole ring on the cytotoxicities of the metal NHC complexes was found. Selectivity index study was also carried out using three human normal cell lines namely OKF6 (oral epithelial cells), HACAT (skin keratinocytes) and BEAS2B (lung epithelial cells). Regrettably, the selectivity of the tested complexes towards the cancer cells was unsatisfactory.

4.4. Experimental

4.4.1. Cell lines

Three human carcinoma cell lines and three human normal cell lines were utilized in this study as shown in **Table 19**.

Table 19. The list of cell lines used in MTT assay to determine the cytotoxicity of the synthesized compounds, including human carcinoma cell lines and normal cell lines.

Group	Name	RRID	Description
Human carcinoma cell lines	H103	CVCL_2457	Oral squamous cells – tongue squamous cell carcinoma
	HCT116	CVCL_0291	Colon epithelial cells – colorectal carcinoma
	MCF7	CVCL_0031	Breast/Mammary epithelial cells – adenocarcinoma
Human normal cell lines	OKF6	CVCL_L222	Oral epithelial cells
	HACAT	CVCL_0038	Skin cells – keratinocytes
	BEAS2B	CVCL_0168	Lung epithelial cells

4.4.2. Maintenance of cell culture

The cell culture media used to culture and maintain the human carcinoma cell lines and human normal cell lines were listed below (**Table 20**).

Table 20. The list of corresponding cell culture media used to culture and maintain the selected human carcinoma cell lines and normal cell lines.

Group	Name	Cell culture medium
Human carcinoma cell lines	H103	Dulbecco's Modified Eagle Medium-F12 (DMEM-F12)
	HCT116	McCoy's 5A medium
	MCF7	Dulbecco's Modified Eagle Medium (DMEM)
Human normal cell lines	OKF6	Keratinocyte-Serum Free Medium (KSFM)
	HaCaT	Dulbecco's Modified Eagle Medium (DMEM)
	Beas2B	Roswell Park Memorial Institute (RPMI) 1640 medium

The cell culture media were supplemented with sodium hydrogen carbonate, 10 % fetal bovine serum (FBS), 100 U/mL penicillin and 100 µg/mL streptomycin in culture flasks. In addition to that, the DMEM-F12 medium for H103 was added with 0.5 µg/mL of sodium hydrocortisone succinate, and KSFM medium for OKF6 was supplemented with calcium chloride at a final concentration of 0.02 mM.

Initially, all adherent cell lines were maintained at 37 °C, 5 % CO₂ and 95 % humidity. Cells that have a confluency of 70-80 % were chosen for cell seeding purpose. The old medium was carefully removed from the cell culture flasks. The cells were then washed thrice with sterile phosphate buffer saline (PBS) with pH 7.4. After washing, PBS was discarded completely before addition of 0.05% trypsin-EDTA solution and distributed evenly over the cell surfaces. The cells were then incubated at 37 °C in 5% CO₂ for around 5 minutes. The flasks were containing the cells were then gently tapped to facilitate cell segregation and were then observed using an inverted microscope (if cell segregation is not satisfactory, the cells were incubated for another 5 minutes). Trypsin activity was inhibited by addition of fresh complete media of 10% FBS. The cells were the counted and diluted to obtain a final concentration of 50,000 cells/mL for seeding cells in the microtiter plate (100 µL cells per well).

4.4.3. MTT cell viability assay

MTT (3-(4,5-dimethylthiazol-2-yl)-2,5-diphenyltetrazolium bromide) cell viability assay was performed to evaluate the cell cytotoxicity effects of the synthesized compounds (Riss et al., 2004). The compounds tested were prepared in 2% DMSO in PBS solution. Positive control utilised in this assay was cisplatin (prepared in 0.9% NaCl solution). The cells were seeded in 96-well microtiter plate at a density of 5000 cells/well in 100µL cell culture medium and incubated at 37 °C (5 % CO₂) for 24 hours. After 18 hours of seeding, the medium was removed and then the cells were incubated at 37 °C for 48 hours in CO₂ incubator with absence and/or presence of various concentrations of compounds of interest ranging from 10, 20, 25, 30, 35 and 40 µM. Given that the compound's treatments containing 0.2 % of final DMSO concentration, 0.2 % DMSO in PBS solution was used as the negative control. After incubation, 10 µL of MTT solution (5 mg/mL in PBS) was added into each well. These plates were incubated again for 4 hours in CO₂ incubator at 37 °C. After that, the medium-MTT solutions are removed and the purple formazan crystals formed were dissolved in 200 µL dimethyl sulfoxide. The resulting MTT-products were determined by measuring the absorbance at 570 nm, with reference wavelength at 620 nm. The experiment was carried out in quadruplicate for each compound/complex, and the medium not containing the complexes served as the control. The cell viability was determined by using the formula: Cell viability % = (optical density of sample / optical density of control) × 100 (solvent controls set to 100% viable cells). IC₅₀ value were defined as the concentrations that show 50% inhibition of proliferation on any tested cell line.

CHAPTER 5 SUMMARY AND FUTURE DIRECTIONS

5.1. Summary

In this study, a series of racemic pyridine-functionalised nickel, palladium and platinum NHC complexes were synthesized and characterized. The basic backbone of the NHC ligands were prepared in two stepwise reactions: reduction of the commercially available 2-benzoylpyridine **61**, followed by halogenation to yield the common 2-(chloro(phenyl)methyl)pyridine **63**. Subsequent reactions with different imidazoles gave the desired imidazolium salts (or NHC precursors) **64** with different R groups at the *N* wingtip [R = Me (**a**), Ph (**b**) and *t*Bu (**c**)] at the imidazole ring. Transmetalation of the imidazolium salts (NHC precursors) into palladium and platinum NHC complexes **65** were achieved by using Ag₂O mediated method with Pd(CH₃CN)₂Cl₂ and Pt(cod)Cl₂ as the transmetalating agents respectively. In contrast, nickel NHC complexes were synthesized via one pot synthesis method with nickel chloride as the transmetalating agent and reflux in the presence of a base. Noted that the racemic metal NHC complexes **65** have a chiral centre within the NHC chelate ring, therefore each racemic metal NHC complexes is made up of equal composition of *R* and *S* enantiomers. Two racemic palladium NHC complexes (**Pd-65**) were separated into enantiomers via optical resolution approach which involved three steps: formation of diastereomers pair upon coordination with sodium salt of chiral amino acid, separation of the diastereomeric pair by fractional crystallization, followed by treatment with 1 M HCl to get the optical active metal NHC complexes (either *R* or *S*) as a result of cleavage of chiral amino acid auxiliary. In this study, complex **Pd-(Rc)-65a** was obtained from the racemic complex **Pd-65a** whereas **Pd-(Sc)-65b** was isolated from the racemic complex **Pd-65b**.

The structures and identities of these synthesized precursors (**62** and **63**), imidazolium salts **64** and metal NHC complexes **65** have been investigated and confirmed by using different spectroscopy techniques including proton (¹H) and carbon (¹³C) nuclear magnetic resonance (NMR) spectroscopy as well as mass spectrometry. Following recrystallisation, the molecular structure of complex **Pd-65a** in solid state had been successfully elucidated via single crystal X ray diffraction (XRD) analysis. The X ray crystallography data had shown that six-membered ring of the platinum NHC complexes adopted a boat conformation with the phenyl ring arranged at the axial position. Two unexpected nickel coordination complexes, i.e. simple nickel coordination complex **72** and nickelate complex **73**, were obtained upon recrystallisation from Ni NHC complexes and studied using X ray crystallography.

Entire series of compounds, inclusive but not limited to, the precursors, imidazolium salts (or NHC precursors), and Group 10 metal NHC complexes that were synthesized previously were evaluated for their antimicrobial activities against a panel of pathogenic microorganisms including Gram positive and Gram bacteria, as well as yeasts by using broth microdilution (BMD) assay. While the imidazolium salts (or NHC precursors) **64** exhibited insubstantial antimicrobial activities than those reported by the literatures, the palladium and platinum NHC complexes **Pd-65** and **Pt-65** shown improved antimicrobial activities upon coordination to metals with minimum inhibitory concentration (MIC) values in the micromolar range. Remarkably, two platinum NHC complexes (**Pt-65b** and **Pt-65c**) exhibited significant antimicrobial activities with MIC as low as 2 μM , which are comparable to silver NHC complexes with renowned antimicrobial profiles. Also, the optically resolved *R* enantiomers of palladium NHC complexes **65** have shown evident antimicrobial activities compared to *S* enantiomers, resembling chiral drugs with only one bioactive enantiomer out of two.

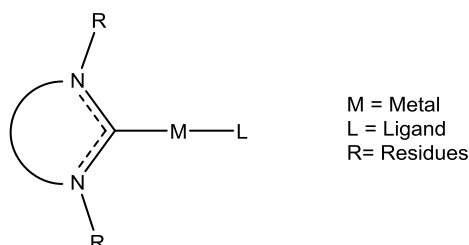
Correspondingly, the anticancer activities of a series of compounds including but not limited to those precursors, imidazolium salts (or NHC precursors), and Group 10 metal NHC complexes synthesized were evaluated against a panel of selected human carcinoma cell lines, including H103 (oral cancer), HCT116 (colon cancer) and MCF7 (breast cancer) by using MTT cell viability assay. Their respective cell cytotoxicity was described in terms of the half maximal inhibitory concentration (IC_{50}). Upon coordination to metals, the cytotoxicity effects of the Pd and Pt NHC complexes **65** increased significantly as compared to the imidazolium salts **64**. Most notably, Pt NHC complex **Pt-65c** displayed outstanding cytotoxicities towards the cancer cells with IC_{50} values that are two to three times lower than that of the anticancer benchmark cisplatin. It was observed that the *R* and *S* enantiomer of palladium NHC complexes **65** have different anticancer profile, in which latter was less cytotoxic towards the cancer cells tested. Lastly but not least, selectivity index study was also carried out using three human normal cell lines namely OKF6 (oral epithelial cells), HACAT (skin keratinocytes) and BEAS2B (lung epithelial cells). However, the experimental results have shown that the tested complexes were not selective towards the cancer cells tested.

Essentially, evidences for the influence of metals, *N* wingtip substituents on the NHC ring, and optical isomerism on the antimicrobial and anticancer activities of these metal NHC complexes have been found. Although the mechanism of action for the reported biological activities is not known at present, it is apparent from this work that these Group 10 metal NHC complexes, especially the platinum NHC complexes, could be some potential drug candidates in the future.

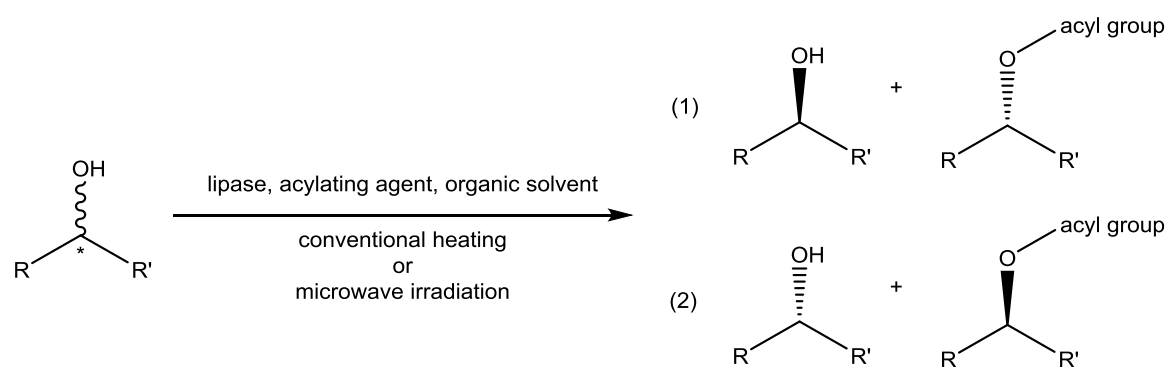
5.2. Future Directions

While encouraging results have been obtained in this rather preliminary study, it is apparent that more in-depth work would be required before undertaking those advanced *in vivo* tests and clinical trials. Besides, there are several aspects of the study which can seek for further improvement or alternatives. For continuation of this study, several approaches can be conducted in the future to optimise these metal NHC complexes are outlined in the following paragraph:

1. Design of novel metal NHC complexes for improvement of the biological activity profiles with respect to structural-activity relationship (SAR). This can be tackled from the perspectives of increasing the complexes' potency and improving their selectivity index. Based on the general structure of metal NHC complex as shown below, one of the approaches would be the incorporation of other known bioactive metals such as silver (Ag), gold (Au), rhodium (Rh), ruthenium (Ru), and others. In addition, different ancillary ligands and/or leaving groups can be included for the construction of new metal NHC complexes such as Cl^- , Br^- , I^- , F^- , BF_4^- , PF_6^- , NO_3^- , PPh_3 and many more. Besides that, different R group can be incorporated at the *N* wingtip of the NHC ligands to study the effects of various side groups. For examples, different long alkyl groups with varying chain length (C_6 to C_{10}) can be used as the *N* substituents to increase the structure lipophilicity and hydrophobicity. As for the aromatic group, the phenyl group can be attached with different electron donating group (EDG) or electron withdrawing group (EWG) to make it more nucleophilic or electrophilic, respectively. Lastly, apart from the *tert*-butyl group which we discussed in this study, effects of steric bulkiness on the bioactivities can be studied by exploring different bulky groups as the *N* substituents, for examples isopropyl and adamantyl group.



2. Perform optical resolution on alcohol complex **62** before subsequent reactions to produce enantiomerically pure imidazolium salt **64** and thereby optically active metal NHC complexes **65**. One established approaches that can be utilized is the enzymatic optical resolution of chiral alcohol complex which involves enantioselective transesterification by lipase in organic solvent, as illustrated in the schematic drawing below (Patel et al., 2000, Bachu et al., 2007, Fogassy et al., 2006).



Scheme 49. General pathway for enzymatic optical resolution of chiral alcohol complex.

3. Evaluation of the antibiofilm activities of these synthesized complexes, *via* biofilm inhibition and biofilm disruption assay, to investigate if the complexes would act on the complex biofilm apart from the planktonic bacteria (investigated using BMD assay).
4. Expansion of the panel of human cancer cell lines and human normal cell lines used in MTT cell viability assay to study the anticancer activities of these metal NHC complexes in a vast variety of cell lines and their respective selectivity.
5. Investigation of the metal NHC complexes or ions localization inside the living cells or organisms using X-ray fluorescence microscopy (XRFM) (Dean et al., 2012).

6. Determination of mechanisms of antimicrobial action (Yan et al., 2013).

a. Time-kill kinetics assay

This assay is to determine the rate of killing for these metal NHC complexes by incubating a mixture of microorganisms and metal NHC complexes together over a period of time.

b. Membrane permeability assay

This assay is to examine the effect of metal NHC complexes on the integrity of bacterial membrane. The permeability of the bacterial outer membrane by these metal NHC complexes can be tested using fluorescent method, whereby colorimetric method can be utilized to test for the permeability of bacterial inner membrane.

c. Confocal laser scanning microscopy assay

This assay is to examine the effect of these metal NHC complexes on the integrity of bacterial membrane.

d. DNA binding assay

This assay basically includes DNA retardation and DNA absorption assays. It is to examine the interaction between these metal NHC complexes and bacterial DNA using fluorescent method.

e. Atomic force microscopy (AFM) imaging

The interaction between these metal NHC complexes and bacterial DNA can be observed using atomic force microscope.

f. Scanning electron microscopy (SEM)

The bacteria treated with metal NHC complexes can be fixed on a glass surface and subjected to SEM to examine the effect of these metal NHC complexes on the bacterial surface morphology.

g. Transmission electron microscopy (TEM)

The bacteria treated with metal NHC complexes can be subjected to TEM to examine the effect of these metal NHC complexes on the intercellular components of bacteria.

7. Determination of mechanisms of anticancer action (Gandin et al., 2014, Ray et al., 2007).

a. Cellular apoptosis analysis by flow cytometry

This assay enables the analysis of the metal NHC complexes-induced cell cycle perturbations and DNA fragmentation after DNA staining with propidium iodide (PI).

b. Cell cycle analysis

This assay can be conducted to determine the effects of metal NHC complexes on the cell cycle. The cells will be probed with different antibodies or markers to deduce the cell cycle stages which the metal NHC complexes exert its effect.

c. Immunofluorescent microscopy

In immunofluorescent analysis, the cells will be stained with antibody and fluorescent probe in order to analyze whether the metal NHC complexes are involve in protein regulation or cell cycle arrest.

d. Western blot analysis

In Western blot analysis, the targeted proteins which are specific to particular cell cycle stage can be identified, and protein-specific antibody can be utilized to investigate the cells treated with metal NHC complexes. This will allow the understanding of the protein targets that are affected by metal NHC complexes.

e. Annexin V/propidium iodide (PI) staining

This assay can be performed to determine the apoptotic stages of the cells treated with the metal NHC complexes. Absence of annexin V and propidium iodide staining indicates viable cells, whereas cells stained positive for annexin alone are early apoptotic cells. Cells stained positive for both annexin V and propidium iodide denote late apoptotic cells, and those stained positive for propidium iodide alone are dead cells which undergo apoptosis or necrosis.

REFERENCES

- ABU-SURRAH, A. S. & KETTUNEN, M. 2006. Platinum group antitumor chemistry: Design and development of new anticancer drugs complementary to cisplatin. *Current Medicinal Chemistry*, 13, 1337-57.
- ADHIKARY, S. D., BOSE, D., MITRA, P., SAHA, K. D., BERTOLASI, V. & DINDA, J. 2012. Au(i)- and Pt(ii)-N-heterocyclic carbene complexes with picoline functionalized benzimidazolin-2-ylidene ligands; synthesis, structures, electrochemistry and cytotoxicity studies. *New Journal of Chemistry*, 36, 759-767.
- AHER, S. B., DUBEY, V., MUSKAWAR, P. N., THENMOZHI, K., GHOSH, A. R. & BHAGAT, P. R. 2017. Cytotoxic behavior of binuclear silver N-heterocyclic carbenes in HCT 116 cells and influence of substitution on cytotoxicity. *Research on Chemical Intermediates*, 1-12.
- AIYELABOLA, T., AKINKUNMI, E., OJO, I., OBUOTOR, E., ADEBAJO, C. & ISABIRYE, D. 2017. Syntheses, Characterization, Resolution, and Biological Studies of Coordination Compounds of Aspartic Acid and Glycine. *Bioinorganic Chemistry and Applications*, 2017, 15.
- ALBADA, B. & METZLER-NOLTE, N. 2016. Organometallic–Peptide Bioconjugates: Synthetic Strategies and Medicinal Applications. *Chemical Reviews*, 116, 11797-11839.
- ALBERT, J., BOSQUE, R., CADENA, M., D'ANDREA, L., GRANELL, J., GONZÁLEZ, A., QUIRANTE, J., CALVIS, C., MESSEGUER, R., BADÍA, J., BALDOMÀ, L., CALVET, T. & FONT-BARDIA, M. 2014a. A new family of doubly cyclopalladated diimines. A remarkable effect of the linker between the metalated units on their cytotoxicity. *Organometallics*, 33, 2862-2873.
- ALBERT, J., GRANELL, J., QADIR, R., QUIRANTE, J., CALVIS, C., MESSEGUER, R., BADÍA, J., BALDOMÀ, L., FONT-BARDIA, M. & CALVET, T. 2014b. Cyclopalladated benzophenone imines: Synthesis, antitumor activity, cell accumulation, DNA interaction, and cathepsin B inhibition. *Organometallics*, 33, 7284-7292.

- ALI, I., LONE, M. N. & ABOUL-ENEIN, H. Y. 2017. Imidazoles as potential anticancer agents. *MedChemComm*, 8, 1742-1773.
- ALI, I., MOHAMMAD NADEEM, L., ZEID, A. A.-O., ABDULRAHMAN, A.-W. & MOHD. MARSIN, S. 2015. Heterocyclic Scaffolds: Centrality in Anticancer Drug Development. *Current Drug Targets*, 16, 711-734.
- ALTMAN, R. A. & BUCHWALD, S. L. 2006. 4,7-Dimethoxy-1,10-phenanthroline: An Excellent Ligand for the Cu-Catalyzed N-Arylation of Imidazoles. *Organic Letters*, 8, 2779-2782.
- ARDUENGO, A. J., HARLOW, R. L. & KLINE, M. 1991. A stable crystalline carbene. *Journal of the American Chemical Society*, 113, 361-363.
- ARDUENGO, A. J., KRAFCZYK, R., SCHMUTZLER, R., CRAIG, H. A., GOERLICH, J. R., MARSHALL, W. J. & UNVERZAGT, M. 1999. Imidazolylidenes, imidazolinyliidenes and imidazolidines. *Tetrahedron*, 55, 14523-14534.
- ASMUS, M. J. & HENDELES, L. 2000. Levalbuterol nebulizer solution: Is it worth five times the cost of albuterol? *Pharmacotherapy: The Journal of Human Pharmacology and Drug Therapy*, 20, 123-129.
- BACHU, P., GIBSON, J. S., SPERRY, J. & BRIMBLE, M. A. 2007. The influence of microwave irradiation on lipase-catalyzed kinetic resolution of racemic secondary alcohols. *Tetrahedron: Asymmetry*, 18, 1618-1624.
- BAKER, M. V., BARNARD, P. J., BERNERS-PRICE, S. J., BRAYSHAW, S. K., HICKEY, J. L., SKELTON, B. W. & WHITE, A. H. 2006. Cationic, linear Au(I) N-heterocyclic carbene complexes: Synthesis, structure and anti-mitochondrial activity. *Dalton Transactions*, 3708-3715.
- BARRETINA, J., CAPONIGRO, G., STRANSKY, N., VENKATESAN, K., MARGOLIN, A. A., KIM, S., WILSON, C. J., LEHÁR, J., KRYUKOV, G. V., SONKIN, D., REDDY, A., LIU, M., MURRAY, L., BERGER, M. F., MONAHAN, J. E., MORAIS, P., MELTZER, J., KOREJWA, A., JANÉ-VALBUENA, J., MAPA, F. A., THIBAUT, J., BRIC-FURLONG, E., RAMAN, P., SHIPWAY, A., ENGELS, I. H., CHENG, J., YU, G. K., YU, J., ASPESI, P., DE SILVA, M., JAGTAP, K., JONES, M. D., WANG, L.,

- HATTON, C., PALESCANDOLO, E., GUPTA, S., MAHAN, S., SOUGNEZ, C., ONOFRIO, R. C., LIEFELD, T., MACCONAILL, L., WINCKLER, W., REICH, M., LI, N., MESIROV, J. P., GABRIEL, S. B., GETZ, G., ARDLIE, K., CHAN, V., MYER, V. E., WEBER, B. L., PORTER, J., WARMUTH, M., FINAN, P., HARRIS, J. L., MEYERSON, M., GOLUB, T. R., MORRISSEY, M. P., SELLERS, W. R., SCHLEGEL, R. & GARRAWAY, L. A. 2012. The Cancer Cell Line Encyclopedia enables predictive modelling of anticancer drug sensitivity. *Nature*, 483, 603.
- BECEIRO, A., TOMÁS, M. & BOU, G. 2013. Antimicrobial Resistance and Virulence: a Successful or Deleterious Association in the Bacterial World? *Clinical Microbiology Reviews*, 26, 185-230.
- BETZER, J.-F., NUTER, F., CHTCHIGROVSKY, M., HAMON, F., KELLERMANN, G., ALI, S., CALMÉJANE, M.-A., ROQUE, S., POUPON, J., CRESTEIL, T., TEULADE-FICHO, M.-P., MARINETTI, A. & BOMBARD, S. 2016. Linking of Antitumor trans NHC-Pt(II) Complexes to G-Quadruplex DNA Ligand for Telomeric Targeting. *Bioconjugate Chemistry*, 27, 1456-1470.
- BILDSTEIN, B., MALAUN, M., KOPACKA, H., WURST, K., MITTERBÖCK, M., ONGANIA, K.-H., OPROMOLLA, G. & ZANELLO, P. 1999. N, N'-Diferrocenyl-N-heterocyclic Carbenes and Their Derivatives. *Organometallics*, 18, 4325-4336.
- BIRNIE, C. R., MALAMUD, D. & SCHNAARE, R. L. 2000. Antimicrobial Evaluation of N-Alkyl Betaines and N-Alkyl-N,N-Dimethylamine Oxides with Variations in Chain Length. *Antimicrobial Agents and Chemotherapy*, 44, 2514-2517.
- BORDI, C. & DE BENTZMANN, S. 2011. Hacking into bacterial biofilms: a new therapeutic challenge. *Annals of intensive care*, 1, 19.
- BOROWIECKI, P., MILNER-KRAWCZYK, M., BRZEZIŃSKA, D., WIELECHOWSKA, M. & PLENKIEWICZ, J. 2013. Synthesis and antimicrobial activity of imidazolium and triazolium chiral ionic liquids. *European Journal of Organic Chemistry*, 2013, 712-720.
- BOURISSOU, D., GUERRET, O., GABBAÏ, F. P. & BERTRAND, G. 2000. Stable carbenes. *Chemical Reviews*, 100, 39-92.

- BUDAGUMPI, S. & ENDUD, S. 2013. Group XII Metal–N-Heterocyclic Carbene Complexes: Synthesis, Structural Diversity, Intramolecular Interactions, and Applications. *Organometallics*, 32, 1537-1562.
- BUDAGUMPI, S., HAQUE, R. A. & SALMAN, A. W. 2012. Stereochemical and structural characteristics of single- and double-site Pd(II)–N-heterocyclic carbene complexes: Promising catalysts in organic syntheses ranging from CC coupling to olefin polymerizations. *Coordination Chemistry Reviews*, 256, 1787-1830.
- BURGOS, C., ANA, E., TAMAYO, L. & TORRELLAS-HIDALGO, R. 2014. Synthesis, characterization and antimicrobial activity of a Pd (II) complex with a 1, 3-diphenylpyrazole-4-carboxaldehyde thiosemicarbazone ligand. *Revista UDCA Actualidad & Divulgación Científica*, 17, 477-486.
- BUTSCH, K., ELMAS, S., GUPTA, N. S., GUST, R., HEINRICH, F., KLEIN, A., VON MERING, Y., NEUGEBAUER, M., OTT, I., SCHÄFER, M., SCHERER, H. & SCHURR, T. 2009. Organoplatinum(II) and -palladium(II) Complexes of Nucleobases and Their Derivatives. *Organometallics*, 28, 3906-3915.
- CEPEDA, V., FUERTES, M. A., CASTILLA, J., ALONSO, C., QUEVEDO, C. & PEREZ, J. M. 2007. Biochemical mechanisms of cisplatin cytotoxicity. *Anticancer Agents Med Chem*, 7, 3-18.
- CETINKAYA, B., CETINKAYA, E., KUCUKBAY, H. & DURMAZ, R. 1996. Antimicrobial activity of carbene complexes of rhodium(I) and ruthenium(II). *Arzneimittelforschung*, 46, 821-3.
- CETINKAYA, B., DEMIR, S., ÖZDEMİR, I., TOUPET, L., SEMERIL, D., BRUNEAU, C. & DIXNEUF, P. H. 2003. η^6 -Mesityl, η^1 -Imidazolinylidene–Carbene–Ruthenium (II) Complexes: Catalytic Activity of their Allenylidene Derivatives in Alkene Metathesis and Cycloisomerisation Reactions. *Chemistry–A European Journal*, 9, 2323-2330.
- CETINKAYA, B., OZDEMİR, I., BINBASIOGLU, B., DURMAZ, R. & GUNAL, S. 1999. Antibacterial and antifungal activities of complexes of ruthenium (II). *Arzneimittelforschung*, 49, 538-40.

- CHAN, B. K., CHANG, N. & GRIMMETT, M. R. 1977. The synthesis and thermolysis of imidazole quaternary salts. *Australian Journal of Chemistry*, 30, 2005-2013.
- CHE, C.-M. & SIU, F.-M. 2010. Metal complexes in medicine with a focus on enzyme inhibition. *Current Opinion in Chemical Biology*, 14, 255-261.
- CHE, C.-M. & SUN, R. W.-Y. 2011. Therapeutic applications of gold complexes: lipophilic gold(III) cations and gold(I) complexes for anti-cancer treatment. *Chemical Communications*, 47, 9554-9560.
- CHE, C. M., SUN, R. W. Y., CHOW, L. F. & YAN, J. 2011. Pharmaceutical composition containing cyclometalated n-heterocyclic carbene complexes for cancer treatment. *Patent*, WO2011050574A1.
- CHEKKAT, N., DAHM, G., CHARDON, E., WANTZ, M., SITZ, J., DECOSSAS, M., LAMBERT, O., FRISCH, B., RUBBIANI, R., GASSER, G., GUICHARD, G., FOURNEL, S. & BELLEMIN-LAPONNAZ, S. 2016. N-Heterocyclic Carbene–Polyethylenimine Platinum Complexes with Potent in Vitro and in Vivo Antitumor Efficacy. *Bioconjugate Chemistry*, 27, 1942-1948.
- CHEN, J., WANG, Z., LU, Y., DALTON, J. T., MILLER, D. D. & LI, W. 2008. Synthesis and antiproliferative activity of imidazole and imidazoline analogs for melanoma. *Bioorganic & Medicinal Chemistry Letters*, 18, 3183-3187.
- CHHABRA, N., ASERI, M. L. & PADMANABHAN, D. 2013. A review of drug isomerism and its significance. *International Journal of Applied and Basic Medical Research*, 3, 16-18.
- CHIANG, M. 2011. *Synthesis, Characterisation And Catalytic Application Of Novel Cyclopalladated Pyridine Functionalized N-Heterocyclic Carbenes Complexes*. PhD Thesis, Nanyang Technological University.
- CHIANG, M., LI, Y., KRISHNAN, D., SUMOD, P., NG, K. H. & LEUNG, P.-H. 2010. Synthesis and characterisation of a novel chiral bidentate pyridine-n-heterocyclic carbene-based palladacycle. *European Journal of Inorganic Chemistry*, 2010, 1413-1418.

- CHTCHIGROVSKY, M., ELOY, L., JULLIEN, H., SAKER, L., SÉGAL-BENDIRDJIAN, E., POUPON, J., BOMBARD, S., CRESTEIL, T., RETAILLEAU, P. & MARINETTI, A. 2013. Antitumor trans-N-Heterocyclic Carbene–Amine–Pt(II) Complexes: Synthesis of Dinuclear Species and Exploratory Investigations of DNA Binding and Cytotoxicity Mechanisms. *Journal of Medicinal Chemistry*, 56, 2074-2086.
- CLSI 2012. Methods for dilution antimicrobial susceptibility test for bacteria that grow anaerobically: Approved standard - Ninth Edition. *CLSI Document M07-A9*, Clinical and Laboratory Institute, Wayne, Pennsylvania.
- ÇOLAK, A. T., ÇOLAK, F., YEŞİLEL, O. Z. & ŞAHİN, E. 2010. Synthesis, spectroscopic, thermal, crystal characterization and biological activity of [Ni(phen)₃][Ni(dipic)₂].17H₂O (H₂dipic:pyridine-2,6-dicarboxylic acid, phen: 1,10-phenanthroline). *Journal of the Iranian Chemical Society*, 7, 384-393.
- CORNELLAS, A., PEREZ, L., COMELLES, F., RIBOSA, I., MANRESA, A. & GARCIA, M. T. 2011. Self-aggregation and antimicrobial activity of imidazolium and pyridinium based ionic liquids in aqueous solution. *Journal of Colloid and Interface Science*, 355, 164-171.
- COSGROVE, S. E. 2006. The relationship between antimicrobial resistance and patient outcomes: mortality, length of hospital stay, and health care costs. *Clinical Infectious Diseases*, 42, S82-S89.
- COSTELLOE, C., METCALFE, C., LOVERING, A., MANT, D. & HAY, A. D. 2010. Effect of antibiotic prescribing in primary care on antimicrobial resistance in individual patients: systematic review and meta-analysis. *BMJ*, 340, c2096.
- COWLEY, R. E., BONTCHEV, R. P., DUESLER, E. N. & SMITH, J. M. 2006. Removing the sting from the tail: Reversible protonation of scorpionate ligands in cobalt (II) tris (carbene) borate complexes. *Inorganic chemistry*, 45, 9771-9779.
- CRABTREE, R. H. 2005. NHC ligands versus cyclopentadienyls and phosphines as spectator ligands in organometallic catalysis. *Journal of Organometallic Chemistry*, 690, 5451-5457.

- CRISÓSTOMO, M. I., WESTH, H., TOMASZ, A., CHUNG, M., OLIVEIRA, D. C. & DE LENCASTRE, H. 2001. The evolution of methicillin resistance in *Staphylococcus aureus*: Similarity of genetic backgrounds in historically early methicillin-susceptible and -resistant isolates and contemporary epidemic clones. *Proceedings of the National Academy of Sciences of the United States of America*, 98, 9865-9870.
- CRUDDEN, C. M. & ALLEN, D. P. 2004. Stability and reactivity of N-heterocyclic carbene complexes. *Coordination Chemistry Reviews*, 248, 2247-2273.
- DAHM, G., BAILLY, C., KARMAZIN, L. & BELLEMIN-LAPONNAZ, S. 2015. Synthesis, structural characterization and in vitro anti-cancer activity of functionalized N-heterocyclic carbene platinum and palladium complexes. *Journal of Organometallic Chemistry*, 794, 115-124.
- DE FRÉMONT, P., MARION, N. & NOLAN, S. P. 2009. Carbenes: Synthesis, properties, and organometallic chemistry. *Coordination Chemistry Reviews*, 253, 862-892.
- DEAN, K. M., QIN, Y. & PALMER, A. E. 2012. Visualizing metal ions in cells: An overview of analytical techniques, approaches, and probes. *Biochimica et Biophysica Acta (BBA) - Molecular Cell Research*, 1823, 1406-1415.
- DEMBERELNYAMBA, D., KIM, K.-S., CHOI, S., PARK, S.-Y., LEE, H., KIM, C.-J. & YOO, I.-D. 2004. Synthesis and antimicrobial properties of imidazolium and pyrrolidinium salts. *Bioorganic & Medicinal Chemistry*, 12, 853-857.
- DOMAGOJ, V. 2008. Apoptotic Pathways as Targets for Therapeutic Intervention *Current Cancer Drug Targets*, 8, 86-86.
- DONLAN, R. M. 2002. Biofilms: microbial life on surfaces. *Emerging infectious diseases*, 8, 881.
- DRAGUTAN, V., DRAGUTAN, I. & DEMONCEAU, A. 2005. Ruthenium Complexes Bearing N-Heterocyclic Carbene (NHC) Ligands. *Platinum Metals Review*, 49, 123-137.
- DRAŠKOVIĆ, N. S., GLIŠIĆ, B. D., VOJNOVIC, S., NIKODINOVIC-RUNIC, J. & DJURAN, M. I. 2017. In vitro antimicrobial activity and cytotoxicity of nickel (II) complexes with different diamine ligands. *J. Serb. Chem. Soc.*, 82, 289-398.

- EDWARDS, G. L., BLACK, D. S. C., DEACON, G. B. & WAKELIN, L. P. G. 2005. In vitro and in vivo studies of neutral cyclometallated complexes against murine leukæmias. *Canadian Journal of Chemistry*, 83, 980-989.
- EKKEHARDT HAHN, F., HEIDRICH, B., PAPE, T., HEPP, A., MARTIN, M., SOLA, E. & ORO, L. A. 2006. Mononuclear and dinuclear bromo bridged iridium(I) complexes with N-allyl substituted imidazolin-2-ylidene ligands. *Inorganica Chimica Acta*, 359, 4840-4846.
- EL-TABL, A. S., MOHAMED ABD EL-WAHEED, M., WAHBA, M. A. & ABD EL-HALIM ABOU EL-FADL, N. 2015. Synthesis, characterization, and anticancer activity of new metal complexes derived from 2-hydroxy-3-(hydroxyimino)-4-oxopentan-2-ylidene)benzohydrazide. *Bioinorganic Chemistry and Applications*, 2015, 126023.
- ENDERS, D. & GIELEN, H. 2001. Synthesis of chiral triazolinylidene and imidazolinylidene transition metal complexes and first application in asymmetric catalysis. *Journal of Organometallic Chemistry*, 617-618, 70-80.
- ENDERS, M., GÖRLING, B., BRAUN, A. B., SELTENREICH, J. E., REICHENBACH, L. F., RISSANEN, K., NIEGER, M., LUY, B., SCHEPERS, U. & BRÄSE, S. 2014. Cytotoxicity and NMR Studies of Platinum Complexes with Cyclooctadiene Ligands. *Organometallics*, 33, 4027-4034.
- FARRELL, N., POVIRK, L. F., DANGE, Y., DEMASTERS, G., GUPTA, M. S., KOHLHAGEN, G., KHAN, Q. A., POMMIER, Y. & GEWIRTZ, D. A. 2004. Cytotoxicity, DNA strand breakage and DNA–protein crosslinking by a novel transplatinum compound in human A2780 ovarian and MCF-7 breast carcinoma cells. *Biochemical Pharmacology*, 68, 857-866.
- FLEMMING, H.-C. & WINGENDER, J. 2010. The biofilm matrix. *Nature Reviews Microbiology*, 8, 623.
- FLIS, S. & SPŁAWIŃSKI, J. 2009. Inhibitory Effects of 5-Fluorouracil and Oxaliplatin on Human Colorectal Cancer Cell Survival Are Synergistically Enhanced by Sulindac Sulfide. *Anticancer Research*, 29, 435-441.

- FLOREA, A. M. & BUSSELBERG, D. 2011. Cisplatin as an anti-tumor drug: cellular mechanisms of activity, drug resistance and induced side effects. *Cancers (Basel)*, 3, 1351-71.
- FOGASSY, E., NÓGRÁDI, M., KOZMA, D., EGRI, G., PÁLOVICS, E. & KISS, V. 2006. Optical resolution methods. *Organic & Biomolecular Chemistry*, 4, 3011-3030.
- FONG, T. T.-H., LOK, C.-N., CHUNG, C. Y.-S., FUNG, Y.-M. E., CHOW, P.-K., WAN, P.-K. & CHE, C.-M. 2016. Cyclometalated Palladium(II) N-Heterocyclic Carbene Complexes: Anticancer Agents for Potent In Vitro Cytotoxicity and In Vivo Tumor Growth Suppression. *Angewandte Chemie International Edition*, 55, 11935-11939.
- FOURNARI, P. 1968. P. deoointet, and E. Laviron. *Bull. SOC. Chim. France*, 2438.
- FRASSOLDATI, A., PINEL, C. & BESSON, M. 2013. Aerobic oxidation of secondary pyridine-derivative alcohols in the presence of carbon-supported noble metal catalysts. *Catalysis Today*, 203, 133-138.
- FREY, G. D., SCHOELLER, W. W., HERDTWECK, E. & HERRMANN, W. A. 2016. Catalyst deactivation through "Oxo-assembling". *Journal of Organometallic Chemistry*, 810, 46-50.
- FUERTE, M. A., ALONSO, C. & PÉREZ, J. M. 2003. Biochemical modulation of cisplatin mechanisms of action: Enhancement of antitumor activity and circumvention of drug resistance. *Chemical Reviews*, 103, 645-662.
- GANDIN, V., TISATO, F., DOLMELLA, A., PELLEI, M., SANTINI, C., GIORGETTI, M., MARZANO, C. & PORCHIA, M. 2014. In Vitro and in Vivo Anticancer Activity of Copper(I) Complexes with Homoscorpionate Tridentate Tris(pyrazolyl)borate and Auxiliary Monodentate Phosphine Ligands. *Journal of Medicinal Chemistry*, 57, 4745-4760.
- GAO, E., LIU, C., ZHU, M., LIN, H., WU, Q. & LIU, L. 2009. *Current Development of Pd(II) Complexes as Potential Antitumor Agents*.
- GARCIA, M. T., RIBOSA, I., PEREZ, L., MANRESA, A. & COMELLES, F. 2013. Aggregation Behavior and Antimicrobial Activity of Ester-Functionalized

- Imidazolium- and Pyridinium-Based Ionic Liquids in Aqueous Solution. *Langmuir*, 29, 2536-2545.
- GARRISON, J. C. & YOUNGS, W. J. 2005. Ag (I) N-heterocyclic carbene complexes: synthesis, structure, and application. *Chemical Reviews*, 105, 3978-4008.
- GASSER, G. & METZLER-NOLTE, N. 2012. The potential of organometallic complexes in medicinal chemistry. *Current Opinion in Chemical Biology*, 16, 84-91.
- GASSER, G., OTT, I. & METZLER-NOLTE, N. 2011. Organometallic anticancer compounds. *Journal of Medicinal Chemistry*, 54, 3-25.
- GAUTIER, A. & CISNETTI, F. 2012. Advances in metal–carbene complexes as potent anti-cancer agents. *Metallomics*, 4, 23-32.
- GHDHAYEB, M. Z., HAQUE, R. A., BUDAGUMPI, S., KHADEER AHAMED, M. B. & ABDUL MAJID, A. M. S. 2017a. Mono- and bis-N-heterocyclic carbene silver(I) and palladium(II) complexes: Synthesis, characterization, crystal structure and in vitro anticancer studies. *Polyhedron*, 121, 222-230.
- GHDHAYEB, M. Z., HAQUE, R. A., BUDAGUMPI, S., KHADEER AHAMED, M. B. & MAJID, A. M. S. A. 2017b. Synthesis, characterization, crystal structure and in vitro anticancer potentials of mono and bimetallic palladium(II)–N–heterocyclic carbene complexes. *Inorganic Chemistry Communications*, 75, 41-45.
- GIACCONE, G. 2000. Clinical perspectives on platinum resistance. *Drugs*, 59, 9-17.
- GODOY, F., SEGARRA, C., POYATOS, M. & PERIS, E. 2011. Palladium catalysts with sulfonate-functionalized-NHC ligands for Suzuki–Miyaura cross-coupling reactions in water. *Organometallics*, 30, 684-688.
- GONZÁLEZ-BOBES, F. & FU, G. C. 2006. Amino Alcohols as Ligands for Nickel-Catalyzed Suzuki Reactions of Unactivated Alkyl Halides, Including Secondary Alkyl Chlorides, with Arylboronic Acids. *Journal of the American Chemical Society*, 128, 5360-5361.
- GONZÁLEZ, M. L., TERCERO, J. M., MATILLA, A., NICLÓS-GUTIÉRREZ, J., FERNÁNDEZ, M. T., LÓPEZ, M. C., ALONSO, C. & GONZÁLEZ, S. 1997. cis-Dichloro(α,ω -diamino carboxylate ethyl ester)palladium(II) as Palladium(II) versus

- Platinum(II) Model Anticancer Drugs: Synthesis, Solution Equilibria of Their Aqua, Hydroxo, and/or Chloro Species, and in Vitro/in Vivo DNA-Binding Properties. *Inorganic Chemistry*, 36, 1806-1812.
- GRAVEL, J. & SCHMITZER, A. R. 2017. Imidazolium and benzimidazolium-containing compounds: from simple toxic salts to highly bioactive drugs. *Org Biomol Chem*.
- GRIDNEV, A. A. & MIHALTSEVA, I. M. 1994. Synthesis of 1-Alkylimidazoles. *Synthetic Communications*, 24, 1547-1555.
- GÜMÜŞ, F., PAMUK, I., ÖZDEN, T., YILDIZ, S., DIRIL, N., ÖKSÜZOĞLU, E., GÜR, S. & ÖZKUL, A. 2003. Synthesis, characterization and in vitro cytotoxic, mutagenic and antimicrobial activity of platinum (II) complexes with substituted benzimidazole ligands. *Journal of inorganic biochemistry*, 94, 255-262.
- HAHN, F. E., HEIDRICH, B., LÜGGER, T. & PAPE, T. 2004. Pd (II) complexes of N-allyl substituted N-heterocyclic carbenes. *Zeitschrift für Naturforschung B*, 59, 1519-1523.
- HAHN, F. E. & JAHNKE, M. C. 2008. Heterocyclic Carbenes: Synthesis and Coordination Chemistry. *Angewandte Chemie International Edition*, 47, 3122-3172.
- HAHN, F. E., RADLOFF, C., PAPE, T. & HEPP, A. 2008. Synthesis of Silver (I) and Gold (I) Complexes with Cyclic Tetra- and Hexacarbene Ligands. *Chemistry—A European Journal*, 14, 10900-10904.
- HAMEURY, S., DE FRÉMONT, P., BREUIL, P.-A. R., OLIVIER-BOURBIGOU, H. & BRAUNSTEIN, P. 2014a. Synthesis and Characterization of Palladium(II) and Nickel(II) Alcoholate-Functionalized NHC Complexes and of Mixed Nickel(II)–Lithium(I) Complexes. *Inorganic Chemistry*, 53, 5189-5200.
- HAMEURY, S., DE FRÉMONT, P., R. BREUIL, P.-A., OLIVIER-BOURBIGOU, H. & BRAUNSTEIN, P. 2014b. Synthesis and characterization of oxygen-functionalised-NHC silver(i) complexes and NHC transmetallation to nickel(ii). *Dalton Transactions*, 43, 4700-4710.

- HANDLEY, D., B HITCHCOCK, P. & LEIGH, G. 2001. Triangulo-pentahalotrimetal complexes of nickel(II) and cobalt(II) with N,N,N',N'-tetramethylethane-1,2-diamine and related compounds. *Inorganica Chimica Acta*, 314, 1-13.
- HAQUE, R. A., CHOO, S. Y., BUDAGUMPI, S., IQBAL, M. A. & AL-ASHRAF ABDULLAH, A. 2015. Silver(I) complexes of mono- and bidentate N-heterocyclic carbene ligands: synthesis, crystal structures, and in vitro antibacterial and anticancer studies. *Eur J Med Chem*, 90, 82-92.
- HAQUE, R. A., GHADHAYEB, M. Z., BUDAGUMPI, S., KHADEER AHAMED, M. B. & ABDUL MAJID, A. M. S. 2016a. Synthesis, crystal structures, and in vitro anticancer properties of new N-heterocyclic carbene (NHC) silver(I)- and gold(I)/(III)-complexes: a rare example of silver(I)-NHC complex involved in redox transmetallation. *RSC Adv.*, 6, 60407-60421.
- HAQUE, R. A., HASANUDIN, N., HUSSEIN, M. A., AHAMED, S. A. & IQBAL, M. A. 2016b. Bis-N-heterocyclic carbene silver(I) and palladium(II) complexes: Efficient antiproliferative agents against breast cancer cells. *Inorganic and Nano-Metal Chemistry*, 47, 131-137.
- HAQUE, R. A., HAZIZ, U. F. M., ABDULLAH, A. A.-A., SHAHEEDA, N. & RAZALI, M. R. 2016c. New non-functionalized and nitrile-functionalized benzimidazolium salts and their silver(I) complexes: Synthesis, crystal structures and antibacterial studies. *Polyhedron*, 109, 208-217.
- HAQUE, R. A., HAZIZ, U. F. M., AMIRUL, A. A., SHAHEEDA, N. & RAZALI, M. R. 2016d. Synthesis of a palladium(II) complex of a N-heterocyclic carbene via transmetalation: crystal structure and antibacterial studies. *Transition Metal Chemistry*, 41, 775-781.
- HAQUE, R. A., SALMAN, A. W., BUDAGUMPI, S., ABDULLAH, A. A.-A. & MAJID, A. M. S. A. 2013. Sterically tuned Ag(i)- and Pd(ii)-N-heterocyclic carbene complexes of imidazol-2-ylidenes: synthesis, crystal structures, and in vitro antibacterial and anticancer studies. *Metallomics*, 5, 760-769.
- HARTINGER, C. G. & DYSON, P. J. 2009. Bioorganometallic chemistry-from teaching paradigms to medicinal applications. *Chemical Society Reviews*, 38, 391-401.

- HARTINGER, C. G., JAKUPEC, M. A., ZORBAS-SEIFRIED, S., GROESSL, M., EGGER, A., BERGER, W., ZORBAS, H., DYSON, P. J. & KEPPLER, B. K. 2008. KP1019, A New Redox-Active Anticancer Agent – Preclinical Development and Results of a Clinical Phase I Study in Tumor Patients. *Chemistry & Biodiversity*, 5, 2140-2155.
- HASHMI, A. S. K. 2010. New pathways in the gold-catalyzed cycloisomerization of furanynes. *Pure and Applied Chemistry*, 82, 1517-1528.
- HE, Y., LV, M.-F. & CAI, C. 2012. A simple procedure for polymer-supported N-heterocyclic carbene silver complex via click chemistry: an efficient and recyclable catalyst for the one-pot synthesis of propargylamines. *Dalton Transactions*, 41, 12428-12433.
- HENRIKSSON, M. L., EDIN, S., DAHLIN, A. M., OLDENBORG, P.-A., ÖBERG, Å., VAN GUELPEL, B., RUTEGÅRD, J., STENLING, R. & PALMQVIST, R. 2011. Colorectal Cancer Cells Activate Adjacent Fibroblasts Resulting in FGF1/FGFR3 Signaling and Increased Invasion. *The American Journal of Pathology*, 178, 1387-1394.
- HENWOOD, A. F., LESIEUR, M., BANSAL, A. K., LEMAUR, V., BELJONNE, D., THOMPSON, D. G., GRAHAM, D., SLAWIN, A. M., SAMUEL, I. D. & CAZIN, C. S. 2015. Palladium (0) NHC complexes: a new avenue to highly efficient phosphorescence. *Chemical Science*, 6, 3248-3261.
- HERRMANN, W. A., ELISON, M., FISCHER, J., KÖCHER, C. & ARTUS, G. R. 1996a. N-Heterocyclic Carbenes: Generation under Mild Conditions and Formation of Group 8–10 Transition Metal Complexes Relevant to Catalysis. *Chemistry—A European Journal*, 2, 772-780.
- HERRMANN, W. A., GOOBEN, L. J. & SPIEGLER, M. 1997. Functionalized imidazoline-2-ylidene complexes of rhodium and palladium. *Journal of organometallic chemistry*, 547, 357-366.
- HERRMANN, W. A., KÖCHER, C., GOOBEN, L. J. & ARTUS, G. R. 1996b. Heterocyclic carbenes: A high-yielding synthesis of novel, functionalized N-heterocyclic carbenes in liquid ammonia. *Chemistry—A European Journal*, 2, 1627-1636.

- HERRMANN, W. A., KÖCHER, C., GOOßEN, L. J. & ARTUS, G. R. J. 1996c. Heterocyclic carbenes: A high-yielding synthesis of novel, functionalized N-heterocyclic carbenes in liquid ammonia. *Chemistry – A European Journal*, 2, 1627-1636.
- HILLIER, A. C., SOMMER, W. J., YONG, B. S., PETERSEN, J. L., CAVALLO, L. & NOLAN, S. P. 2003. A combined experimental and theoretical study examining the binding of N-heterocyclic carbenes (NHC) to the Cp*RuCl (Cp* = η^5 -C₅Me₅) moiety: Insight into stereoelectronic differences between unsaturated and saturated NHC ligands. *Organometallics*, 22, 4322-4326.
- HINDI, K. M., MEDVETZ, D. A., PANZNER, M., TESSIER, C. & YOUNGS, W. J. 2009a. Metal complexes incorporated within biodegradable nanoparticles and their use. *Patent*, WO2008150830A2.
- HINDI, K. M., PANZNER, M. J., TESSIER, C. A., CANNON, C. L. & YOUNGS, W. J. 2009b. The medicinal applications of imidazolium carbene–metal complexes. *Chemical Reviews*, 109, 3859-3884.
- HINDI, K. M., SICILIANO, T. J., DURMUS, S., PANZNER, M. J., MEDVETZ, D. A., REDDY, D. V., HOGUE, L. A., HOVIS, C. E., HILLIARD, J. K., MALLET, R. J., TESSIER, C. A., CANNON, C. L. & YOUNGS, W. J. 2008. Synthesis, stability, and antimicrobial studies of electronically tuned silver acetate N-heterocyclic carbenes. *Journal of Medicinal Chemistry*, 51, 1577-1583.
- HINTERMANN, L. 2007. Expedient syntheses of the N-heterocyclic carbene precursor imidazolium salts IPr· HCl, IMes· HCl and IXy· HCl. *Beilstein journal of organic chemistry*, 3, 22.
- HOPKINSON, M. N., RICHTER, C., SCHEDLER, M. & GLORIUS, F. 2014. An overview of N-heterocyclic carbenes. *Nature*, 510, 485-496.
- HU, W., LUO, Q., MA, X., WU, K., LIU, J., CHEN, Y., XIONG, S., WANG, J., SADLER, P. J. & WANG, F. 2009. Arene control over thiolate to sulfinate oxidation in albumin by organometallic ruthenium anticancer complexes. *Chemistry*, 15, 6586-94.

- HUANG, J. & NOLAN, S. P. 1999. Efficient cross-coupling of aryl chlorides with aryl Grignard reagents (Kumada reaction) mediated by a palladium/imidazolium chloride system. *Journal of the American Chemical Society*, 121, 9889-9890.
- HUANG, J., STEVENS, E. D., NOLAN, S. P. & PETERSEN, J. L. 1999. Olefin metathesis-active ruthenium complexes bearing a nucleophilic carbene ligand. *Journal of the American Chemical Society*, 121, 2674-2678.
- HUERTOS, M. A., PÉREZ, J., RIERA, L. & MENÉNDEZ-VELÁZQUEZ, A. 2008. From N-Alkylimidazole Ligands at a Rhenium Center: Ring Opening or Formation of NHC Complexes. *Journal of the American Chemical Society*, 130, 13530-13531.
- IGAU, A., GRUTZMACHER, H., BACEIREDO, A. & BERTRAND, G. 1988. Analogous. alpha., alpha.'-bis-carbenoid, triply bonded species: synthesis of a stable. lambda. 3-phosphino carbene-. lambda. 5-phosphaacetylene. *Journal of the American Chemical Society*, 110, 6463-6466.
- ISLAM, M. S., RICHARDS, J. P. & OJHA, A. K. 2012. Targeting drug tolerance in mycobacteria: a perspective from mycobacterial biofilms. *Expert review of anti-infective therapy*, 10, 1055-1066.
- JAFARPOUR, L., STEVENS, E. D. & NOLAN, S. P. 2000. A sterically demanding nucleophilic carbene: 1, 3-bis (2, 6-diisopropylphenyl) imidazol-2-ylidene). Thermochemistry and catalytic application in olefin metathesis. *Journal of Organometallic Chemistry*, 606, 49-54.
- JIANG, W., SAXENA, A., SONG, B., WARD, B. B., BEVERIDGE, T. J. & MYNENI, S. C. B. 2004. Elucidation of Functional Groups on Gram-Positive and Gram-Negative Bacterial Surfaces Using Infrared Spectroscopy. *Langmuir*, 20, 11433-11442.
- JOHNSON, J. I., DECKER, S., ZAHAREVITZ, D., RUBINSTEIN, L. V., VENDITTI, J. M., SCHEPARTZ, S., KALYANDRUG, S., CHRISTIAN, M., ARBUCK, S., HOLLINGSHEAD, M. & SAUSVILLE, E. A. 2001. Relationships between drug activity in NCI preclinical in vitro and in vivo models and early clinical trials. *British Journal Of Cancer*, 84, 1424.

- KANJILAL, S., SUNITHA, S., REDDY, P. S., KUMAR, K. P., MURTY, U. S. N. & PRASAD, R. B. N. 2009. Synthesis and evaluation of micellar properties and antimicrobial activities of imidazole-based surfactants. *European Journal of Lipid Science and Technology*, 111, 941-948.
- KANTCHEV, E. A. B., O'BRIEN, C. J. & ORGAN, M. G. 2007. Palladium Complexes of N-Heterocyclic Carbenes as Catalysts for Cross-Coupling Reactions—A Synthetic Chemist's Perspective. *Angewandte Chemie International Edition*, 46, 2768-2813.
- KARATAS, M. O., OLGUNDENIZ, B., GUNAL, S., OZDEMIR, I., ALICI, B. & CETINKAYA, E. 2016. Synthesis, characterization and antimicrobial activities of novel silver(I) complexes with coumarin substituted N-heterocyclic carbene ligands. *Bioorg Med Chem*, 24, 643-50.
- KASCATAN-NEBIOGLU, A., MELAIYE, A., HINDI, K., DURMUS, S., PANZNER, M. J., HOGUE, L. A., MALLETT, R. J., HOVIS, C. E., COUGHENOUR, M., CROSBY, S. D., MILSTED, A., ELY, D. L., TESSIER, C. A., CANNON, C. L. & YOUNGS, W. J. 2006. Synthesis from caffeine of a mixed N-heterocyclic carbene–silver acetate complex active against resistant respiratory pathogens. *Journal of Medicinal Chemistry*, 49, 6811-6818.
- KASCATAN-NEBIOGLU, A., PANZNER, M. J., TESSIER, C. A., CANNON, C. L. & YOUNGS, W. J. 2007. N-Heterocyclic carbene–silver complexes: A new class of antibiotics. *Coordination Chemistry Reviews*, 251, 884-895.
- KELLAND, L. 2007. The resurgence of platinum-based cancer chemotherapy. *Nat Rev Cancer*, 7, 573-584.
- KHOJASTEH, R. R. & MATIN, S. J. 2015. Synthesis, characterization, and antibacterial activities of some metal complexes of heptadentate schiff base ligand derived from acetylacetone. *Russian Journal of Applied Chemistry*, 88, 921-925.
- KIM, H. & KANG, S. K. 2014. Crystal structure of phenyl(pyridin-2-yl)methanol. *Acta Crystallographica Section E*, 70, o947.
- KIYOMORI, A., MARCOUX, J.-F. & BUCHWALD, S. L. 1999. An efficient copper-catalyzed coupling of aryl halides with imidazoles. *Tetrahedron Letters*, 40, 2657-2660.

- KÜHL, O. 2009. Sterically induced differences in N-heterocyclic carbene transition metal complexes. *Coordination Chemistry Reviews*, 253, 2481-2492.
- KUMAR, A., NAAZ, A., PRAKASHAM, A., GANGWAR, M. K., BUTCHER, R. J., PANDA, D. & GHOSH, P. 2017. Potent Anticancer Activity with High Selectivity of a Chiral Palladium N-Heterocyclic Carbene Complex. *ACS Omega*, 2, 4632-4646.
- LAPPERT, M. F. 1988. The coordination chemistry of electron-rich alkenes (enetetramines). *Journal of Organometallic Chemistry*, 358, 185-213.
- LEE, J.-Y., LEE, J.-Y., CHANG, Y.-Y., HU, C.-H., WANG, N. M. & LEE, H. M. 2015. Palladium Complexes with Tridentate N-Heterocyclic Carbene Ligands: Selective “Normal” and “Abnormal” Bindings and Their Anticancer Activities. *Organometallics*, 34, 4359-4368.
- LEE, K. M., LEE, C. K. & LIN, I. J. 1997. A Facile Synthesis of Unusual Liquid-Crystalline Gold (I) Dicarbene Compounds. *Angewandte Chemie International Edition in English*, 36, 1850-1852.
- LEMKE, J., PINTO, A., NIEHOFF, P., VASYLYEVA, V. & METZLER-NOLTE, N. 2009. Synthesis, structural characterisation and anti-proliferative activity of NHC gold amino acid and peptide conjugates. *Dalton Trans*, 7063-70.
- LI, K., ZOU, T., CHEN, Y., GUAN, X. & CHE, C.-M. 2015. Pincer-Type Platinum(II) Complexes Containing N-Heterocyclic Carbene (NHC) Ligand: Structures, Photophysical and Anion-Binding Properties, and Anticancer Activities. *Chemistry – A European Journal*, 21, 7441-7453.
- LIN, I. J. B. & VASAM, C. S. 2007. Preparation and application of N-heterocyclic carbene complexes of Ag(I). *Coordination Chemistry Reviews*, 251, 642-670.
- LIU, W., BENS DORF, K., PROETTO, M., HAGENBACH, A., ABRAM, U. & GUST, R. 2012. Synthesis, characterization, and in vitro studies of bis[1,3-diethyl-4,5-diarylimidazol-2-ylidene]gold(I/III) complexes. *Journal of Medicinal Chemistry*, 55, 3713-3724.

- LIU, W. & GUST, R. 2013. Metal N-heterocyclic carbene complexes as potential antitumor metallodrugs. *Chem Soc Rev*, 42, 755-73.
- LIU, W. & GUST, R. 2016. Update on metal N-heterocyclic carbene complexes as potential anti-tumor metallodrugs. *Coordination Chemistry Reviews*, 329, 191-213.
- MAH, T.-F. C. & O'TOOLE, G. A. 2001. Mechanisms of biofilm resistance to antimicrobial agents. *Trends in Microbiology*, 9, 34-39.
- MAHAVORASIRIKUL, W., VIYANANT, V., CHAJAROENKUL, W., ITHARAT, A. & NA-BANGCHANG, K. 2010. Cytotoxic activity of Thai medicinal plants against human cholangiocarcinoma, laryngeal and hepatocarcinoma cells in vitro. *BMC Complementary and Alternative Medicine*, 10, 55.
- MAILLIET, P., MARINETTI, A. & SKANDER, M. 2009. Platinum-N-heterocyclic carbene derivatives, preparation thereof and therapeutic use thereof. *Patent*, WO2009118475A2.
- MARION, N., DE FRÉMONT, P., PUIJK, I. M., ECARNOT, E. C., AMOROSO, D., BELL, A. & NOLAN, S. P. 2007. N-heterocyclic carbene–palladium complexes [(NHC)Pd(acac)Cl]: Improved synthesis and catalytic activity in large-scale cross-coupling reactions. *Advanced Synthesis & Catalysis*, 349, 2380-2384.
- MARLOYE, M., BERGER, G., GELBCKE, M. & DUFRASNE, F. 2016. A survey of the mechanisms of action of anticancer transition metal complexes. *Future Medicinal Chemistry*, 8, 2263-2286.
- MARZO, A. & HEFTMANN, E. 2002. Enantioselective analytical methods in pharmacokinetics with specific reference to genetic polymorphic metabolism. *Journal of Biochemical and Biophysical Methods*, 54, 57-70.
- MATHEWS, C. J., SMITH, P. J. & WELTON, T. 2004. N-donor complexes of palladium as catalysts for Suzuki cross-coupling reactions in ionic liquids. *Journal of Molecular Catalysis A: Chemical*, 214, 27-32.
- MAURO, C. & GIOVANNI, N. 2007. Trans-Platinum Complexes in Cancer Therapy. *Anti-Cancer Agents in Medicinal Chemistry*, 7, 111-123.

- MCDERMOTT, J. X., WHITE, J. F. & WHITESIDES, G. M. 1976. Thermal decomposition of bis (phosphine) platinum (II) metallocycles. *Journal of the American Chemical Society*, 98, 6521-6528.
- MCGUINNESS, D. S., CAVELL, K. J., SKELTON, B. W. & WHITE, A. H. 1999. Zerovalent Palladium and Nickel Complexes of Heterocyclic Carbenes: Oxidative Addition of Organic Halides, Carbon–Carbon Coupling Processes, and the Heck Reaction. *Organometallics*, 18, 1596-1605.
- MCKEAGE, M. 1995. Comparative adverse effect profiles of platinum drugs. *Drug Safety*, 13, 228-244.
- MELAIYE, A., SIMONS, R. S., MILSTED, A., PINGITORE, F., WESEMIOTIS, C., TESSIER, C. A. & YOUNGS, W. J. 2004. Formation of water-soluble pincer silver(I)–carbene complexes: A novel antimicrobial agent. *Journal of Medicinal Chemistry*, 47, 973-977.
- MELAIYE, A., SUN, Z., HINDI, K., MILSTED, A., ELY, D., RENEKER, D. H., TESSIER, C. A. & YOUNGS, W. J. 2005. Silver(I)–imidazole cyclophane gem-diol complexes encapsulated by electrospun tecophilic nanofibers: Formation of nanosilver particles and antimicrobial activity. *Journal of the American Chemical Society*, 127, 2285-2291.
- MJOS, K. D. & ORVIG, C. 2014. Metallodrugs in medicinal inorganic chemistry. *Chem Rev*, 114, 4540-63.
- MOHAMED, A. M., PALMER, R. A., SOAYED, A. A., REFAAT, H. M. & BASHER, D. E. 2014. The Ni (II) Complex of 2-Hydroxy-Pyridine-N-Oxide 2-Isothionate: Synthesis, Characterization, Biological Studies, and X-ray Crystal Structures using (1) Cu K α Data and (2) Synchrotron Data. *J Mater Sci Nanotechnol*, 2, 101.
- MOLLER, T., WONNEBERGER, P., KRETZSCHMAR, N. & HEY-HAWKINS, E. 2014. P-chiral phosphorus heterocycles: a straightforward synthesis. *Chemical Communications*, 50, 5826-5828.
- MORÁN, C., CLAPÉS, P., COMELLES, F., GARCÍA, T., PÉREZ, L., VINARDELL, P., MITJANS, M. & INFANTE, M. R. 2001. Chemical Structure/Property Relationship in Single-Chain Arginine Surfactants. *Langmuir*, 17, 5071-5075.

- MUENZNER, J. K., REHM, T., BIRSACK, B., CASINI, A., DE GRAAF, I. A. M., WORAWUTPUTTAPONG, P., NOOR, A., KEMPE, R., BRABEC, V., KASPARKOVA, J. & SCHOBERT, R. 2015. Adjusting the DNA Interaction and Anticancer Activity of Pt(II) N-Heterocyclic Carbene Complexes by Steric Shielding of the Trans Leaving Group. *Journal of Medicinal Chemistry*, 58, 6283-6292.
- MUMTAZ, A., SAEED, A., FATIMA, N., DAWOOD, M., RAFIQUE, H. & IQBAL, J. 2016. Imidazole and its derivatives as potential candidates for drug development. *Bangladesh Journal of Pharmacology*, 11, 756.
- NG, K. H., LI, Y., TAN, W. X., CHIANG, M. & PULLARKAT, S. A. 2013. Synthesis and characterization of conformationally rigid chiral pyridine-N-heterocyclic carbene-based palladacycles with an unexpected Pd-N bond cleavage. *Chirality*, 25, 149-59.
- NGUYEN, L. A., HE, H. & PHAM-HUY, C. 2006. Chiral Drugs: An Overview. *International Journal of Biomedical Science : IJBS*, 2, 85-100.
- NICHOLSON, K. M., PHILLIPS, R. M., SHNYDER, S. D. & BIBBY, M. C. 2002. In vitro and in vivo activity of LS 4477 and LS 4559, novel analogues of the tubulin binder estramustine. *European Journal of Cancer*, 38, 194-204.
- NOLAN, S. P. 2011. The Development and Catalytic Uses of N-Heterocyclic Carbene Gold Complexes. *Accounts of Chemical Research*, 44, 91-100.
- O'TOOLE, G., KAPLAN, H. B. & KOLTER, R. 2000. Biofilm formation as microbial development. *Annual Reviews in Microbiology*, 54, 49-79.
- OEHNINGER, L., RUBBIANI, R. & OTT, I. 2013. N-Heterocyclic carbene metal complexes in medicinal chemistry. *Dalton Transactions*, 42, 3269-3284.
- ÖFELE, K. 1968. Pentacarbonyl (2, 3-diphenylcyclopropenyldene)-chromium (0). *Angewandte Chemie International Edition in English*, 7, 950-950.
- OLIVEIRA, D. C., TOMASZ, A. & DE LENCASTRE, H. 2002. Secrets of success of a human pathogen: molecular evolution of pandemic clones of meticillin-resistant *Staphylococcus aureus*. *The Lancet Infectious Diseases*, 2, 180-189.

- ONAR, G., KARATAŞ, M. O., BALCIÖĞLU, S., TOK, T. T., GÜRSES, C., KILIÇ-CIKLA, I., ÖZDEMİR, N., ATEŞ, B. & ALICI, B. 2018. Benzotriazole functionalized N-heterocyclic carbene–silver (I) complexes: Synthesis, cytotoxicity, antimicrobial, DNA binding, and molecular docking studies. *Polyhedron*, 153, 31-40.
- ONG, Y. C., ROY, S., ANDREWS, P. C. & GASSER, G. 2019. Metal Compounds against Neglected Tropical Diseases. *Chemical Reviews*, 119, 730-796.
- OTT, I. & GUST, R. 2007. Non platinum metal complexes as anti-cancer drugs. *Archiv der Pharmazie*, 340, 117-126.
- ÖZDEMİR, I., DEMİR, S., ÇETINKAYA, B., TOUPET, L., CASTARLENAS, R., FISCHMEISTER, C. & DIXNEUF, P. H. 2007. Chelating η⁶-Arene-η¹-carbene Ligands in Ruthenium Complexes. *European journal of inorganic chemistry*, 2007, 2862-2869.
- ÖZDEMİR, İ., DENIZCI, A., ÖZTÜRK, H. T. & ÇETINKAYA, B. 2004. Synthetic and antimicrobial studies on new gold(I) complexes of imidazolidin-2-ylidenes. *Applied Organometallic Chemistry*, 18, 318-322.
- ÖZDEMİR, İ., TEMELLI, N., GÜNAL, S. & DEMİR, S. 2010. Gold(I) complexes of N-heterocyclic carbene ligands containing benzimidazole: Synthesis and antimicrobial activity. *Molecules*, 15, 2203.
- PAGES, B. J., ANG, D. L., WRIGHT, E. P. & ALDRICH-WRIGHT, J. R. 2015. Metal complex interactions with DNA. *Dalton Transactions*, 44, 3505-3526.
- PANKEY, G. & SABATH, L. 2004. Clinical relevance of bacteriostatic versus bactericidal mechanisms of action in the treatment of Gram-positive bacterial infections. *Clinical infectious diseases*, 38, 864-870.
- PATEL, R. N., BANERJEE, A., NANDURI, V., GOSWAMI, A. & COMEZOGU, F. 2000. Enzymatic resolution of racemic secondary alcohols by lipase B from *Candida antarctica*. *Journal of the American Oil Chemists' Society*, 77, 1015-1019.

- PATIL, S. A., PATIL, S. A., PATIL, R., KERI, R. S., BUDAGUMPI, S., BALAKRISHNA, G. R. & TACKE, M. 2015. N-heterocyclic carbene metal complexes as bio-organometallic antimicrobial and anticancer drugs. *Future Medicinal Chemistry*, 7, 1305-1333.
- PATRA, M. & GASSER, G. 2012. Organometallic compounds: An opportunity for chemical biology? *ChemBioChem*, 13, 1232-1252.
- PATRA, M. & GASSER, G. 2017. The medicinal chemistry of ferrocene and its derivatives. *Nature Reviews Chemistry*, 1, 0066.
- PATRICK, G. L. 2013. *An introduction to medicinal chemistry*, New York, NY, Oxford University Press.
- PEÑA-MORÁN, O., VILLARREAL, M., ÁLVAREZ-BERBER, L., MENESES-ACOSTA, A. & RODRÍGUEZ-LÓPEZ, V. 2016. Cytotoxicity, Post-Treatment Recovery, and Selectivity Analysis of Naturally Occurring Podophyllotoxins from *Bursera fagaroides* var. *fagaroides* on Breast Cancer Cell Lines. *Molecules*, 21, 1013.
- QUIRANTE, J., RUIZ, D., GONZALEZ, A., LÓPEZ, C., CASCANTE, M., CORTÉS, R., MESSEGUER, R., CALVIS, C., BALDOMÀ, L., PASCUAL, A., GUÉRARDEL, Y., PRADINES, B., FONT-BARDÍA, M., CALVET, T. & BIOT, C. 2011. Platinum(II) and palladium(II) complexes with (N,N') and (C,N,N')- ligands derived from pyrazole as anticancer and antimalarial agents: Synthesis, characterization and in vitro activities. *Journal of Inorganic Biochemistry*, 105, 1720-1728.
- RADULOVIĆ, V., BACCHI, A., PELIZZI, G., SLADIĆ, D., BRČESKI, I. & ANDJELKOVIĆ, K. 2006. Synthesis, Structure, and Antimicrobial Activity of Complexes of Pt(II), Pd(II), and Ni(II) with the Condensation Product of 2-(Diphenylphosphino)benzaldehyde and Semioxamazine. *Monatshefte für Chemie / Chemical Monthly*, 137, 681-691.
- RAMAN, N., JOSEPH, J., SAKTHIVEL, A. & JEYAMURUGAN, R. 2009. Synthesis, structural characterisation and antimicrobial studies of novel Schiff base copper (II) complexes. *Journal of the Chilean Chemical Society*, 54, 354-357.
- RAMOS-LIMA, F. J., MONEO, V., QUIROGA, A. G., CARNERO, A. & NAVARRO-RANNINGER, C. 2010. The role of p53 in the cellular toxicity by active trans-platinum

- complexes containing isopropylamine and hydroxymethylpyridine. *European Journal of Medicinal Chemistry*, 45, 134-141.
- RAY, S., ASTHANA, J., TANSKI, J. M., SHAIKH, M. M., PANDA, D. & GHOSH, P. 2009. Design of nickel chelates of tetradentate N-heterocyclic carbenes with subdued cytotoxicity. *Journal of Organometallic Chemistry*, 694, 2328-2335.
- RAY, S., MOHAN, R., SINGH, J. K., SAMANTARAY, M. K., SHAIKH, M. M., PANDA, D. & GHOSH, P. 2007. Anticancer and Antimicrobial Metallopharmaceutical Agents Based on Palladium, Gold, and Silver N-Heterocyclic Carbene Complexes. *Journal of the American Chemical Society*, 129, 15042-15053.
- REEDIJK, J. 2008. Metal-Ligand Exchange Kinetics in Platinum and Ruthenium Complexes. *Platinum Metals Review*, 52, 2-11.
- REHM, T., ROTHEMUND, M., MUENZNER, J. K., NOOR, A., KEMPE, R. & SCHOBERT, R. 2016. Novel cis-[(NHC)₁(NHC)₂(L)Cl]platinum(II) complexes – synthesis, structures, and anticancer activities. *Dalton Transactions*, 45, 15390-15398.
- RELLER, L. B., WEINSTEIN, M., JORGENSEN, J. H. & FERRARO, M. J. 2009. Antimicrobial Susceptibility Testing: A Review of General Principles and Contemporary Practices. *Clinical Infectious Diseases*, 49, 1749-1755.
- RIDUAN, S. N. & ZHANG, Y. 2013. Imidazolium salts and their polymeric materials for biological applications. *Chemical Society Reviews*, 42, 9055-9070.
- RIEB, J., DOMINELLI, B., MAYER, D., JANDL, C., DRECHSEL, J., HEYDENREUTER, W., SIEBER, S. A. & KUHN, F. E. 2017. Influence of wing-tip substituents and reaction conditions on the structure, properties and cytotoxicity of Ag(I)- and Au(I)-bis(NHC) complexes. *Dalton Transactions*, 46, 2722-2735.
- RIT, A., PAPE, T. & HAHN, F. E. 2011. Polynuclear architectures with di- and tricarbene ligands. *Organometallics*, 30, 6393-6401.
- RIXE, O., ORTUZAR, W., ALVAREZ, M., PARKER, R., REED, E., PAULL, K. & FOJO, T. 1996. Oxaliplatin, tetraplatin, cisplatin, and carboplatin: Spectrum of activity in drug-

- resistant cell lines and in the cell lines of the national cancer institute's anticancer drug screen panel. *Biochemical Pharmacology*, 52, 1855-1865.
- ROLAND, S., JOLIVALT, C., CRESTEIL, T., ELOY, L., BOUHOURS, P., HEQUET, A., MANSUY, V., VANUCCI, C. & PARIS, J.-M. 2011. Investigation of a series of silver–N-heterocyclic carbenes as antibacterial agents: Activity, synergistic effects, and cytotoxicity. *Chemistry – A European Journal*, 17, 1442-1446.
- RONCONI, L. & SADLER, P. J. 2007. Using coordination chemistry to design new medicines. *Coordination Chemistry Reviews*, 251, 1633-1648.
- ROSENBERG, B., VAN CAMP, L. & KRIGAS, T. 1965. Inhibition of Cell Division in *Escherichia coli* by Electrolysis Products from a Platinum Electrode. *Nature*, 205, 698-699.
- ROUT, L., JAMMI, S. & PUNNIYAMURTHY, T. 2007. Novel CuO nanoparticle catalyzed C–N cross coupling of amines with iodobenzene. *Organic letters*, 9, 3397-3399.
- SALEEM, K., WANI, W. A., HAQUE, A., LONE, M. N., HSIEH, M. F., JAIRAJPURI, M. A. & ALI, I. 2013. Synthesis, DNA binding, hemolysis assays and anticancer studies of copper(II), nickel(II) and iron(III) complexes of a pyrazoline-based ligand. *Future Med Chem*, 5, 135-46.
- SAMANTARAY, M. K., DASH, C., SHAIKH, M. M., PANG, K., BUTCHER, R. J. & GHOSH, P. 2011. Gold (III) N-heterocyclic carbene complexes mediated synthesis of β -enaminones from 1, 3-dicarbonyl compounds and aliphatic amines. *Inorganic chemistry*, 50, 1840-1848.
- SCHMIDT, C., KARGE, B., MISGELD, R., PROKOP, A., FRANKE, R., BRÖNSTRUP, M. & OTT, I. 2017. Gold(I) NHC Complexes: Antiproliferative Activity, Cellular Uptake, Inhibition of Mammalian and Bacterial Thioredoxin Reductases, and Gram-Positive Directed Antibacterial Effects. *Chemistry – A European Journal*, 23, 1869-1880.
- SCHMITT, F., DONNELLY, K., MUENZNER, J. K., REHM, T., NOVOHRADSKY, V., BRABEC, V., KASPARKOVA, J., ALBRECHT, M., SCHOBERT, R. & MUELLER, T. 2016. Effects of histidin-2-ylidene vs. imidazol-2-ylidene ligands on the anticancer

- and antivasular activity of complexes of ruthenium, iridium, platinum, and gold. *Journal of Inorganic Biochemistry*, 163, 221-228.
- SCOTT, N. M., DORTA, R., STEVENS, E. D., CORREA, A., CAVALLO, L. & NOLAN, S. P. 2005. Interaction of a bulky N-heterocyclic carbene ligand with Rh(I) and Ir(I). Double C–H activation and isolation of bare 14-electron Rh(III) and Ir(III) complexes. *Journal of the American Chemical Society*, 127, 3516-3526.
- SHEIKHSHOAIE, I., LOTFI, N., SIELER, J., KRAUTSCHEID, H. & KHALEGHI, M. 2018. Synthesis, structures and antimicrobial activities of nickel(II) and zinc(II) diaminomaleonitrile-based complexes. *Transition Metal Chemistry*, 43, 555-562.
- SKANDER, M., RETAILLEAU, P., BOURRIÉ, B., SCHIO, L., MAILLIET, P. & MARINETTI, A. 2010. N-Heterocyclic Carbene-Amine Pt(II) Complexes, a New Chemical Space for the Development of Platinum-Based Anticancer Drugs. *Journal of Medicinal Chemistry*, 53, 2146-2154.
- STORR, T., THOMPSON, K. H. & ORVIG, C. 2006. Design of targeting ligands in medicinal inorganic chemistry. *Chemical Society Reviews*, 35, 534-544.
- STROHFELDT, K. & TACKE, M. 2008. Bioorganometallic fulvene-derived titanocene anti-cancer drugs. *Chemical Society Reviews*, 37, 1174-1187.
- SUN, R. W.-Y., CHOW, A. L.-F., LI, X.-H., YAN, J. J., CHUI, S. S.-Y. & CHE, C.-M. 2011. Luminescent cyclometalated platinum(II) complexes containing N-heterocyclic carbene ligands with potent in vitro and in vivo anti-cancer properties accumulate in cytoplasmic structures of cancer cells. *Chemical Science*, 2, 728-736.
- SURESH, P. & PITCHUMANI, K. 2008. Per-6-amino- β -cyclodextrin as an Efficient Supramolecular Ligand and Host for Cu(I)-Catalyzed N-Arylation of Imidazole with Aryl Bromides. *The Journal of Organic Chemistry*, 73, 9121-9124.
- TANDON, R., SINGH, I., LUXAMI, V., TANDON, N. & PAUL, K. 2019. Recent Advances and Developments of in vitro Evaluation of Heterocyclic Moieties on Cancer Cell Lines. *The Chemical Record*, 19.

- TERAO, J., WATANABE, H., IKUMI, A., KUNIYASU, H. & KAMBE, N. 2002. Nickel-Catalyzed Cross-Coupling Reaction of Grignard Reagents with Alkyl Halides and Tosylates: Remarkable Effect of 1,3-Butadienes. *Journal of the American Chemical Society*, 124, 4222-4223.
- TEYSSOT, M.-L., JARROUSSE, A.-S., MANIN, M., CHEVRY, A., ROCHE, S., NORRE, F., BEAUDOIN, C., MOREL, L., BOYER, D. & MAHIOU, R. 2009. Metal-NHC complexes: a survey of anti-cancer properties. *Dalton Transactions*, 6894-6902.
- THOMPSON, K. H. & ORVIG, C. 2006. Metal complexes in medicinal chemistry: new vistas and challenges in drug design. *Dalton Transactions*, 761-764.
- TOBISU, M., SHIMASAKI, T. & CHATANI, N. 2008. Nickel-Catalyzed Cross-Coupling of Aryl Methyl Ethers with Aryl Boronic Esters. *Angewandte Chemie International Edition*, 47, 4866-4869.
- VAN BEUSICHEM, M. & FARRELL, N. 1992. Activation of the trans geometry in platinum antitumor complexes. Synthesis, characterization, and biological activity of complexes with the planar ligands pyridine, N-methylimidazole, thiazole, and quinoline. Crystal and molecular structure of trans-dichlorobis(thiazole)platinum(II). *Inorganic Chemistry*, 31, 634-639.
- VOUTCHKOVA, A. M., APPELHANS, L. N., CHIANESE, A. R. & CRABTREE, R. H. 2005. Disubstituted imidazolium-2-carboxylates as efficient precursors to N-heterocyclic carbene complexes of Rh, Ru, Ir, and Pd. *Journal of the American Chemical Society*, 127, 17624-17625.
- WANG, D. & LIPPARD, S. J. 2005. Cellular processing of platinum anticancer drugs. *Nat Rev Drug Discov*, 4, 307-320.
- WANG, H. M. J. & LIN, I. J. B. 1998. Facile Synthesis of Silver(I)-Carbene Complexes. Useful Carbene Transfer Agents. *Organometallics*, 17, 972-975.
- WANZLICK, H. W. & SCHÖNHERR, H. J. 1968. Direct synthesis of a mercury salt-carbene complex. *Angewandte Chemie International Edition in English*, 7, 141-142.

- WHEATE, N. J., WALKER, S., CRAIG, G. E. & OUN, R. 2010. The status of platinum anticancer drugs in the clinic and in clinical trials. *Dalton Transactions*, 39, 8113-8127.
- WHO, W. H. O. 2014. *Antimicrobial resistance: global report on surveillance*, World Health Organization.
- WINSTON, S., STYLIANIDES, N., TULLOCH, A. A., WRIGHT, J. A. & DANOPOULOS, A. A. 2004. Picoline and pyridine functionalised chelate N-heterocyclic carbene complexes of nickel: synthesis and structural studies. *Polyhedron*, 23, 2813-2820.
- WISE, R., HART, T., CARS, O., STREULENS, M., HELMUTH, R., HUOVINEN, P. & SPRENGER, M. 1998. Antimicrobial resistance. British Medical Journal Publishing Group.
- XUE, F., CAI, C., SUN, H., SHEN, Q. & RUI, J. 2008. β -Ketoimine as an efficient ligand for copper-catalyzed N-arylation of nitrogen-containing heterocycles with aryl halides. *Tetrahedron Letters*, 49, 4386-4389.
- YAN, J., WANG, K., DANG, W., CHEN, R., XIE, J., ZHANG, B., SONG, J. & WANG, R. 2013. Two Hits Are Better than One: Membrane-Active and DNA Binding-Related Double-Action Mechanism of NK-18, a Novel Antimicrobial Peptide Derived from Mammalian NK-Lysin. *Antimicrobial Agents and Chemotherapy*, 57, 220-228.
- YAN, J. J., CHOW, A. L.-F., LEUNG, C.-H., SUN, R. W.-Y., MA, D.-L. & CHE, C.-M. 2010. Cyclometalated gold(III) complexes with N-heterocyclic carbene ligands as topoisomerase I poisons. *Chemical Communications*, 46, 3893-3895.
- YOUNGS, W., TESSIER, C., KOFRON, W., SIMONS, R. & GARRISON, J. 2004. Carbene porphyrins and carbene porphyrinoids, methods of preparation and uses thereof. *Patent*, WO2002038566A2.
- YOUNGS, W. J., TESSIER, C. A., GARRISON, J., QUEZADA, C., MELAIYE, A., PANZNER, M. & DURMAS, S. 2005. Metal complexes of N-heterocyclic carbenes as radiopharmaceuticals and antibiotics. *Patent*, US20070021401A1.
- ZHANG, D. & ZI, G. 2015. N-heterocyclic carbene (NHC) complexes of group 4 transition metals. *Chemical Society Reviews*, 44, 1898-1921.

- ZHANG, J.-J., CHE, C.-M. & OTT, I. 2015. Caffeine derived platinum(II) N-heterocyclic carbene complexes with multiple anti-cancer activities. *Journal of Organometallic Chemistry*, 782, 37-41.
- ZHANG, X., LIU, B., LIU, A., XIE, W. & CHEN, W. 2009. Steric Bulkiness-Dependent Structural Diversity in Nickel (II) Complexes of N-Heterocyclic Carbenes: Synthesis and Structural Characterization of Tetra-, Penta-, and Hexacoordinate Nickel Complexes. *Organometallics*, 28, 1336-1349.
- ZHONG, W., FEI, Z., SCOPELLITI, R. & DYSON, P. J. 2016. Alcohol-Induced C–N Bond Cleavage of Cyclometalated N-Heterocyclic Carbene Ligands with a Methylene-Linked Pendant Imidazolium Ring. *Chemistry – A European Journal*, 22, 12138-12144.
- ZHOU, J. & FU, G. C. 2003. Cross-Couplings of Unactivated Secondary Alkyl Halides: Room-Temperature Nickel-Catalyzed Negishi Reactions of Alkyl Bromides and Iodides. *Journal of the American Chemical Society*, 125, 14726-14727.
- ZHOU, J., GUPTA, K., AGGARWAL, S., ANEJA, R., CHANDRA, R., PANDA, D. & JOSHI, H. C. 2003. Brominated derivatives of noscapine are potent microtubule-interfering agents that perturb mitosis and inhibit cell proliferation. *Molecular Pharmacology*, 63, 799-807.
- ZHOU, Y., ZHANG, X., CHEN, W. & QIU, H. 2008. Synthesis, structural characterization, and luminescence properties of multinuclear silver complexes of pyrazole-functionalized NHC ligands containing Ag–Ag and Ag– π interactions. *Journal of Organometallic Chemistry*, 693, 205-215.
- ZOU, T., LOK, C.-N., FUNG, Y. M. E. & CHE, C.-M. 2013. Luminescent organoplatinum(II) complexes containing bis(N-heterocyclic carbene) ligands selectively target the endoplasmic reticulum and induce potent photo-toxicity. *Chemical Communications*, 49, 5423-5425.

APPENDIX 1: X Ray Crystallographic Data

Table 21. Crystallographic data of racemic complex Pt-65a.

Empirical formula	C ₁₆ H ₁₅ Cl ₂ N ₃ Pt·C ₂ H ₆ OS	
Formula Weight	593.43	
Temperature	239(2) K	
Wavelength	0.71076 Å	
Crystal system	monoclinic	
Space group	P 21/n	
Unit cell dimensions	$a = 9.781(3) \text{ \AA}$	$\alpha = 90^\circ$
	$b = 15.685(7) \text{ \AA}$	$\beta = 103.703(13)^\circ$
	$c = 13.896(5) \text{ \AA}$	$\gamma = 90^\circ$
Volume	2071.0(14) Å ³	
Z	4	
Density (calculated)	1.903 Mg/m ³	
Absorption coefficient	7.146 mm ⁻¹	
F(000)	1144	
Crystal size	0.34 × 0.30 × 0.12 mm ³	
Theta range for data collection	2.899 to 25.044°	
Index ranges	-11 ≤ h ≤ 11, -18 ≤ k ≤ 18, -16 ≤ l ≤ 16	
Reflection collected	19516	
Independent reflections	3646 [R(int) = 0.1182]	
Completeness to theta = 25.044°	99.6%	
Absorption correction	None	
Max. and min. transmission	0.481 and 0.195	
Refinement method	Full-matrix least squares on F ²	
Data / restraints / parameters	3646 / 0 / 238	
Goodness-of-fit on F ²	1.051	
Final R indices [I > 2σ(I)]	R1 = 0.0611, wR2 = 0.1664	
R indices (all data)	R1 = 0.0932, wR2 = 0.1977	
Largest diff. peak and hole	1.277 and -3.621 e.Å ⁻³	

Table 22. Crystallographic data of unexpected nickel complex 72.

Empirical formula	C ₁₀ H ₂₀ Cl ₂ N ₄ NiO ₂	
Formula Weight	357.91	
Temperature	293(2) K	
Wavelength	0.71073Å	
Crystal system	triclinic	
Space group	P -1	
Unit cell dimensions	$a = 6.2281(8) \text{ \AA}$	$\alpha = 107.050(11)^\circ$
	$b = 8.1875(11) \text{ \AA}$	$\beta = 109.143(11)^\circ$
	$c = 8.6744(10) \text{ \AA}$	$\gamma = 96.894(10)^\circ$
Volume	387.89(9) Å ³	
Z	1	
Density (calculated)	1.532 Mg/m ³	
Absorption coefficient	1.598 mm ⁻¹	
F(000)	186	
Crystal size	0.50 × 0.50 × 0.5 mm ³	
Theta range for data collection	4.3430 to 29.4410°	
Index ranges	-8<=h<=8, -8<=k<=11, -11<=l<=10	
Reflection collected	2761	
Independent reflections	1799 [R(int) = 0.0264]	
Completeness to theta = 25.242°	98.9%	
Absorption correction	Multi-scan	
Max. and min. transmission	0.64927 and 1.00000	
Refinement method	Full-matrix least squares on F ²	
Data / restraints / parameters	1799 / 3 / 94	
Goodness-of-fit on F ²	1.069	
Final R indices [I>2Sigma(I)]	R1 = 0.0351, wR2 = 0.0837	
R indices (all data)	R1 = 0.0447, wR2 = 0.0922	
Largest diff. peak and hole	1.277 and -3.621 e.Å ⁻³	

Table 23. Crystallographic data of unexpected nickelate complex 73.

Empirical formula	C ₃₈ H ₄₄ C ₁₄ N ₆ Ni	
Formula Weight	785.04	
Temperature	298(2) K	
Wavelength	1.54184 Å	
Crystal system	triclinic	
Space group	P 1	
Unit cell dimensions	$a = 9.8671(11) \text{ \AA}$	$\alpha = 76.191(10)^\circ$
	$b = 10.7163(12) \text{ \AA}$	$\beta = 73.299(10)^\circ$
	$c = 11.0690(13) \text{ \AA}$	$\gamma = 999.6(2)^\circ$
Volume	999.6(2) Å ³	
Z	1	
Density (calculated)	1.304 Mg/m ³	
Absorption coefficient	3.421 mm ⁻¹	
F(000)	410	
Crystal size	0.50 × 0.50 × 0.4 mm ³	
Theta range for data collection	4.480 to 74.039°	
Index ranges	-12 ≤ h ≤ 12, -13 ≤ k ≤ 11, -13 ≤ l ≤ 13	
Reflection collected	5876	
Independent reflections	4407 [R(int) = 0.0240]	
Completeness to theta = 67.684°	98.49%	
Absorption correction	Multi-scan	
Max. and min. transmission	0.43129 and 1.00000	
Refinement method	Full-matrix least squares on F ²	
Data / restraints / parameters	4407 / 63 / 449	
Goodness-of-fit on F ²	1.038	
Final R indices [I > 2Sigma(I)]	R1 = 0.0569, wR2 = 0.1505	
R indices (all data)	R1 = 0.0585, wR2 = 0.1546	
Largest diff. peak and hole	0.402 and -0.918 e.Å ⁻³	

APPENDIX 2: NMR Spectral Data

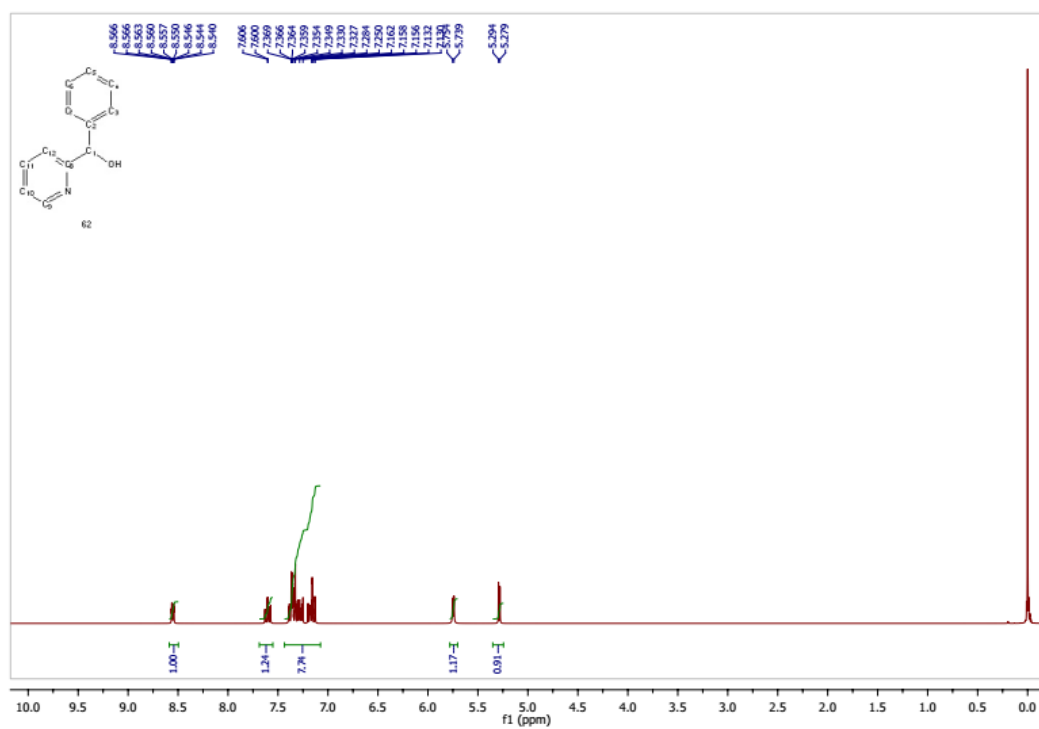


Figure 7. ¹H NMR spectrum of phenyl(pyridine-2-yl)methanol, 62.

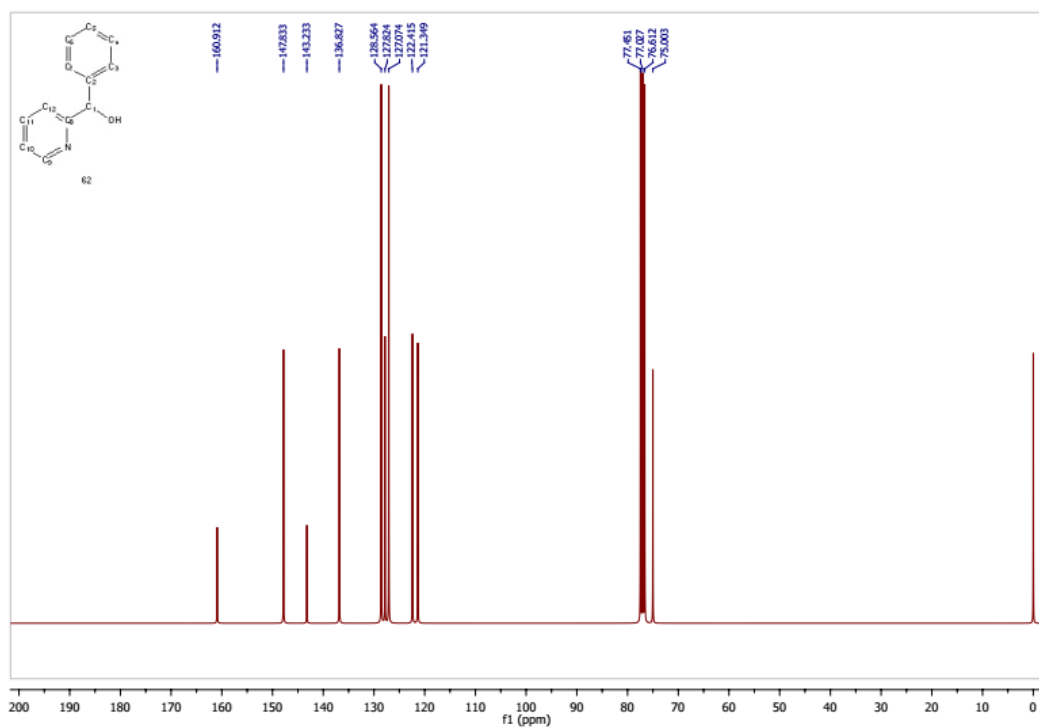


Figure 8. ¹³C NMR spectrum of phenyl(pyridine-2-yl)methanol, 62.

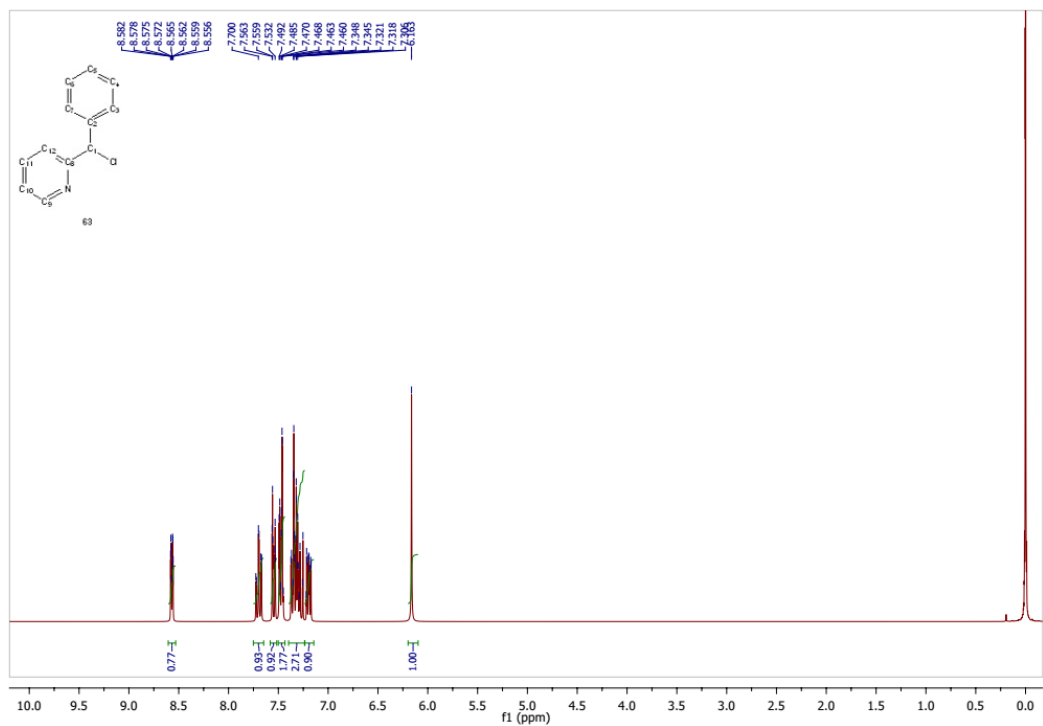


Figure 9. ¹H NMR spectrum of 2-(chloro(phenyl)methyl)pyridine, 63.

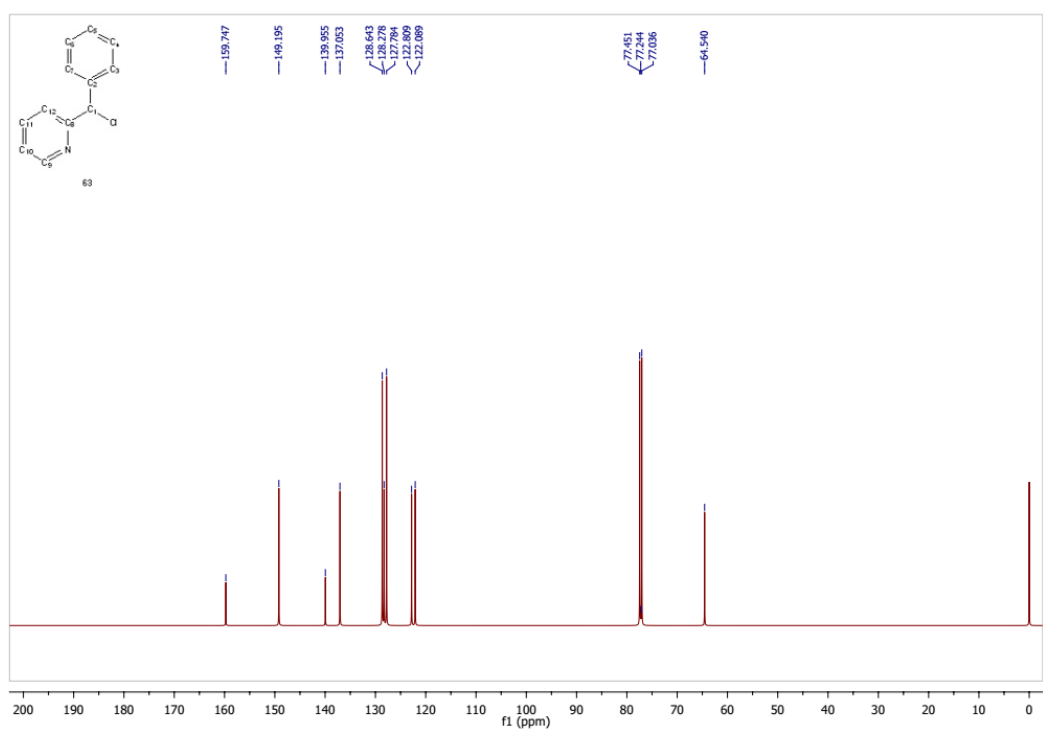


Figure 10. ¹³C NMR spectrum of 2-(chloro(phenyl)methyl)pyridine, 63.

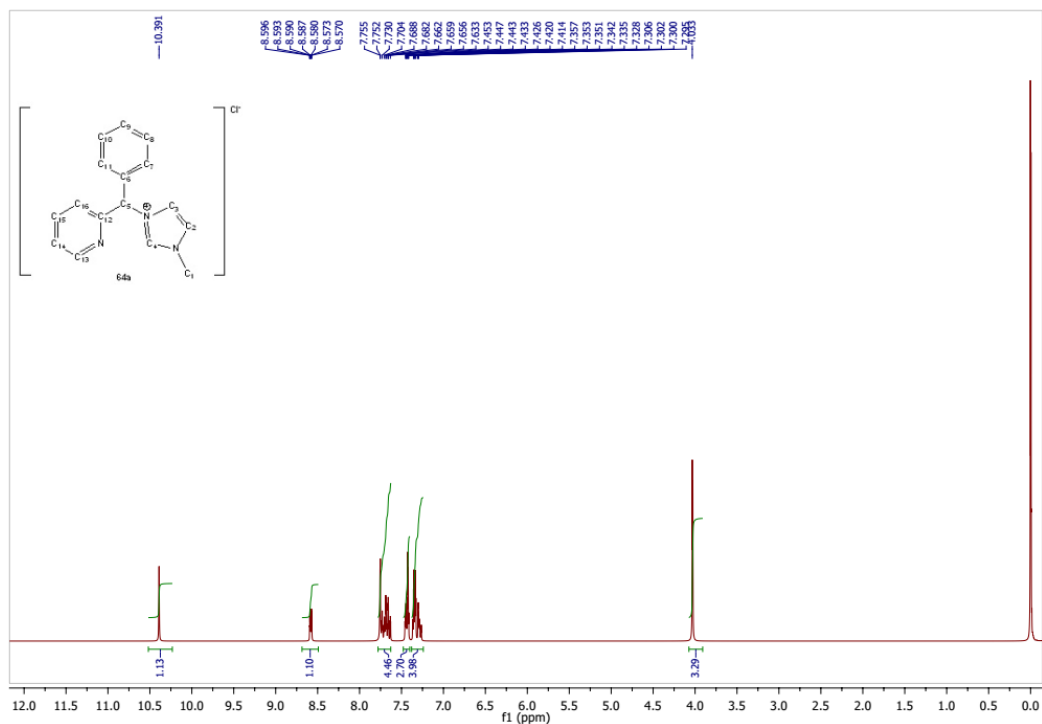


Figure 11. ^1H NMR spectrum of imidazolium-based salt, 64a.

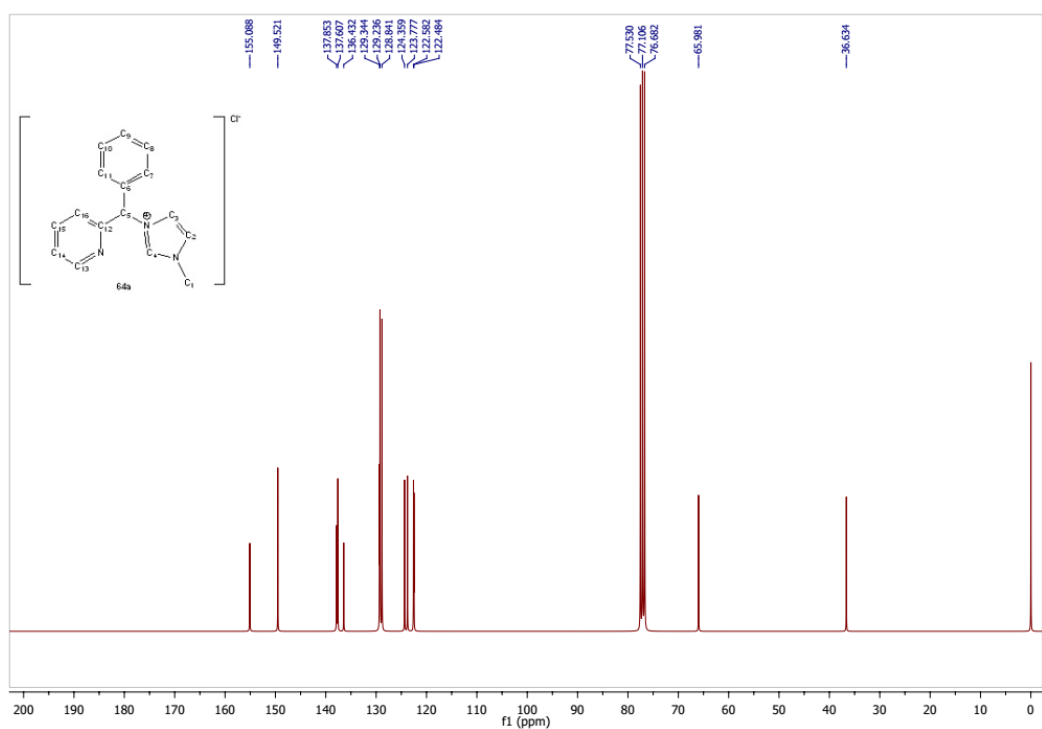


Figure 12. ^{13}C NMR spectrum of imidazolium-based salt, 64a.

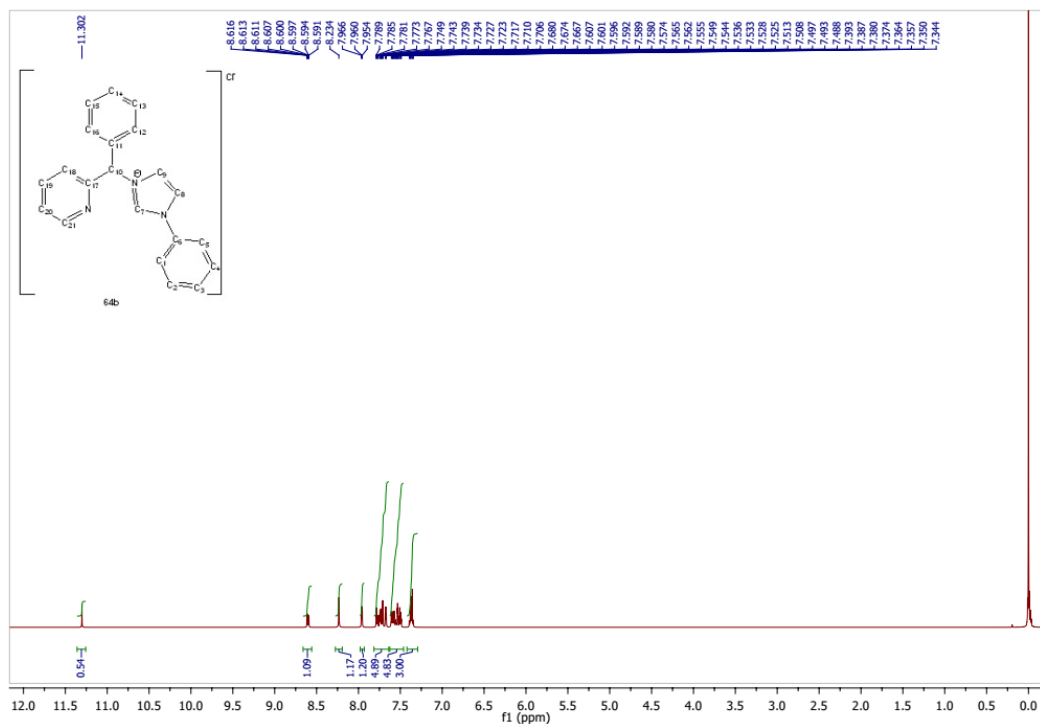


Figure 13. ¹H NMR spectrum of imidazolium-based salt, 64b.

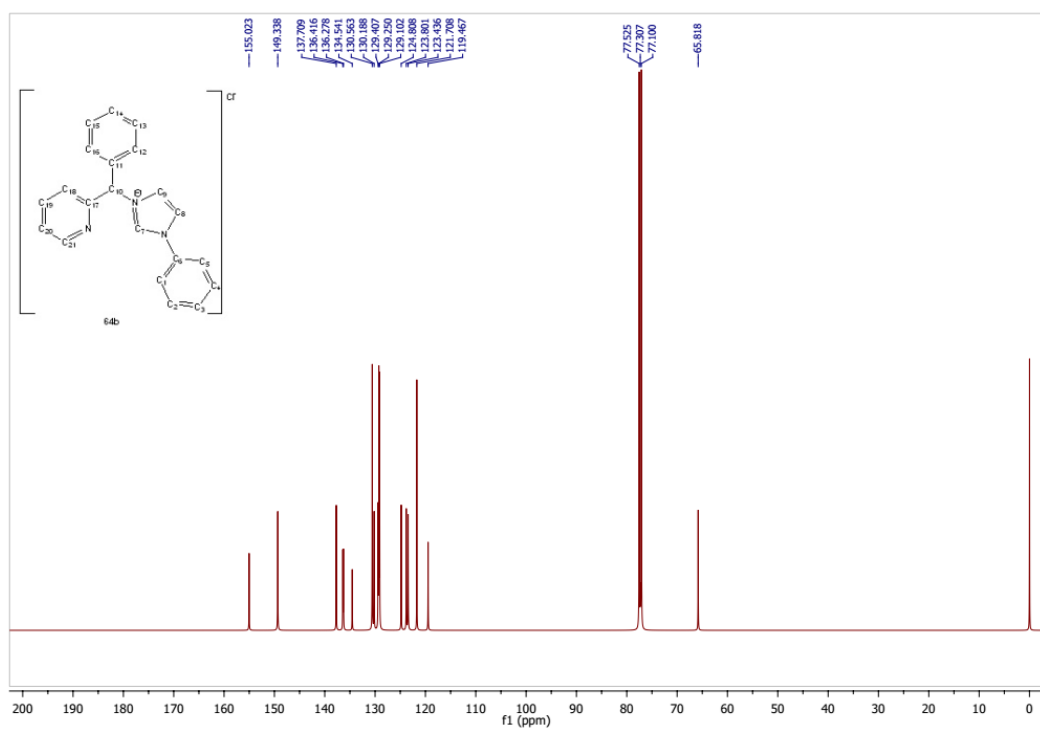


Figure 14. ¹³C NMR spectrum of imidazolium-based salt, 64b.

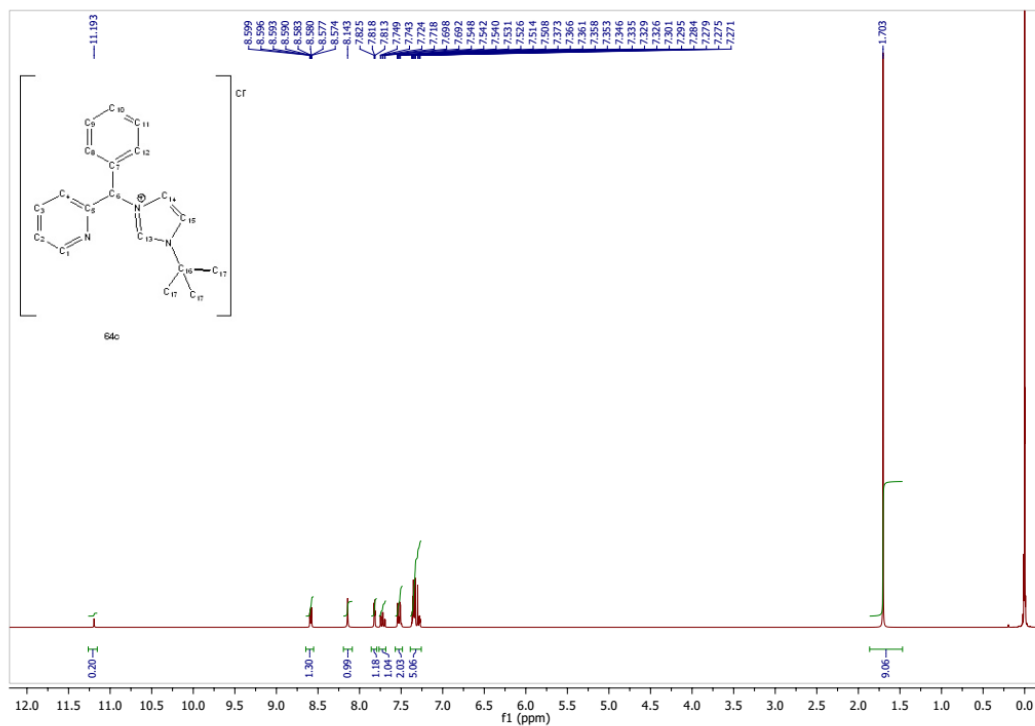


Figure 15. ¹H NMR spectrum of imidazolium-based salt, 64c.

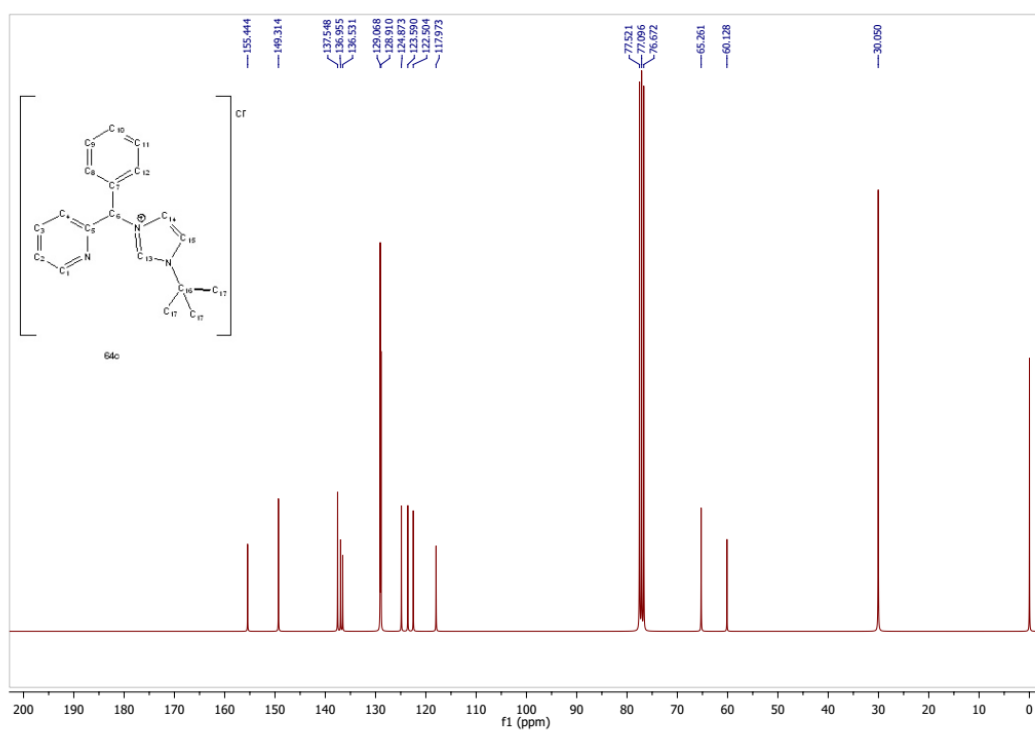


Figure 16. ¹³C NMR spectrum of imidazolium-based salt, 64c.

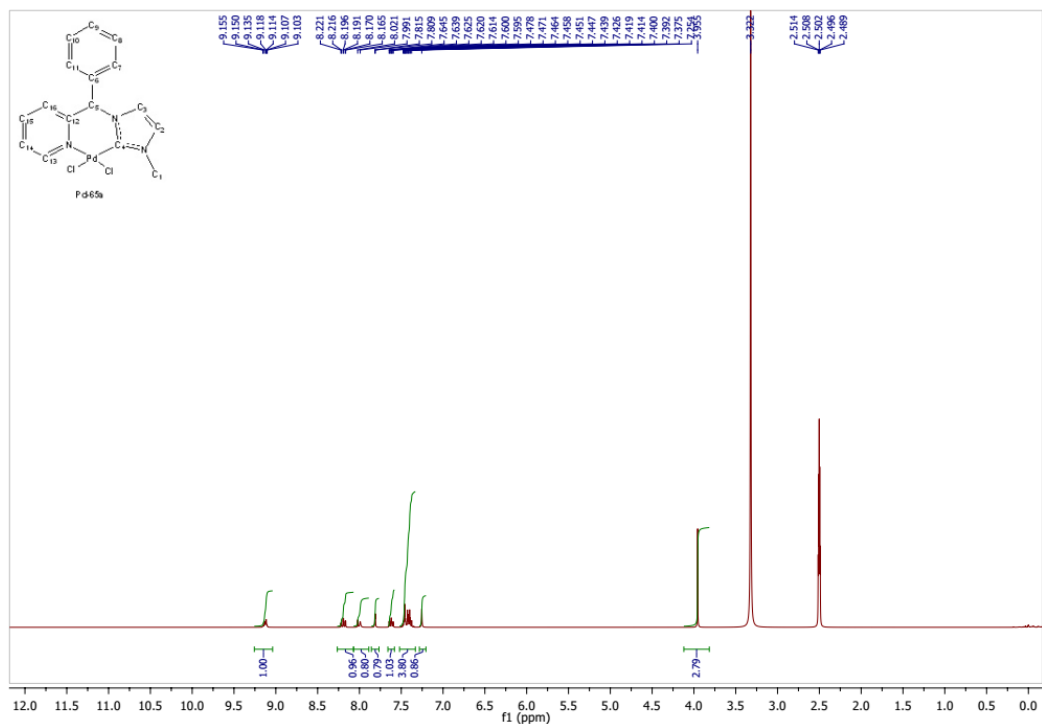


Figure 17. ¹H NMR spectrum of racemic Pd NHC complex (±)-Pd-65a.

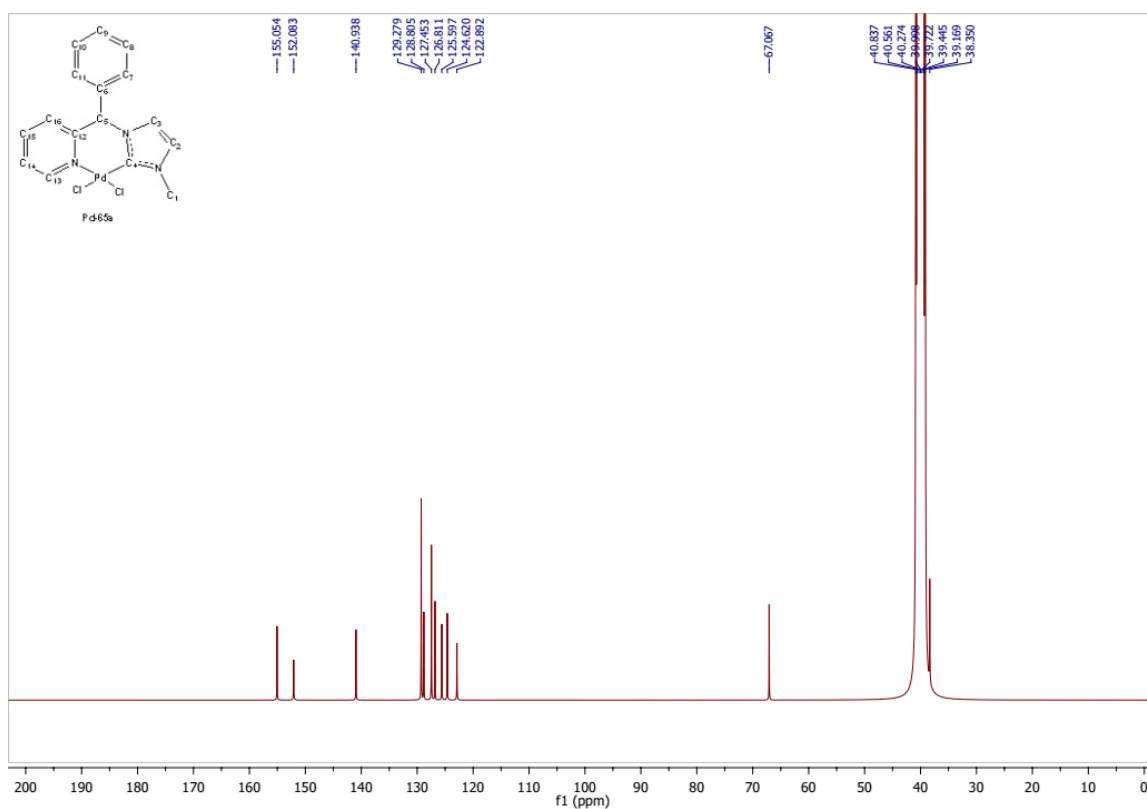


Figure 18. ¹³C NMR spectrum of racemic Pd NHC complex (±)-Pd-65a.

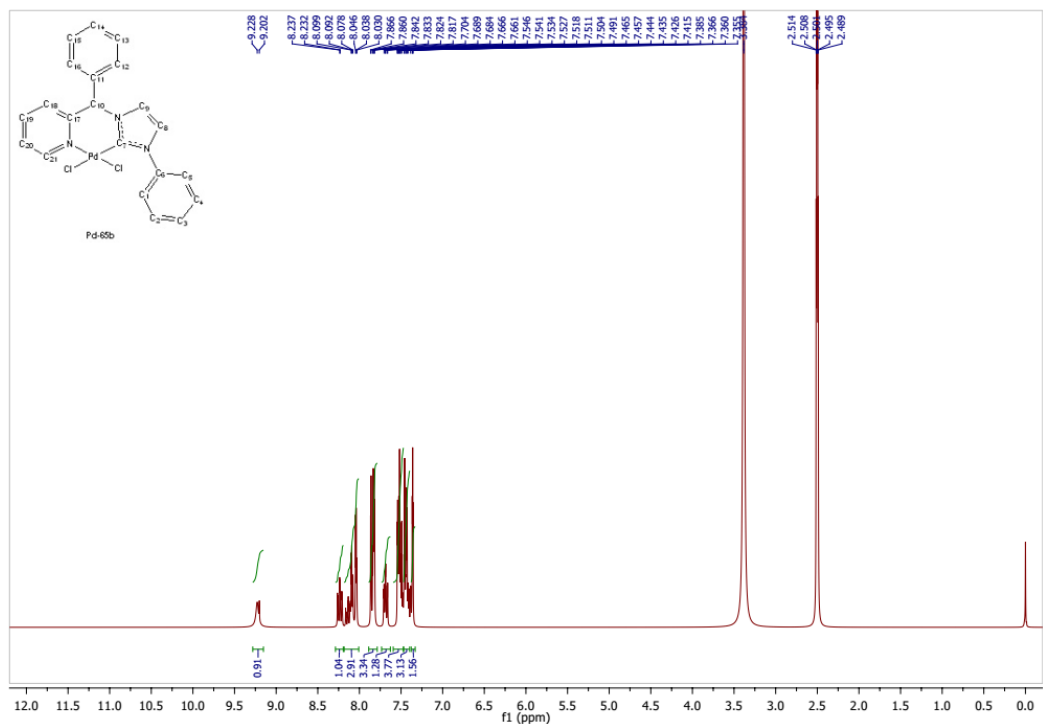


Figure 19. ¹H NMR spectrum of racemic Pd NHC complex (±)-Pd-65b.

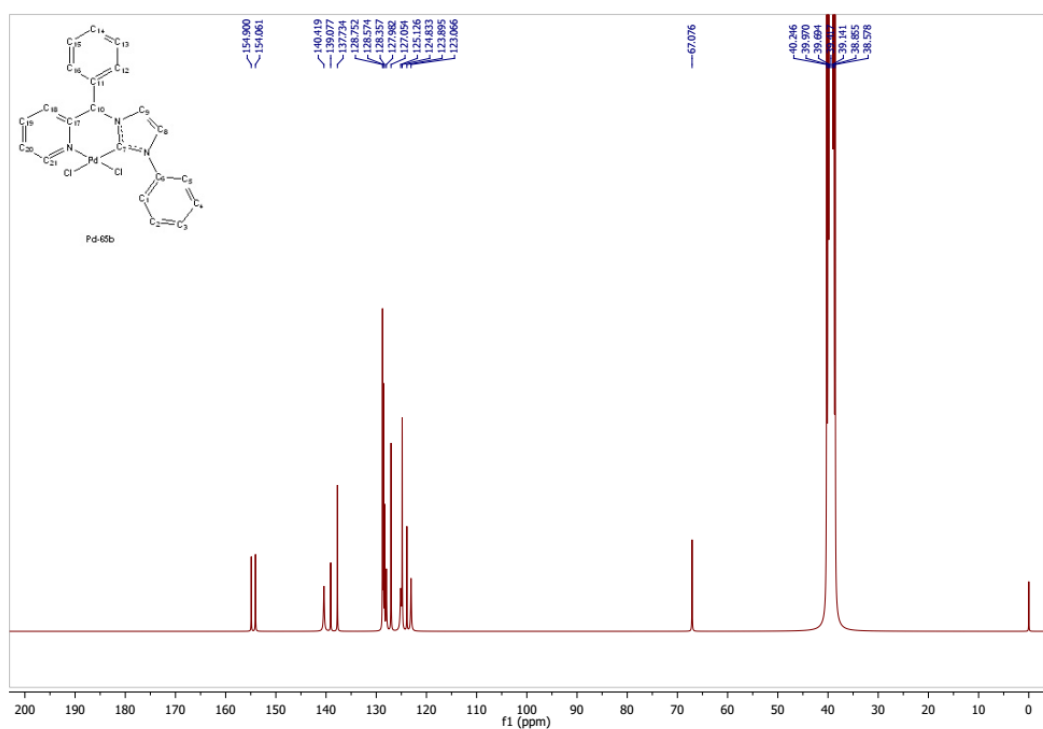


Figure 20. ¹³C NMR spectrum of racemic Pd NHC complex (±)-Pd-65b.

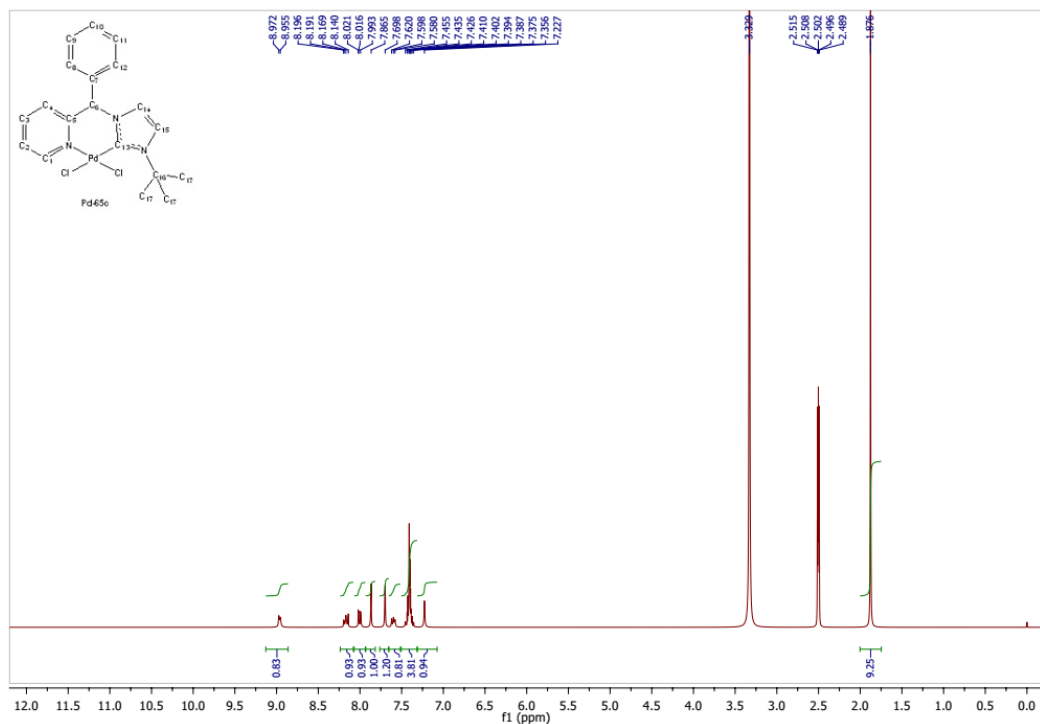


Figure 21. ¹H NMR spectrum of racemic Pd NHC complex (±)-Pd-65c.

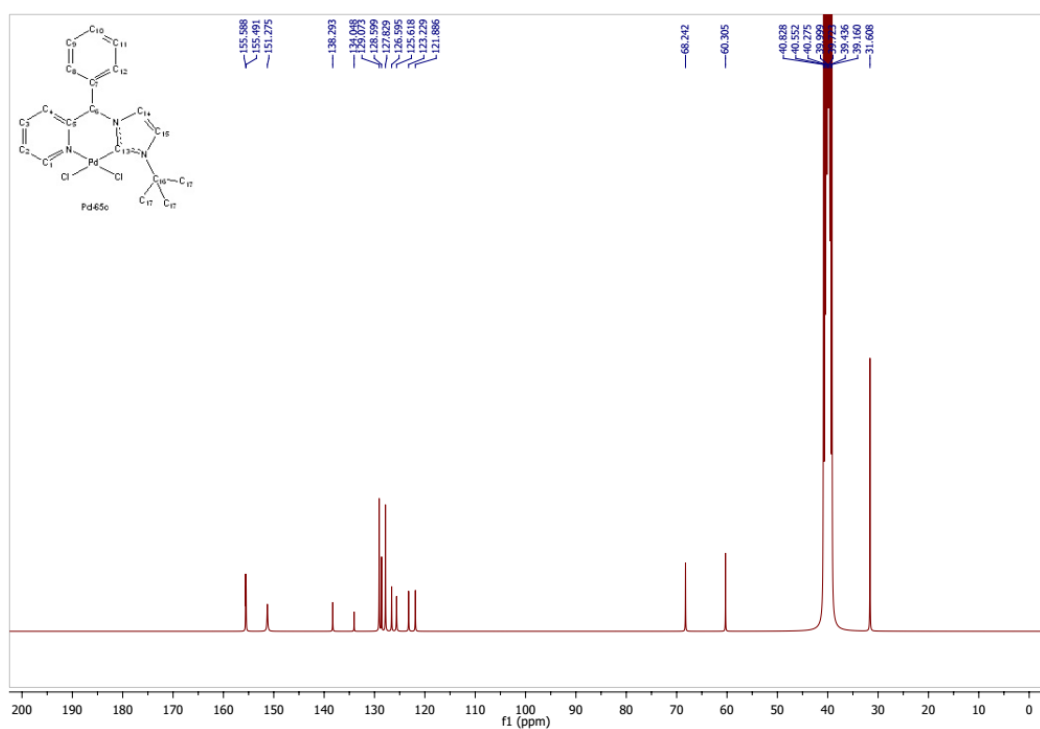


Figure 22. ¹³C NMR spectrum of racemic Pd NHC complex (±)-Pd-65c.

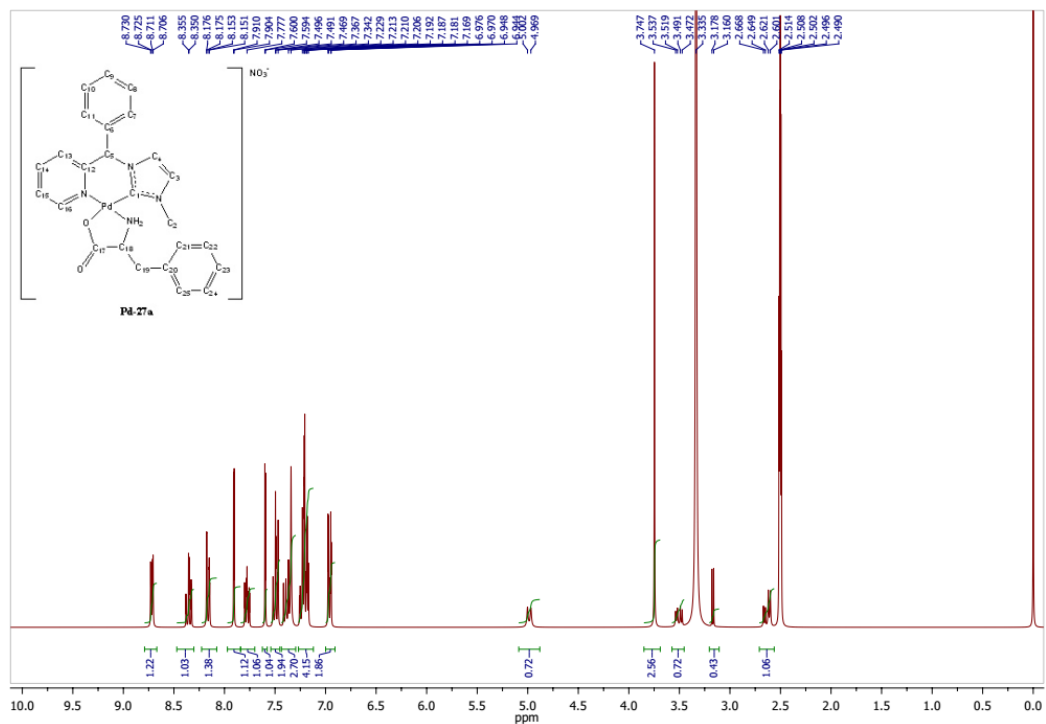


Figure 23. ¹H NMR spectrum of diastereomer Pd-(*Rc,Sc*)-68a.

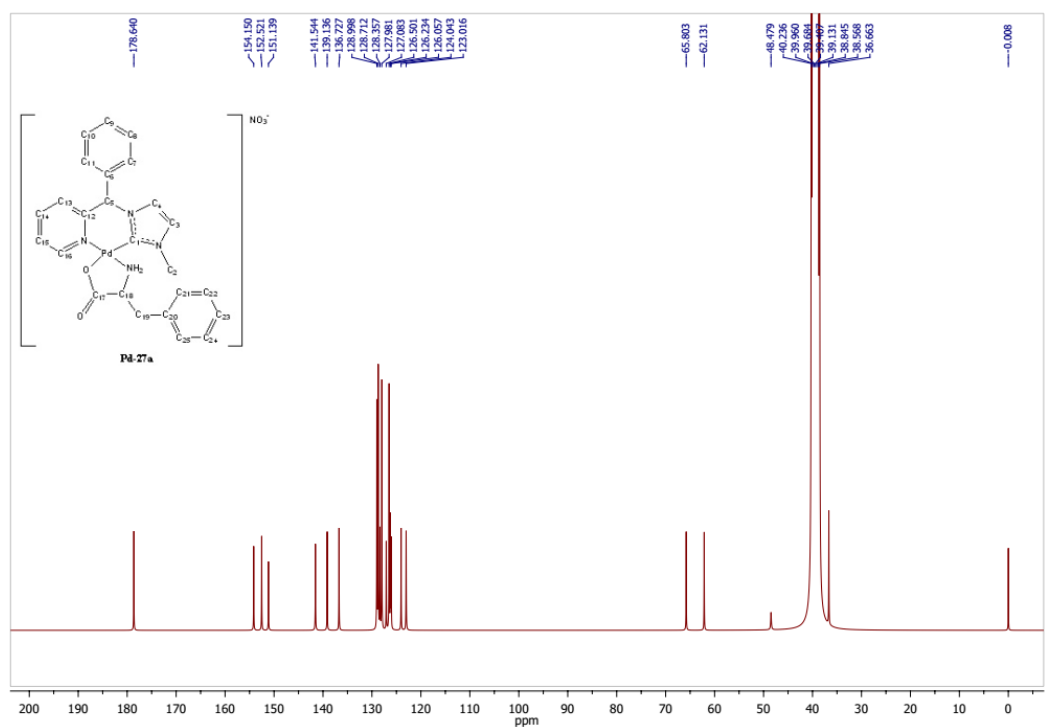


Figure 24. ¹³C NMR spectrum of diastereomer Pd-(*Rc,Sc*)-68a.

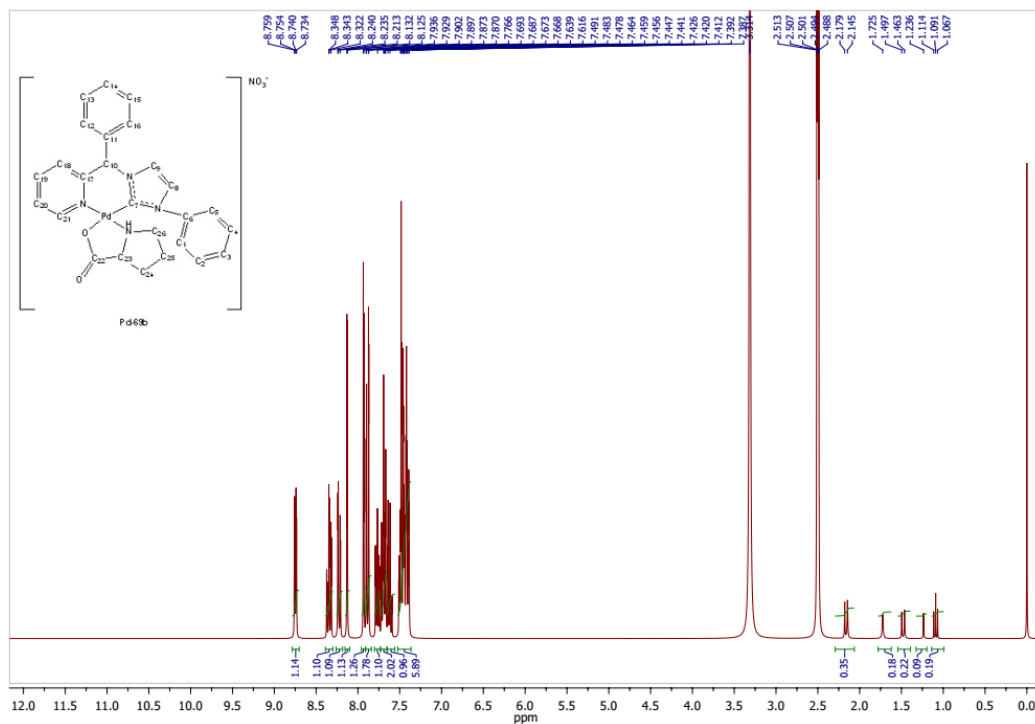


Figure 25. ^1H NMR spectrum of diastereomer Pd-(*Sc,Sc*)-69b.

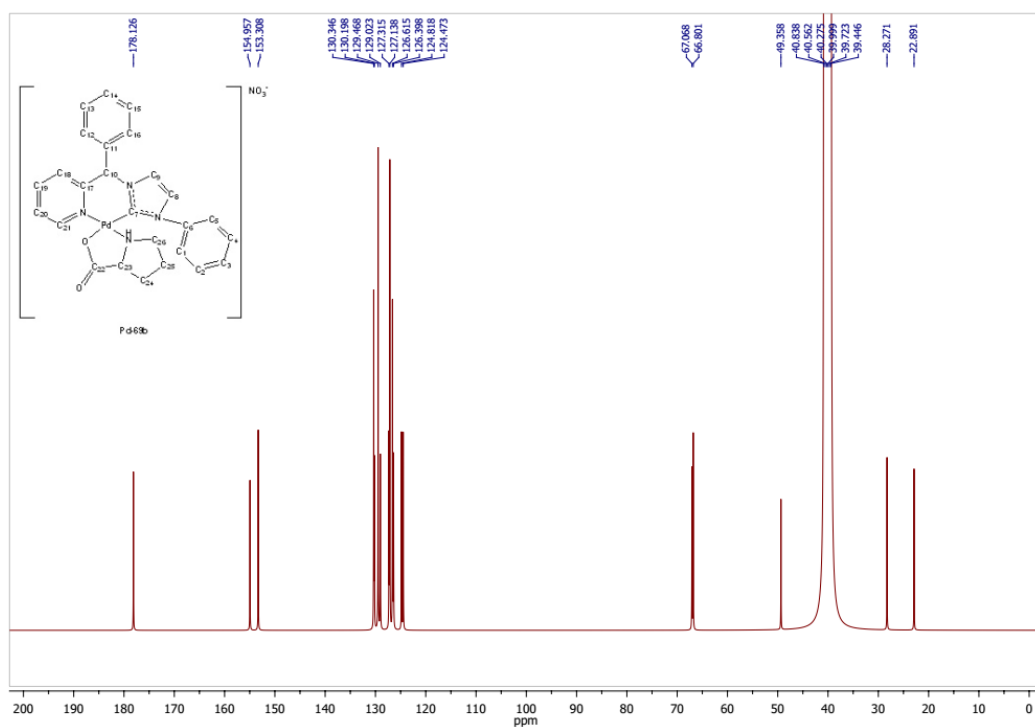


Figure 26. ^{13}C NMR spectrum of diastereomer Pd-(*Sc,Sc*)-69b.

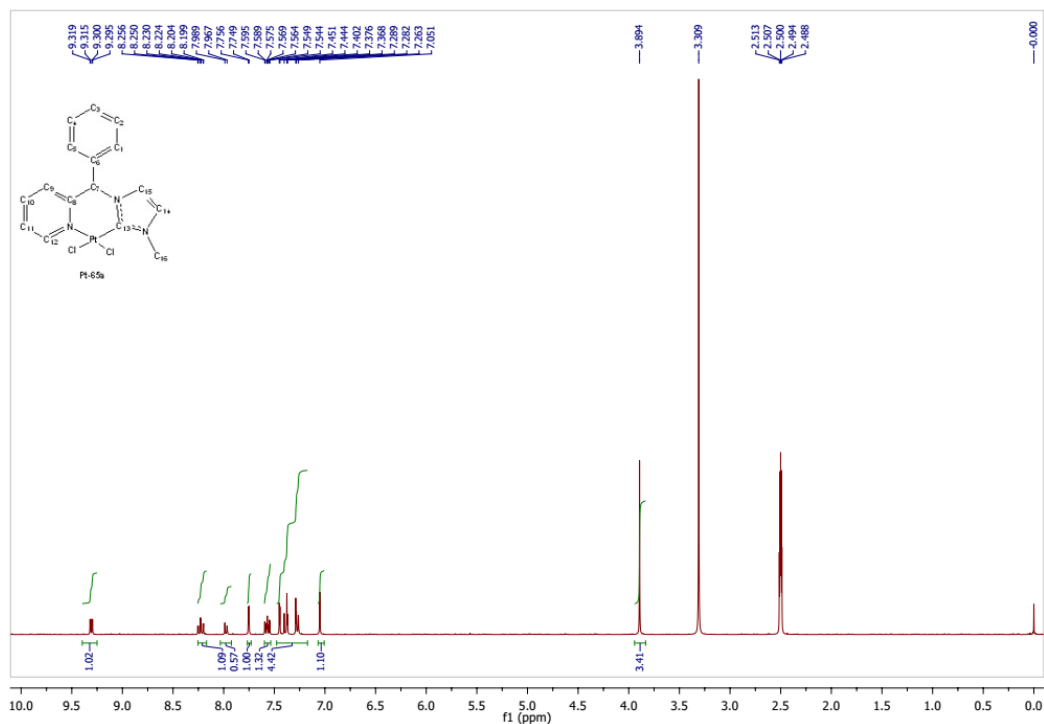


Figure 27. ¹H NMR spectrum of racemic Pt NHC complex (±)-Pt-65a.

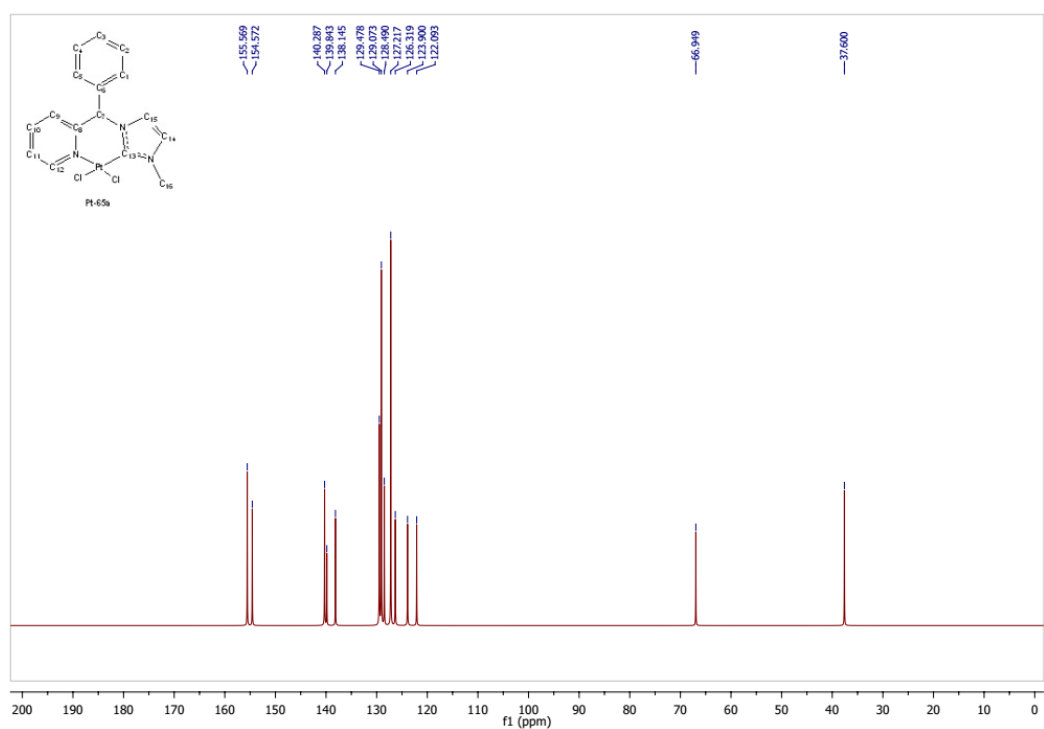


Figure 28. ¹³C NMR spectrum of racemic Pt NHC complex (±)-Pt-65a.

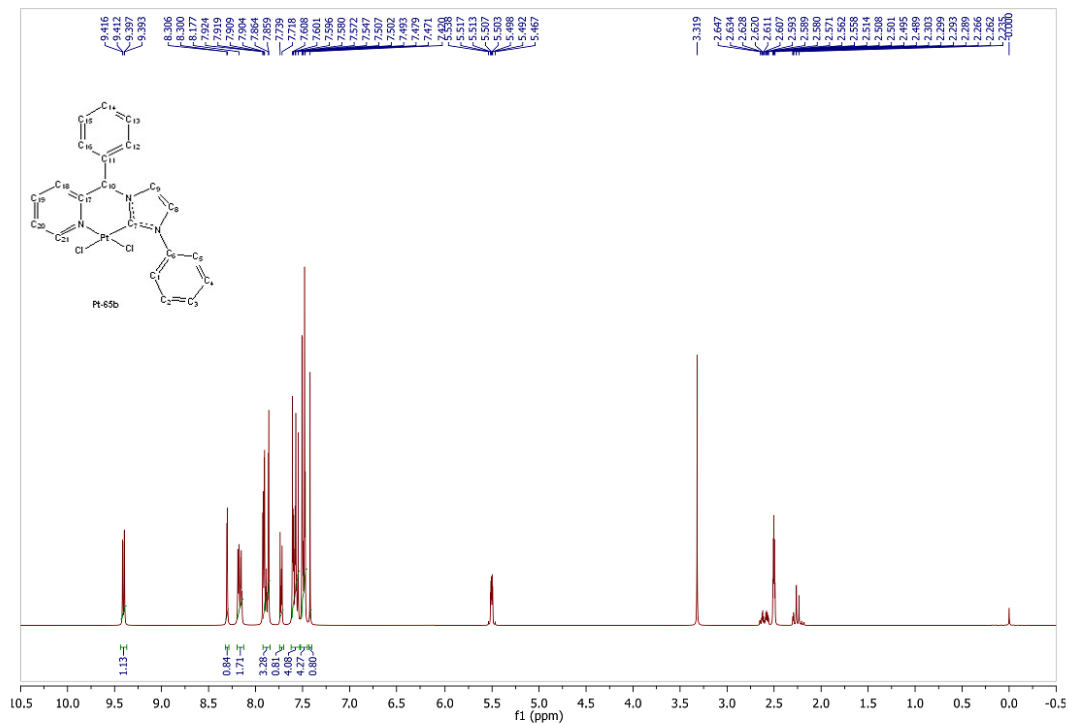


Figure 29. ¹H NMR spectrum of racemic Pt NHC complex (±)-Pt-65b.

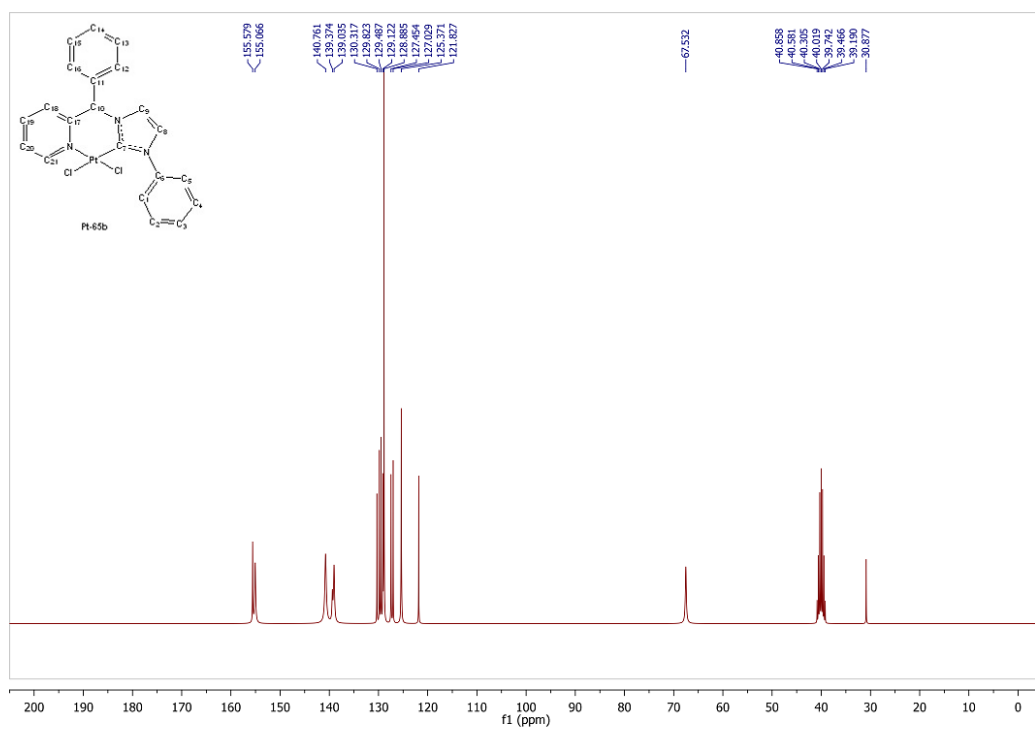


Figure 30. ¹³C NMR spectrum of racemic Pt NHC complex (±)-Pt-65b.

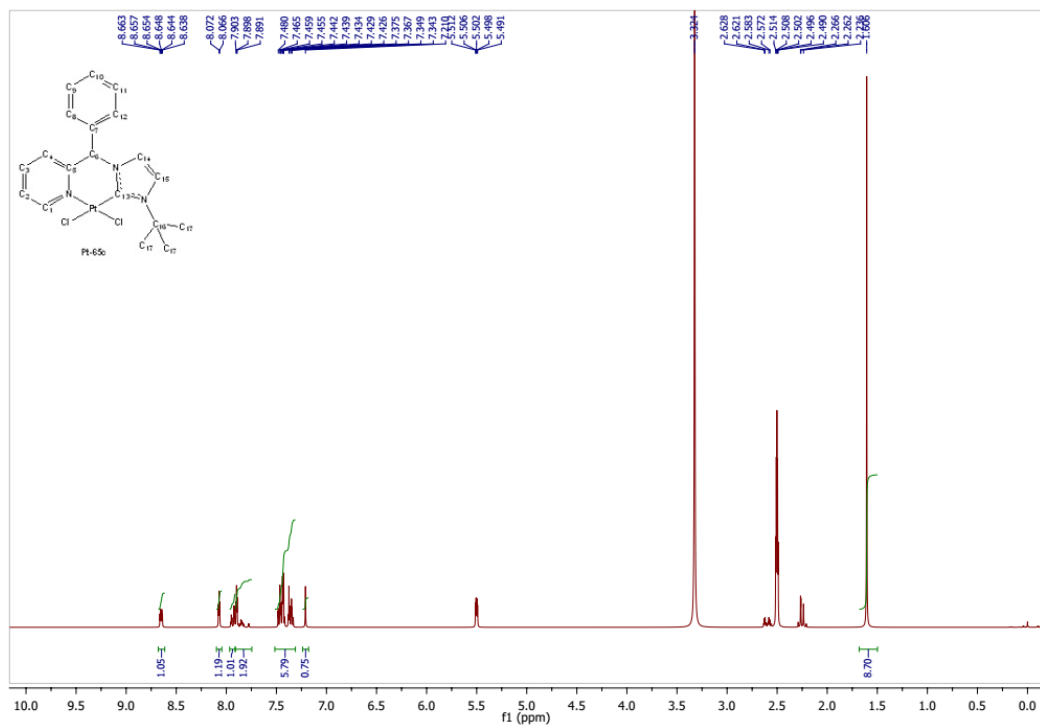


Figure 31. ¹H NMR spectrum of racemic Pt NHC complex (±)-Pt-65c.

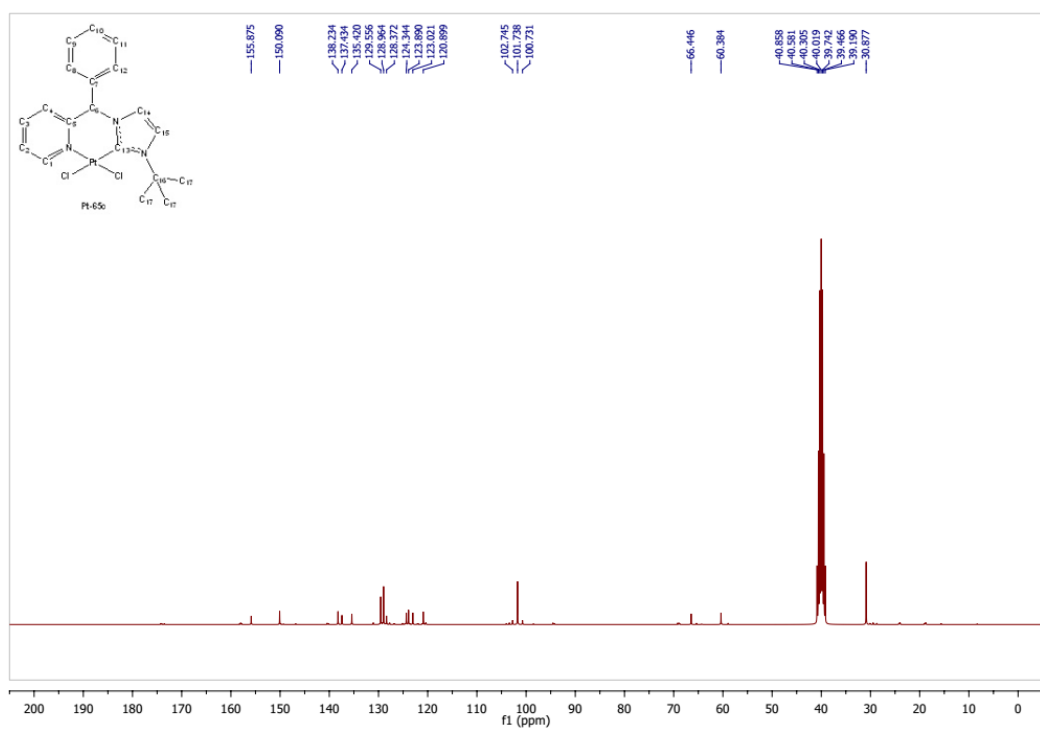


Figure 32. ¹³C NMR spectrum of racemic Pt NHC complex (±)-Pt-65c.

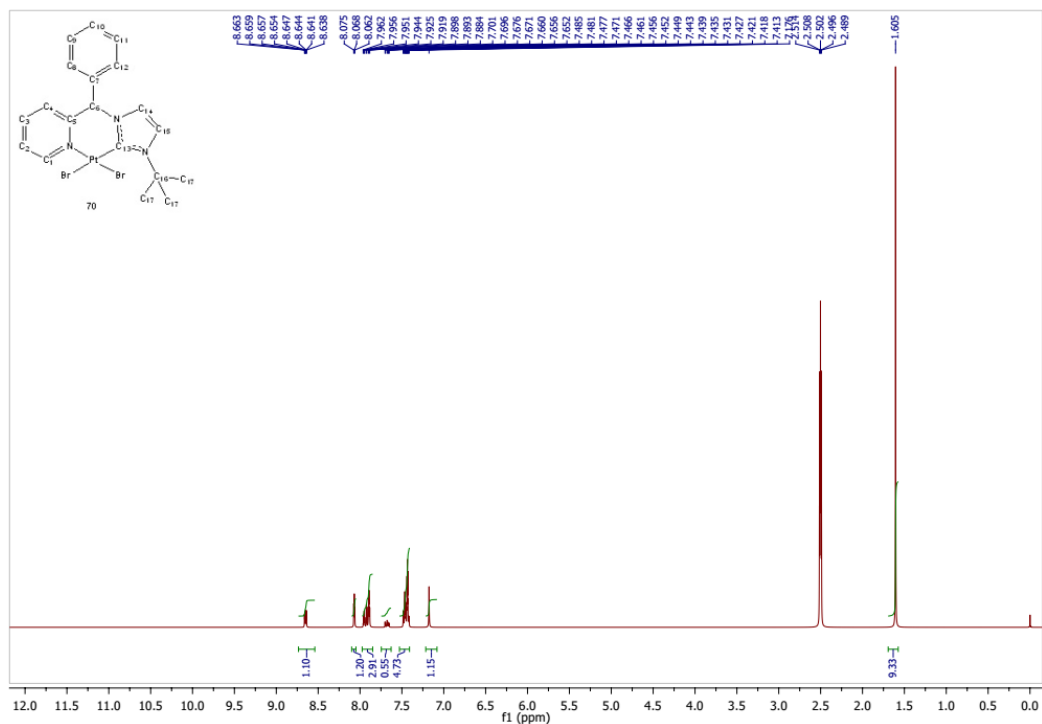


Figure 33. ¹H NMR spectrum of racemic dibromide Pt NHC complex (±)-70.

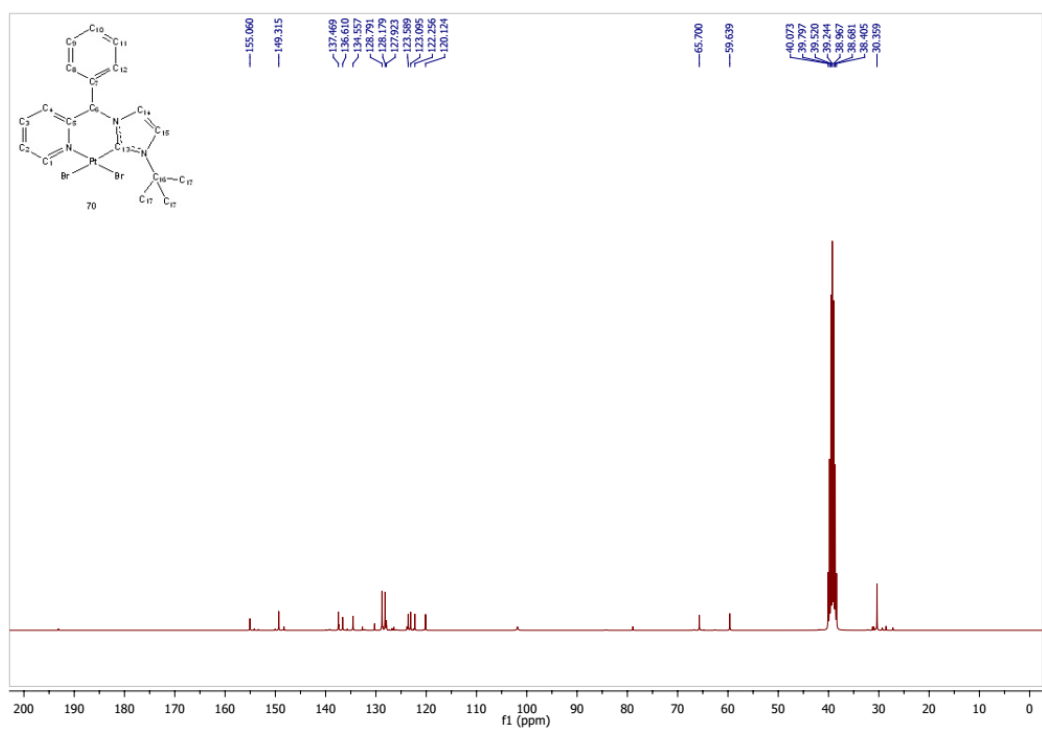


Figure 34. ¹³C NMR spectrum of racemic dibromide Pt NHC complex (±)-70.

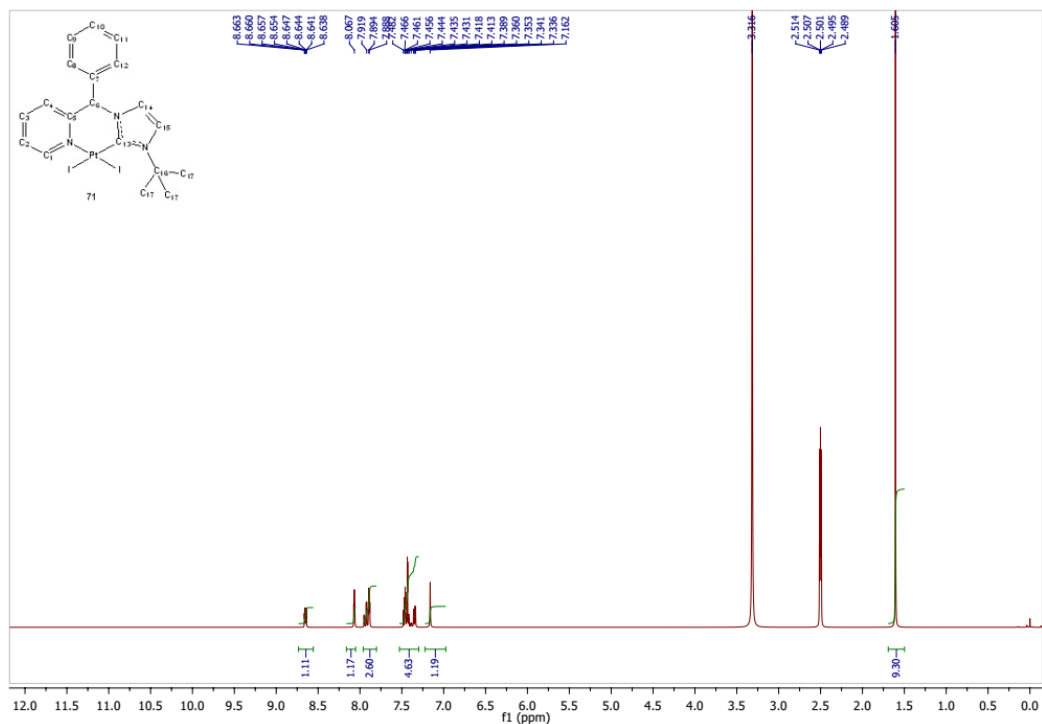


Figure 35. ¹H NMR spectrum of racemic diiodo Pt NHC complex (±)-71.

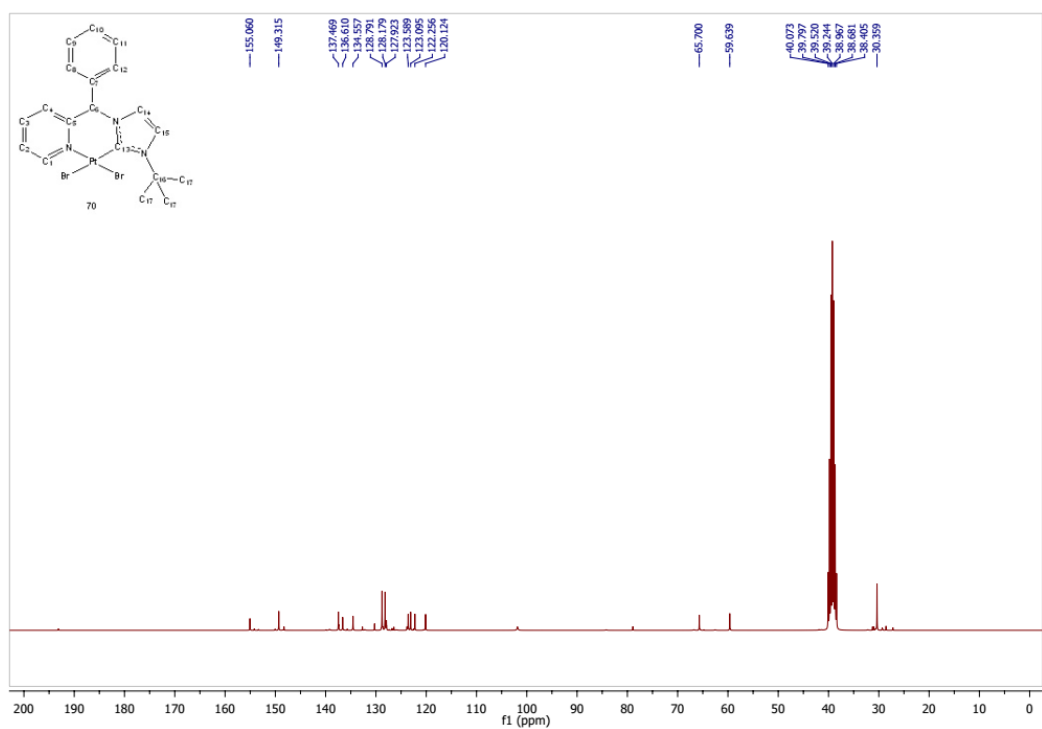


Figure 36. ¹³C NMR spectrum of racemic diiodo Pt NHC complex (±)-71.

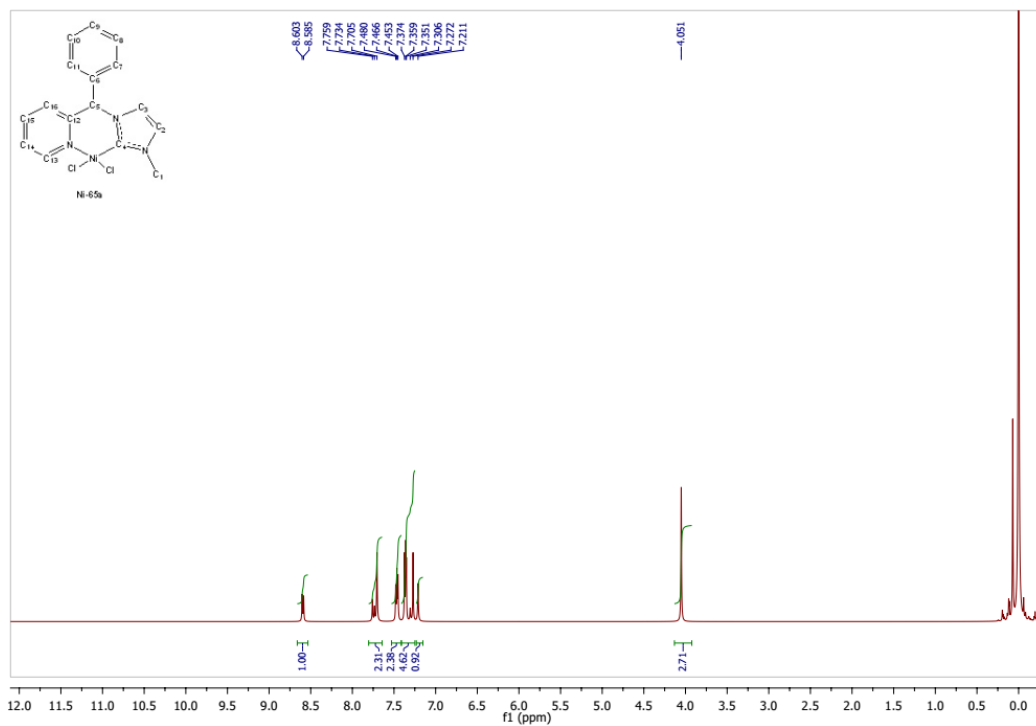


Figure 37. ¹H NMR spectrum of racemic Ni NHC complex (±)-Ni-65a.

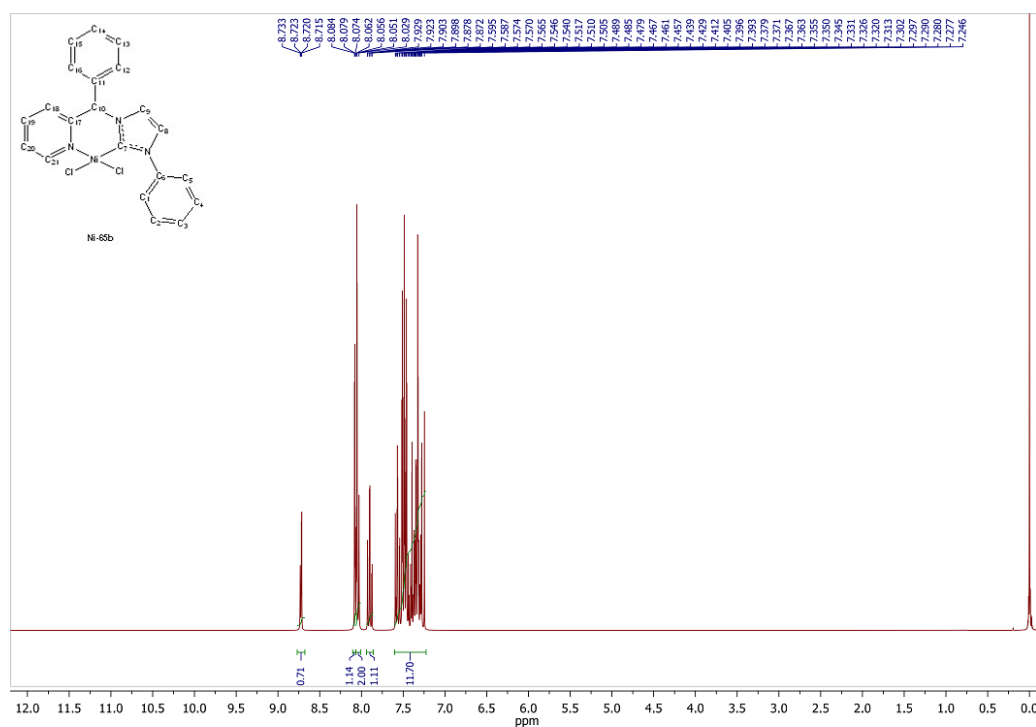


Figure 38. ¹H NMR spectrum of racemic Ni NHC complex (±)-Ni-65b.

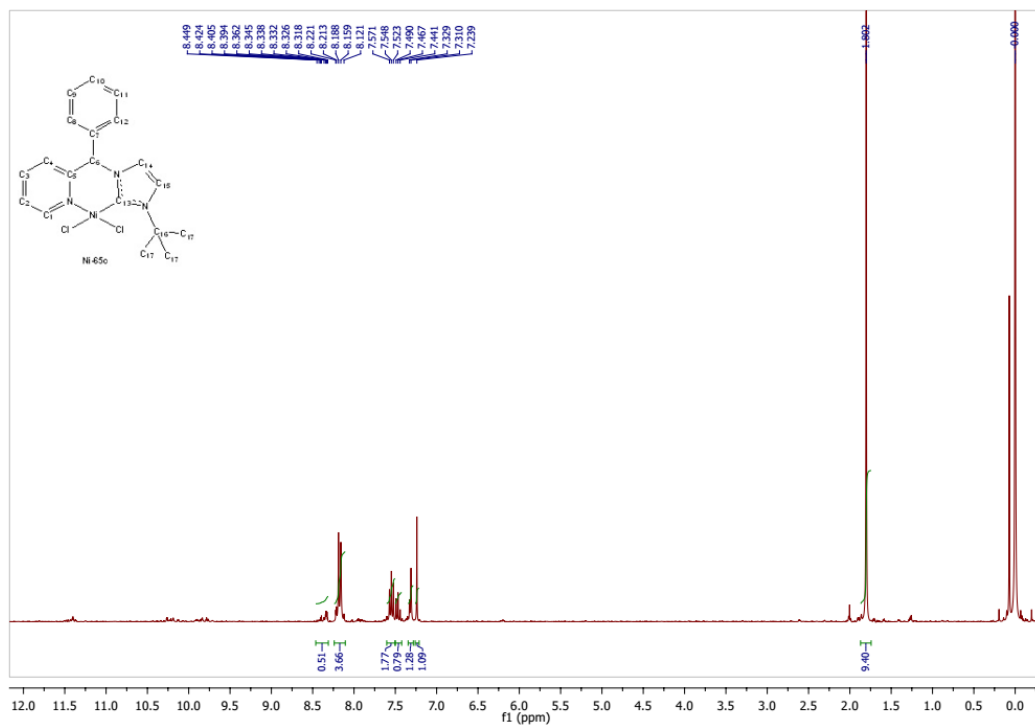


Figure 39. ¹H NMR spectrum of racemic Ni NHC complex (±)-Ni-65c.

APPENDIX 3: LCMS Spectral Data

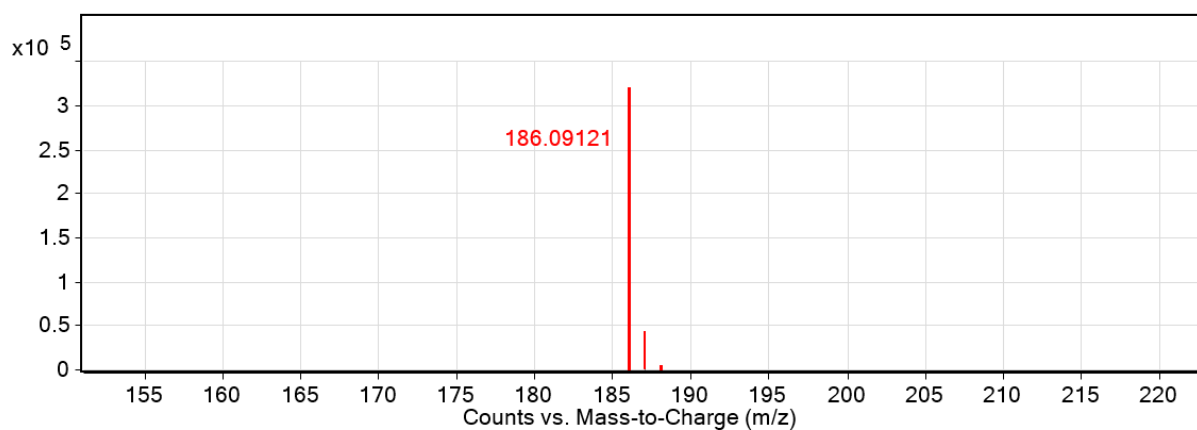


Figure 40. LCMS spectrum of phenyl(pyridine-2-yl)methanol, 62.

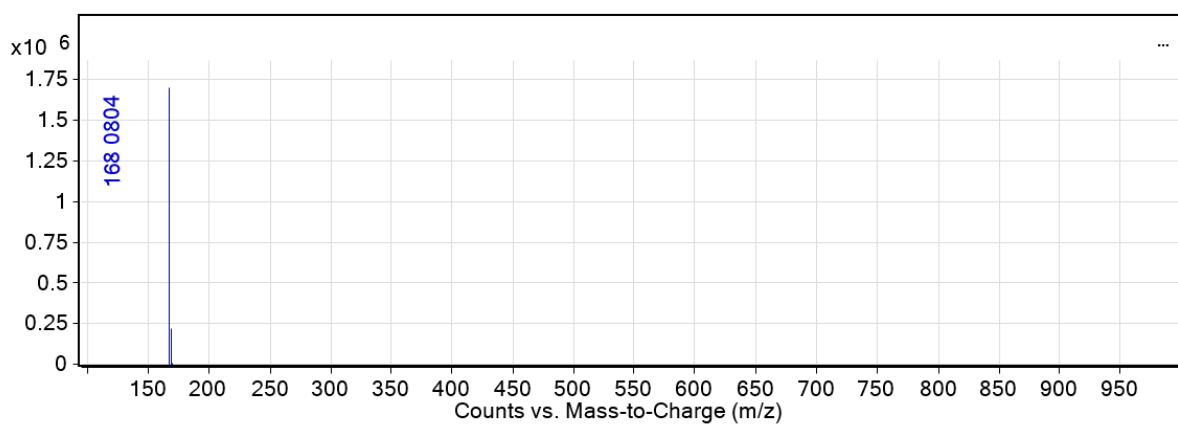


Figure 41. LCMS spectrum of 2-(chloro(phenyl)methyl)pyridine, 63

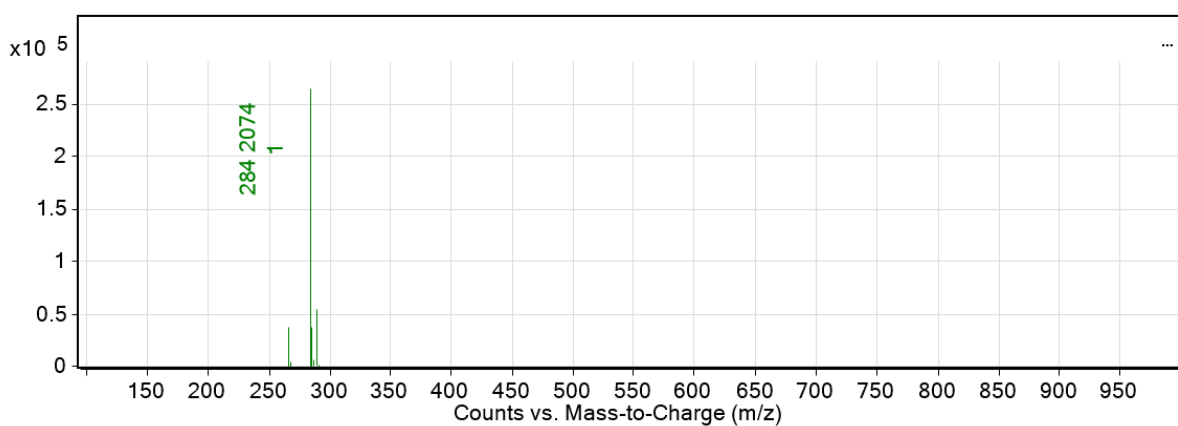


Figure 42. LCMS spectrum of imidazolium-based salt, 64a.

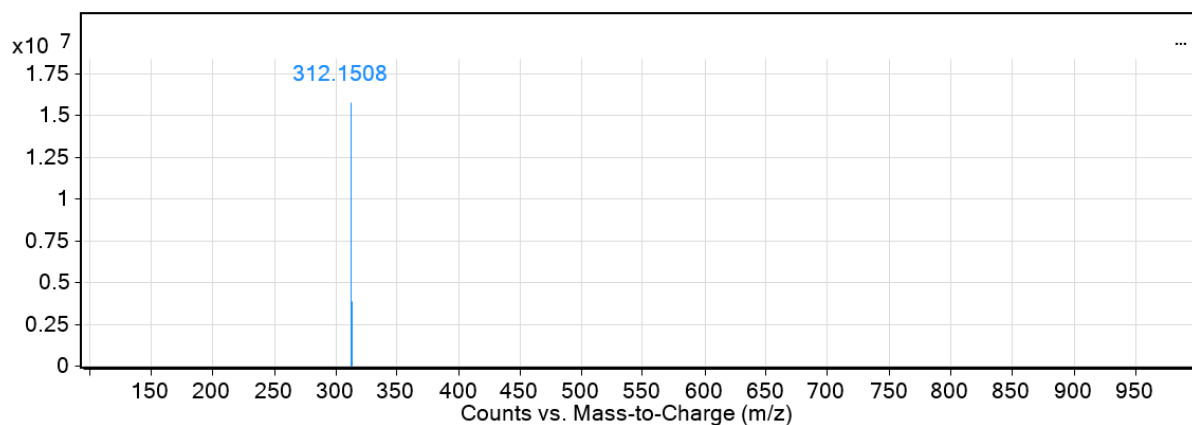


Figure 43. LCMS spectrum of imidazolium-based salt, 64b.

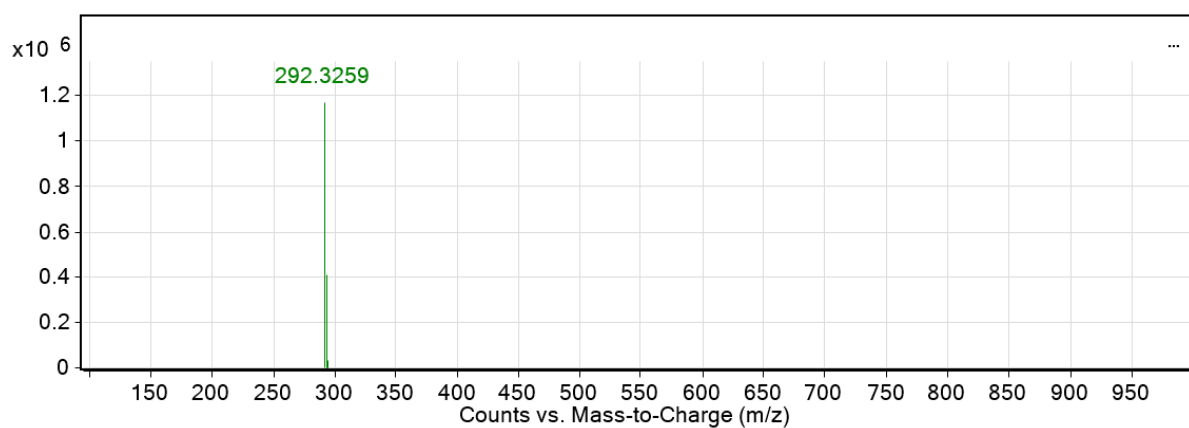


Figure 44. LCMS spectrum of imidazolium-based salt, 64c.

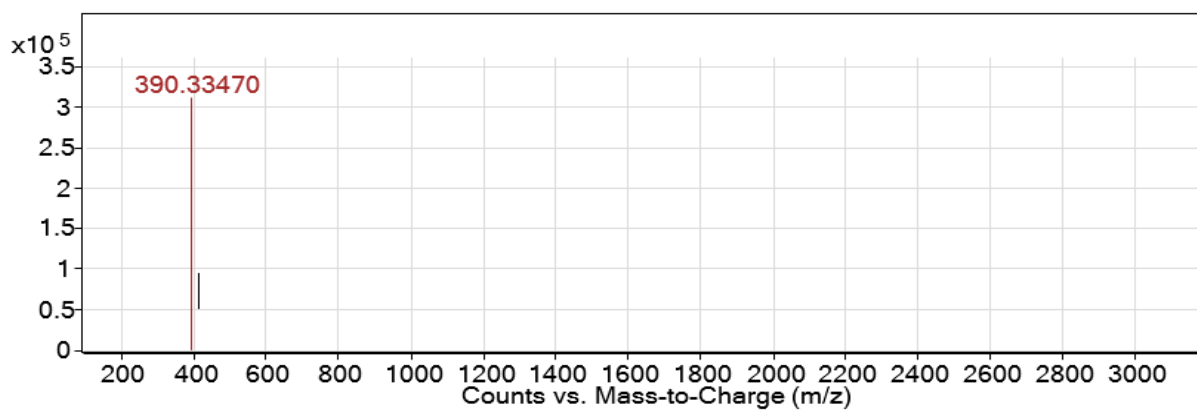


Figure 45. LCMS spectrum of racemic Pd NHC complex (\pm)-Pd-65a.

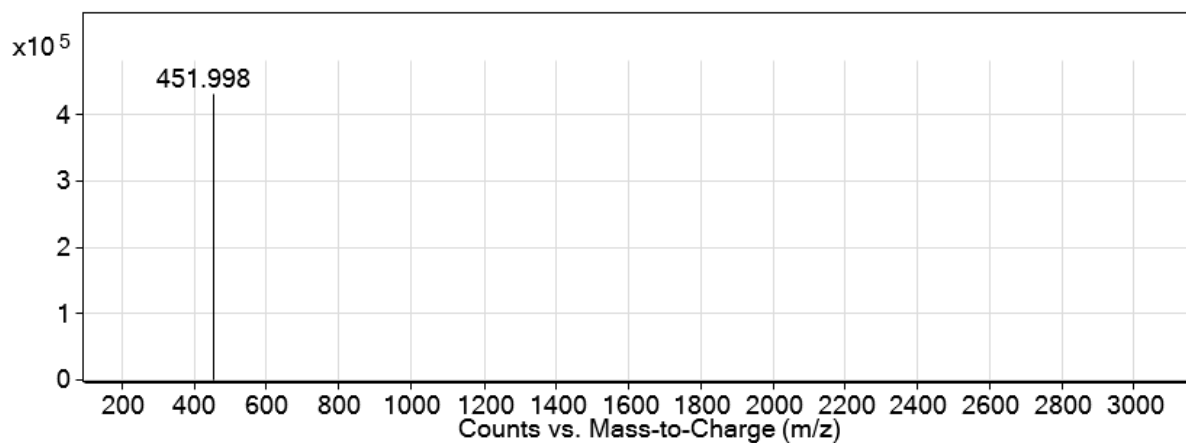


Figure 46. LCMS spectrum of racemic Pd NHC complex (±)-Pd-65b.

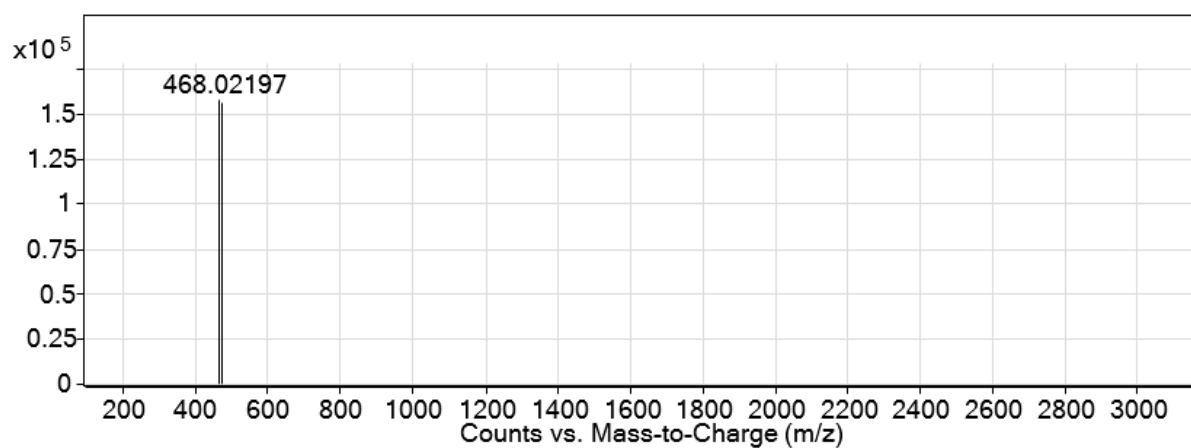


Figure 47. LCMS spectrum of racemic Pd NHC complex (±)-Pd-65c.

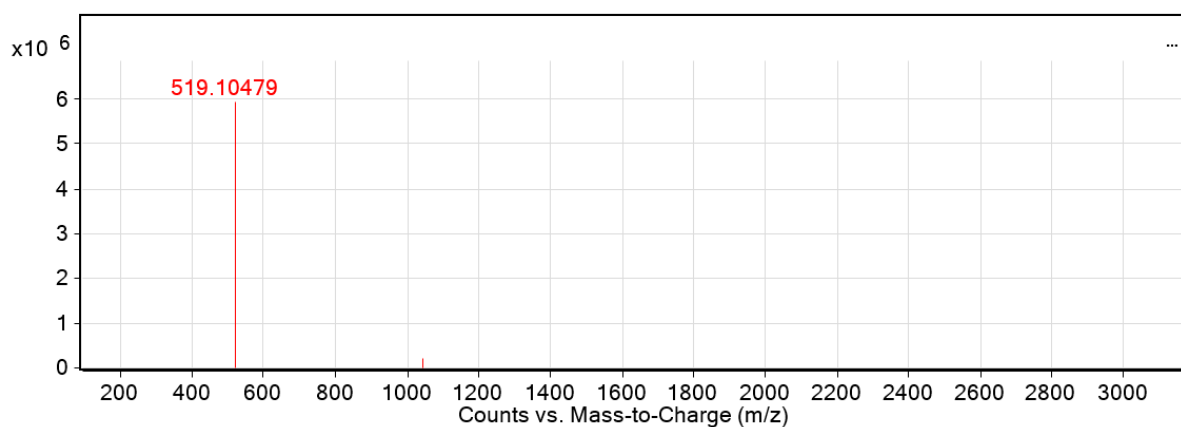


Figure 48. LCMS spectrum of diastereomer Pd-(*R_c*,*S_c*)-68a.

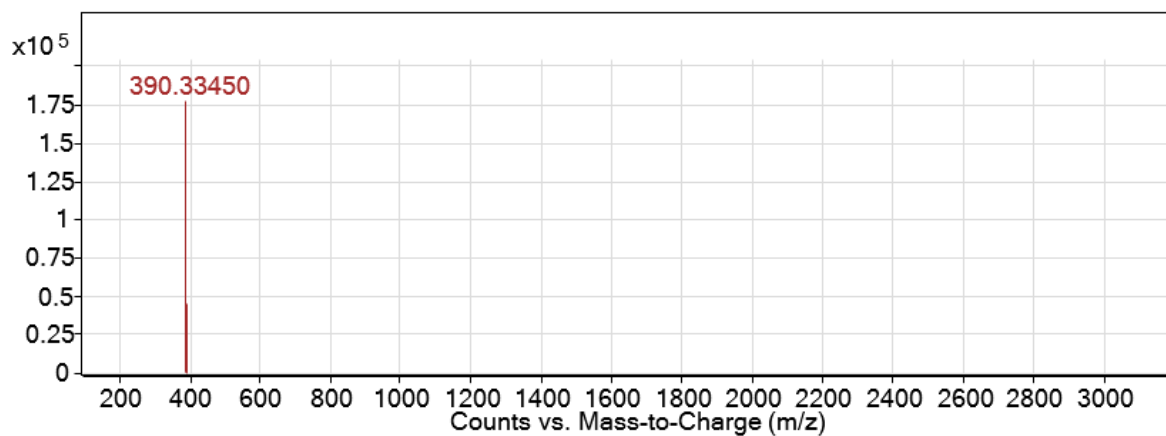


Figure 49. LCMS spectrum of enantiomer Pd NHC complex (R)-Pd-65a.

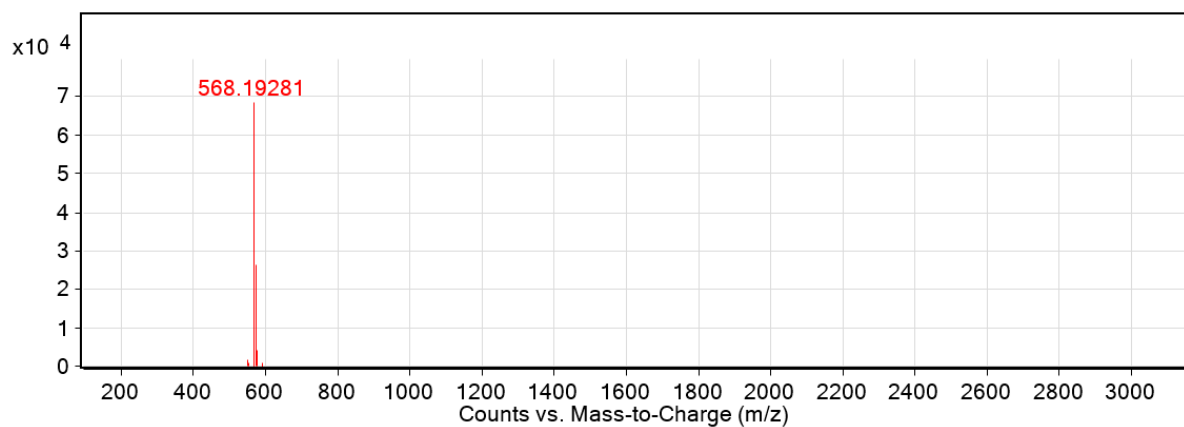


Figure 50. LCMS spectrum of diastereomer Pd-(Sc,Sc)-69b.

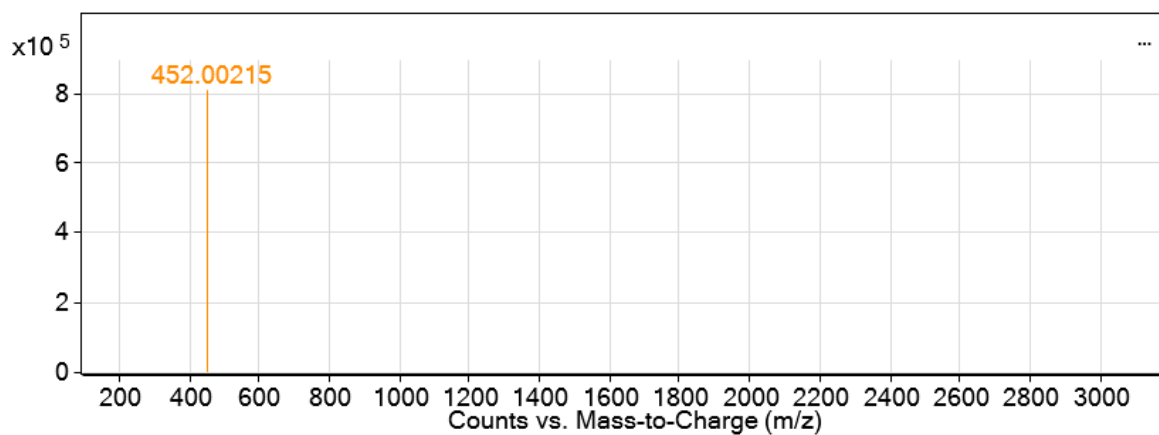


Figure 51. LCMS spectrum of enantiomer Pd NHC complex (S)-Pd-65b.

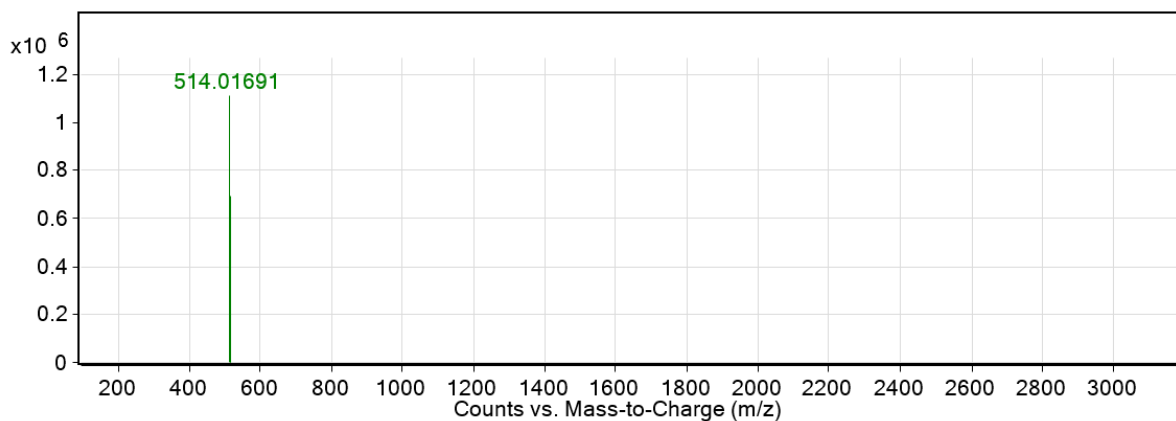


Figure 52. LCMS spectrum of racemic Pt NHC complex (±)-Pt-65a.

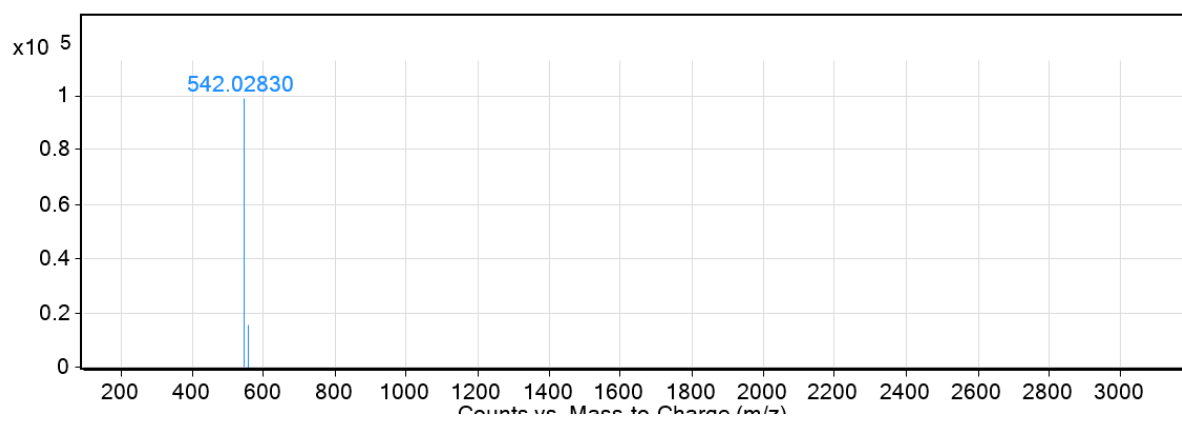


Figure 53. LCMS spectrum of racemic Pt NHC complex (±)-Pt-65b.

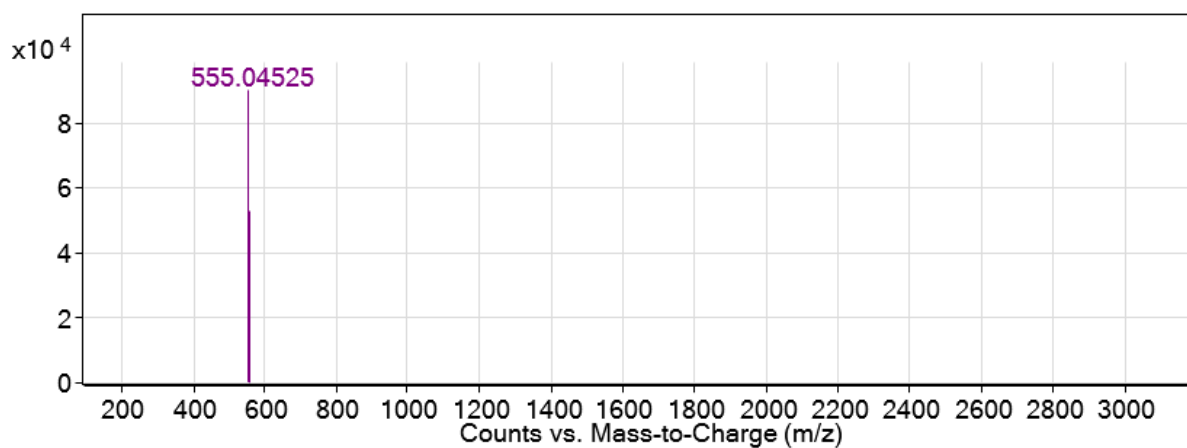


Figure 54. LCMS spectrum of racemic Pt NHC complex (±)-Pt-65c.

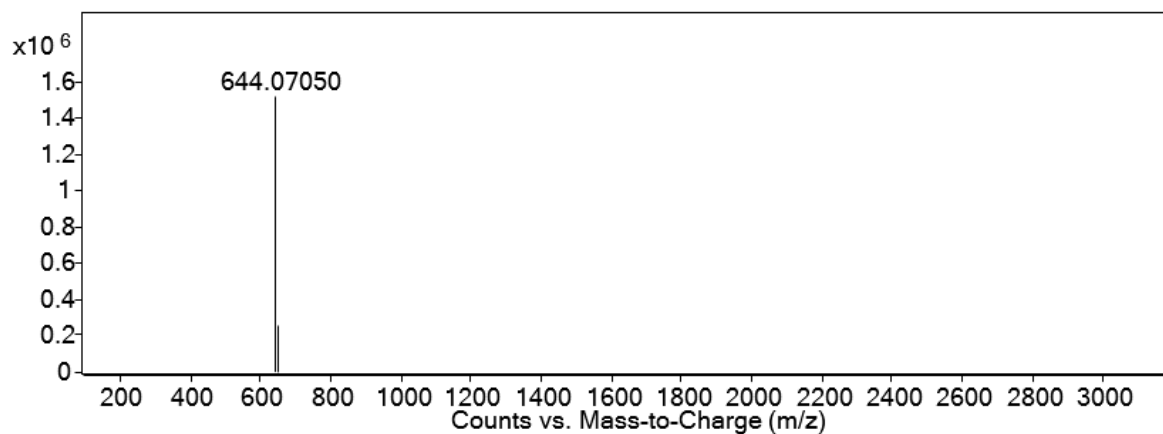


Figure 55. LCMS spectrum of racemic dibromide Pt NHC complex (±)-70.

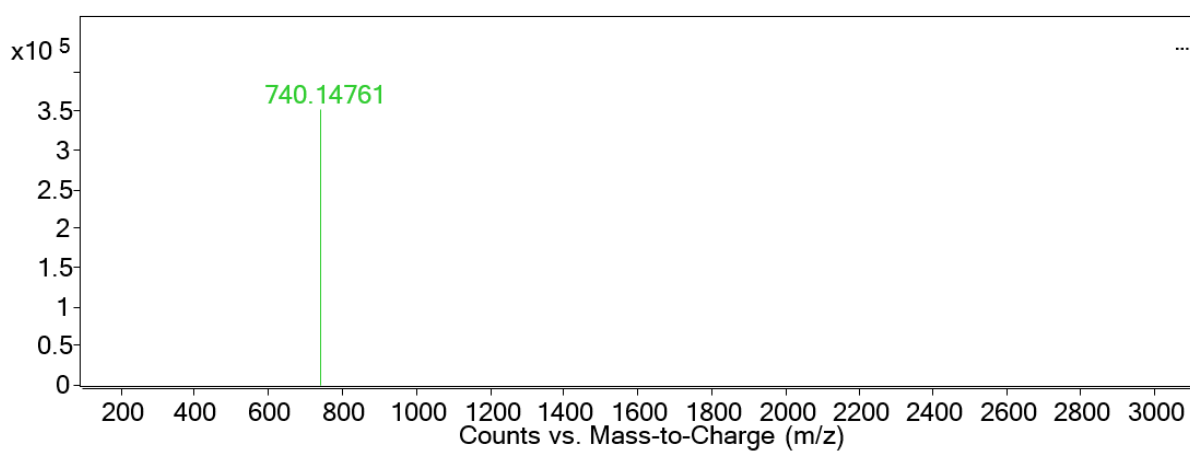


Figure 56. LCMS spectrum of racemic diiodo Pt NHC complex (±)-71.

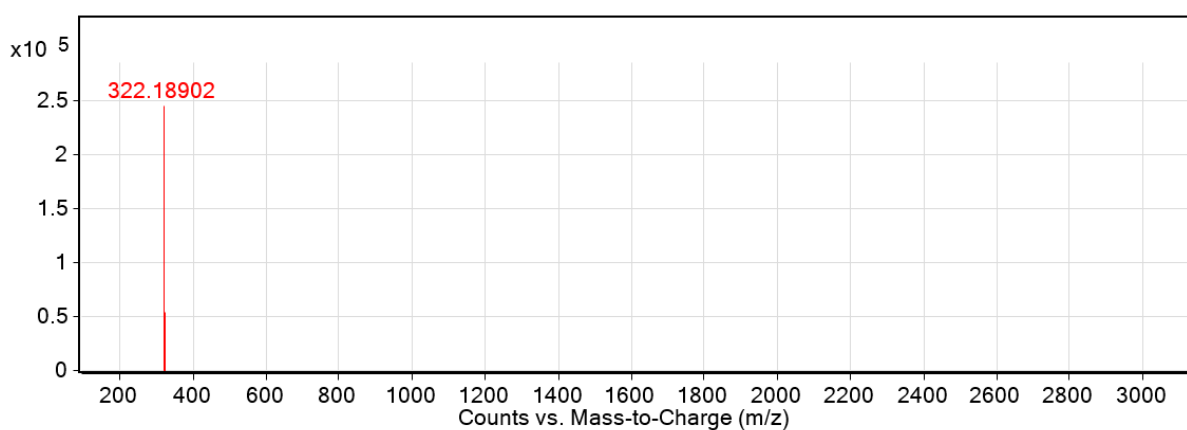


Figure 57. LCMS spectrum of unexpected Ni complex 72.

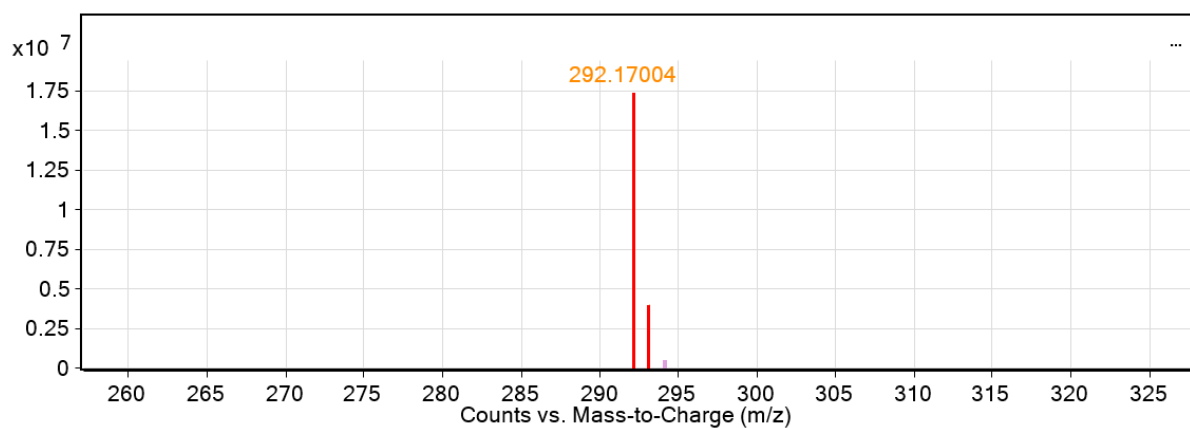


Figure 58. LCMS spectrum of unexpected nickelate complex 73.

APPENDIX 4: Plots of MTT cell viability assay

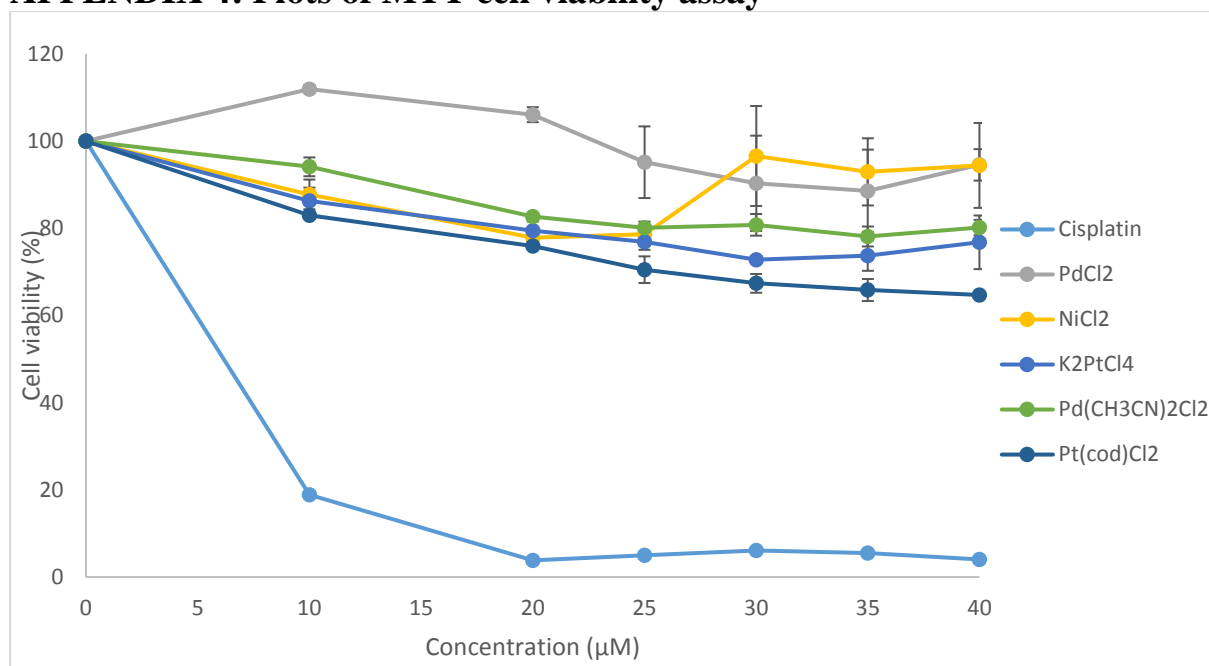


Figure 59. Cytotoxicity of cisplatin, metal salts, and transmetalating agents against H103 after 48 hours of treatment. Cell viability was assessed using MTT cell viability assay at 570 nm (reference wavelength at 620 nm). The cell viability is reported in mean with error bars of ± 1 SEM.

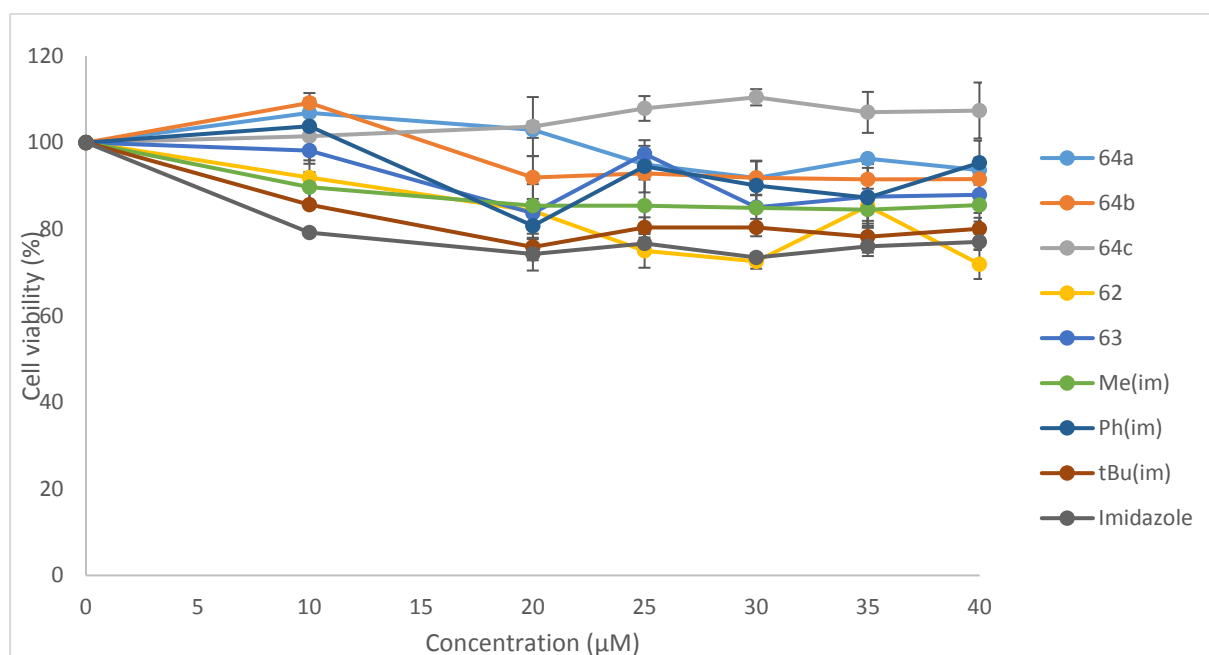


Figure 60. Cytotoxicity of precursors (62 and 63), imidazolium salts 64 and different imidazoles against H103 after 48 hours of treatment. Cell viability was assessed using MTT cell viability assay at 570 nm (reference wavelength at 620 nm). The cell viability is reported in mean with error bars of ± 1 SEM.

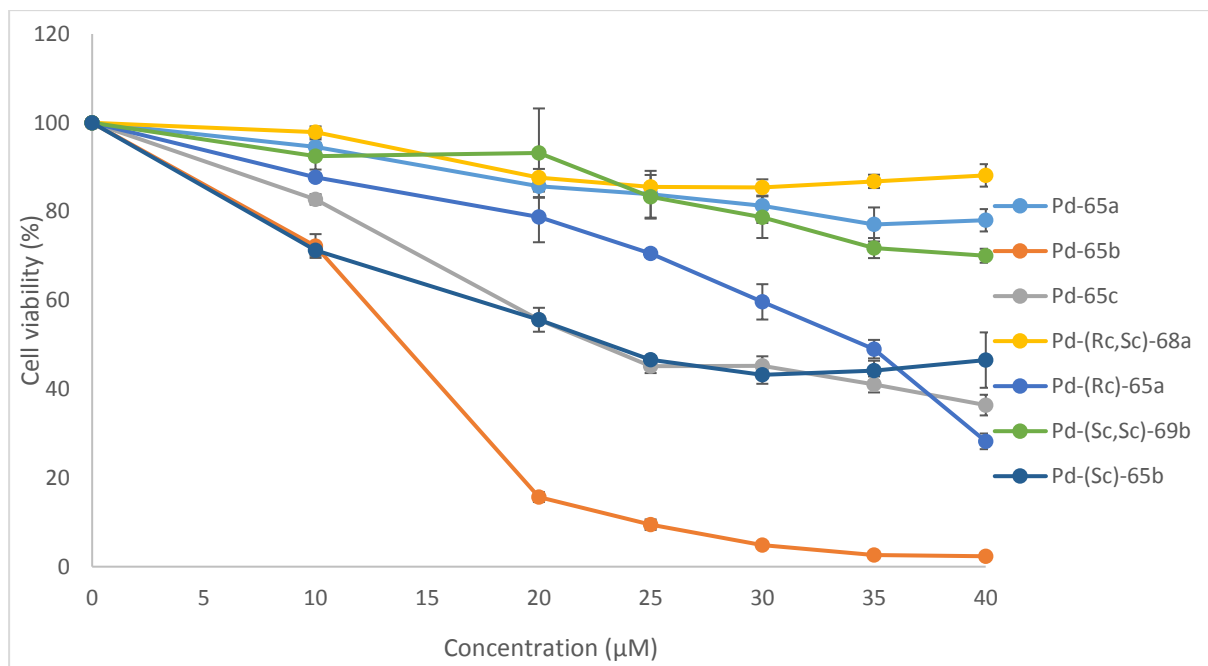


Figure 61. Cytotoxicity of Pd NHC complexes and diastereomers against H103 after 48 hours of treatment. Cell viability was assessed using MTT cell viability assay at 570 nm (reference wavelength at 620 nm). The cell viability is reported in mean with error bars of ± 1 SEM.

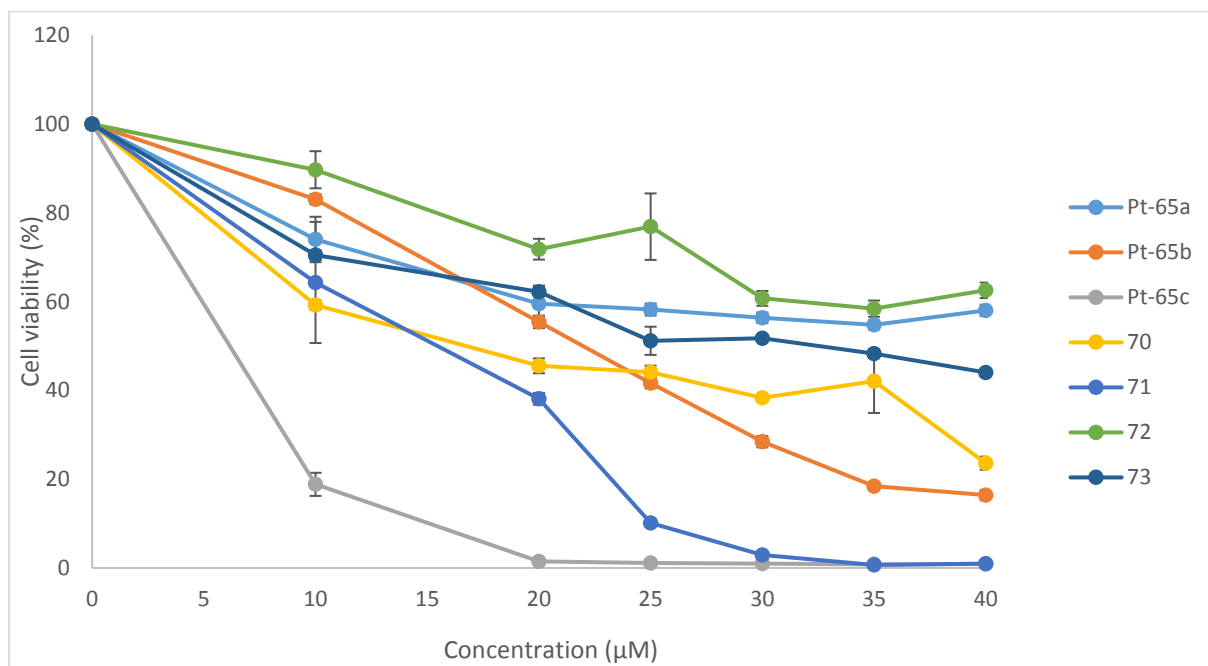


Figure 62. Cytotoxicity of Pt NHC complexes and Ni complexes against H103 after 48 hours of treatment. Cell viability was assessed using MTT cell viability assay at 570 nm (reference wavelength at 620 nm). The cell viability is reported in mean with error bars of ± 1 SEM.

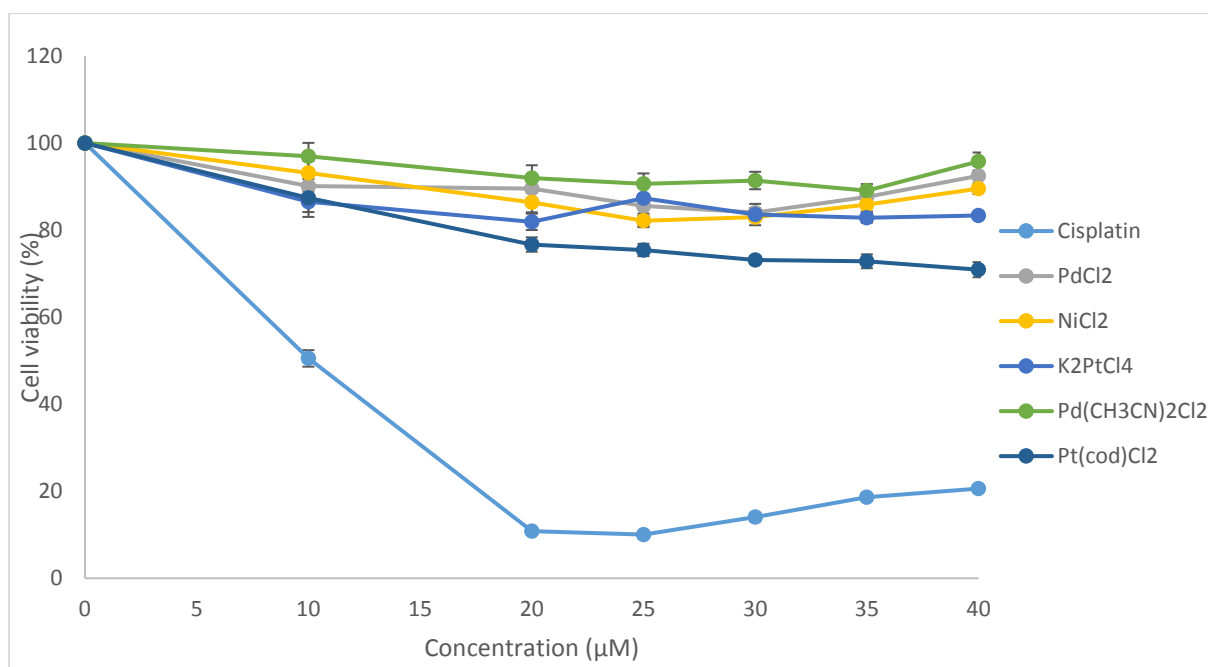


Figure 63. Cytotoxicity of cisplatin, metal salts, and transmetalating agents against HCT116 after 48 hours of treatment. Cell viability was assessed using MTT cell viability assay at 570 nm (reference wavelength at 620 nm). The cell viability is reported in mean with error bars of ± 1 SEM.

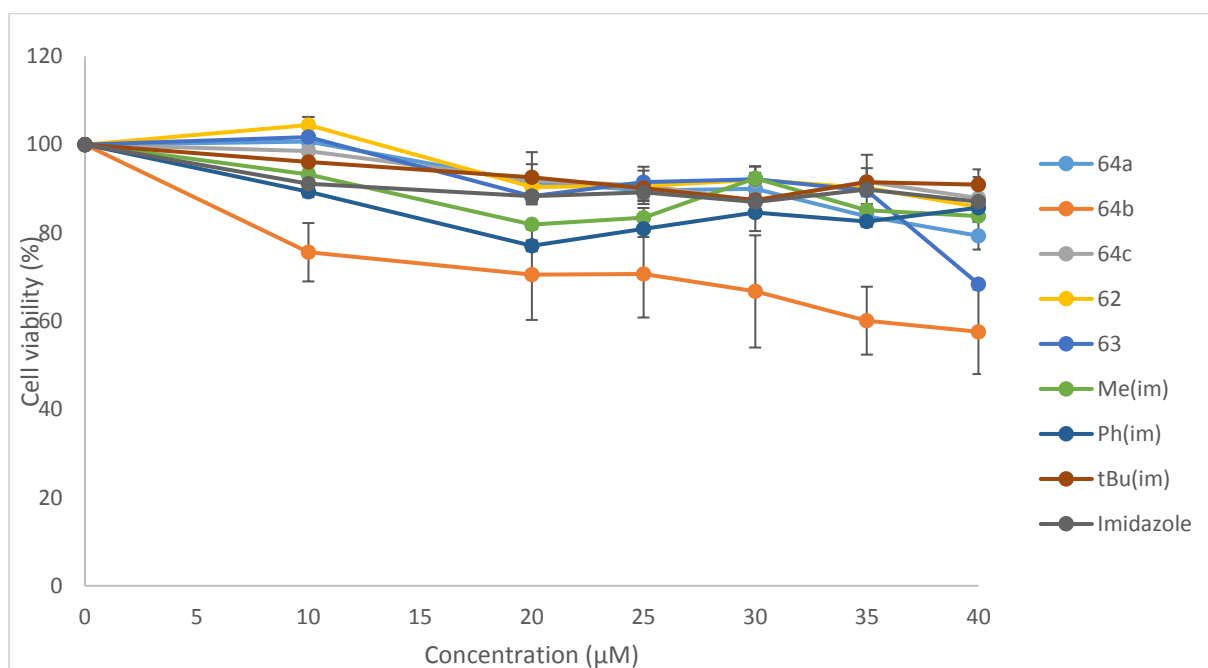


Figure 64. Cytotoxicity of precursors (62 and 63), imidazolium salts 64 and different imidazoles against HCT116 after 48 hours of treatment. Cell viability was assessed using MTT cell viability assay at 570 nm (reference wavelength at 620 nm). The cell viability is reported in mean with error bars of ± 1 SEM.

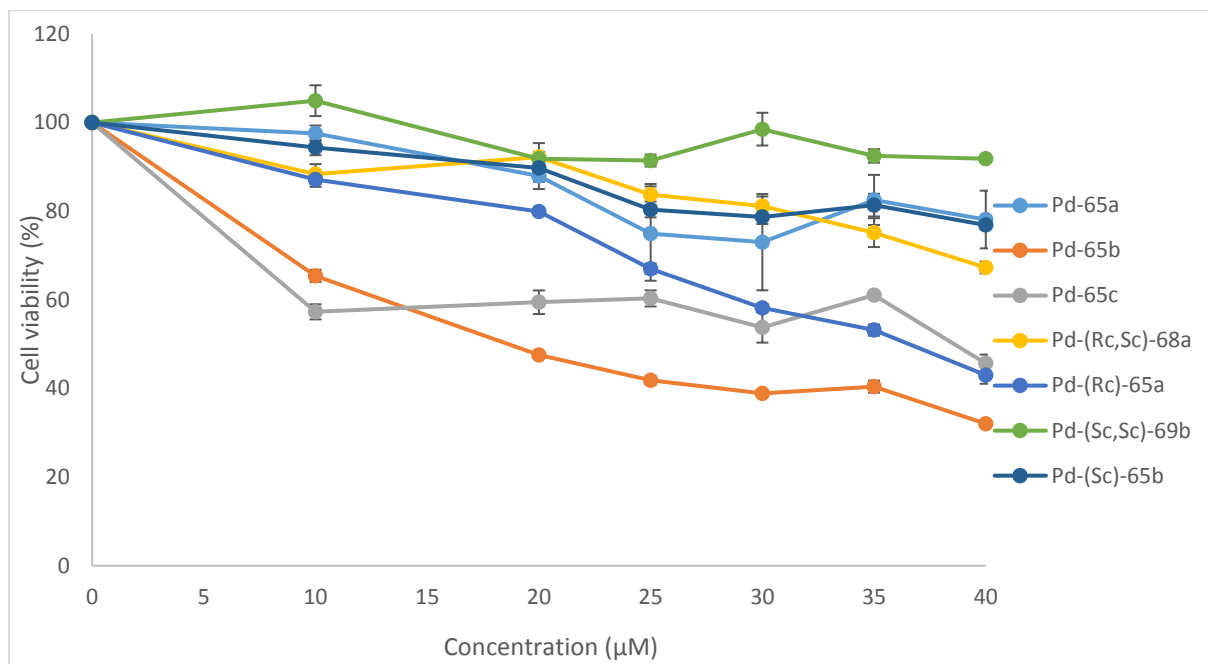


Figure 65. Cytotoxicity of Pd NHC complexes and diastereomers against HCT116 after 48 hours of treatment. Cell viability was assessed using MTT cell viability assay at 570 nm (reference wavelength at 620 nm). The cell viability is reported in mean with error bars of ± 1 SEM.

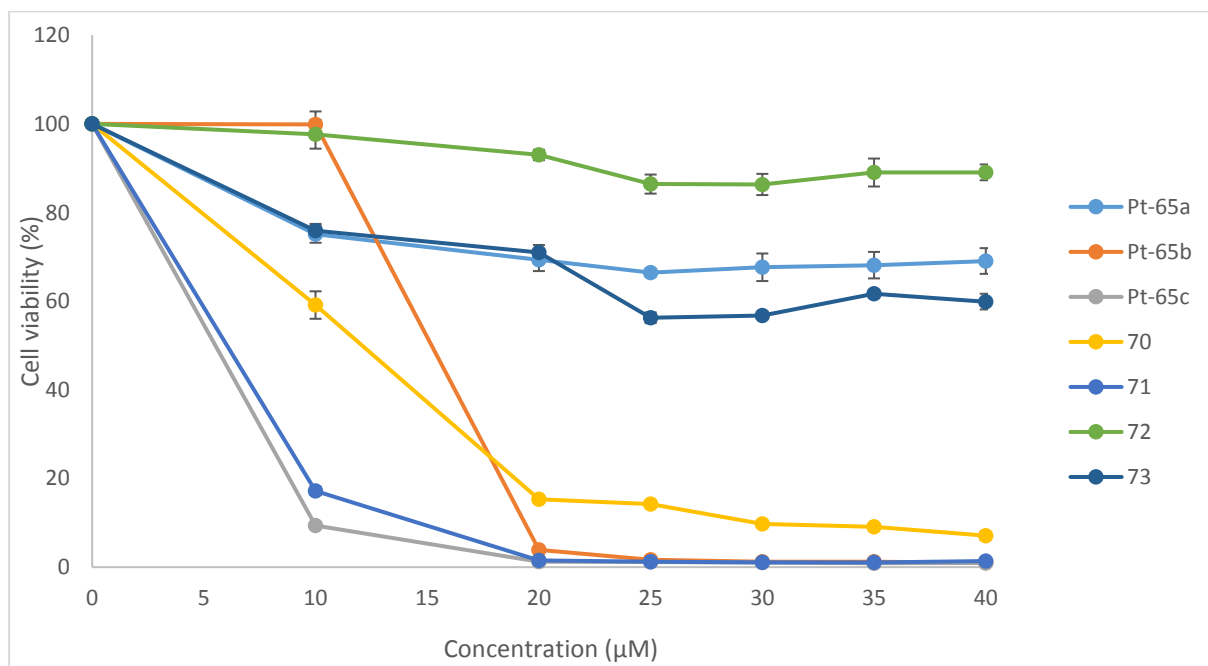


Figure 66. Cytotoxicity of Pt NHC complexes and Ni complexes against HCT116 after 48 hours of treatment. Cell viability was assessed using MTT cell viability assay at 570 nm (reference wavelength at 620 nm). The cell viability is reported in mean with error bars of ± 1 SEM.

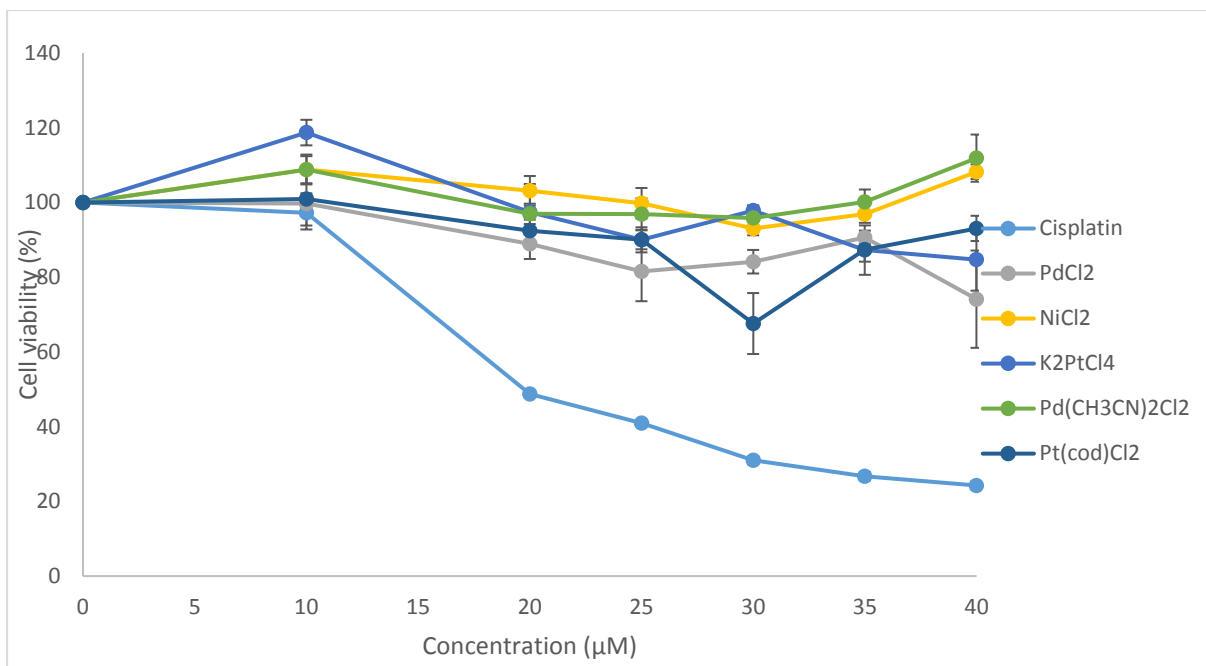


Figure 67. Cytotoxicity of cisplatin, metal salts, and transmetalating agents against MCF7 after 48 hours of treatment. Cell viability was assessed using MTT cell viability assay at 570 nm (reference wavelength at 620 nm). The cell viability is reported in mean with error bars of ± 1 SEM.

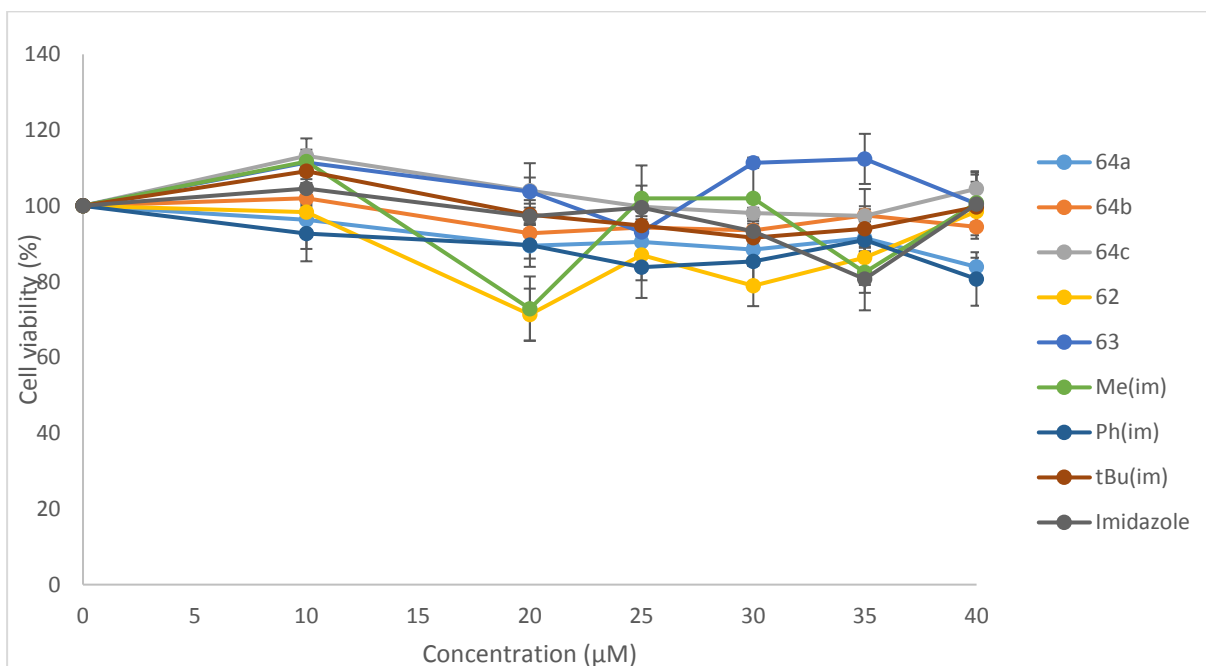


Figure 68. Cytotoxicity of precursors (62 and 63), imidazolium salts 64 and different imidazoles against MCF7 after 48 hours of treatment. Cell viability was assessed using MTT cell viability assay at 570 nm (reference wavelength at 620 nm). The cell viability is reported in mean with error bars of ± 1 SEM.

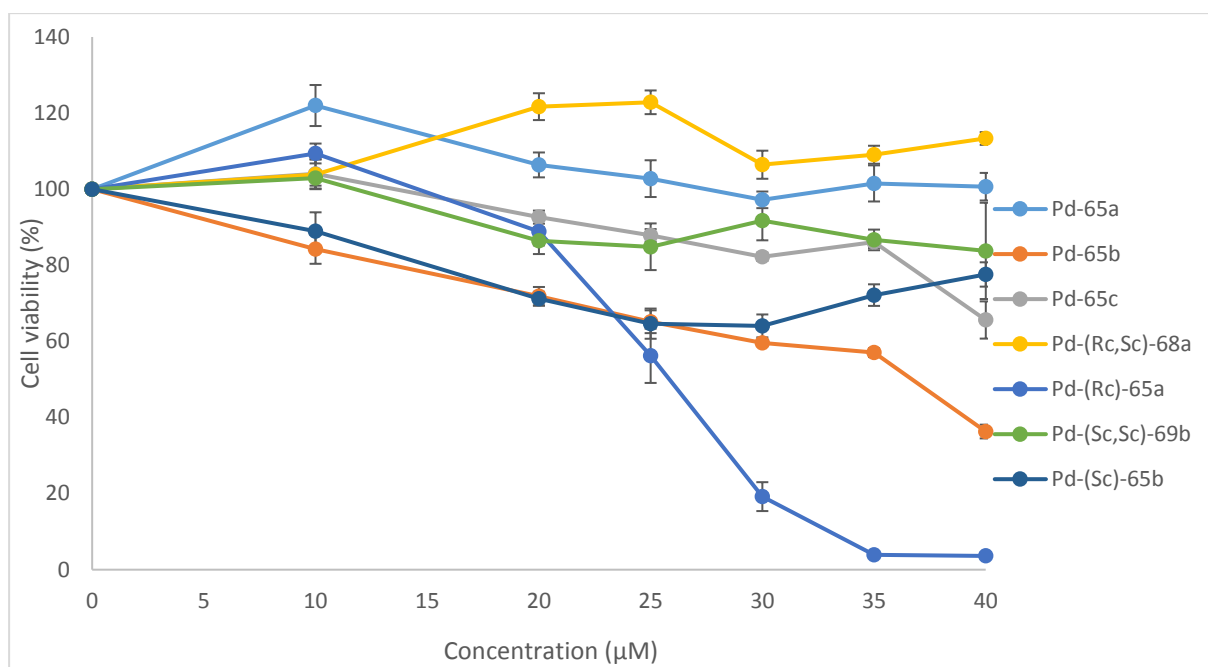


Figure 69. Cytotoxicity of Pd NHC complexes and diastereomers against MCF7 after 48 hours of treatment. Cell viability was assessed using MTT cell viability assay at 570 nm (reference wavelength at 620 nm). The cell viability is reported in mean with error bars of ± 1 SEM.

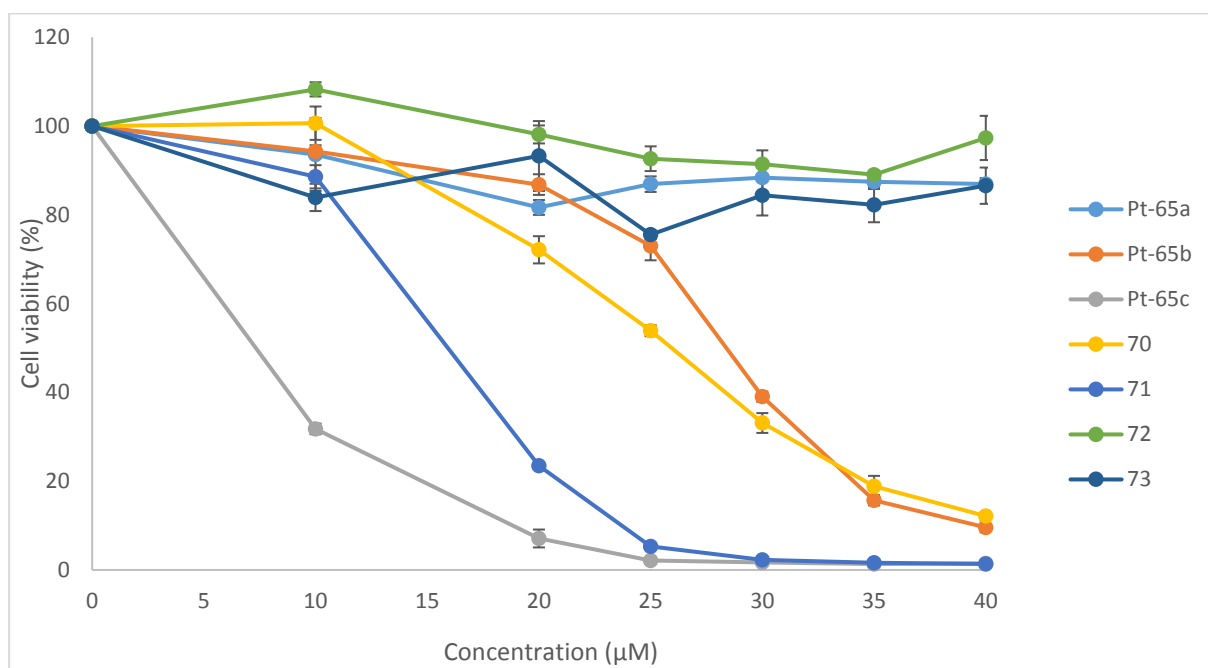


Figure 70. Cytotoxicity of Pt NHC complexes and Ni complexes against MCF7 after 48 hours of treatment. Cell viability was assessed using MTT cell viability assay at 570 nm (reference wavelength at 620 nm). The cell viability is reported in mean with error bars of ± 1 SEM.

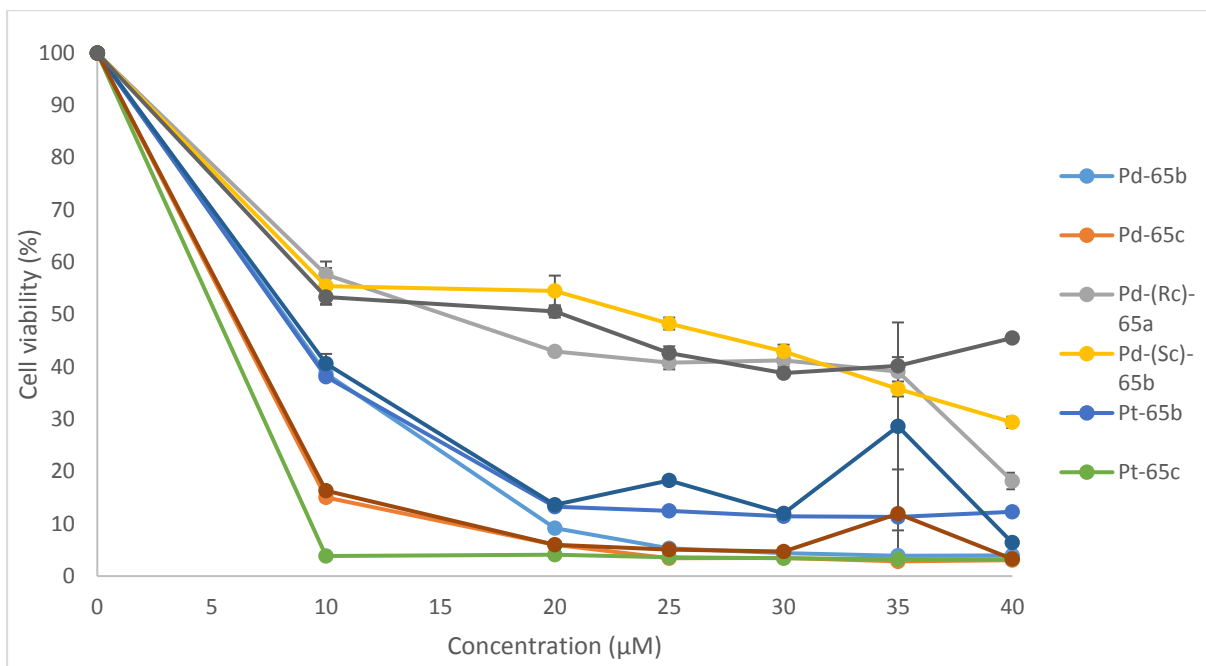


Figure 71. Cytotoxicity of selected complexes against OKF6 after 48 hours of treatment. Cell viability was assessed using MTT cell viability assay at 570 nm (reference wavelength at 620 nm). The cell viability is reported in mean with error bars of ± 1 SEM.

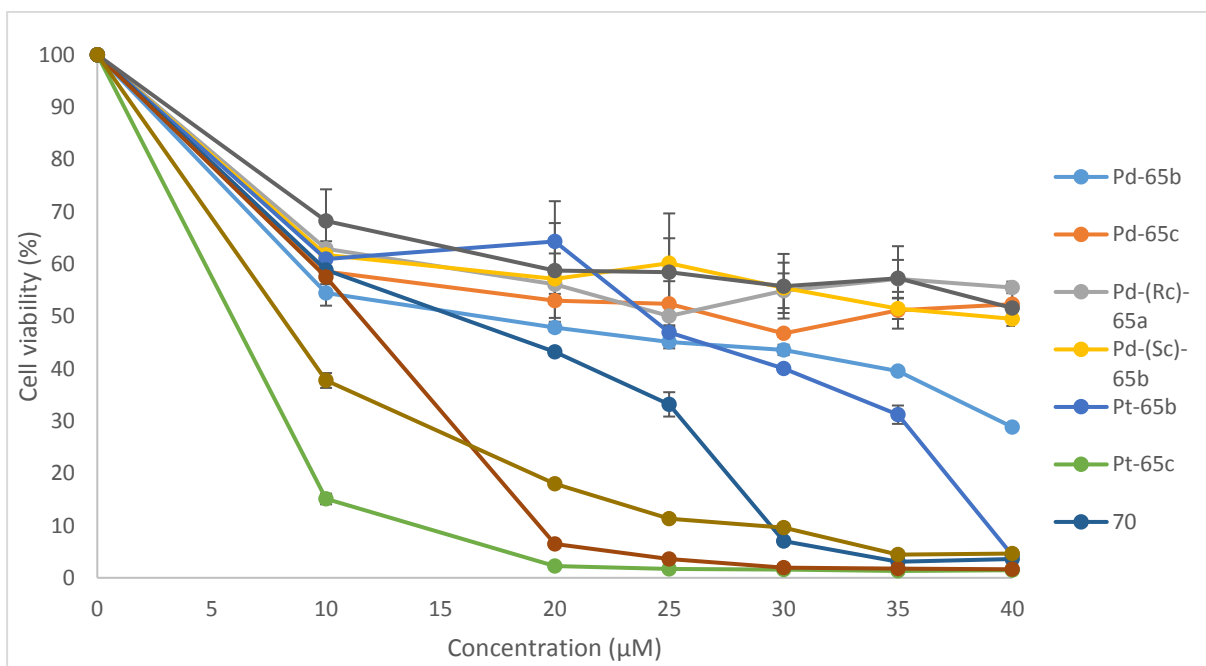


Figure 72. Cytotoxicity of selected complexes against HACAT after 48 hours of treatment. Cell viability was assessed using MTT cell viability assay at 570 nm (reference wavelength at 620 nm). The cell viability is reported in mean with error bars of ± 1 SEM.

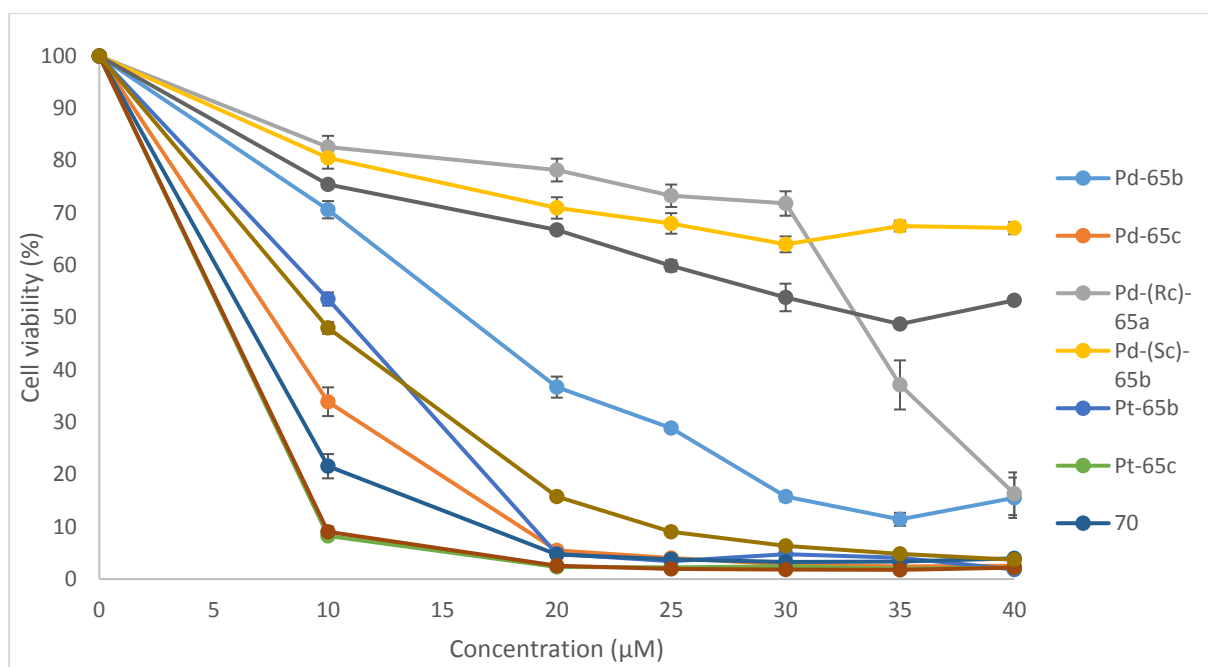


Figure 73. Cytotoxicity of selected complexes against BEAS2B after 48 hours of treatment. Cell viability was assessed using MTT cell viability assay at 570 nm (reference wavelength at 620 nm). The cell viability is reported in mean with error bars of ± 1 SEM.

APPENDIX 5: Published publication #1

Received: 16 October 2017 | Revised: 28 February 2018 | Accepted: 2 March 2018
DOI: 10.1002/aoc.4377



FULL PAPER

WILEY Applied Organometallic Chemistry

Palladium complexes of bidentate pyridine *N*-heterocyclic carbenes: Optical resolution, antimicrobial and cytotoxicity studies

Kar Bee Choo | Wee Li Mah | Sui Mae Lee | Wai Leng Lee | Yuen Lin Cheow

School of Science, Monash University
Malaysia, Jalan Lagoon Selatan, 47500
Bandar Sunway, Selangor, Malaysia

Correspondence

Yuen Lin Cheow, School of Science,
Monash University Malaysia, Jalan
Lagoon Selatan, 47500 Bandar Sunway,
Selangor, Malaysia.
Email: cheow.yuen.lin@monash.edu

Funding information

Ministry of Higher Education (MOHE),
Malaysia via Fundamental Research
Grant Scheme, Grant/Award Number:
(FRGS) (FRGS/1/2014/ST01/MUSM/03/1)

A series of bidentate pyridine-functionalized palladium *N*-heterocyclic carbene (Pd NHC) complexes with various wingtip substituents (R = methyl, phenyl and *tert*-butyl) have been synthesized and evaluated for their potential biomedical applications as antimicrobials and antiproliferative drug candidates. The obtained Pd NHC complexes were applied in a standard broth microdilution assay for determination of their antimicrobial activities against thirteen strains of pathogenic microorganisms. In addition to that, cytotoxic activities of the Pd NHC complexes were also evaluated against three human cancer cell lines, namely breast (MCF-7), colon (HCT116) and oral (H103) cancer cells, using a standard MTT assay. Upon coordination to palladium, the Pd NHC complexes show significant antimicrobial activities with minimum inhibitory concentrations in the micromolar range, and they are cytotoxic to the tested carcinomas with IC₅₀ ranging from 13 to 38 μM. Evidences for influence of both wingtip substituents and optical isomerism on the biological activities of the complexes have been found.

KEYWORDS

antimicrobial activity, cytotoxicity, *N*-heterocyclic carbene, palladium NHC complexes

1 | INTRODUCTION

The clinical success of platinum-based drugs like cisplatin and its second-generation analogues, carboplatin and oxaliplatin, in the treatment of different types of cancer has had an enormous impact on the discovery of novel metallopharmaceutical agents.^[1] However, platinum-based drugs have several substantial drawbacks including poor aqueous solubility (1 mg ml⁻¹), severe side effects like nephrotoxicity, neurotoxicity, ototoxicity, nausea and vomiting, effectiveness against a relatively narrow range of tumour types, as well as drug resistance phenomena, which have lowered the applicability and efficacy of these agents.^[2] These unresolved disadvantages have stimulated research on the development of novel

transition metal complexes containing improved organic ligands, in particular the group 10 metals, using cisplatin as a prototype.

Metal *N*-heterocyclic carbene (NHC) complexes have received ample attention due to their highlighted applications in catalysis, material science and biomedicine.^[3] Research on their therapeutic potential is one of the most active areas within the emerging field of bioorganometallic chemistry, with over 300 transition metal NHC complexes being reported as potential antimicrobials and anti-tumour drugs over the past three years.^[4] Their therapeutic potential is further accentuated by a number of patents held by several universities and 'big pharma' in recent years.^[5] NHCs are a class of ligands similar to phosphine ligands, which are well

known for their capability to form complexes with almost all main group metals and transition metals. They are generally derived from persistent carbenes which are stable compounds of divalent carbons. NHCs are generally defined as heterocyclic species containing a carbene carbon and at least one nitrogen atom within the ring structures.^[6]

A number of group 10 metal NHC complexes have been reported for their potential anticancer activities. Recent studies have depicted the possible mode of action of group 10 metal NHC complex-based anticancer drug-like candidates as these metal centres appear promising in altering cell migration, DNA replication and condensation or DNA fragmentation.^[7] Apart from the interference with nucleic acids, a recent review has provided a general insight into the mechanisms of anticancer action of group 10 metal complexes, which include reactive oxygen species production associated with redox mechanisms, cell cycle arrest, endoplasmic reticulum stress-mediated apoptosis, mitochondria-associated apoptosis and binding to cytochrome, and binding to essential amino acids causing protein dysfunctions to name a few.

Both belonging to group 10, palladium and platinum display similar chemistry. Hence palladium has become a target for chemotherapeutics development especially as a component of anticancer drugs. There are a number of novel mononuclear, binuclear and multinuclear palladium NHC (Pd NHC) complexes with reduced cross-resistance to cisplatin, decreased toxicity and high specificity that have been developed. Ray *et al.* reported a study of two Pd NHC complexes: one bis(NHC) complex and one mixed complex with NHC and pyridine ligands. Both complexes demonstrated potent cytotoxic activity against HeLa (cervical cancer), MCF-7 (breast cancer) and HCT116 (colon adenocarcinoma) cell lines in the micromolar range.^[9] Interestingly, the pyridine-functionalized Pd NHC complex was 2- to 20-fold more cytotoxic than cisplatin. Yet, high cytotoxicity against cancer cells is not limited to Pd-bis(NHC) complexes. Wang *et al.* have explored a heteroleptic Pd NHC- π -allyl complex containing a pendant amine group that exhibited up to 10-fold increased cytotoxicity compared to cisplatin when tested against breast cancer cell lines (MCF-7 and MDA-MB-231) and glioblastoma cells (U-87 MG).^[10] Recently, a new Pd NHC complex derived from a binuclear silver NHC complex was shown to exhibit significant antiproliferative activity against MCF-7 cells with IC_{50} of 2.5 μ M, a value comparable with that of the standard drug used in the study, tamoxifen ($IC_{50} = 2.4 \mu$ M).^[11] The promising *in vitro* antiproliferative activities of Pd NHC complexes have prompted us to explore their potential as anticancer agents.

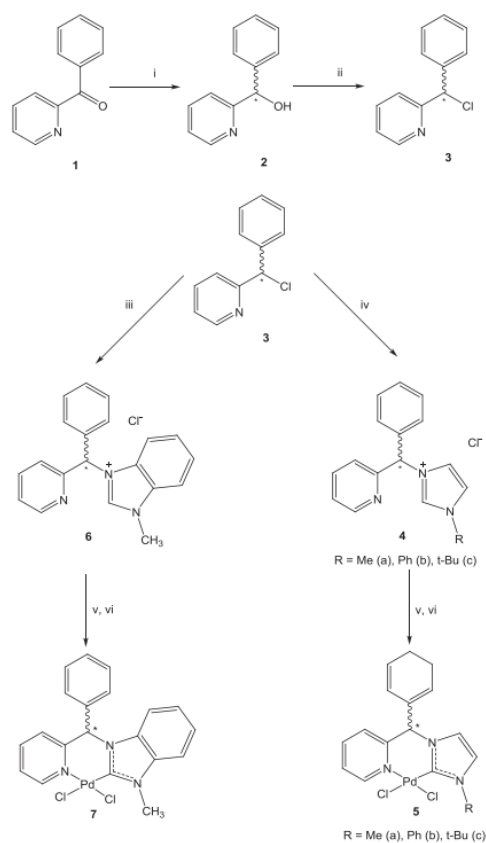
The impetus for the antimicrobial study came from the knowledge that a number of elemental metals are well known for their antimicrobial activities, for example silver. Though there is no previous report on the antimicrobial properties of any Pd NHC complexes, a number of transition metal NHC complexes have been shown to exhibit significant antimicrobial activities against Gram-positive and/or Gram-negative bacteria with minimum inhibitory concentration (MIC) below 10 μ g ml⁻¹, including silver, gold, rhodium and ruthenium NHC complexes among others.^[3n,5c,9,12] Other organometallic complexes containing palladium as the metal centre that exhibit significant antimicrobial activities have also been reported previously. For instance, a binuclear palladium complex with N₄O₄ Schiff base ligand, a palladium dicyclohexyldithiocarbamate complex and a palladium *N*-methylbenzylpiperidinedithiocarbamate complex have been shown to be effective against a range of Gram-positive and Gram-negative bacteria, as well as *Candida albicans* at MIC below 50 μ g ml⁻¹.^[13] Thus, in order to explore the potential biomedical applications of the synthesized Pd NHC complexes, we decided to study their antimicrobial properties.

Previously, Leung's group reported the synthesis and characterization of a series of novel cyclopalladated pyridine-functionalized NHC dichloride complexes showing interesting conformational behaviour and exhibiting remarkable activities in catalytic allylic alkylation reactions.^[14] In this paper, we report the influence of optical isomerism and various wingtip substituents in the structure of pyridine-functionalized Pd NHC complexes on the antimicrobial activity and cytotoxicity against cancer cells. As the literature implies, the metal centre plays an important role in interacting with biological targets while lipophilicity is maintained at an optimum level by adjusting the side chain in the metal NHC complex.^[15]

2 | RESULTS AND DISCUSSION

2.1 | Synthesis of Pd NHC Complexes

The synthesis of the targeted complexes followed established procedures with some minor modifications (Scheme 1).^[14b,c] Initially, the commercially available 2-benzoylpyridine (**1**) was reduced to phenyl(pyridine-2-yl)methanol (**2**), followed by halogenation to give 2-(chloro(phenyl)methyl)pyridine (**3**). Then, the targeted pyridine-functionalized imidazolium salts **4a**, **4b** and **4c** and benzimidazolium salt **6** were obtained by reacting with their respective imidazoles (1-methylimidazole, 1-phenylimidazole and 1-*tert*-butylimidazole) and 1-methylbenzimidazole under reflux for 48 h.^[14b,16] The pyridine-functionalized Pd NHC complexes (\pm)-**5** and



SCHEME 1 Synthesis pathway of racemic Pd NHC complexes. Reagents and conditions: (i) NaBH_4 , EtOH, 1 h, 90 °C, 1:1 EtOAc– H_2O ; (ii) methanesulfonyl chloride, Et_3N , DCM, overnight, r.t., 1:4 EtOAc–hexane; (iii) 1-methylbenzimidazole, CH_3CN , reflux, 48 h; (iv) 1-methylimidazole (a)/1-phenylimidazole (b)/1-*tert*-butylimidazole (c), CH_3CN , reflux, 48 h; (v) Ag_2O , CH_2Cl_2 , r.t., overnight, in dark; (vi) $\text{Pd}(\text{CH}_3\text{CN})_2\text{Cl}_2$, CH_3CN , r.t., overnight, in dark

(\pm)-**7** could be obtained by reaction of the imidazolium salts and benzimidazolium with silver(I) oxide, followed by a transmetalation reaction using bis(acetonitrile)palladium (II) chloride. Four pyridine-functionalized Pd NHC complexes were synthesized for the purpose of biomedical studies. All synthesized compounds and complexes were characterized using ^1H NMR and ^{13}C NMR spectroscopy. The obtained spectroscopic data were consistent with previous literature.^[14]

In the ^1H NMR spectra, the acidic proton (NHCN) signal of compounds **4** and **6** confirmed the formation of the salts, resonating in a low field for all salts. For example, the characteristic imidazolium proton peak

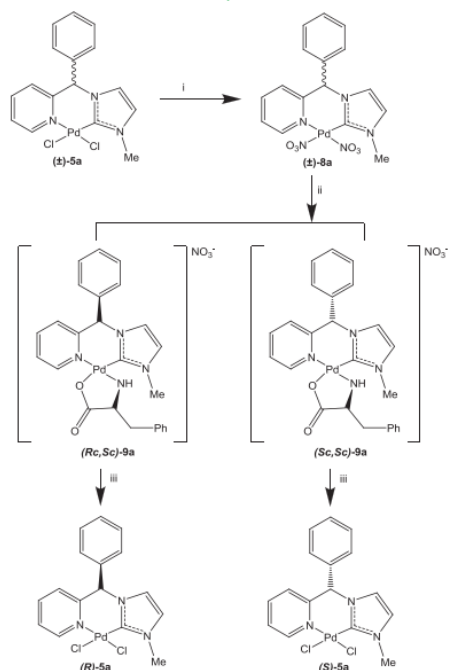
was observed at 10.39, 11.30 and 11.19 ppm for compounds **4a**, **4b** and **4c**, respectively; whereas the characteristic benzimidazolium proton peak was found at 11.33 ppm for compound **6**. Apart from that, their identities were also confirmed by the resonance of the various wingtip groups on the heterocyclic ring, such as a singlet in the ^1H NMR spectra at 4.03 and 4.30 ppm for the methyl group in compounds **4a** and **6**, respectively, as well as a singlet at 1.70 ppm for the *tert*-butyl group in compound **4c**. For all the salts, the proton at the chiral centre has a downfield shift appearing in the aromatic proton region (6.25 to 7.90 ppm) and was indistinguishable from other aromatic protons.

In this study, we synthesized the transition metal complexes with NHC ligands via transmetalation through the corresponding $\text{Ag}(\text{I})$ -NHC complexes which act as a transfer agent. This method is very well established and very attractive compared to other procedures, which often require inert or harsher conditions.^[17] In this case, silver oxide acts as a base as well as a metalation agent. The simplicity of the Ag -carbene bond formation attracts interest because of the great affinity of the electron exchange taking place between carbene C and Ag centre. The NHC species are good electronic donors whereby Ag acts as an excellent acceptor of electron density. The overall electronic exchange is the best example of a σ d donation from carbene C to the Ag centre and a π back-donation from Ag to carbene C.^[15]

As expected, ^1H NMR spectra of Pd NHC complexes in $\text{DMSO}-d_6$ confirm the successful deprotonation of imidazolium moieties indicating coordination of the ligand to the metal centre. The characteristic change was the disappearance of the characteristic NHCN proton signal of imidazolium salts **4a–c** and benzimidazolium salt **6** in the ^1H NMR spectra upon palladium coordination in (\pm)-**5a–c** and (\pm)-**7**. Similarly, the proton at the chiral centre shifted downfield and fell within the aromatic region, thus unidentifiable from other aromatic protons. In addition, there was a general downfield shift in the ^1H NMR spectra upon metal coordination. The obtained values lie within the range reported in the literature.^[14] In most cases, no NCN resonance was observable the ^{13}C NMR spectra of the synthesized Pd NHC complexes in $\text{DMSO}-d_6$. This is not unusual since metal NHC complexes with similar behaviour have been reported. The reason for the absence of carbene signals is still unclear; nevertheless a fast dynamic behaviour combined with the poor relaxation of quaternary NCN could account for it.^[18]

2.2 | Optical Resolution of Pd NHC Complexes

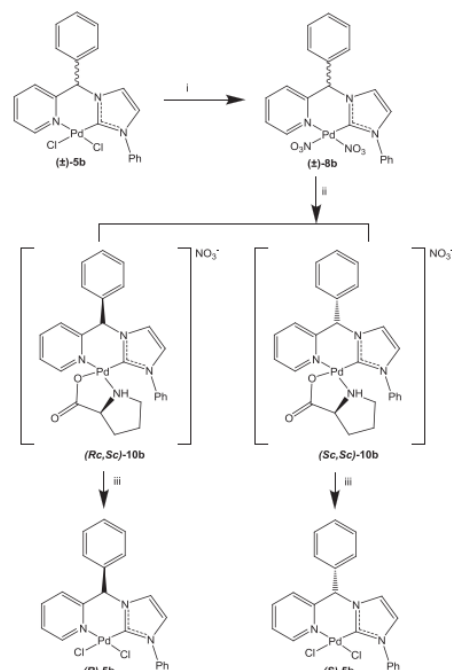
Following a literature method, the optical resolution of the racemic Pd NHC complex (\pm)-**5a** was initiated by



SCHEME 2 Optical resolution of racemic complex (\pm)-**5a**. Reagents and conditions: (i) AgNO_3 , MeOH, r.t., 3 h, in dark; (ii) sodium (*Sc*)-phenylalaninate, MeOH, r.t., 2 h; (iii) 1 M HCl, MeOH, r.t., 1 h

switching the counter ions present in the diastereomic complexes from chloride to nitrate, and sodium-(*Sc*)-phenylalaninate was used as the resolving reagent (Scheme 2).^[14b] Fractional crystallization method was employed to yield the less soluble diastereomers (*Rc,Sc*)-**9a** from methanol and diethyl ether. Whereas the optically active (*R*)-**5a** was obtained by stirring an equimolar methanol solution of diastereomers (*Rc,Sc*)-**9a** with 1 M HCl. Their identities were confirmed with ^1H NMR and ^{13}C NMR, also in agreement with a previous report.^[14b] Slow diffusion of diethyl ether into the methanol solution of the (*Sc,Sc*)-**9a**-enriched mother liquor is performed to allow the remaining (*Rc,Sc*)-**9a** to crystallize out. The diastereomers (*Rc,Sc*)-**9a** and (*Sc,Sc*)-**9a** were distinguished with the presence of two distinct sets of proton resonances for each of the diastereomers. For example, NH_2 in (*Rc,Sc*)-**9a** was characterized as a doublet and a multiplet at 5.00 and 5.98–6.01 ppm, respectively, while in (*Sc,Sc*)-**9a**, the NH_2 protons were present at around 7.00 ppm.

The literature has reported the optical resolution of the racemic Pd NHC complex (\pm)-**5b** using sodium-(*Sc*)-



SCHEME 3 Optical resolution of racemic complex (\pm)-**5b**. Reagents and conditions: (i) AgNO_3 , MeOH, r.t., 3 h, in dark; (ii) sodium (*Sc*)-prolinate, MeOH, r.t., 2 h; (iii) 1 M HCl, MeOH, r.t., 1 h

prolinate without changing the counter anion present in the diastereomic complexes.^[14a] In our case, the two resulting diastereomers could not be separated resulting in several failed attempts of crystallization. The problem was finally overcome by changing the counter anion. After switching the counter anion from chloride to nitrate, successful optical resolution of racemic complex (\pm)-**5b** was achieved using sodium-(*Sc*)-prolinate as the auxiliary ligand (Scheme 3). Fractional crystallization from methanol and diethyl ether yielded the less soluble diastereomers (*Sc,Sc*)-**10b**. The identity of (*Sc,Sc*)-**10b** was confirmed through NMR and in agreement with the literature.^[14a] Slow diffusion of diethyl ether into a methanol solution of the (*Rc,Sc*)-**10b**-enriched mother liquor is performed to allow the remaining (*Sc,Sc*)-**10b** to crystallize out. Similarly, the optically active (*S*)-**5b** was obtained by stirring a methanol solution of diastereomers (*Sc,Sc*)-**10b** with 1 M HCl. The optically active (*S*)-**5b** was isolated as a yellow powder. Unfortunately, the optical resolution of (\pm)-**5c** was unsuccessful despite changing the ancillary chloride ligand and use of various sodium-amino acid salts. Meanwhile, the optical resolution of (\pm)-**7** is on-going.

TABLE 1 Cell viability (half inhibitory concentration) IC_{50} values of screened imidazolium salts, Pd NHC complexes and cisplatin against human breast MCF-7, human colon HCT116 and human oral H103 tumour cells incubated for 48 h

Complex	Half inhibitory concentration, IC_{50} (μM) ^a		
	MCF-7	HCT116	H103
4a	>40	>40	>40
4b	>40	>40	>40
4c	>40	>40	>40
(\pm)- 5a	>40	>40	>40
(\pm)- 5b	36.70	18.64	13.93
(\pm)- 5c	>40	38.60	22.69
(<i>Rc,Sc</i>)- 9a	>40	>40	>40
(<i>R</i>)- 5a	25.84	36.57	34.53
(<i>Sc,Sc</i>)- 10b	>40	>40	>40
(<i>S</i>)- 5b	>40	23.11	>40
Cisplatin	5.83	8.37	5.44

^aCells were exposed to various concentrations of complexes for 48 h and cell viability was assessed using MTT assay. The IC_{50} values were calculated from a graph of mean \pm SEM, which are experiments performed in quadruplicate, and tabulated.

2.3 | Cytotoxicity Studies of Pd NHC Complexes

It is well known that metal complexes generally display cytotoxic activity. In this study, the cytotoxic effects of the synthesized ligands and Pd NHC complexes were evaluated using *in vitro* 3-(4,5-dimethylthiazol-2-yl)-2,5-diphenyltetrazolium bromide (MTT) assays against human breast (MCF-7), human colon (HCT116) and human oral (H103) cancer cell lines. The obtained IC_{50} values are summarized in Table 1. Cisplatin was utilized as a positive control as it is an anti-tumour drug. These cell lines were exposed to various concentrations of complexes, from 0 to 40 μM , for 48 h. The MTT assay results show that the synthesized ligands and complexes have an inhibitory effect on these cancer cells in a dose-dependent manner.

Notably, the corresponding precursor ligands, imidazolium salts **4**, shows no cytotoxicity up to 40 μM suggesting that the growth inhibition of cancer cells is likely the consequence of incorporation of metal cations (Table 1). Instead, the cytotoxic effects observed in the racemic Pd NHC complexes (\pm)-**5** is speculated to be mainly due to the metal–ligand interaction with cellular components. In general, the bulkier Pd NHC complexes (\pm)-**5b** and (\pm)-**5c** have shown only moderate cytotoxic effect compared to their analogue (\pm)-**5a**, with IC_{50} ranging from 13.93 to 38.60 μM against the tested carcinoma

cell lines. This structure–activity relationship may be attributed to the central metal atom as explained by Tweedy's chelation theory and overall lipophilicity of the compounds.^[19] Besides that, it is known that the steric factors (bulk, size and shape) of drug can affect how easily it can approach and interact with a binding site. Bulky substituents may act like a steric shield and hinder the ideal interaction between a compound and its binding site; alternatively, they may help to orientate the compound appropriately for maximum binding and increased activity.^[20] The literature has suggested that the mode of action of Pd NHC complexes is due to covalent bonding at the minor groove of DNA causing cross-linking of the bases (especially with guanine), and the square planar configuration enabled intercalation of the compounds with the DNA involving a π – π stacking.^[21] A mode of action involving a block of the cell cycle at the G2/M phase also has been proposed for Pd NHC complexes.^[10]

Interestingly, the optically active enantiomer (*R*)-**5a** was shown to be cytotoxic with IC_{50} around 25–36 μM against the three cell lines tested as compared to the racemic Pd NHC complex (\pm)-**5a** (Table 1). Conversely, as opposed to the enantiomer (*R*)-**5a** which has enhanced cell cytotoxicity against the carcinomas after optical resolution, the IC_{50} values (*S*)-**5b** were higher than that of racemic Pd NHC complex (\pm)-**5b** with reduced cytotoxicity. Similar to their antimicrobial properties, it is speculated that the cell toxicity of (*R*)-enantiomers is more evident compared to (*S*)-enantiomers. The cell cytotoxicity effects of these active complexes were comparable to those of other reported organic anticancer agents, including noscapine (IC_{50} of 20–35 μM) and estramustine (IC_{50} of 0.5–17 μM).^[22] Yet, a *trans*-Pd NHC complex with impressive cell cytotoxicity against HeLa, HCT116 and MCF-7 carcinoma cells with IC_{50} of 0.8 to 4 μM , and twice as effective as cisplatin, has been reported.^[10] On the other hand, in a recent study where Kumar *et al.* investigated five enantiomeric pairs of Pd NHC complexes derived from 1,2,4-triazole, no influence on the cytotoxicity was observed in regards to the chirality as both enantiomers of all five enantiomeric pairs exhibited near-equal activities, whereby one of the enantiomeric pair was shown to be 3- to 27-fold more active than the benchmark cisplatin against human carcinoma cell lines.^[23] Mechanistic studies of the potent chiral Pd NHC complex revealed that it interfered with cancer cell proliferation by arresting the cells at the G2 phase; caused production of reactive oxygen species in the mitochondria which led to cell death; and was involved in inducing p53-dependent programmed cell death in MCF-7 cells.^[23] Nevertheless, it is known that for a racemic complex, in this case Pd NHC complexes (\pm)-**5**, each enantiomer

possesses its own pharmacological activities that can be null, similar, different or opposite.^[24] Even though the Pd NHC complexes showed lower cytotoxic effects compared to cisplatin, the racemic Pd NHC complexes (\pm)-**5b** and (\pm)-**5c** have exhibited substantial cell cytotoxicities against the carcinoma cells tested. Therefore, it is important to separate the enantiomers via optical resolution and evaluate their respective bioactivities. Also, the IC₅₀ values of metal NHC complexes have been previously reported to vary within different cell lines; hence it is conceivable that these Pd NHC complexes could show greater potency in other cell types.

2.4 | Antimicrobial Studies of Pd NHC Complexes

The antimicrobial effects of metal NHC complexes have recently attracted increased attention. In this study, we screened the synthesized pyridine-functionalized imidazolium salts **4a–c**, benzimidazolium salts **6**, racemic Pd NHC complexes (\pm)-**5a–c** and (\pm)-**7**, the diastereomers (*Rc,Sc*)-**9a** and (*Sc,Sc*)-**10b** as well as the optically active enantiomers (*R*)-**5a** and (*S*)-**5b** against a series of pathogenic microorganisms including Gram-negative and Gram-positive bacteria as well as *Candida albicans* by using broth microdilution assay. An antibiotic, chloramphenicol, was used as the reference drug in the antimicrobial assay. Chloramphenicol is a type of broad-spectrum antibiotic that exerts antimicrobial effect through protein synthesis inhibition by binding to the 50S ribosomal subunit. The MIC values of the synthesized complexes for the tested microorganism strains are presented in Table 2.

Overall, the Gram-positive bacterial strains were inhibited by low micromolar concentrations of the synthesized complexes, whereas substantially lower efficacies against Gram-negative bacterial strains were observed. The different susceptibility of Gram-positive and Gram-negative bacteria can be attributed to their morphological differences. The outer peptidoglycan layer of Gram-positive bacteria is not an effective permeability layer. On the other hand, the outer membrane of Gram-negative bacteria contains structural lipopolysaccharide components, thereby making the cell wall impermeable to lipophilic solutes while porins, membrane transport proteins, constitute a selective barrier to the hydrophilic solutes. The compounds synthesized were not soluble in a wide array of solvents but DMSO, and they were made up of several conjugated rings, which give rise their hydrophobicity (i.e. lipophilicity). Therefore, the lack of efficacy against Gram-negative bacteria was not surprising.^[25]

It was found that all microorganisms were considerably resistant to the ligands **4a–c** and **6**. Although **4a–c**

showed antimicrobial activities at 5 mM or below against some pathogens, this is not comparable to other imidazolium salts which were reported to have MIC values in the micromolar range.^[26] Nevertheless, the antimicrobial activities increased markedly upon coordination to palladium ((\pm)-**5a–c**). For example, Pd NHC complex (\pm)-**5c** displayed antimicrobial activities against all the microorganism strains tested, with the lowest MIC value of 16 μ M (or 7 μ g ml⁻¹) against *B. subtilis* (Table 2). The lack of antimicrobial activity of Pd NHC complex (\pm)-**5a** compared to (\pm)-**5b** and (\pm)-**5c** was not surprising. This is because antimicrobial activity is often dependent on the chain length of the *N*-substituted imidazolium salts, in which the lowest MIC values were achieved by compounds with long alkyl chains (C₈ to C₁₆).^[26b,d] Longer alkyl chains are thought to be associated with disruption of bacterial membranes, probably due to the integration of the long hydrocarbon chain with the lipid bilayer of the cell membrane, leading to leakage of cell contents.^[27] Also, the extended conjugated ring of the benzimidazolium salt **6** and the racemic Pd NHC complex (\pm)-**7** have been shown to exhibit no improved antimicrobial activities against the microorganisms tested compared to their imidazolium-based counterparts, imidazolium salt **4a** and Pd NHC complex (\pm)-**5a**. These results agree with reports in the literature; the side groups on the benzimidazole ring influence the antimicrobial activities, where the combined steric and electronic constraints imposed by the methyl group and pyridine moiety may be responsible for the decreased activities.^[28]

Remarkably, while the racemic complex (\pm)-**5a** did not show any antimicrobial activity at the highest concentration tested (0.5 mM), its corresponding purified enantiomer (*R*)-**5a** was shown to inhibit the microorganisms tested. In contrast, this is not the same for Pd NHC complex **5b**, where both the racemic (\pm)-**5b** and the optically pure (*S*)-**5b** did not show any antimicrobial activity at the highest concentration tested (0.5 mM). This may be attributed to the antimicrobial property of Pd NHC complexes being more prominent in the (*R*)-enantiomers instead of (*S*)-enantiomers. It is not uncommon that there is only one major bioactive enantiomer out of two in racemic drugs.^[29] The most famous example would be thalidomide, where (*R*)-thalidomide is effective against morning sickness while (*S*)-thalidomide is teratogenic.^[30] Therefore, optical resolution is important so that each of the enantiomers can be evaluated for their respective bioactive potentials.

The findings suggest that the antimicrobial activity occurs due to a synergy between the metal and the ligand, as evidenced by the improved antimicrobial activity of the synthesized Pd NHC complexes despite the poorer antimicrobial activities as observed in the imidazolium salts

TABLE 2 Minimum inhibitory concentration (MIC) and minimum bactericidal concentration (MBC) of the synthesized complexes against selected microorganisms^a

Microorganisms tested	MIC (mM)						PdCl ₂	Chloramphenicol							
	4a	4b	4c	6	(±)-5a	(±)-5b			(±)-5c	(±)-7	(Rc,Sc)-9a	(R)-5a	(Sc,Sc)-10b	(S)-5b	
<i>Bacillus cereus</i> ATCC 8188	5	2.5	5	>5	>0.5	0.25	0.063	>0.5	>0.5	0.125	>0.5	>0.5	>0.5	>0.5	0.006
<i>Bacillus subtilis</i> ATCC 14579	5	2.5	5	>5	>0.5	0.063	0.016	>0.5	>0.5	0.25	>0.5	>0.5	>0.5	>0.5	0.006
<i>Staphylococcus aureus</i> ATCC 29213	2.5	1.25	2.5	>5	>0.5	0.125	0.125	>0.5	>0.5	0.25	>0.5	>0.5	>0.5	>0.5	0.025
<i>Staphylococcus aureus</i> ATCC 6538P	2.5	1.25	2.5	>5	>0.5	0.25	0.031	>0.5	0.125	0.031	>0.5	>0.5	>0.5	>0.5	0.025
<i>Staphylococcus aureus</i> ATCC 43300 ^b	5	1.25	5	>5	>0.5	0.5	0.063	>0.5	0.125	0.031	>0.5	>0.5	>0.5	>0.5	0.025
<i>Staphylococcus aureus</i> ATCC 33591 ^b	>5	5	>5	>5	>0.5	0.25	0.125	>0.5	>0.5	0.25	>0.5	>0.5	>0.5	>0.5	0.05
<i>Enterococcus faecalis</i> ATCC 29212	>5	>5	>5	>5	>0.5	0.25	0.125	>0.5	>0.5	0.25	>0.5	>0.5	>0.5	>0.5	0.05
<i>Enterococcus faecalis</i> ATCC 700802 ^c	>5	>5	>5	>5	>0.5	0.25	0.125	>0.5	>0.5	0.25	>0.5	>0.5	>0.5	>0.5	0.05
<i>Escherichia coli</i> ATCC 25922	>5	5	>5	>5	>0.5	0.5	0.125	>0.5	0.5	0.125	>0.5	>0.5	>0.5	>0.5	0.025
<i>Klebsiella pneumoniae</i> ATCC 10031	>5	2.5	>5	>5	>0.5	>0.5	0.25	>0.5	0.5	0.125	>0.5	>0.5	>0.5	>0.5	0.003
<i>Pseudomonas aeruginosa</i> ATCC 10145	>5	>5	>5	>5	>0.5	>0.5	0.25	>0.5	0.5	0.125	>0.5	>0.5	>0.5	>0.5	>0.05
<i>Shigella flexneri</i> ATCC 12022	5	1.25	5	>5	>0.5	0.5	0.25	>0.5	0.5	0.125	>0.5	>0.5	>0.5	>0.5	0.006
<i>Candida albicans</i> IMR	2.5	1.25	5	5	>0.5	0.5	0.25	>0.5	>0.5	0.25	>0.5	>0.5	>0.5	>0.5	>0.05
MBC (mM)		4a	4b	4c	6	(±)-5a	(±)-5b	(±)-5c	(±)-7	(Rc,Sc)-9a	(R)-5a	(Sc,Sc)-10b	(S)-5b	PdCl ₂	Chloramphenicol
<i>Bacillus cereus</i> ATCC 8188	5	2.5	5	>5	>5	>0.5	0.5	0.25	>0.5	>0.5	0.25	>0.5	>0.5	>0.5	>0.05
<i>Bacillus subtilis</i> ATCC 14579	>5	2.5	>5	>5	>5	>0.5	>0.5	0.25	>0.5	>0.5	0.25	>0.5	>0.5	>0.5	>0.05
<i>Staphylococcus aureus</i> ATCC 29213	5	5	5	>5	>0.5	0.5	0.5	0.5	>0.5	>0.5	>0.5	>0.5	>0.5	>0.5	>0.05
<i>Staphylococcus aureus</i> ATCC 6538P	5	5	5	>5	>0.5	>0.5	>0.5	0.125	>0.5	>0.5	>0.5	>0.5	>0.5	>0.5	>0.05
<i>Staphylococcus aureus</i> ATCC 43300 ^b	5	2.5	5	>5	>0.5	0.5	0.5	0.5	>0.5	>0.5	>0.5	>0.5	>0.5	>0.5	>0.05
<i>Staphylococcus aureus</i> ATCC 33591 ^b	>5	>5	>5	>5	>0.5	>0.5	>0.5	0.125	>0.5	>0.5	0.5	>0.5	>0.5	>0.5	>0.05
<i>Enterococcus faecalis</i> ATCC 29212	>5	>5	>5	>5	>0.5	>0.5	>0.5	0.5	>0.5	>0.5	0.5	>0.5	>0.5	>0.5	>0.05
<i>Enterococcus faecalis</i> ATCC 700802 ^c	>5	>5	>5	>5	>0.5	>0.5	>0.5	0.5	>0.5	>0.5	0.5	>0.5	>0.5	>0.5	>0.05
<i>Escherichia coli</i> ATCC 25922	>5	5	>5	>5	>0.5	0.5	0.5	0.5	>0.5	>0.5	0.5	>0.5	>0.5	>0.5	>0.05
<i>Klebsiella pneumoniae</i> ATCC 10031	>5	5	>5	>5	>0.5	>0.5	>0.5	0.5	>0.5	0.5	0.125	>0.5	>0.5	>0.5	0.003
<i>Pseudomonas aeruginosa</i> ATCC 10145	>5	>5	>5	>5	>0.5	>0.5	>0.5	0.5	>0.5	>0.5	0.25	>0.5	>0.5	>0.5	>0.05
<i>Shigella flexneri</i> ATCC 12022	5	5	>5	>5	>0.5	0.5	0.25	>0.5	>0.5	0.5	0.25	>0.5	>0.5	>0.5	0.05
<i>Candida albicans</i> IMR	5	2.5	5	>5	>0.5	>0.5	0.5	0.5	>0.5	>0.5	0.5	>0.5	>0.5	>0.5	>0.05

^aThe antimicrobial assay was performed in triplicate. The compounds with no antimicrobial activity were reported as more than the maximum working concentration tested in mM.^bMethicillin-resistant *S. aureus*.^cVancomycin-resistant enterococci.

and PdCl₂. Based on Tweedy's chelation theory, the ion polarity of Pd(II) is reduced by overlapping of the ligand orbitals and the exchange of the partial positive charge of the metal ion to the donor atoms of the ligands; thereby the delocalization of π -electrons on the chelate ring increases and improves the lipophilicity of the complexes.^[31] The increased lipophilicity allows the complex to penetrate the lipid membrane and block the metal binding sites on enzymes, which might result in the disturbance of cellular respiration and protein synthesis, thus inhibiting cell growth.^[32] In general, DNA is considered to be the main target of group 10 metalodrugs through the formation of intra- and inter-strand adducts, while metal bonding to sulfur-containing groups in proteins was also reported.^[33]

3 | CONCLUSIONS

A series of pyridine-functionalized imidazolium salts and Pd NHC complexes were synthesized and characterized by spectroscopic techniques. Antimicrobial activities and cytotoxic effects of these ligands and Pd NHC complexes against three human cancer cell lines were reported. Although the mechanism of action is not known at present, it is clear from this work that the nature of various wingtip substituents of the NHC ligand has a profound effect on the biological activities of the resulting Pd NHC complexes. Besides, optical isomerism might play a role in the biological activity, as illustrated by the racemic Pd NHC complexes (\pm)-**5a** and (\pm)-**5b**, and their respective enantiomers. Therefore, it is important to resolve the racemic metal NHC complexes into their respective enantiomers. The optical resolution of the racemic Pd NHC complexes (\pm)-**5c** and (\pm)-**7** is currently in progress.

4 | EXPERIMENTAL

4.1 | General Procedures

All the commercially available chemicals and solvents were used without prior drying or purification. Reactions involving air-sensitive compounds were performed under a positive pressure of nitrogen. Phenyl(pyridine-2-yl)methanol (**2**), bis(acetonitrile)palladium chloride (PdCl₂(CH₃CN)₂), 1-phenylimidazole and 1-*tert*-butylimidazole were prepared according to literature methods with some modifications. Mass spectra were recorded with an Agilent 1290 Infinity LC system coupled to an Agilent 6520 Accurate-Mass Q-TOF mass spectrometer with dual ESI source. Optical activity of the diastereomers and enantiomers was determined using a

Rudolph AUTOPOL VI automatic polarimeter at 436 nm. ¹H NMR and ¹³C NMR spectroscopy was performed with a Bruker Avance 300 NMR spectrometer. The number of protons (*n*) for a given resonance is indicated by *n* H. Coupling constants are reported as a *J* value in Hz. ¹H NMR signals are reported as δ in units of parts per million (ppm) downfield from SiMe₄ (δ = 0.00 ppm). ¹³C NMR signals are reported as δ in units of parts per million (ppm) relative to the signal of chloroform-*d* (δ = 77.16 ppm, triplet) and DMSO-*d*₆ (δ = 39.52 ppm, septet). All chemical shifts reported are referenced to the chemical shifts of their respective residual solvent resonances. Unless stated otherwise, all NMR experiments were carried out at 300 K. See the supporting information for the NMR spectra of all synthesized compounds, imidazolium salts and Pd NHC complexes.

4.2 | Synthesis of Phenyl(pyridin-2-yl)methanol (**2**)

The method for reduction of 2-benzoylpyridine to **2** was modified from the literature.^[16] Sodium borohydride (2.04 g, 54 mmol) in 50 ml of 95% ethanol was added dropwise into a solution of 2-benzoylpyridine (5 g, 27 mmol) in 50 ml of 95% ethanol on an ice bath. The reaction mixture was stirred continuously for 1 h until the reaction was completed. Then, 100 ml of water was added to the reaction mixture and the solution was heated at 90 °C for 15 min. Then, the solution was extracted with ethyl acetate thrice and the solvent was evaporated under reduced pressure to afford a pale green oil. Slow evaporation of a solution in ethanol at room temperature yielded the clear crystal solid, 5.01 g, 96.43%. ¹H NMR (300 MHz, CDCl₃, δ , ppm): 5.29 (d, 1 H, *J*_{H,H} = 4.5 Hz, OH), 5.75 (d, 1 H, *J*_{H,H} = 4.5 Hz, H1), 7.13–7.39 (m, 7 H, arom.), 7.60 (td, 1 H, *J*_{H,H} = 7.8 Hz, *J*_{H,H} = 1.8 Hz, arom.) and 8.55 (dq, 1 H, *J*_{H,H} = 5.1 Hz, *J*_{H,H} = 1.2 Hz, arom.). ¹³C NMR (75 MHz, CDCl₃, δ , ppm): 75.00 (C1), 121.35, 122.42, 127.07, 127.82, 128.56, 136.83, 143.23, 147.83 and 160.91 (arom.). MS *m/z*: [M + H]⁺ calcd for C₁₂H₁₂NO 186.2298, found 186.0912.

4.3 | Synthesis of 2-(Chloro(phenyl)methyl)pyridine (**3**)

Compound **2** (1.85 g, 10.5 mmol) and triethylamine (3.4 ml, 24.4 mmol) in 32 ml of CH₂Cl₂ was stirred in an ice bath. Methanesulfonyl chloride (1.2 ml, 15.8 mmol) was added dropwise into the stirring solution. The reaction mixture was left to warm up slowly to room temperature. The reaction mixture was allowed to stir overnight and then poured into a saturated aqueous NaHCO₃ solution. The aqueous layer was extracted with

chloroform thrice. The combined organic layers were washed with water, dried over anhydrous MgSO_4 and evaporated *in vacuo* to give a red liquid. The resultant red liquid was subjected to column chromatography (ethyl acetate–hexane 1:4 v/v) to give a yellow oil, 1.52 g, 74.32%. The spectral data for this compound are consistent with those reported in the literature.^[14b] ^1H NMR (300 MHz, CDCl_3 , δ , ppm): 6.16 (s, 1 H, H1), 7.20 (ddd, 1 H, $J_{\text{H,H}} = 7.5$ Hz, $J_{\text{H,H}} = 4.8$ Hz, $J_{\text{H,H}} = 1.2$ Hz, arom.), 7.25–7.37 (m, 3 H, arom.), 7.45–7.49 (m, 2 H, arom.), 7.55 (dt, 1 H, $J_{\text{H,H}} = 7.8$ Hz, $J_{\text{H,H}} = 0.9$ Hz, arom.), 7.70 (td, 1 H, $J_{\text{H,H}} = 7.8$ Hz, $J_{\text{H,H}} = 1.8$ Hz, arom.) and 8.57 (dq, 1 H, $J_{\text{H,H}} = 4.8$, $J_{\text{H,H}} = 0.9$ Hz, H9). ^{13}C NMR (75 MHz, CDCl_3 , δ , ppm): 64.54 (C12), 122.09 and 122.81 (arom.), 127.78 (C10), 128.28 (C12), 128.64 and 137.05 (arom.), 139.96 (C12), 149.19 (C8) and 159.75 (C9). MS m/z : $[\text{M} + \text{H}]^+$ calcd for $\text{C}_{12}\text{H}_{11}\text{NCl}$ 204.6754, found 204.0574.

4.4 | Synthesis of Pyridine-Functionalized Imidazolium Salts 4

Liquid 1-methylimidazole (**a**) or 1-phenylimidazole (**b**) or 1-*tert*-butylimidazole (**c**) (1 mol equiv.) was added to a stirring solution of compound **3** (1 mol equiv.) in 50 ml of CH_3CN . The reaction mixture was heated at refluxing temperature for 48 h. Then, the reaction mixture was reduced *in vacuo* and the resulting oil was stirred in diethyl ether. The diethyl ether layer was decanted away to give ligands **4a**, **4b** and **4c**. The spectral data for these compounds are consistent with those reported in the literature.^[14]

4.4.1 | Synthesis of 1-methyl-3-[phenyl(pyridin-2-yl)methyl]-1H-imidazolium chloride (4a)

Hygroscopic off-white solid, 2.97 g, 45.75%. ^1H NMR (300 MHz, CDCl_3 , δ , ppm): 4.03 (s, 3 H, CH_3), 7.26–7.37 (m, 4 H, arom.) 7.41–7.46 (m, 3 H, arom.), 7.63–7.76 (m, 4 H, arom.), 8.57–8.60 (m, 1 H, H13) and 10.39 (s, 1 H, H4). ^{13}C NMR (75 MHz, CDCl_3 , δ , ppm): 36.63 (C1), 65.98 (C5), 122.48 (C2), 122.58 (C3), 123.78 (C14), 124.36 (C16), 128.84, 129.24, 129.34, 136.43 and 137.61 (arom.), 137.85 (C15), 149.52 (arom.) and 155.09 (C13). MS (ESI) m/z : $[\text{M} - \text{Cl}]^+$ calcd for $\text{C}_{16}\text{H}_{16}\text{N}_3$ 250.1344, found 250.1952.

4.4.2 | Synthesis of 1-phenyl-3-[phenyl(pyridin-2-yl)methyl]-1H-imidazolium chloride (4b)

Brown oil, 2.71 g, 28.81%. ^1H NMR (300 MHz, CDCl_3 , δ , ppm): 7.34–7.39 (m, 3 H, arom.), 7.49–7.61 (m, 5 H, arom.),

7.67–7.79 (m, 5 H, arom.), 7.96 (t, 1 H, $J_{\text{H,H}} = 1.8$ Hz, arom.), 8.23 (s, 1 H, H10), 8.60 (dq, 1 H, $J_{\text{H,H}} = 0.9$ Hz, $J_{\text{H,H}} = 4.8$ Hz, H21) and 11.30 (s, 1 H, H7). ^{13}C NMR (75 MHz, CDCl_3 , δ , ppm): 65.82 (C10), 119.47 (C8), 121.71 (C20), 123.44 (C18), 123.80, 124.81, 129.10, 129.25, 129.41, 130.19, 130.56, 134.54, 136.28, 136.42, 137.71 and 149.34 (arom.), 155.02 (C17). MS (ESI) m/z : $[\text{M} - \text{Cl}]^+$ calcd for $\text{C}_{21}\text{H}_{18}\text{N}_3$ 312.1501, found 312.1508.

4.4.3 | Synthesis of 1-*tert*-butyl-3-[phenyl(pyridin-2-yl)methyl]-1H-imidazolium chloride (4c)

Brown solid, 8.24 g, 54.00%. ^1H NMR (300 MHz, CDCl_3 , δ , ppm): 1.70 (s, 9 H, H17), 7.27–7.37 (m, 5 H), 7.50–7.55 (m, 2H), 7.72 (td, 1 H, $J_{\text{H,H}} = 1.8$ Hz, $J_{\text{H,H}} = 7.8$ Hz), 7.81–7.83 (m, 1 H), 8.14 (s, 1 H), 8.59 (dq, 1 H, $J_{\text{H,H}} = 0.9$ Hz, $J_{\text{H,H}} = 4.8$ Hz, H1) and 11.19 (s, 1 H, H13). ^{13}C NMR (75 MHz, CDCl_3 , δ , ppm): 30.05 (C17), 60.13 (C16), 65.26 (C6), 117.97 (C15), 122.50 (C14), 123.60 (C2), 124.87 (C4), 128.91, 129.07, 136.53 and 136.96 (arom.), 137.55 (C3), 149.30 (arom.) and 155.44 (C1). MS (ESI) m/z : $[\text{M} - \text{Cl}]^+$ calcd for $\text{C}_{19}\text{H}_{22}\text{N}_3$ 292.1814, found 292.3259.

4.5 | Synthesis of Pyridine-Functionalized Benzimidazolium Salt 6

Liquid 1-methylbenzimidazole (1 mol equiv.) was added to a stirring solution of compound **3** (1 mol equiv.) in 50 ml of CH_3CN . The reaction mixture was heated at refluxing temperature for 48 h. Then, the reaction mixture was reduced *in vacuo* and the resulting oil was stirred in diethyl ether. The diethyl ether layer was decanted away to give ligand **6**. The spectral data are consistent with those reported in the literature.^[14c] Brown oil, 2.55 g, 62.3%. ^1H NMR (300 MHz, CDCl_3 , δ , ppm): 4.30 (s, 3 H, H1), 7.28–7.30 (m, 1 H, H18), 7.31 (m, 5 H, arom.), 7.46–7.49 (m, 1 H, arom.), 7.55–7.64 (m, 2 H, arom.), 7.64–7.70 (m, 2 H, arom.), 7.75–7.78 (m, 1 H, arom.), 7.82 (td, 1 H, $J_{\text{H,H}} = 7.8$, $J_{\text{H,H}} = 1.8$ Hz, arom.), 8.56 (dd, 1 H, $J_{\text{H,H}} = 6$, $J_{\text{H,H}} = 1.2$ Hz, H17), 11.23 (s, 1 H, H8). ^{13}C NMR (75 MHz, CDCl_3 , δ , ppm): 33.93 (C1), 66.83 (C9), 112.56, 115.80, 124.12, 124.59, 126.78, 126.91, 128.88, 129.44, 129.55, 131.40, 134.71, 138.11, 143.81, 149.71 and 154.55 (arom.), 160.20 (C17). MS (ESI) m/z : $[\text{M} - \text{Cl}]^+$ calcd for $\text{C}_{20}\text{H}_{18}\text{N}_3$ 300.14, found 299.14.

4.6 | Synthesis of Pyridine-Functionalized Pd NHC Complexes

To a solution of pyridine-functionalized NHC ligands **4a**, **4b**, **4c** or **6** (1 mol equiv.) in 30 ml of CH_2Cl_2 , Ag_2O

(0.5 mol equiv.) was added in the dark. The reaction mixture was stirred at room temperature for 12 h and was filtered through a short plug of celite. A $\text{PdCl}_2(\text{CH}_3\text{CN})_2$ suspension (1 mol equiv. in 100 ml of CH_3CN) was added to the filtrate in the dark. The reaction mixture was then allowed to stir overnight at room temperature and was filtered through celite the next day. The filtrate was reduced *in vacuo* to approximately 50 ml and then 200 ml of diethyl ether to yield the Pd NHC complexes. The spectral data for these compounds are consistent with those reported in the literature.^[14]

4.6.1 | Synthesis of racemic complex (\pm)-5a

Orange-yellow solid 2.10 g, 37.55%. ^1H NMR (300 MHz, $\text{DMSO}-d_6$, δ , ppm): 3.96 (s, 3 H, H2), 7.26 (s, 1 H, H5), 7.35–7.50 (m, 5 H, arom.), 7.60–7.65 (m, 1 H, H15), 7.81 (d, 1 H, $J_{\text{H,H}} = 1.8$ Hz, H4), 8.00–8.02 (m, 1 H, H13), 8.20 (td, 1 H, $J_{\text{H,H}} = 1.5$ Hz, $J_{\text{H,H}} = 7.8$ Hz, H14) and 9.10–9.16 (m, 1 H, H16). ^{13}C NMR (75 MHz, $\text{DMSO}-d_6$, δ , ppm): 38.35 (C2), 67.07 (C5), 122.89 (C3), 124.62 (C4), 125.60 (C15), 126.81 (C13), 127.45, 128.81, 129.28 and 140.94 (arom.), 152.08 (C14), and 155.06 (C16).

4.6.2 | Synthesis of racemic complex ($\pm\pm$)-5b

Orange-yellow solid 1.50 g, 39.88%. ^1H NMR (300 MHz, $\text{DMSO}-d_6$, δ , ppm): 7.36–7.55 (m, 10 H, arom.), 7.69 (t, 1 H, $J_{\text{H,H}} = 6.9$ Hz, $J_{\text{H,H}} = 1.5$ Hz, H20), 7.82–7.87 (m, 3 H, arom.), 8.03–8.10 (m, 2 H, H18 and H9), 8.23 (td, 1 H, $J_{\text{H,H}} = 8.1$ Hz, $J_{\text{H,H}} = 1.5$ Hz, H19) and 9.20–9.23 (m, 1 H, H21). ^{13}C NMR (75 MHz, $\text{DMSO}-d_6$, δ , ppm): 67.08 (C10), 123.07 (C9), 123.90 (C8), 124.83 (C20), 125.13 (C18), 127.05, 127.98, 128.36, 128.57, 128.75, 137.73 and 139.08 (arom.) 140.42 (C19), 154.06 (arom.) and 154.90 (C21).

4.6.3 | Synthesis of racemic complex (\pm)-5c

Orange-yellow solid 4.39 g, 60.00%. ^1H NMR (300 MHz, $\text{DMSO}-d_6$, δ , ppm): 1.88 (s, 9 H, H17), 7.23 (s, 1 H, H6), 7.36–7.46 (m, 1 H, arom.), 7.58–7.62 (m, 1 H, H2), 7.70 (s, 1 H, H15), 7.87 (s, 1 H, H14), 7.99–8.02 (m, 1 H, H4), 8.14–8.20 (m, 1 H, H3) and 8.96 (d, 1 H, $J_{\text{H,H}} = 5.1$ Hz, H1). ^{13}C NMR (75 MHz, $\text{DMSO}-d_6$, δ , ppm): 29.99 (C17), 58.67 (C16), 66.61 (C6), 120.27 (C15), 121.61 (C14), 123.99 (C2), 124.98 (C4), 126.21, 126.95, 127.43, 136.67 and 139.06 (arom.), 149.64 (C3), 153.86 (arom.) and 153.98 (C1).

4.6.4 | Synthesis of racemic complex (\pm)-7

Orange-yellow solid 1.63 g, 61.10%. ^1H NMR (300 MHz, $\text{DMSO}-d_6$, δ , ppm): 4.19 (s, 3 H, H1), 7.34–7.38 (m, 3 H, Ph), 7.48–7.57 (m, 2 H, Ph), 7.67 (d, 1 H, $J_{\text{H,H}} = 1.5$ Hz, arom.), 7.80–7.82 (m, 1 H, H19), 7.93–8.00 (m, 1 H, H9), 8.16–8.21 (m, 2 H, H17 and H4), 8.25–8.28 (m, 1 H, H18), 9.03–9.25 (m, 1 H, H20). ^{13}C NMR (75 MHz, $\text{DMSO}-d_6$, δ , ppm): 35.77 (C1), 63.71 (C9), 111.33, 112.52, 124.57, 125.05, 127.28, 127.45, 128.96, 129.47, 132.42, 134.67, 136.26, and 138.51 (arom.), 143.20 (C18), 150.32 and 155.07 (arom.).

4.7 | Optical Resolution of Racemic Pd NHC Complex (\pm)-5a

To a suspension of the racemic complex (\pm)-5a (2.08 g, 4.86 mmol) in 20 ml of MeOH, AgNO_3 (1.74 g, 9.72 mmol) was added. The reaction mixture was allowed to stir in the dark at room temperature for 3 h and was filtered through a short plug of celite. The orange filtrate was treated with sodium (*Sc*)-phenylalanate (0.11 g, 4.86 mmol) in 100 ml of MeOH. The reaction was then stirred for 2 h and was concentrated to approximately 50 ml and was left to stand overnight. From the diastereomic mixture, only complex (*Rc,Sc*)-9a crystallized out as off-white crystals the next day and was isolated and washed with MeOH. The mother liquor for the diastereomer was enriched with (*Sc,Sc*)-9a. The spectral data for the diastereomer are consistent with previous literature.^[14b]

Diastereomer (*Rc,Sc*)-9a. Off-white solid. $[\alpha]_{436} + 78.6$ (c 0.05, DMSO), lit.^[14b] $[\alpha]_{436} + 83.3$ (c 0.5, DMSO). ^1H NMR (300 MHz, $\text{DMSO}-d_6$, δ , ppm): 2.63 (dd, 1 H, $J_{\text{H,H}} = 6.0$ Hz, $J_{\text{H,H}} = 14.4$ Hz, H18), 3.17 (d, 1 H, $J_{\text{H,H}} = 5.4$ Hz, H19), 3.47–3.54 (m, 1 H, H19), 3.75 (s, 3 H, H2), 4.99 (d, 1 H, $J_{\text{H,H}} = 9.9$ Hz, NH), 5.99–6.02 (m, 1 H, NH), 6.94–6.98 (d, 2 H, arom.), 7.17–7.26 (m, 4 H, arom.), 7.34–7.42 (m, 3 H, arom.), 7.47–7.52 (m, 2 H, arom.), 7.60 (d, 1 H, $J_{\text{H,H}} = 1.8$ Hz, arom.), 7.75–7.80 (m, 1 H, arom.), 7.91 (d, 1 H, $J_{\text{H,H}} = 1.8$ Hz, arom.), 8.15–8.18 (m, 1 H, arom.), 8.35 (td, 1 H, $J_{\text{H,H}} = 1.8$ Hz, $J_{\text{H,H}} = 7.8$ Hz, arom.) and 8.72 (dd, 1 H, $J_{\text{H,H}} = 1.5$ Hz, $J_{\text{H,H}} = 5.7$ Hz, H16). ^{13}C NMR (75 MHz, $\text{DMSO}-d_6$, δ , ppm): 36.66 (C2), 48.48 (C19), 62.13 (C5), 65.80 (C18), 123.02 (C3), 124.04 (C4), 126.06 (C15), 126.23 (C13), 126.50, 127.08, 127.98, 128.36, 128.71, 129.00, 136.73, 139.14, 141.54, 151.14 and 152.52 (Ph), 154.15 (C16) and 178.64 (C17).

The optically active (*R*)-5a was obtained by stirring a methanol solution of diastereomer (*Rc,Sc*)-9a with 1 M HCl. The optically active (*R*)-5a was isolated as a yellow powder, 59%. $[\alpha]_{436} + 87.4$ (c 0.05, DMSO), lit.^[14b] $[\alpha]_{436} - 12.5$ (c 0.5, DMSO).

4.8 | Optical Resolution of Racemic Pd NHC Complex (\pm)-5b

To a suspension of the racemic complex (\pm)-5b (0.26 g, 0.53 mmol) in 20 ml of MeOH, AgNO₃ (0.18 g, 1.06 mmol) was added. The reaction mixture was allowed to stir in the dark at room temperature for 3 h and was filtered through celite. The orange filtrate was treated with sodium (Sc)-prolinate (0.07 g, 0.53 mmol) in 100 ml of MeOH. The reaction was then stirred for 2 h and was concentrated to approximately 50 ml and was left to stand overnight. From the diastereomeric mixture, only complex (Sc,Sc)-10b crystallized out as off-white crystals the next day and was isolated and washed with MeOH. The mother liquor was enriched with (Rc,Sc)-10b. The spectral data for the diastereomer are consistent with previous literature.^[14c]

Diastereomer (Sc,Sc)-10b. Off-white solid. $[\alpha]_{436}^{25}$ -153.2 (c 0.05, DMSO), lit.^[14c] $[\alpha]_{436}^{25}$ -167 (c 0.5, DMSO). ¹H NMR (300 MHz, DMSO-*d*₆, δ , ppm): 1.07–1.12 (m, 1 H, H24), 1.20–1.26 (m, 1 H, H25), 1.46–1.50 (m, 1 H, H25), 1.69–1.75 (m, 1 H, H26), 2.15–2.18 (m, 1 H, H26), 7.39–7.49 (m, 6 H, arom.), 7.62–7.64 (m, 1 H, arom.), 7.67–7.72 (m, 2 H, arom.), 7.75–7.79 (m, 1 H, arom.), 7.87–7.90 (m, 2 H, arom.), 7.93–7.94 (m, 1 H, arom.), 8.13 (d, 1 H, $J_{H,H}$ = 2.1 Hz, arom.), 8.22 (dd, 1 H, $J_{H,H}$ = 7.8 Hz, $J_{H,H}$ = 1.5 Hz, arom.), 8.35 (td, 1 H, $J_{H,H}$ = 7.8 Hz, $J_{H,H}$ = 1.5 Hz, H19) and 8.75 (dd, 1 H, $J_{H,H}$ = 6.0 Hz, $J_{H,H}$ = 1.8 Hz, H21). ¹³C NMR (75 MHz, DMSO-*d*₆, δ , ppm): 22.90 (C24), 28.27 (C25), 49.36 (C26), 66.80 (C10), 67.07 (C23), 124.47 (C9), 124.82 (C8), 126.40 (C20), 126.62 (C18), 127.14, 127.32, 129.02, 129.47, 130.20, 130.35, 153.31 and 153.45 (Ph), 154.96 (C21) and 178.13 (C22).

The optically active (S)-5b was obtained by stirring a methanol solution of diastereomer (Sc,Sc)-10b with 1 M HCl. The optically active (S)-5b was isolated as a yellow powder in 50% yield. $[\alpha]_{436}^{25}$ -45.7 (c 0.05, DMSO), lit.^[14c] $[\alpha]_{436}^{25}$ -27.8 (c 0.2, MeOH).

4.9 | Evaluation of Antimicrobial Activity

The broth microdilution assay was conducted with 96-well microtiter plates according to a protocol stated by the Clinical and Laboratory Standards Institute with some amendments.^[25] The compounds tested were prepared in 10% DMSO in phosphate-buffered saline (PBS) solution. Overnight bacteria culture in Mueller–Hinton broth (MHB) was adjusted to match 0.5 McFarland standard and diluted 1:100 in MHB. Into each well of the 96-well microtiter plate, the compounds of interest were serially diluted two-fold with MHB to obtain final working concentrations between 0.5 mM and 0.39 μ M

(for Pd complexes) or 5 mM and 3.9 μ M (for NHC ligands) in 100 μ l of broth. Then, 100 μ l of 1:100 diluted bacterial suspensions was added into each well prior to incubation at 37 °C for 24 h. The well with the lowest concentration of compounds that had no observed growth was determined as the MIC. The content of clear wells was streaked on Mueller–Hinton agar (MHA) and incubated overnight. The minimum bactericidal concentration was determined as the lowest concentration of compound in which the inoculum did not give bacterial growth on the MHA. The experiment was performed in triplicate.

4.10 | Evaluation of Cytotoxicity

Cytotoxicity studies of the synthesized compounds and metal NHC complexes along with cisplatin were carried out using HCT116, H103 and MCF-7 cell lines. MTT cell viability assay was performed to evaluate the cell cytotoxicity effects of the synthesized compounds.^[34] The three human carcinoma cell lines were from American Type Culture Collection (ATCC). The compounds tested were prepared in 2% DMSO in PBS solution. Positive control utilized in this assay was cisplatin (prepared in 0.9% NaCl solution). The cells were seeded in a 96-well microtiter plate at a density of 5000 cells per well in 100 μ l of cell culture medium and incubated at 37 °C (5% CO₂) for 24 h. After 18 h of seeding, the medium was removed and then the cells were incubated at 37 °C for 48 h in the CO₂ incubator with absence and/or presence of various concentrations of compounds of interest ranging from 0 to 40 μ M. After incubation, 10 μ l of MTT solution (5 mg ml⁻¹ in PBS) was added into each well. These plates were incubated again for 4 h in the CO₂ incubator at 37 °C. After that, the medium–MTT solutions are removed and the purple formazan crystals formed were dissolved in 200 μ l of DMSO. The resulting MTT products were determined by measuring the absorbance at 570 nm, with reference wavelength at 620 nm. The cell viability was determined by using the formula: cell viability (%) = (optical density of sample/optical density of control) \times 100 (solvent controls set to 100% viable cells). IC₅₀ values were defined as the concentrations that show 50% inhibition of proliferation on any tested cell line.

ACKNOWLEDGEMENTS

We are grateful for financial support from the Ministry of Higher Education (MOHE), Malaysia via Fundamental Research Grant Scheme (FRGS) (FRGS/1/2014/ST01/MUSM/03/1) and the School of Science, Monash University Malaysia.

ORCID

Yuen Lin Cheow  <http://orcid.org/0000-0002-0336-2328>

REFERENCES

- [1] a) L. Kelland, *Nat. Rev. Cancer* **2007**, *7*, 573; b) O. Rixe, W. Ortuzar, M. Alvarez, R. Parker, E. Reed, K. Paull, T. Fojo, *Biochem. Pharmacol.* **1996**, *52*, 1855; c) B. Rosenberg, L. Van Camp, T. Krigas, *Nature* **1965**, *205*, 698; d) D. Wang, S. J. Lippard, *Nat. Rev. Drug Discov.* **2005**, *4*, 307; e) N. J. Wheate, S. Walker, G. E. Craig, R. Oun, *Dalton Trans.* **2010**, *39*, 8113.
- [2] a) A. M. Florea, D. Busselberg, *Cancers (Basel)* **2011**, *3*, 1351; b) M. A. Fuentes, C. Alonso, J. M. Pérez, *Chem. Rev.* **2003**, *103*, 645; c) G. Giaccone, *Drugs* **2000**, *59*, 9; d) M. McKeage, *Drug Saf.* **1995**, *13*, 228.
- [3] a) S. Budagumpi, S. Endud, *Organometallics* **2013**, *32*, 1537; b) S. Budagumpi, R. A. Haque, A. W. Salman, *Coord. Chem. Rev.* **2012**, *256*, 1787; c) V. Dragutan, I. Dragutan, A. Demonceau, *Plat. Met. Rev.* **2005**, *49*, 123; d) G. D. Frey, W. W. Schoeller, E. Herdtweck, W. A. Herrmann, *J. Organomet. Chem.* **2016**, *810*, 46; e) A. Gautier, F. Cisnetti, *Metallomics* **2012**, *4*, 23; f) F. E. Hahn, C. Radloff, T. Pape, A. Hepp, *Chem.–A Eur. J.* **2008**, *14*, 10900; g) R. A. Haque, S. Y. Choo, S. Budagumpi, M. A. Iqbal, A. Al-Ashraf Abdullah, *Eur. J. Med. Chem.* **2015**, *90*, 82; h) A. S. K. Hashmi, *Pure Appl. Chem.* **2010**, *82*, 1517; i) Y. He, M.-f. Lv, C. Cai, *Dalton Trans.* **2012**, *41*, 12428; j) A. F. Henwood, M. Lesieur, A. K. Bansal, V. Lemaur, D. Beljonne, D. G. Thompson, D. Graham, A. M. Slawin, I. D. Samuel, C. S. Cazin, *Chem. Sci.* **2015**, *6*, 3248; k) K. M. Hindi, M. J. Panzner, C. A. Tessier, C. L. Cannon, W. J. Youngs, *Chem. Rev.* **2009**, *109*, 3859; l) W. Hu, Q. Luo, X. Ma, K. Wu, J. Liu, Y. Chen, S. Xiong, J. Wang, P. J. Sadler, F. Wang, *Chemistry* **2009**, *15*, 6586; m) E. A. B. Kantchev, C. J. O'Brien, M. G. Organ, *Angew. Chem. Int. Ed.* **2007**, *46*, 2768; n) A. Kascatan-Nebioglu, M. J. Panzner, C. A. Tessier, C. L. Cannon, W. J. Youngs, *Coord. Chem. Rev.* **2007**, *251*, 884; o) W. Liu, R. Gust, *Chem. Soc. Rev.* **2013**, *42*, 755; p) L. Oehninger, R. Rubbiani, I. Ott, *Dalton Trans.* **2013**, *42*, 3269; q) S. A. Patil, S. A. Patil, R. Patil, R. S. Keri, S. Budagumpi, G. R. Balakrishna, M. Tacke, *Future Med. Chem.* **2015**, *7*, 1305; r) A. Rit, T. Pape, F. E. Hahn, *Organomet.* **2011**, *30*, 6393; s) M. K. Samantaray, C. Dash, M. M. Shaikh, K. Pang, R. J. Butcher, P. Ghosh, *Inorg. Chem.* **2011**, *50*, 1840; t) D. Zhang, G. Zi, *Chem. Soc. Rev.* **2015**, *44*, 1898.
- [4] W. Liu, R. Gust, *Coord. Chem. Rev.* **2016**, *329*, 191.
- [5] a) C. M. Che, R. W. Y. Sun, L. F. Chow, J. Yan, *Pharmaceutical composition containing cyclometalated n-heterocyclic carbene complexes for cancer treatment*, Google Patents, **2011**; b) K. M. Hindi, D. A. Medvetz, M. Panzner, C. Tessier, W. J. Youngs, *Metal complexes incorporated within biodegradable nanoparticles and their use*, Google Patents, **2009**; c) K. M. Hindi, T. J. Siciliano, S. Durmus, M. J. Panzner, D. A. Medvetz, D. V. Reddy, L. A. Hogue, C. E. Hovis, J. K. Hilliard, R. J. Mallet, C. A. Tessier, C. L. Cannon, W. J. Youngs, *J. Med. Chem.* **2008**, *51*, 1577; d) P. Mailliet, A. Marinetti, M. Skander, *Platinum-N-heterocyclic carbene derivatives, preparation thereof and therapeutic use thereof*, Google Patents, **2009**; e) W. Youngs, C. Tessier, W. Kofron, R. Simons, J. Garrison, *Carbene porphyrins and carbene porphyrinoids, methods of preparation and uses thereof*, Google Patents, **2004**; f) W. J. Youngs, C. A. Tessier, J. Garrison, C. Quezada, A. Melaiye, M. Panzner, S. Durmas, *Metal complexes of N-heterocyclic carbenes as radiopharmaceuticals and antibiotics*, Google Patents, **2005**.
- [6] a) D. Bourissou, O. Guerret, F. P. Gabbaï, G. Bertrand, *Chem. Rev.* **2000**, *100*, 39; b) P. de Frémont, N. Marion, S. P. Nolan, *Coord. Chem. Rev.* **2009**, *253*, 862.
- [7] B. J. Pages, D. L. Ang, E. P. Wright, J. R. Aldrich-Wright, *Dalton Trans.* **2015**, *44*, 3505.
- [8] M. Marloye, G. Berger, M. Gelbcke, F. Dufrasne, *Future Med. Chem.* **2016**, *8*, 2263.
- [9] S. Ray, R. Mohan, J. K. Singh, M. K. Samantaray, M. M. Shaikh, D. Panda, P. Ghosh, *J. Am. Chem. Soc.* **2007**, *129*, 15042.
- [10] C.-H. Wang, W.-C. Shih, H. C. Chang, Y.-Y. Kuo, W.-C. Hung, T.-G. Ong, W.-S. Li, *J. Med. Chem.* **2011**, *54*, 5245.
- [11] R. A. Haque, N. Hasanudin, M. A. Hussein, S. A. Ahamed, M. A. Iqbal, *Inorg. Nano-Met. Chem.* **2016**, *47*, 131.
- [12] a) B. Cetinkaya, E. Cetinkaya, H. Kucukbay, R. Durmaz, *Arzneimittelforschung* **1996**, *46*, 821; b) B. Cetinkaya, I. Ozdemir, B. Binbasioglu, R. Durmaz, S. Gunal, *Arzneimittelforschung* **1999**, *49*, 538; c) A. Melaiye, R. S. Simons, A. Milsted, F. Pingitore, C. Wesdemiotis, C. A. Tessier, W. J. Youngs, *J. Med. Chem.* **2004**, *47*, 973; d) İ. Özdemir, A. Denizci, H. T. Öztürk, B. Çetinkaya, *Appl. Organomet. Chem.* **2004**, *18*, 318; e) A. Melaiye, Z. Sun, K. Hindi, A. Milsted, D. Ely, D. H. Reneker, C. A. Tessier, W. J. Youngs, *J. Am. Chem. Soc.* **2005**, *127*, 2285; f) M. V. Baker, P. J. Barnard, S. J. Berners-Price, S. K. Brayshaw, J. L. Hickey, B. W. Skelton, A. H. White, *Dalton Trans.* **2006**, 3708; g) A. Kascatan-Nebioglu, A. Melaiye, K. Hindi, S. Durmus, M. J. Panzner, L. A. Hogue, R. J. Mallet, C. E. Hovis, M. Coughenour, S. D. Crosby, A. Milsted, D. L. Ely, C. A. Tessier, C. L. Cannon, W. J. Youngs, *J. Med. Chem.* **2006**, *49*, 6811; h) İ. Özdemir, N. Temelli, S. Günal, S. Demir, *Molecules* **2010**, *15*, 2203; i) S. Roland, C. Jolival, T. Cresteil, L. Eloy, P. Bouhours, A. Hequet, V. Mansuy, C. Vanucci, J.-M. Paris, *Chem. A Eur. J.* **2011**, *17*, 1442; j) W. Liu, K. Bendorf, M. Proetto, A. Hagenbach, U. Abram, R. Gust, *J. Med. Chem.* **2012**, *55*, 3713; k) R. A. Haque, U. F. M. Haziz, A. A.-A. Abdullah, N. Shaheeda, M. R. Razali, *Polyhedron* **2016**, *109*, 208; l) M. O. Karatas, B. Olgunzeniz, S. Gunal, I. Ozdemir, B. Alici, E. Cetinkaya, *Bioorg. Med. Chem.* **2016**, *24*, 643.
- [13] F. Shaheen, A. Badshah, M. Gielen, M. Dusek, K. Fejfarova, D. de Vos, B. Mirza, *J. Organomet. Chem.* **2007**, *692*, 3019.
- [14] a) M. Chiang, *Synthesis, Characterisation And Catalytic Application Of Novel Cyclopalladated Pyridine Functionalized N-Heterocyclic Carbenes Complexes*, in *School of Physical and Mathematical Sciences*, Nanyang Technological University, Singapore, **2011**, p. PhD; b) M. Chiang, Y. Li, D. Krishnan, P. Sumod, K. H. Ng, P.-H. Leung, *Eur. J. Inorg. Chem.* **2010**, *2010*, 1413; c) K. H. Ng, Y. Li, W. X. Tan, M. Chiang, S. A. Pullarkat, *Chirality* **2013**, *25*, 149.
- [15] S. B. Aher, V. Dubey, P. N. Muskawar, K. Thenmozhi, A. R. Ghosh, P. R. Bhagat, *Res. Chem. Intermed.* **2017**, *1*.

- [16] H. Kim, S. K. Kang, *Acta Crystallographica Section E* **2014**, *70*, 0947.
- [17] J. Rieb, B. Dominelli, D. Mayer, C. Jandl, J. Drechsel, W. Heydenreuter, S. A. Sieber, F. E. Kuhn, *Dalton Trans.* **2017**, *46*, 2722.
- [18] J. C. Garrison, W. J. Youngs, *Chem. Rev.* **2005**, *105*, 3978.
- [19] a) A. S. El-Tabl, M. Mohamed Abd El-Waheed, M. A. Wahba, N. Abd El-Halim Abou El-Fadl, *Bioinorg. Chem. Appl.* **2015**, *2015*, 126023; b) N. Raman, J. Joseph, A. Sakthivel, R. Jeyamurugan, *J. Chil. Chem. Soc.* **2009**, *54*, 354.
- [20] a) T. Moller, P. Wonneberger, N. Kretzschmar, E. Hey-Hawkins, *Chem. Commun.* **2014**, *50*, 5826; b) G. L. Patrick, *An introduction to medicinal chemistry*, 5th ed., Oxford University Press, New York, NY **2013**, xxiii.
- [21] R. W.-Y. Sun, A. L.-F. Chow, X.-H. Li, J. J. Yan, S. S.-Y. Chui, C.-M. Che, *Chem. Sci.* **2011**, *2*, 728.
- [22] a) K. M. Nicholson, R. M. Phillips, S. D. Shnyder, M. C. Bibby, *Eur. J. Cancer* **2002**, *38*, 194; b) J. Zhou, K. Gupta, S. Aggarwal, R. Aneja, R. Chandra, D. Panda, H. C. Joshi, *Mol. Pharmacol.* **2003**, *63*, 799.
- [23] A. Kumar, A. Naaz, A. Prakasham, M. K. Gangwar, R. J. Butcher, D. Panda, P. Ghosh, *ACS Omega* **2017**, *2*, 4632.
- [24] L. A. Nguyen, H. He, C. Pham-Huy, *Int. J. Biol. Sci.: IJBS* **2006**, *2*, 85.
- [25] CLSI, *CLSI Document M07-A9*, Clinical and Laboratory Institute, Wayne, PA **2012**.
- [26] a) A. Mumtaz, A. Saeed, N. Fatima, M. Dawood, H. Rafique, J. Iqbal, *Bangladesh J. Pharmacogenomics* **2016**, *11*, 756; b) D. Demberelnyamba, K.-S. Kim, S. Choi, S.-Y. Park, H. Lee, C.-J. Kim, I.-D. Yoo, *Bioorg. Med. Chem.* **2004**, *12*, 853; c) S. N. Riduan, Y. Zhang, *Chem. Soc. Rev.* **2013**, *42*, 9055; d) P. Borowiecki, M. Milner-Krawczyk, D. Brzezińska, M. Wielechowska, J. Pleniewicz, *Eur. J. Org. Chem.* **2013**, *2013*, 712; e) J. Gravel, A. R. Schmitzer, *Org. Biomol. Chem.* **2017**.
- [27] C. R. Birnie, D. Malamud, R. L. Schnaare, *Antimicrob. Agents Chemother.* **2000**, *44*, 2514.
- [28] a) C. J. Goin, V. W. Mayer, *Mutat. Res./Genet. Toxicol.* **1995**, *343*, 185; b) F. Gümüş, I. Pamuk, T. Özden, S. Yıldız, N. Diril, E. Öksüzöglü, S. Gür, A. Özkul, *J. Inorg. Biochem.* **2003**, *94*, 255; c) F. Hatch, M. Colvin, *Mutat. Res. Fundam. Mol. Mech. Mutagen.* **1997**, *376*, 87.
- [29] a) M. J. Asmus, L. Hendeles, *Pharmacother. J. Hum Pharmacol. Drug Ther.* **2000**, *20*, 123; b) A. Marzo, E. Heftmann, *J. Biochem. Biophys. Methods* **2002**, *54*, 57.
- [30] a) N. Chhabra, M. L. Aseri, D. Padmanabhan, *Int. J. Appl. Basic Med. Res.* **2013**, *3*, 16; b) C. Mauro, N. Giovanni, *Anticancer Agents Med. Chem.* **2007**, *7*, 111.
- [31] a) A. E. Burgos, C. L. Tamayo, R. Torrellas-Hidalgo, *Revista U. D.C.A Actualidad & Divulgación Científica* **2014**, *17*, 477; b) M. A. Neelakantan, M. Esakkiammal, S. S. Mariappan, J. Dharmaraja, T. Jeyakumar, *Indian J. Pharm. Sci.* **2010**, *72*, 216.
- [32] R. Prabhakaran, S. V. Renukadevi, R. Karvembu, R. Huang, J. Mautz, G. Huttner, R. Subashkumar, K. Natarajan, *Eur. J. Med. Chem.* **2008**, *43*, 268.
- [33] G. Sava, A. Bergamo, P. J. Dyson, *Dalton Trans.* **2011**, *40*, 9069.
- [34] T. L. Riss, R. A. Moravec, A. L. Niles, H. A. Benink, T. J. Worzella, L. Minor, in *Assay Guidance Manual* (Eds: G. S. Sittampalam, N. Gal-Edd, M. Arkin, D. Auld, C. Austin, B. Bejcek, M. Glicksman, J. Inglese, V. Lemmon, Z. Li, J. McGee, O. McManus, L. Minor, A. Napper, T. Riss, O. J. Trask, J. Weidner), Eli Lilly and National Center for Advancing Translational Sciences, Bethesda, MD **2004**.

SUPPORTING INFORMATION

Additional Supporting Information may be found online in the supporting information tab for this article.

How to cite this article: Choo KB, Mah WL, Lee SM, Lee WL, Cheow YL. Palladium complexes of bidentate pyridine *N*-heterocyclic carbenes: Optical resolution, antimicrobial and cytotoxicity studies. *Appl Organometal Chem.* 2018;32:e4377. <https://doi.org/10.1002/aoc.4377>

